INVESTIGATING THE ROLE OF PELLINO3 IN TNF SIGNALLING

A thesis presented to the National University of Ireland, Maynooth for the degree of Doctor of Philosophy

By

Bingwei Wang

Institute of Immunology, Department of Biology

National University of Ireland Maynooth

October 2011

Supervisor: Prof. Paul Moynagh

CONTENTS:

ABSTRACT

Tumor necrosis factor (TNF) is an important modulator of the innate immune system, responsible for the activation of immune cells as well as the removal of damaged cells. Aberrant TNF signalling can cause a number of pathologic conditions. TNF binding to TNF receptor 1 triggers the activation of nuclear factor kappa B (NF-κB) leading to pro-inflammatory gene expression as well as the activation of the caspase cascade leading to death. In this study we observed that knockdown or knockout of the ubiquitin E3 ligase, Pellino3, sensitizes cells to TNF-induced apoptosis. Suppressed expression of Pellino3 leads to the activation of NF-κB, thereby inducing the expression of a series of antiapoptotic proteins, indicating that the increased apoptosis that is observed in Pellino3-knockdown or –deficient cells is not due to the regulation of the NF-κB pathway. We found that Pellino3 deficiency enhanced formation of the death-induced signalling complex in response to TNF. Pellino3 directly interacts with DISC components, RIP1 and caspase-8, but not FADD. Furthermore we show that Pellino3 regulates the formation of DISC and apoptosis in a manner that is dependent on the FHA domain but independent of the RING-like domain of Pellino3. The physiological importance of Pellino3 as a regulator of TNF signalling is confirmed by Pellino3-deficient mice showing increased sensitivity to TNF-induced apoptosis and greatly increased lethality in response to TNF administration. These findings define Pellino3 as a novel regulator of TNF signalling and a critical determining factor in dictating whether TNF induces cell survival or death.

ACKNOWLEDGEMENTS

First and foremost, I would like to thank my supervisor, Professor Paul Moynagh. Paul, thank you for the chance gave me to come and study in Ireland that never happened in my dream. Your unstinting support, advice and encouragement have made this work possible. Also sorry for all the corrections that you have to make on my thesis. It must be a terrible work to correct the English wrote by a "Chingilsh" writer.

To all the members of the molecular immunology lab, you have all in your own way helped me throughout these last three years. Lisa, your laughter makes me happy everyday. Although we are not "B.F.F.", I missed you every single day you were not in. Mark, thank you for always being there for us, you are a really good friend. Paola, you are such a Warm-hearted person, thank you for all your help. Nezira, thank you for all the thesises you found for me. All other members of the lab: Siobhan, Alan, Fiachra, Ruaidhrí and Anne, I thank you all for being you. You make me happy to come into work every day, and I am glad to work in a place with such special people. Thanks to everyone who took time from their busy schedules to correct my thesis.

Thanks to my parents and my younger sister for taking excellent care of my daughter and for supporting throughout. Thanks to my daughter, Sihan, for the joy and happiness you bring to me.

A special thanks to my husband and coworker, Dr. Shuo Yang. Thank you for everything you did for me. That is much more than I can say.

ABBREVIATIONS

A:	alanine
ABIN-1:	A20 binding and inhibitor of NF-κB
AP-1:	activator protein-1
Apaf1:	apoptosis-inducing factor1
APS:	ammonium persulfate
Bcl:	B cell lymphoma
BID:	BH3 interacting domain death agonist
BLAST:	blast local alignment search tool
ATP:	adenosine triphosphate
bp:	base pair
BSA:	bovine serum albumin
C:	carboxy; cysteine
cAMP:	cyclic adenosine 3’ 5’ -monophosphate
CARD:	caspase-recruiting domain
CD14:	cluster of differentiation antigen 14
cDNA:	complementary DNA
cFLIP:	cellular FADD-Like IL-1-beta converting enzyme inhibitor protein
CHX:	cycloheximide
cIAP1:	cellular Inhibitor of apoptosis protein1
CpG:	2′-deoxyribo cytidine-phosphate-guanosine
CREB:	cAMP-responsive element binding protein
CYLD:	cylindromatosis
DAMPs:	danger-associated molecular patterns
DAPI:	4′ 6-diamidino-2-phenylindole
DC:	dendritic cell
DD:	death domain
DED:	death effector domain

DEPC:	diethylpyrocarbonate
D-Gal:	D-galactosamine
DISC:	death inducing signalling complex
DMEM:	Dulbecco's Modified Eagle's medium
DMSO:	dimethylsulfoxide
DNA:	deoxyribonucleic acid
dNTPs :	deoxyribonucleic triphosphates
dsRNA:	double-stranded RNA
dToll:	*Drosophila* Toll
DTT:	dithiothreitol
E.coli:	*Escherichia coli*
EDTA:	ethylenediaminetetraacetic acid
EGFP:	enhanced-green fluorescent protein
ELISA:	enzyme-linked immunosorbant assay
EMSA:	electrophoresis mobility shift assay
ER:	endoplasmic reticulum
ERK:	extracellular signal regulated kinase
EST:	expressed sequence tag
FACS:	fluorescence activated cell sorting
FADD:	Fas-associated death domain
FBS:	foetal bovine serum
FHA:	forkhead-associated
FITC:	fluorescein isothiocyanate
Fn:	fibronectin III domain
g:	gravitation
GAPDH:	glyceraldehyde-3-phosphate dehydrogenase
GFP:	green fluorescent protein
GLUD:	glutamate dehydrogenase
GLUL:	glutamate-ammonia ligase
GPI:	glycosylphosphatidylinositol
hr:	hour

H&E:	haematoxylin and eosin
H_2O_2:	hydrogen peroxide solution
H_2SO_4:	sulphuric acid
HBSS:	Hank's balanced salt solution
HEK:	human embryonic kidney
HEPE:	hydroxyeicosapentaenoic acid
HRP:	horseradish-peroxidase
HSP:	heat shock protein
HCl:	hydrochloric acid
ID:	intermediary domain
IFN:	interferon
Ig:	immunoglobulin
IKK:	IκB Kinase
IL:	interleukin
IL-1R:	IL1 receptor
IL-1Ra:	IL-1 receptor antagonist
IL-1RacP:	IL-1 receptor accessory protein
IPTG:	isopropyl β-D-1 thiogalactopyranoside
IRAK:	IL-1 receptor associated kinase
IRF:	interferon-regulatory factor
IPTG:	isopropyl β-D-1 thiogalactopyranoside
ISRE:	interferon-stimulated response element
IκB:	inhibitor of κB
JNK:	c-Jun N-terminal kinase
K:	lysine
Kb:	kilobase
kD:	kilodalton
LB:	lysogeny broth
LPS:	lipopolysaccharide
LRR:	leucine-rich repeat
MAPK:	mitogen activated protein kinase

MAPKK:	MAPK kinase
MAPKKK:	MAPKK kinase
MD2:	myeloid differentiation protein2
MEF:	mouse embryonic fibroblast
min:	minute
MKK:	mitogen activated protein kinase kinase
ml:	milli liter
mM:	milli molar
M-MLV:	moloney murine leukemia virus
mRNA:	messenger RNA
MSCV:	murine stem cell virus
MTT:	3- 4 5-dimethylthiazol-2-yl -2 5-diphenyltetrazolium bromide
MyD88:	myeloid differentiation protein 88
Na_3VO_4:	sodium orthovanadate
NaCl:	sodium chloride
NADPH:	nicotinamide adenine dinucleotide phosphate
NaOH:	sodium hydroxide
Nec-1:	necrostatin-1
NEMO:	NF-κB essential modulator
NF-κB:	nuclear factor kappa B
ng:	nanogrammes
NIK:	NF-κB Inducing Kinase
Ni-NTA:	nickel-nitrilotriacetic acid
NK:	natural killer
NLS:	nuclear localization sequence
nM:	nanomolar
NOX1:	NADPH oxidase1
NOXA1:	NOX activator 1
NOXO1:	NOX organizer 1
nt:	nucleotide
NTP:	nucleotide triphospahte

OD:	optical density
PAGE:	polyacrylamide gel electrophoresis
PAMP:	pathogen-associated molecular pattern
PARP:	poly-ADP-ribose- polymerase
PBMC:	peripheral blood mononuclear cell
PBS:	phosphate buffered saline
PCR:	polymerase chain reaction
pDC:	plasmacytoid dendritic cell
PGN:	peptidoglycan
PGRP:	peptidoglycan recognition protein
PMSF:	phenylmethylsulfonyl fluoride
Poly I:C:	polyinosinic-polycytidylic acid
PRR:	pattern-recognition receptor
PYGL:	glycogen phosphorylase
R:	arginine
RANTES:	regulated upon activation normal T cell expressed and secreted
RHIM:	RIP homotypic interaction motif
RING:	really interesting new gene
RIP:	receptor interacting protein
RNA:	ribonucleic acid
ROS:	reactive oxygen species
RPMI:	roswell park memorial institute
RT:	room temperature; reverse transcriptase
s:	second; serine
SAPK:	stress-activated protein kinase
SARM:	sterile α and heat-armadillo motifs
SDS:	sodium dodecyl sulphate
SIMRA:	stabilized immune-modulatory RNA
siRNA:	small interfering RNA
SOC:	super optimal broth with catabolic repressor
SOCS:	suppressor of cytokine signalling

SODD:	silencer of death domain
ssRNA:	single-stranded RNA
SUMO:	small-ubiquitin-related-modifier
TAB:	TAK1-binding protein
TACE:	TNFα-converting enzyme
TAE:	Tris-acetate-EDTA
TAK1:	TGF-β-activated protein kinase 1
TANK:	TRAF-family-member-associated NF-κB activator
Taq:	*Thermophilus aquaticus*
TBE:	Tris-Borate-EDTA
TBK1:	TANK binding kinase
TBS:	Tris-buffered saline
TBST:	Tris-buffered saline containing Tween 20
Tc:	threshold cycle
TD:	transactivation domain
TE:	Tris-EDTA
TEMED:	N N N' N' - Tetramethylethylene-diamine
TGF-β:	transforming growth factor-β
TIR:	Toll-IL-1 receptor domain
TIRAP:	TIR domain-containing protein
TLR:	Toll-like receptor
TMB:	3 3' 5 5'-Tetramethylbenzidine
TNF α:	tumour necrosis factor alpha
TNFR:	TNF receptor
Tollip:	Toll-interacting protein
TRADD:	TNF receptor –associated death domain
TRAF:	TNF receptor associated factor
TRAILR:	TNF-related apoptosis-inducing ligand receptor
TRAM:	TRIF-related adaptor molecule
TRIF:	TIR domain-containing adaptor inducing IFN-β
TUNEL:	terminal deoxynucleotidyl transferase mediated dutp nick end

	labeling
Ubc:	ubiquitin conjugating enzyme
USP21:	ubiquitin specific peptidase 21
UV:	ultraviolet light
UXT-V1	ubiquitously expressed transcript-v1
WT:	wild-type
XIAP:	X chromosome-linked IAP
Z-VAD-fmk:	benzyloxycarbonyl-valine-alanine-aspartate-fluoromethyl ketone
μg:	micro grammes
μl:	micro liter
μM:	micromolar

CHAPTER ONE: INTRODUCTION

1.1 The immune system

The immune system is an organism's defence system against disease and acts by identifying and killing invading pathogens. It protects the organism from bacterial, parasitic, fungal and viral infections and from the growth of tumor cells. The immune system is typically divided into two major branches: the innate immune system and the adaptive immune system. The latter is found only in vertebrates.

1.1.1 The innate immune system

The innate immune system reacts in a non-specific manner to the type of pathogenic threat. Its effects are immediate and initiated a very short time after exposure to an antigen. It has long been considered to be non-specific and that its main function is to contain infection until the adaptive immune response can be induced. However, in the last few years it has become clear that innate immunity shows some specificity and is able to discriminate molecular structures that are conserved among broad groups of microorganisms. For example, all gram-negative bacteria contain lipopolysaccharide (LPS) in the bacterial cell wall. A receptor that can recognize the conserved lipid A moiety of LPS has therefore the potential to detect the presence of virtually any gram-negative bacteria infection. These molecular structures, like LPS, are known as pathogen-associated molecular patterns (PAMPs) and the receptors of the innate immune system that evolved to recognize them are called pattern-recognition receptors (PRRs). The innate immune defence is highly efficient at distinguishing self from non-self, through the use of PRRs.

1.1.2 The adaptive immune system

The adaptive immune system provides vertebrates with the ability to recognize and remember specific pathogens and react more quickly each time the pathogen is subsequently encountered. While all multicellullar organisms appear to have some form of host defence system, only vertebrates have developed the adaptive immune system (Thompson, 1995). There are two major branches of the adaptive immune responses: humoral immunity and cell-mediated immunity. Humoral immunity is mediated by B-lymphocytes and involves the production of antibodies in specific response to an antigen. Cell-mediated immunity is mediated by T-lymphocytes and involves the activation of macrophages, natural killer (NK) cells, antigen-specific cytotoxic T-lymphocytes, and the release of various cytokines in response to an antigen. The adaptive immune system, relying on clonally expressed receptors, has the advantage of flexibility and immunologic memory. However, the triggering of adaptive immunity is dependent on the innate immune system. The cooperation between the innate and adaptive immune systems leads to highly efficient recognition and elimination of pathogens (Clark and Kupper, 2005).

1.1.3 The inflammatory response

Inflammation, which is mainly due to cells of the innate immune system, is a complex biological response to harmful stress, such as pathogens, damaged cells or irritants. Inflammation is a protective attempt to prevent spreading of infection and to initiate the healing process. Inflammation is characterised by redness and swelling of tissue in the affected area and these symptoms are due to vasodilation of the blood vessels allowing cells of the immune system to congregate in the affected area. Inflammation is triggered by the recognition of danger-associated molecular patterns (DAMPs) or PAMPs and then facilitated by endogenous cytokines such as TNF and interleukin 1 (IL-1). Spontaneous secretion of TNF or IL-1β can also initiate inflammation. Once receptors such as Toll-like receptors (TLRs), TNF receptor (TNFR) and IL-1 receptor (IL-1R) are activated, various intracellular signal transduction pathways are initiated culminating in expression of inflammatory genes.

1.2 TLR signalling pathways

1.2.1 TLRs

The Toll protein was initially identified in *Drosophia* as a gene involved in dorsoventral polarity in the developing embryo. Subsequent studies have shown that the Toll protein plays an essential role in the defence against fungal infections (Lemaitre et al., 1996). Further studies led to the identification of a mammalian homolog of Toll, and this represented the characterisation of TLR4 as the first member of the TLR family (Medzhitov et al., 1997). To date, 13 mammalian TLRs (named TLR1 to TLR13) have been identified, 10 of which are found in humans. All TLRs are type I transmembrane proteins containing an extracellular leucine-rich repeat (LRR) domain, a transmembrane region, and a cytoplasmic Toll/IL-1 receptor (TIR) domain, which shares high sequence homology to the corresponding domain in the IL-1 receptor. The LRR domain has been inferred to be the ligand-sensing motif, responsible for molecular recognition (Kobe and Deisenhofer, 1995). All LRRs have a highly conserved segment. The repeat numbers and their distinct arrangement in TLRs differ with isoforms and species. The TIR domain of TLRs consists of approximately 150 amino acids and shows high similarity to that of the IL-1 receptor family. The TIR domain plays a central role in TLR signalling. It is present in both TLRs and adapter molecules and once the TLRs have bound their ligands, the TLR TIR domains act as a scaffold to recruit downstream TIR domain-containing adaptor proteins through TIR-TIR interactions (Dunne and O'Neill, 2003). The structure of TLRs is presented in Figure 1-1.

The TLR family members are expressed on the cells of the innate and adaptive immune systems. However, TLRs are differentially localized within the cell. TLR1, TLR2, TLR4, TLR5 TLR6 and TLR10 are all located on the cell surface, whereas TLR3, TLR7, TLR8 and TLR9 are located within the endosome and recognize intracellular pathogens. Each TLR recognizes distinct PAMPs (Table 1-1) (Roach et al., 2005).

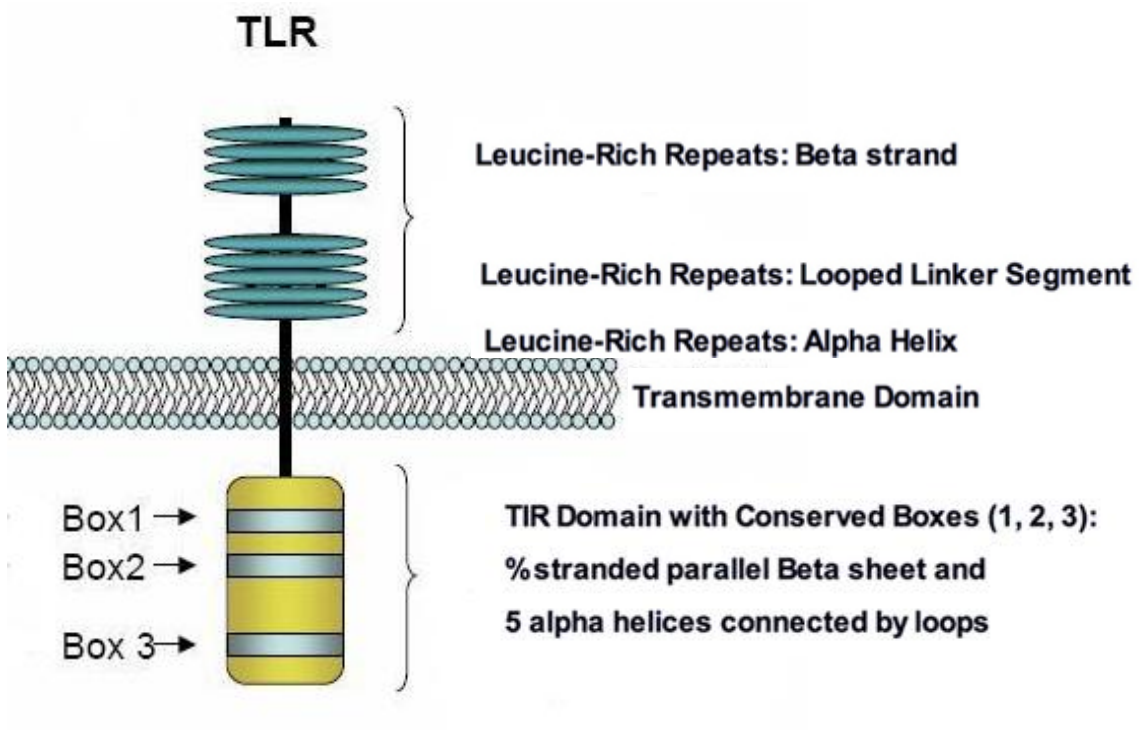

Figure 1-1 TLR Structure.

The mammalian TLR family are type I transmembrane proteins containing multiple leucine-rich repeats and one or two cysteine-rich regions in the large and divergent ligand-binding ectodomain; a short transmembrane region; and a conserved cytoplasmic domain TIR domain characterized by the presence of three highly homologous regions (known as boxes 1, 2 and 3).

Adapted from (Akira and Takeda, 2004).

Receptor	Ligands	Origin of ligands
TLR1	Tri-acyl lipopeptides	Bacteria, mycobacteria
	Soluble factors	Neisseria meningitides
TLR2	Lipoprotein/lipopeptides	A variety of pathogens
	Peptidoglycan	Gram-positive bacteria
	Lipoteichoic acid	Gram-positive bacteria
	Lipoarabinomannan	Mycobacteria
	A phenol-soluble modulin	*Staphylococcus epidermidis*
	Glycoinositolphospholipids	*Trypanosoma cruzi*
	Glycolipids	*Treponema maltophilum*
	Porins	Neisseria
	Zymosan	Fungi
	Atypical LPS	*Leptospira interrogans*
	Atypical LPS	*Porphyromonas gingivalis*
	LPS	*Porphyromonas gingivali*s
	HSP70	Host
TLR3	Double-stranded RNA	Virus
TLR4	LPS	Gram-negative bacteria
	Taxol	Plant
	Fusion protein	RSV
	Envelope proteins	MMTV
	HSP60	*Chlamydia pneumoniae*
	HSP60	Host
	HSP70	Host
	Type III repeat extra domain A of fibronectin	Host
	Oligosaccharides of hyaluronic acid	Host
	Polysaccharide fragments of heparan sulfate	Host
	Fibrinogen	Host
TLR5	Flagellin	Bacteria
TLR6	Di-acyl lipopeptides	Mycoplasma
TLR7	Imidazoquinoline	Synthetic compounds
	Loxoribine	Synthetic compounds
	Bropirimine	Synthetic compounds
	Sigle-stranded RNA	Virus
TLR8	Imidazoquinoline	Synthetic compounds
	Sigle-stranded RNA	Virus
TLR9	CpG DNA	Bacteria
TLR10	N.D.	N.D.
TLR11	Uropathogenic *E.coli* strains	Uropathogenic bacteria
	Profilin-like molecule	

Table 1-1 Toll-like receptors and their ligands

N.D.: not determined

Adapted from (Akira and Takeda, 2004)

1.2.1.1 Extracellular TLRs

TLR4 was the first TLR identified in mammals with the ability to recognize LPS, which, as mentioned, is a glycolipid component of the gram-negative bacterial cell wall (Poltorak et al., 1998). TLR4 requires some accessory proteins to recognize LPS, including CD14 (cluster of differentiation antigen 14), a glycosylphosphatidylinositol (GPI) -anchored membrane glycoprotein, and myeloid differentiation protein2 (MD2), a secretory protein. LPS is first transferred to soluble CD14 by a lipid transferase LPS-binding protein (LBP) (Jiang et al., 2000). LPS is then delivered to the TLR4/MD2 complex on the cell surface by CD14 (da Silva Correia et al., 2001). TLR4 can also recognize some other ligands including Taxol, an antitumor agent derived from a plant, fusion protein from respiratory syncytial virus (RSV), envelope proteins from moloney murine leukemia virus (MMLV), heat shock protein 60 (HSP60), HSP70, the extra domain A of fibronectin oligosaccharides of hyaluronic acid, polysaccharide fragments of heparan sulfate and fibrinogen (Kawasaki et al., 2000; Kawasaki et al., 2000; Rassa et al., 2002; Bulut et al., 2002; Vabulas et al., 2002; Okamura et al., 2001;, Termeer et al., 2002; Johnson et al., 2002; Smiley et al., 2001).

The genes encoding TLR1, TLR2, TLR6 and TLR10 are closely related and show high sequence homology to each other. Overall, TLR1 shares 69.3% amino acid sequence identity with TLR6, but the TIR domains of both receptors exhibit over 90% identity. They have a similar genomic structure and locate in tandem on the same chromosome (Takeuchi et al., 1999; Takeda et al., 2003; Du et al., 2000). TLR2 has been reported to recognize a variety of different molecules from gram-positive and gram-negative bacteria, fungi, viruses and parasites (Miyake, 2007). This wide array of recognition is made possible by the collaboration of TLR2 either with TLR1 or TLR6, by virtue of the formation of heterodimers between TLR2 and TLR1or TLR6 (Ozinsky et al., 2000). From the sequence homology, TLR10 also belongs to the TLR1 gene family. It exists only in human as its expression has not been detected in mice. TLR10 can form

complexes as homodimers or heterodimers, in association with TLR1 or TLR2 (Hasan et al., 2005).

TLR5 is expressed in monocytes, immature dendritic cells, endothelial cells, macrophages and epithelial cells (Vabulas et al., 2002). TLR5 can recognize flagellin, a protein that makes up the filament of bacterial flagella and plays important roles in bacterial chemotaxis, bacterial adherence and invasion of host tissues (Hayashi et al., 2001). So far, flagellin is the only known ligand for TLR5. Although the focus of some research, the mechanism by which flagellin is recognized by TLR5 is still unknown (Jacchieri et al., 2003; Mizel et al., 2003).

TLR11 is not expressed in human but has been detected in mouse bladder and kidney. It recognizes uropathogenic *E.coli* strains and a profilin-like molecule from intracellular protozoans such as *Toxoplasma gondii* (Yarovinsky et al., 2005).

TLR12 and TLR13 have also been discovered in mouse, but remain to be characterised at the functional level.

1.2.1.2 Intracellular TLRs

TLR3, TLR7, TLR8 and TLR9 are all located in the intracellular endosome membrane, a prime location to recognize their PAMPs, viral and bacterial nucleic acids. Translocation of these TLRs from the endoplasmic reticulum (ER) to the endosome or endolysosome is dependent on the membrane protein UNC93B1 (Kim et al., 2008) and the ER-resident chaperone gp96 (Saitoh and Miyake, 2009).

TLR3 recognizes double-stranded RNA (dsRNA), which is generated by many viruses during their replicative stages within host cells (Alexopoulou et al., 2001). TLR3 is unique amongst the other TLRs in that it lacks a critical proline residue that is highly conserved in the TIR domain of other TLRs. TLR3 protein is encoded by exons 2 through 5, while other TLRs are encoded by only 1 or 2 exons (Hoshino et al., 1999). TLR3 is expressed in a variety cells such as T lymphocytes, NK cells, macrophages and mast cells. TLR3 is located in acidic endosomes where it binds dsRNA via its ectodomain (Gauzzi et al., 2010). Polyinosinic:polycytidylic acid (Poly (I:C)) is a stable

synthetic dsRNA analogue which is extensively used as a TLR3 ligand to mimic activation of TLR3 by viral infection (Field et al., 1967).

TLR7 and TLR8 are similar in sequence and able to recognize single-stranded RNA (ssRNA), rich in guanosine or uridine, derived from viruses. TLR7 has also been reported to respond to synthetic antiviral imidazoquinoline compounds such as R848, loxoribine and imiquimod (Hemmi et al., 2002; Diebold et al., 2004; Heil et al., 2004). Furthermore TLR7 and TLR8 recognize synthetic oligoribonucleotides known as stabilized immune-modulatory RNA (SIMRA) compounds (Lan et al., 2007). Recently, a study on TLR8-deficient mice showed murine TLR8 had the ability to control TLR7 expression, thereby regulating myeloid cells and preventing autoimmunity (Demaria et al., 2010).

TLR9 recognizes unmethylated cytosine phosphate guanine (CpG) motifs of ssDNA, which is commonly present in bacteria and viruses. Activation of TLR9 induces secretion of cytokine and chemotactic factors and is involved in activation of proapoptotic signals (Theiner et al., 2008; Liang et al., 2010).

1.2.2 TLR Signalling

TLR-signal transduction can be broadly categorized into myeloid differentiation primary-response protein 88 (MyD88)-dependent and MyD88-independent pathways with the latter also termed the TIR-domain-containing adaptor protein inducing interferon β (TRIF)-dependent pathway. All TLRs, except TLR3, use the MyD88-dependent pathway to activate NF-κB, p38 and c-Jun N-terminal kinse/stress-activated protein kinase (JNK/SAPK) mitogen-activated protein kinase (MAPK) pathways. TLR3 and TLR4 are both capable of initiating the TRIF-dependent pathway, inducing inflammatory cytokines and type I interferons such as interferon-α and β (IFNα/β) (Bagchi et al., 2007).

1.2.2.1 The MyD88-dependent pathway

Upon stimulation by a cognate ligand, all TLRs, except TLR3, recruit MyD88, which has a TIR domain, an intermediary domain (ID) and a death domain (DD). In addition

to MyD88, TLR2 and TLR4 recruit MyD88-adaptor-like protein (MAL, also known as TIR-domain containing adapter protein, TIRAP), which serves as a bridge between the TIR domain of TLR2 and TLR4 and MyD88. MyD88 then recruits the members of the IL-1 receptor-associated kinase (IRAK) family with IRAK first being described as a protein kinase activity that co-precipitated with IL-1R1 (Martin et al., 1994). IRAK4 binds to MyD88 by its DD, triggering hyperphosphorylation of IRAK1 and IRAK2 (Kawagoe, et al. 2008). Activated IRAKs subsequently dissociate from MyD88 and interact with downstream adaptor TNFR-associated factor 6 (TRAF6), which acts as an E3 ubiquitin ligase. The complex associates with the pre-formed TGF-β-activated protein kinase 1 (TAK1) – TAK1 binding protein1 (TAB1)-TAB2-TAB3 complex. TAK1 then phosphorylates IKKβ in a complex with its related IKK kinase and the scaffolding protein IKKγ. The activated IKKβ can directly phosphorylate inhibitor of NF-κB (IκB) leading to its degradation allowing for NF-κB translocation into nucleus, where it initiates transcription of NF-κB responsive genes (Ninomiya-Tsuji, et al. 1999; O'Neill 2002).

TAK1 also phosphorylates and activates MAPK kinase kinase (MKK) 3/6 and MKK7, resulting in downstream phosphorylation of both p38 and JNK MAPKs, respectively. P38 MAPK and JNKs can then translocate to the nucleus and regulate expression of their target genes (Wang, et al. 2001).

Signalling molecules in the above pathway are subject to tight control and this is facilitated in many cases by their posttranslational modification. Phosphorylation and ubiquitination are especially important modifications that regulate these pathways. Reversible protein phosphorylation, principally on serine, threonine or tyrosine residues, is one of the most important posttranslational modifications that regulate the function, localization, and binding specificity of target proteins (Stock et al., 1989). Protein kinases and phosphatases are the enzymes responsible for determining the phosphorylation state of particular proteins. Protein kinases modify proteins by chemically adding phosphate groups to them, while protein phosphatases remove the phosphate group from its substrate by hydrolysing phosphoric acid monoesters into a phosphate ion and a molecule with a free hydroxyl group (Cohen, 1992).

Ubiquitination is another important reversible posttranslational modification, which regulates many biological processes including cell cycle progression, apoptosis, cell proliferation and DNA repair. Ubiquitin is a highly evolutionarily conserved 8-kDa polypeptide consisting of 76 amino acids, containing seven lysine (K) residues (K6, K11, K27, K29, K33, K48 and K63) that can participate in chain linkage formation (Baboshina and Haas, 1996). Ubiquitination occurs by the coordinated action of three distinct classes of enzymes named E1 (ubiquitin-activating enzyme), E2 (ubiquitin-conjugating enzyme) and E3 (ubiquitin ligase). Ubiquitin is first activated by an E1, in an ATP-dependent reaction. The activated ubiquitin is then transferred to an E2, forming an E2-Ub thioester. The E2 enzyme-ubiquitin complex, in the presence of an E3 protein, is attached to a target protein via the C terminal glycine residue of ubiquitin and a lysine residue in the target protein (Alkalay et al., 1995). Following an initial monoubiquitination event, the covalently attached ubiquitin itself can be subjected to ubiquitination at one of its 7 lysine residues and this process can be repeated leading to the formation of an ubiquitin polymer and thus polyubiquitination of the target protein. Polyubiquitin chains, which are linked via linkages at their K48 residues, are recognized by the 26S proteasome leading to degradation of the ubiquitinated protein and the recycling of ubiquitin. The formation of K63-linked chains is not a signal for degradation but instead such chains act as docking site for the recruitment of various proteins. It is interesting to note that E3 ubiquitin ligases that catalyze K63-linked polyubiquitination also have a tendency to promote autoubiquitination (Deng et al., 2000). TRAF-6 is one such E3 ligase that catalyzes the formation of K63-linked polyubiquitin chain on itself and this allows for its recruitment of the TAK-1/TAB and IKK complexes by virtue of the ubiquitin-binding domains of TAB proteins and IKKγ respectively (Xia, et al. 2009). This brings TAK1 into close proximity with the IKKs allowing for phosphorylation and activation of the latter by TAK1.

Whilst most attention has focused on NF-κB as the major transcription factor that is activated by the Myd88 pathway, TLR7 and TLR9 can also employ MyD88 in plasmacytoid dendritic cells (pDCs) to activate IRF7 that induces type I interferon expression. In this pathway MyD88 recruits IRAK4, TRAF6, TRAF3 and IRAK1. IRF7

becomes phosphorylated in this complex allowing for its translocation into the nucleus where it can regulate IFN transcription (Kawai and Akira, 2008).

1.2.2.2 The TRIF-dependent pathway

The TRIF-dependent pathway or MyD88-independent signalling pathway is only initiated by TLR3 and TLR4. TLR4 is the only TLR that utilizes both the MyD88-dependent pathway and the TRIF-dependent pathway (Amati et al., 2006; Foster et al., 2007; O'Neill, 2006; Pandey and Agrawal, 2006). Unlike TLR3, TLR4 needs a bridging adaptor TRIF-related adaptor molecule (TRAM) for activating TRIF (Fitzgerald et al., 2003). TRIF interacts with TRAF3 and TRAF6 through TRAF-binding motifs, which exist in its N-terminal portion to initiate downstream signalling.

In response to TLR3, TRAF3 plays a critical pole in activating two IKK-related kinases; TRAF-family-member associated NF-κB activator (TANK)-binding kinase 1 (TBK1) and IKKε (also call inducible IKK or IKKi). Activation of TBK1 and IKKε leads to the phosphorylation of interferon regulatory factors 3 (IRF3) and IRF7. IRF3 and IRF7 dimerise and in turn translocate to the nucleus, resulting in induction of type I IFNs and expression of IFN-inducible genes (Hacker et al., 2006).

Although TRAF6 has been showed to interact with TRIF, its role in TRIF signalling is still controversial. In contrast to TRAF6-deficient mouse embryonic fibroblasts (MEFs), TRIF signalling was not affected in TRAF6-deficient macrophage (Gohda et al., 2004; Hacker et al., 2006).

TRIF also recruits receptor interacting protein1 (RIP1) and RIP3 by its C-terminal RIP homotypic interaction motif (RHIM) (Meylan et al., 2004). RIP1 is then polyubiquitinated and activates TAK1 resulting in the activation of the NF-κB pathway (Cusson-Hermance et al., 2005). RIP3 plays an inhibitory role in the TRIF-RIP1-NF-κB pathway..

The schematic representation of TLR pathway is presented in Figure 1-2.

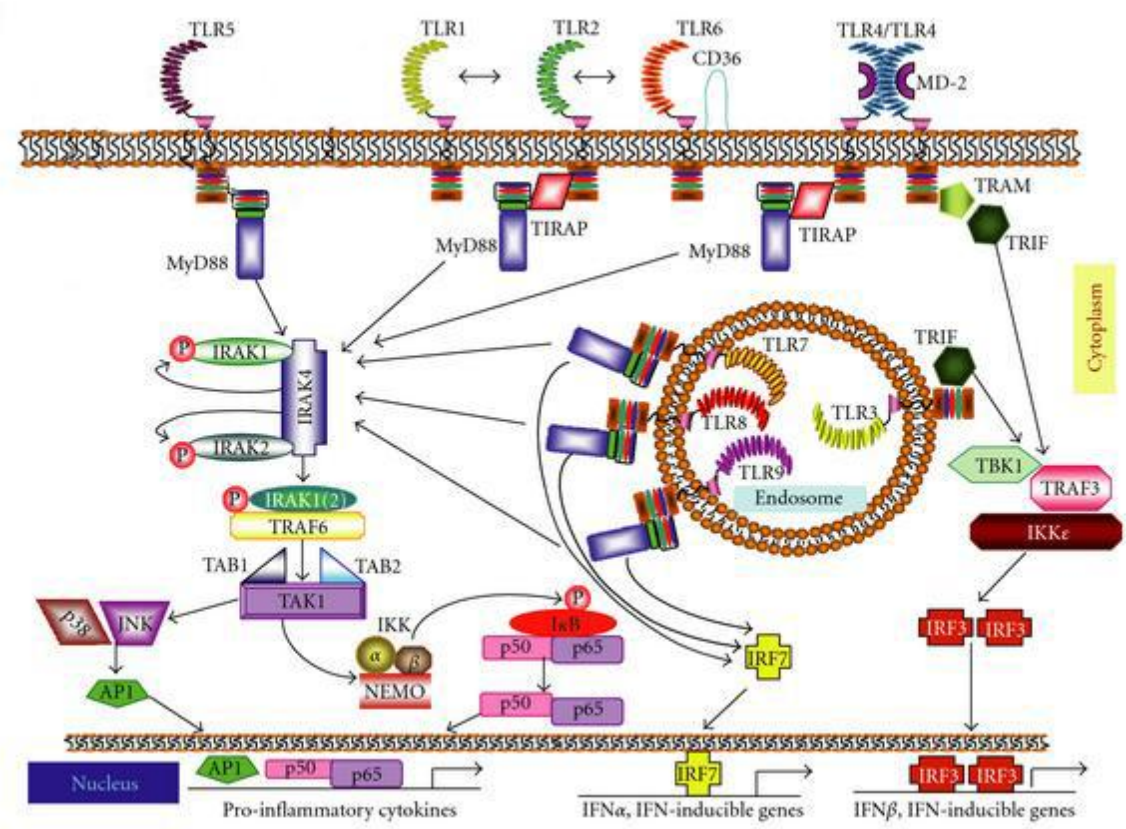

Figure 1-2 Overview of TLR signalling pathways.

Upon stimulation by a cognate ligand, all TLRs, except TLR3, recruit MyD88. In addition to MyD88, TLR2 and TLR4 recruit TIRAP, which serves as a bridge between the TIR domain of TLR2 and TLR4 and MyD88. MyD88 then recruits the members of IRAK family. IRAK4 binds to MyD88 by its DD, triggering hyperphosphorylation of IRAK1 and IRAK2. Activated IRAKs subsequently dissociate from MyD88 and interact with downstream adaptor TRAF6. The complex associates with the pre-formed TAK1-TAB2-TAB3 complex. TAK1 then phosphorylates IKKβ in a complex with its related IKK kinase and the scaffolding protein IKKγ. The activated IKKβ can directly phosphorylate IκB leading to its degradation allowing for NF-κB translocation into nucleus, where it initiates transcription of NF-κB responsive genes. TAK1 also trigers phosphorylation of both p38 and JNK MAPKs. TLR7 and TLR9 can also employ MyD88 in plasmacytoid dendritic cells to activate IRF7 that induces type I interferon expression. TLR3 and TLR4 both signal through the adaptor TRIF, which interacts with TRAF3 to activate the noncanonical IKKs, TBK1, and IKKε resulting in the dimerization and activation of IRF3, which then translocates into the nucleus activating the transcription of IFN$\beta$and IFN-inducible genes.

Adapted from (Loiarro, 2010)

1.3 IL-1R signaling pathway

Whilst TLRs are primary triggers of the inflammatory response, inflammation can be triggered by TLR-induced expression of endogenous pro-inflammatory cytokines. IL-1 is a key proinflammatory cytokine that plays a determining role in the regulation of a broad spectrum of immune and inflammatory responses. IL-1 can regulate a number of genes, including genes for other cytokines, cytokine receptors, acute-phase reactants, growth factors, tissue remodeling enzymes, extracellular matrix components and adhesion molecules (Dinarello, 1996; O'Neill, 1995). Furthermore, IL-1 can also induce expression of its own genes in a positive-feedback loop (Gaestel et al., 2009). Although the original IL-1 family comprised only IL-1α and IL-1β, more members of the IL-1 family have been identified, including IL-1R antagonist (IL-1Ra), IL-18, IL-36Ra, IL-36α, IL-37, IL-36β, IL-36γ, IL-38 and IL-33, which are encoded by 11 distinct genes (Dinarello, 2011). IL-1α and IL-1β are mainly produced by activated macrophages, monocytes and dendritic cells, but other cell types, such as epithelial cells (Hoffmann et al., 2005), endothelial cells (Bandman et al., 2002) and fibroblasts (Holzberg et al., 2003) can also make these cytokines.

IL-1 signals through two distinct subunits of its receptor: IL-1R1 and IL-1R accessory protein (IL-1RacP). Once bound with IL-1, IL-1R and IL-1RacP form a complex, which recruits MyD88 and Toll-interacting protein (Tollip) to the receptor to facilitate downstream signal propagation. Competitive binding by IL-1Ra to IL-1R1 can block such IL-1 mediated signalling (Aksentijevich et al., 2009). Like TLRs, IL-1R1 utilises the MyD88-dependent pathway to activate NF-κB and this is due to IL-1R1 and TLRs sharing the TIR homology domain in their intracellular regions. MyD88 and Tollip serve as adaptors to recruit IRAK4 to the receptor allowing subsequent phosphorylation of IRAK1 and IRAK2. Tollip and IRAK1 exist as a

complex in resting cell, where Tollip blocks phosphorylation and the kinase activity of IRAK1 (Brissoni et al., 2006). After receptor activation, the complex is recruited to the receptor, resulting in the rapid autophosphorylation of IRAK1 and its dissociation from the receptor. In parallel, IRAK1 phosphorylates Tollip, leading to the dissociation of Tollip from IRAK1 and its rapid ubiquitylation and degradation. TRAF6 is subsequently recruited and activated as described previously for the MyD88-dependent pathway.

The schematic representation of IL-R1 pathway is presented in Figure 1-3.

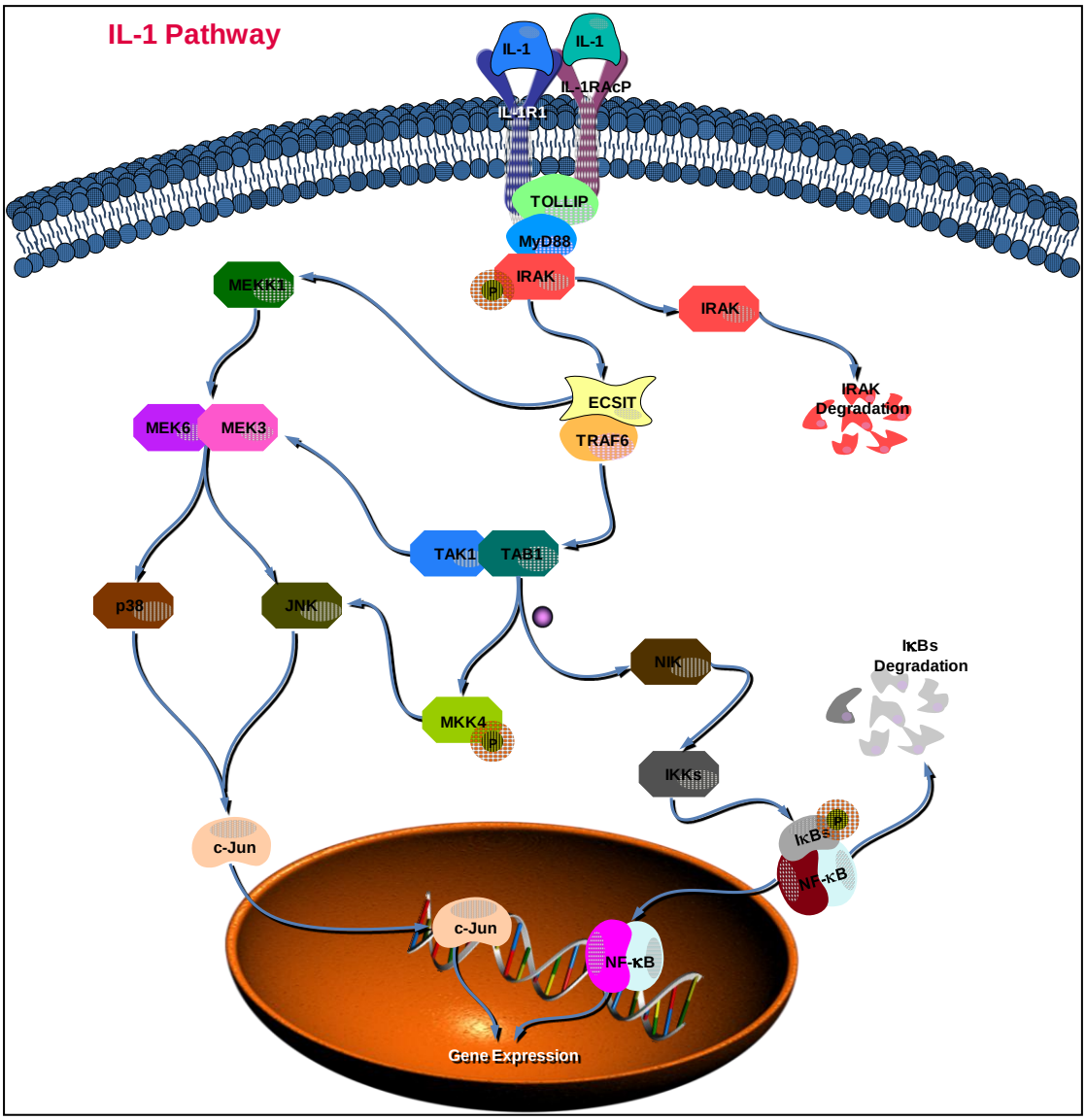

Figure 1-3 Signal transduction through IL-1R.

After IL-1 is bound, a complex is formed between the IL-1R and IL-1RacP. The cytosolic proteins MyD88 and TolliP are recruited to this complex, where they function as adaptors, recruiting IRAK in turn. IRAK1 activates and recruits TRAF6 to the IL-1 receptor complex. Eventually, phosphorylated IRAK is ubiquitinated and degraded. TRAF6 activates two pathways, one leading to NF-κB activation and another leading to c-Jun activation. The TRAF associated protein ECSIT leads to c-Jun activation through the MAPK/JNK signaling system. TRAF6 also signals through the TAB1/TAK1 kinases to trigger the degradation of IκB, and activation of NF-κB.

Adapted from (https://www.qiagen.com/geneglobe/pathwayview.aspx?pathwayID=237)

1.4 TNFR signalling pathway

1.4.1 TNF

Like IL-1, TNF is a critical TLR-induced cytokine that orchestrates the inflammatory response. TNF was first discovered more than one hundred years ago. In 1984, TNF was isolated and its encoding cDNA was cloned and expressed (Haranaka et al., 1984). Human TNF is synthesized as a 233 amino acid protein that is then cleaved to a 157 amino acid protein by TNF-converting enzyme (TACE) (Kriegler et al., 1988). A wide range of cells produce TNF. The primary sources *in vivo* are cells of monocytic lineage, such as macrophages, astroglia, microglia, langerhans cells, Kupffer cells and alveolar macrophages (Pfeffer et al., 1993). Although it was initially characterised as a cytokine that could kill tumor cells, TNF has been subsequently implicated in a wide arrange of biological processes such as cell proliferation, differentiation, apoptosis, lipid metabolism, insulin resistance, endothelial function and coagulation (Gaur and Aggarwal, 2003; Locksley et al., 2001). TNF is not detectable in the serum from a healthy individual. However, TNF is a critical component of effective immune surveillance and is required for proper proliferation and function of immune cells. TNF has been shown to play roles in a wide spectrum of human diseases, such as cancer, Alzheimer disease, heart failure, allograft rejection, diabetes (type II), cerebral malaria, acquired immunodeficiency syndrome, rheumatoid arthritis and Crohn's disease (Aggarwal, 2003).

1.4.2 TNFR

TNF signals through two receptors, TNFR1 (CD120a; p55/60) and TNFR2 (CD120b; p75/80) (Wallach et al., 1999). TNFR1 is expressed in most mammalian tissues whereas TNFR2 is mostly confined to immune cells. Containing four cysteine-rich

domains, the extracellular domains of TNFR1 and TNFR2 are highly conserved (Banner et al., 1993). TNFR1 has a special intracellular death domain containing 80 amino acids, which is required for death signalling (Chen and Goeddel, 2002). However, TNFR2 does not contain a death domain (Grell et al., 1995). TNFR1 is the main signalling receptor for TNF in most cell types. TNF signalling can be regulated by controlling the processing and release of its receptor. Thus, in response to TNF stimulation, TNFR1 can be cleaved by a sheddase enzyme and shed from cells as a 34-kDa soluble TNFR1 (Reddy et al., 2000). In the second pathway the full-length 55-kDa TNFR1 can be released to the extracellular compartment within exosome-like vesicles (Hawari et al., 2004).

1.4.3 TNFR downstream signaling

TNF binding to TNFR1 triggers the activation of NF-κB leading to pro-inflammatory gene expression or activation of the caspase cascade, apoptosis / necroptosis leading to death (Chen and Goeddel, 2002; Galluzzi and Kroemer, 2008). These pathways are subject to counter-regulation and this is best appreciated by discussion of the signalling components of these pathways.

1.4.3.1 Activation of NF-κB

Upon binding of TNF, the trimerisation of TNFR1 will release silencer of death domain (SODD) (Jiang et al., 1999). This will result in the binding of TNF receptor – associated death domain (TRADD) via its death domain (Jiang et al., 1999). TRADD then can recruit a number of additional proteins including TRAF2, TRAF5 and RIP1 to form a new complex termed complex I (Chen and Goeddel, 2002). TRAF2 then recruits the E3 ubiquitin ligase cellular inhibitor of apoptosis protein1 (cIAP1) and cIAP2. The recruitment of cIAP1/cIAP2 causes the K63-linked ubiquitination of RIP1 and TRAF2 (Ea et al., 2006). The K63-linked polyubiquitin chain on K377 in RIP1

serves as a scaffold to recruit the complex of TAK1 and TAB2/3. The newly formed complex subsequently activates the IKKα/β/γ heterocomplex. Activated IKK phosphorylates the NF-κB inhibitor IκBα resulting in its K48-linked ubiquitination and degradation of IκBα allowing NF-κB dimers to translocate to the nucleus (Wu et al., 2006).

Whilst NF-κB is a key driver of pro-inflammatory gene expression it can also promote the transcription of a series of prosurvival genes, such as cellular Fas-associated death domain-like IL-1-β converting enzyme inhibitor protein 1 (cFLIP1), cIAP1, cIAP2, B cell lymphoma x (Bcl-x), X chromosome-linked IAP (XIAP) (Micheau et al., 2001; Mahoney et al., 2008; Tao et al., 2006; Dutta et al., 2006). These genes can inhibit and counter-regulate the caspase and apoptotic cascade that can also be triggered by TNF.

1.4.3.2 Induction of Apoptosis

Apoptosis, an important cell clearance mechanism, plays an essential role in multiple biological processes, including embryonic development, selection in the immune system, immune tolerance and many human diseases (Lawen, 2003). Apoptotic cells are characterised by several morphological changes, including cell shrinkage, plasma membrane blebbing, nuclear fragmentation, chromatin condensation and chromosomal DNA fragmentation. In contrast to necrosis, apoptosis produces compact membrane-enclosed structures, called apoptotic bodies, which are engulfed by macrophages and quickly removed before the contents of the cell can spill out onto surrounding cells and cause an inflammatory response (Saraste and Pulkki, 2000).

Caspases are cysteine proteases that are the integral players during apoptosis and are named due to their specificity for aspartic acid residues that precede their cleavage sites (Thornberry, 1997). Caspases are synthesized as inactive zymogens, termed procaspases. Upon maturation, the procaspases become proteolytically processed to

generate a small and a large subunit that assemble into active enzymes consisting of two large and two small subunits. The proapoptotic caspases can be divided into the group of initiator caspases, including caspase-2, -8, -9, -10, and executioner caspases, caspase-3, -6, -7. Initiator caspases cleave inactive pro-forms of executioner caspases, thereby activating them. Effector caspases in turn cleave a number of different target proteins within the cell to trigger the apoptotic process (Salvesen and Dixit, 1997).

RIP1 is a key signalling molecule that determines whether TNF induces activation of NF-κB and survival or triggers apoptosis/necroptsis. When ubiquitinated by cIAP1 and cIAP2, RIP tends to bias the TNF pathway towards activation of NF-κB whereas in its unubiquitinated form it promotes apoptosis. Several proteins are known to induce deubiquitination of RIP1. They include cylindromatosis (CYLD), cezanne, ubiquitin specific peptidase 21 (USP21) and A20 (Hitomi et al., 2008; Enesa et al., 2008; Xu et al. 2010; Shembade et al., 2010). Wang et al. reported that second mitochondria-derived activator of caspase (SMAC) mimetics, which are tetrapeptides based on the amino acid sequence from the SMAC protein that binds to IAP family members and were originally designed to repress IAP inhibition of the caspases, can also favour increased levels of unubiqutinated RIP1 by accelerating cIAP1/2 degradation (Wang et al., 2008). In its unubiquitinated state RIP1 can interact with Fas-associated death domain (FADD) protein via the DD of the latter. FADD subsequently recruits procaspase-8 through its death effector domain (DED). This complex is named death inducing signalling complex (DISC), also known as Complex II (Scaffidi et al., 1999). Procaspase-8 is then cleaved into the active p18/p12 fragments by autoproteolytic self-activation (Ashkenazi and Dixit, 1998). Activated caspase-8 can either directly activate caspase-3, or cleave BH3 interacting domain death agonist (BID), a proapoptotic Bcl-2 family member (Scaffidi et al., 1998; Stennicke et al., 1998; Li et al., 1998; Stennicke et al., 1998). Truncated form of Bid (tBID)is then translocated to the mitochondria, resulting in the release of cytochrome c, apoptosis-inducing factor1 (Apaf1), caspase-9 and ATP, which will further activate

caspase-3 and caspase-7. Activated caspases then cleave intracellular substrates, triggering apoptosis (Li et al., 1998). RIP1 can also be cleaved by caspase-8 during this period, abolishing its NF-κB inducing ability. In addition, cleaved RIP1 can promote TRADD and FADD interaction (Lin et al., 1999b).

Both of the apoptotic pathways described are tightly controlled by regulators of caspase activation. DISC can be inhibited by cFLIP, which can prevent the interaction between procaspase-8 and FADD by competitive binding to the former (Irmler et al., 1997; Wang et al., 2008). TBid–induced apoptosis can be inhibited by Bcl2 or Bclx, which block cytochrome c release or by XIAP, which blocks caspase-9 activation ((Yi et al., 2003; Tao et al., 2006; Datta et al., 2000). The ability of NF-κB to induce cFLIP and Bcl2 underlies the counter-regulatory effects of NF-κB on the apoptotic pathway.

1.4.3.3 Induction of necroptosis

Necrosis refers to a caspase-independent cell death mechanism biochemically characterized by mitochondria swelling, nuclear flocculation and uncontrolled cell lysis (Golstein and Kroemer, 2007). Necrosis has been considered for a long time as an accidental, uncontrolled form of cell death. However, accumulating evidences show that necrotic cell death is regulated by complex signal transduction pathway, which is termed necroptosis (Degterev et al., 2005). Studies showed that cell death induced by necroptosis contributed to embryonic development and adult tissue homeostasis and like apoptosis necroptosis could be induced by specific ligands and regulated by genetic, epigenetic, and pharmacological factors (Golstein and Kroemer, 2007). Necroptosis depends on the kinase activities of RIP1 and RIP3 (Degterev et al., 2008; He et al., 2009). Identification of the RIP1 inhibitor, necrostatin-1 (Nec-1) made it possible to study the functions of RIP1 in regulating the downstream pathway of NF-κB activation, apoptosis and necroptosis (Degterev et al., 2005).

RIP3 plays a switch-like role in TNF-induced apoptosis and necroptosis (He et al., 2009). RIP3 binds to RIP1 through their RHIM domains (Sun et al., 2002). Activated caspase-8 inactivates RIP1 and RIP3 by proteolytic cleavage. If a caspase-8 dependent apoptosis pathway is inhibited, necroptosis will occur after death receptor activation. RIP3 regulates the phosphorylation of RIP1. The complex will be further stabilized by the phosophorylation of RIP1 and RIP3 (Cho et al., 2009). RIP1 kinase inhibitor Nec-1 has also been reported to have the ability to prevent the recruitment of both RIP1 and RIP3 to complex I (He et al., 2009). RIP3 will interact with several bioenergetic enzymes such as glycogen phosphorylase (PYGL), glutamate-ammonia ligase (GLUL) and glutamate dehydrogenase (GLUD), further enhancing their kinase activity and triggering downstream reactive oxygen species (ROS) overproduction. Extra ROS, thereby can result in malfunction of mitochondria, leading to TNF-induced necroptosis (Galluzzi and Kroemer, 2008).

In addition, the complex containing TNFR1, TRADD, RIP1 recruits NADPH oxidase1 (NOX1) and the other signalling components NOX organizer 1 (NOXO1), NOX activator 1 (NOXA1) and Rac1. Upon activation of Nox1, NOXO1-TRADD interaction promotes oxidase activation, resulting in the generation of superoxide anions and hydrogen peroxide eventually contributing to necroptosis (Kim et al., 2007).

The schematic representation of TNFR1 pathway is presented in Figure 1-4.

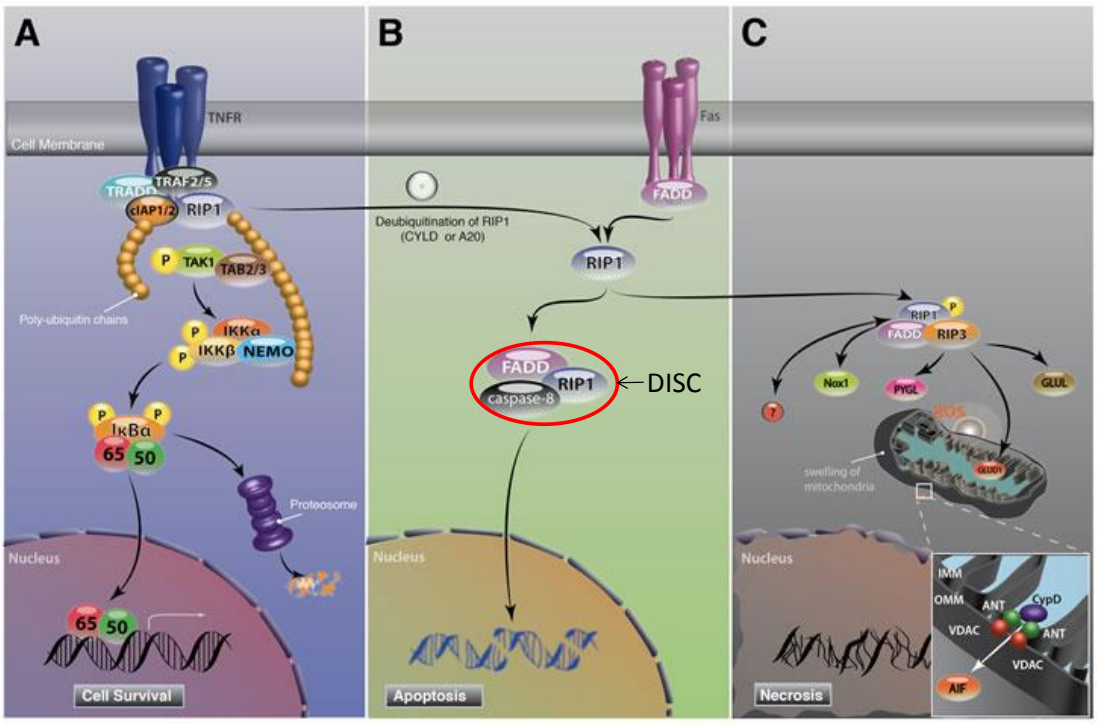

Figure 1-4 TNFR1-elicited signalling pathways.

A. In response to TNF-α stimulation, RIP1 is recruited to TNFR and forms a membrane associated complex I with TRADD, TRAF2/5 and cIAP1/2, which in turn leads to polyubiquitination of RIP1 and pro-survival NF-κB activation. B. when RIP1 is unubiquitinated by A20 or CYLD, deubiquitination of RIP1 leads to the formation of cytosolic DISC with FADD and caspase-8. Activation of caspase-8 in DISC leads to apoptosis induction. During apoptosis, RIP1 is cleaved and inactivated by caspase-8. C. In conditions where caspases are blocked or cannot be activated efficiently, RIP1 binds to RIP3 leading to necrosis.

Adapted from (Murakami, 2011).

1.5 Downstream signalling in inflammatory pathways

It is clear from above that the primary objectives of pro-inflammatory signalling pathways are to activate transcription factors like NF-κB and IRFs and to induce the expression of a range of pro-inflammatory genes.

1.5.1 NF-κB

NF-κB was discovered as a basally active nuclear factor necessary for transcription of the kappa light chain gene of activated B cells (Sen and Baltimore, 1986). However in many other cell types, NF-κB can serve as a first responder to harmful stimuli as the transcription factor is present in an inactive state in the cytosol forgoing the need for new protein synthesis to react to pathogenic threat. NF-κB inducing agents include ROS, TNF, IL-1β, TLR ligands, isoproterenol, cocaine and ionizing radiation.

The NF-κB family has five conserved members in mammals: p50 (also known as NF-κB1, precursor p100), p52 (also known as NF-κB2, precursor p100), p65 (RelA), RelB and cRel (Ghosh et al., 1998). All of the proteins have an N-terminal Rel homology domain, which is responsible for DNA binding, dimerization to other family members and binding to IκBs. P65, RelB and c-Rel have a C-terminal transactivation domain (TD), which is essential for transaction activity. In contrast p50 and p52 lack a TD (Wei, 2008 #324). NF-κB proteins can exist as either homo- or heterodimers. In the cytoplasm of unstimulated cells, the dimers are inactive due to their association with IκB proteins, IκBα, IκBβ, IκBγ and IκBε, which mask the nuclear localization sequences of NF-κB proteins (Karin and Ben-Neriah, 2000). NF-κB is further regulated in the nucleus by the nuclear IκB family members IκBζ, IκBNS and Bcl-3 (Yamamoto and Takeda, 2008).

There are two signalling pathways leading to the activation of NF-κB, known as classical and the alternative pathways. Signalling through TNFR, IL-1R or TLRs, as described above, leads to activation of the classical NF-κB pathway. In response to stimulation, the IKK complex comprising IKKα, IKKβ and IKKγ is activated and phosphorylates IκB, leading to IκB polyubiquitylation and degradation. Liberated from IκB, p50-RelA heterodimers can then translocate from the cytoplasm into the nucleus, triggering the transcription of a plethora of genes (Zandi et al., 1997). The non-canonical pathway is responsible for the activation of p52/RelB complexes and regulates the generation of B and T lymphocytes. In this pathway, NF-κB inducing kinase (NIK) is activated upon ligand-receptor association, resulting in phosphorylation and activation of IKKα-IKKα complex. The activated IKKα complex in turn phosphorylates and subsequently induces proteasomal processing of the precursor protein p100 into a mature p52 subunit. P52-RelB heterodimers then translocate to nucleus and regulate a distinct class of genes (Dejardin, 2006).

The extensive list of NF-κB inducible genes includes genes for proinflammatory cytokines such as IL-1, IL-6 and TNF, as well as genes for chemokines such as IL-8 and RANTES (regulated upon activation normal T cell expressed and secreted) (Ghosh et al., 1998). NF-κB also upregulates the expression of cell adhesion molecules and induces a number of growth factors and antiapoptotic proteins. These proteins take part in many aspects of inflammatory response and NF-κB enhances the host cell division and inhibits apoptosis in response to harmful stimuli.

The schematic representation of NF-κB pathway is presented in Figure 1-5.

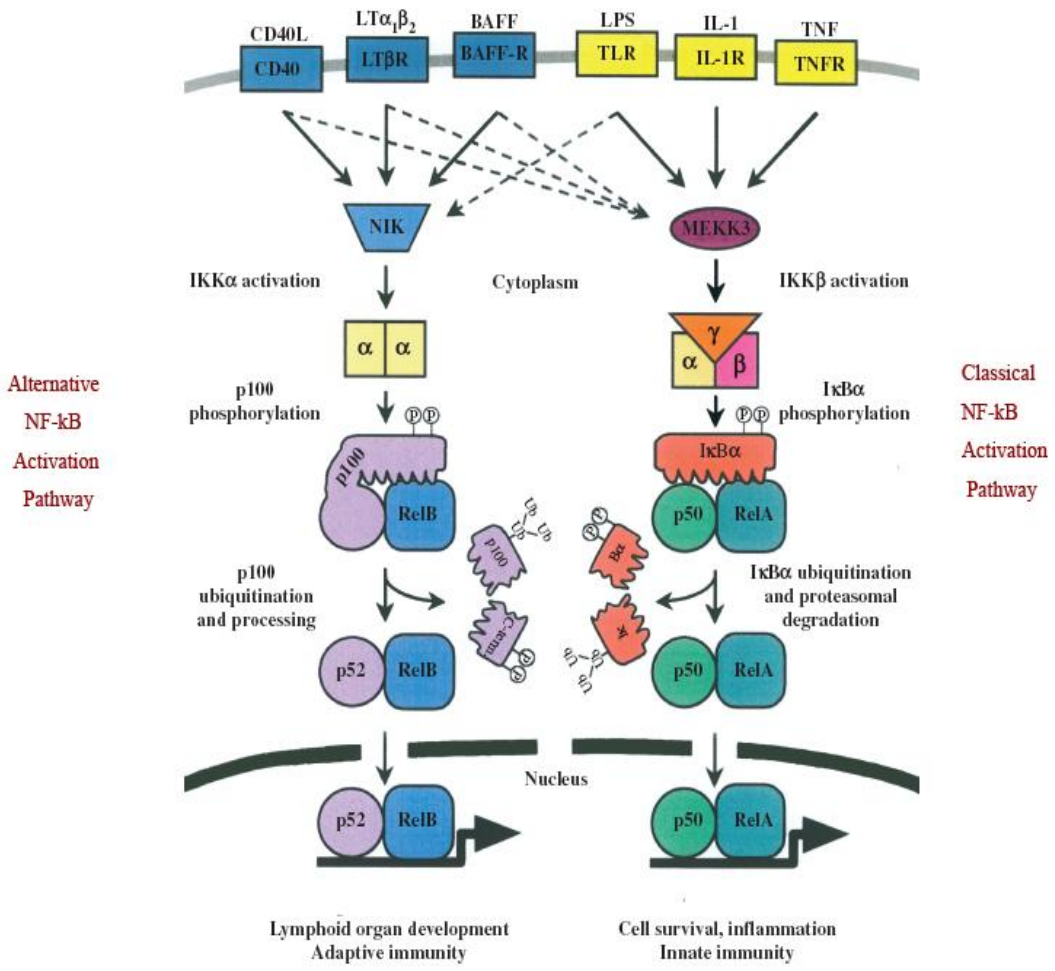

Figure 1-5 Activation of NF-κB by the alternative and the classical pathways.

Left: classical NF-κB pathway. In response to stimulation, the IKK complex comprising IKKα, IKKβ and IKKγ is activated and phosphorylates IκB, leading to IκB polyubiquitylation and degradation. Liberated from IκB, p50-RelA heterodimers can then translocate from the cytoplasm into the nucleus, triggering the transcription of a plethora of genes. Right: non-canonical pathway. In this pathway, NIK is activated upon ligand-receptor association, resulting in phosphorylation and activation of IKKα-IKKα complex. The activated IKKα complex in turn phosphorylates and subsequently induces proteasomal processing of the precursor protein p100 into a mature p52 subunit. P52-RelB heterodimers then translocate to nucleus and regulate a distinct class of genes.

Adapted from (Weih and Caamano, 2003)

1.5.2 MAPK

MAPK pathways exist in all eukaryotic cells, regulating cellular activities from proliferation, differentiation, development and transformation to apoptosis. There are 3 extensively studied groups of mammalian MAPKs including the extracellular signal-regulated kinase (ERK), JNK/SAPK and p38 MAPK. In general, ERK1 and ERK2 are activated in response to growth factors and phorbol esters and function in regulating meiosis, mitosis, and postmitotic processes in differentiated cells (Johnson and Lapadat, 2002). The JNK and p38 kinases are more responsive to stress stimuli such as cytokines, ultraviolet irradiation, heat shock, and osmotic shock and are involved in cell differentiation and apoptosis (Chen et al., 2001).

Each family of MAPKs is composed of a set of three evolutionarily conserved kinases, which are activated in series: a MAPK, a MAPKK (MAPK kinase) and a MAPKKK (MAPKK kinase). To date, at least 14 MAPKKKs, 7 MAPKKs, and 12 MAPKs have been identified in mammalian cells (Widmann et al., 1999). Stimuli from outside the cell initiate the cascade in which MAPKKK phosphorylates and activates a dual-specificity protein kinase (MAPKK) that, in turn, phosphorylates and activates a MAP kinase. MAPK cascade specificity is decided by the substrate selection. Through this way information is sent to the nucleus.

The schematic representation of MAPK pathway is presented in Figure 1-6.

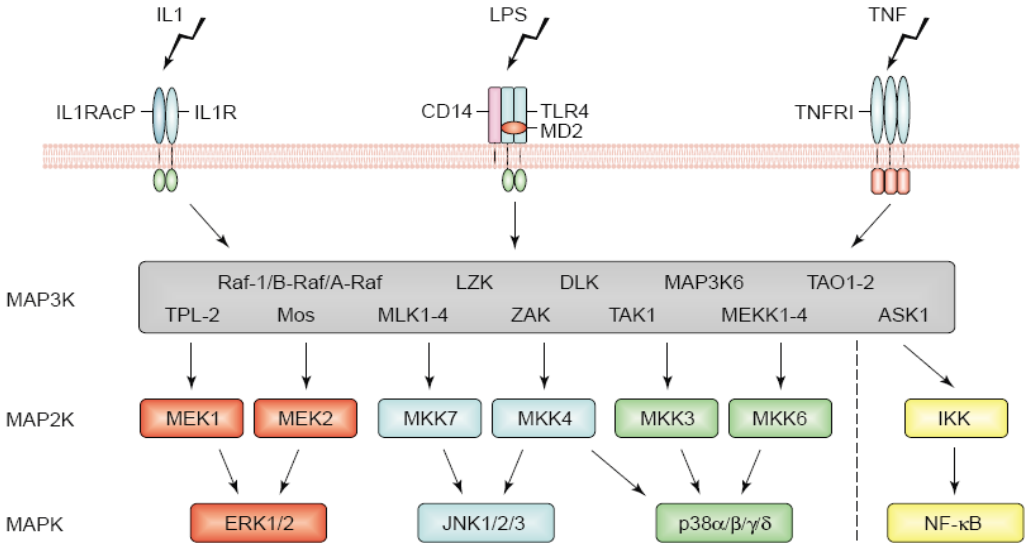

Figure 1-6 MAP kinase activation by innate immunoreceptors.

Stimuli from outside the cell initiate the cascade in which MAPKKK phosphorylates and activates a dual-specificity protein kinase (MAPKK) that, in turn, phosphorylates and activates a MAPK. MAPK cascade specificity is decided by the substrate selection. Through this way information is sent to the nucleus.

Adapted from (Symons et al., 2006)

1.5.3 IRFs

IRFs were originally characterised as transcriptional regulators of IFN, which are responsible for inducing transcription of antiviral genes and inhibiting viral replication (Mamane et al., 1999). There are nine members of the IRF family identified so far. All IRFs have a N-terminal DNA-binding domain, characterized by five tryptophan repeat elements located within the first 150aa of the protein, which mediates binding to specific promoter sequences in IFN-stimulated genes. IRF proteins interact with other family members or other factors through their C-terminal IRF-association domain (Honda et al., 2006). IRF3, IRF5 and IRF7 were reported to serve as direct transducers of virus-mediated signalling and play an essential role in the transcription of IFNα/β (Barnes et al., 2003). IRF3 and IRF-7 are involved in the TLR3/TLR4 pathways. TBK-1 and IKKε phosphorylate IRF3 and IRF7 on their c-

terminal, resulting in IRF homo- and hetero-dimerization, nuclear localization, and association with the co-activator CBP/p300 (Lin et al., 1999a).

1.6 The Pellino family

Pellino was first identified as a protein that interacts with Pelle, the *Drosophila* homologue of IRAK, in a yeast two-hybrid screen (Grosshans et al., 1999). There are four closely related mammalian isoforms described to date, named Pellino1, Pellino2, Pellino3 short and long (Rich et al., 2000; Resch et al., 2001; Jensen and Whitehead, 2003b). The protein sequences of the three mammalian Pellino proteins are highly conserved (Figure 1-). Pellino1 shares 82% amino acid sequence identity with Pellino2, whilst Pellino3 has 84-85% amino acid identity with Pellino1 and Pellino2, respectively (Jiang et al., 2003). The Pellino3 splice variants are 27aa and 25aa longer than Pellino1 and Pellino2 with an additional leader sequence respectively at their N terminus. Pellino3 long also has a 24aa insert at the N terminus compared with Pellino3 short (Jensen and Whitehead, 2003b). The Pellino proteins are also highly conserved among different species, hinting at an important function (Griffin et al., 2011; Haghayeghi et al., 2010).

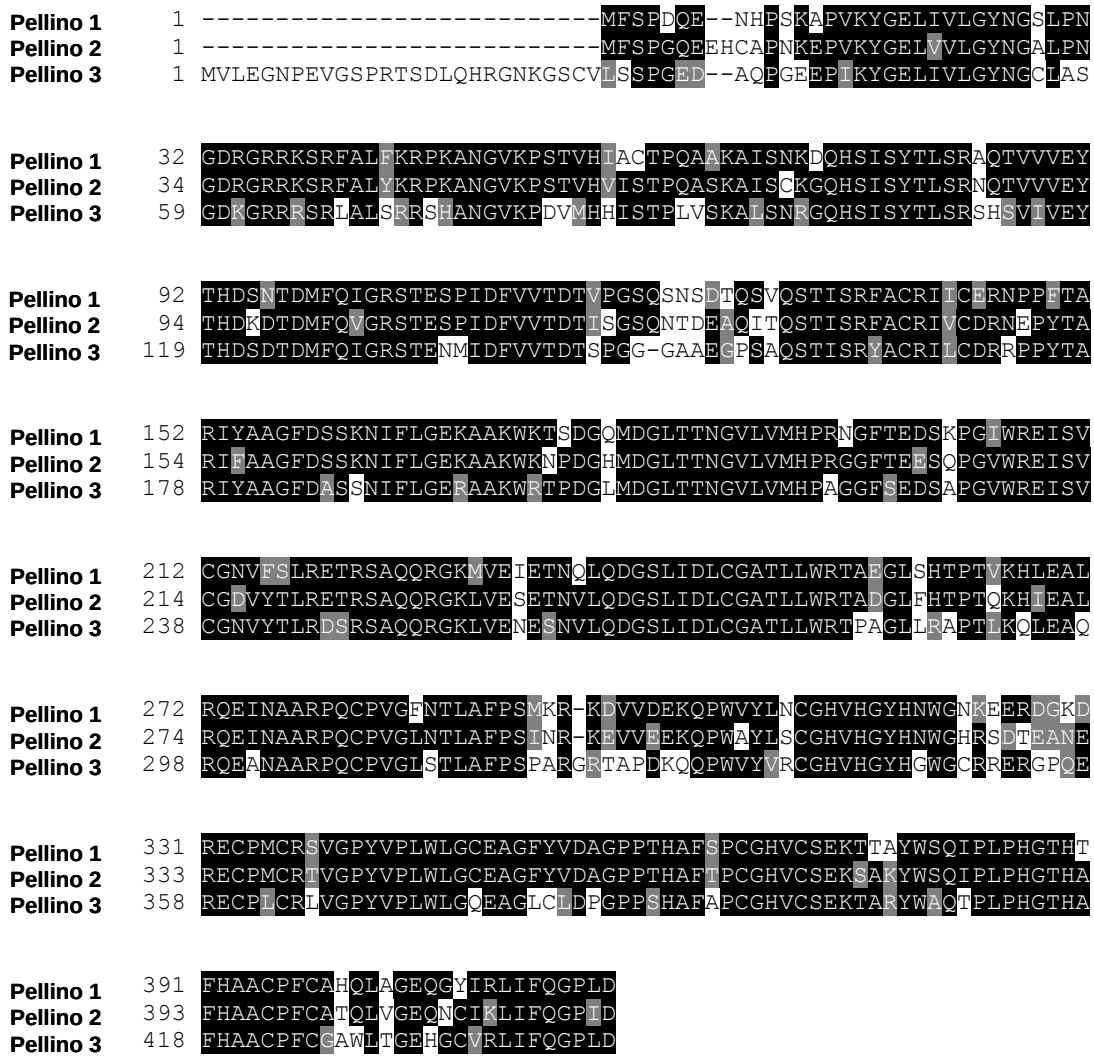

Figure 1-7 An alignment of the amino acid sequences of human Pellino1, 2 and 3

Sequence identity is represented by black shading and sequence similarity by grey shading.

All Pellino proteins contain a C-terminal really interesting new gene (RING)-like domain. The classical RING domain contains a Cys3HisCys4 amino acid motif, which can bind two zinc atoms, whilst the RING-like domain of the Pellino proteins is CysHisCys2CysHisCys2 (Ardley and Robinson, 2005). Many proteins containing a RING domain have an E3 ubiquitin ligase activity. Both recombinant and endogenous forms of Pellinos have been shown in *in vitro* ubiquitination assays to possess E3 ligase activity, which confers the ability of Pellinos to directly catalyse K63-linked polyubiquitination of IRAK (Ordureau et al., 2008). However, the RING domain of Pellino proteins is not required for IRAK1 binding (Lin et al., 2008). Intriguingly, IRAK-Pellino interactions also result in polyubiquitylation of the Pellino proteins, which subsequently trigger Pellinos degradation (Butler et al., 2007). Although Pellinos possess the ability to mediate K63-linked polyubiquitination, Pellino proteins, in an *in vitro* setting, can catalyse the formation of K48-linked polyubiquitin chains (Ordureau et al., 2008).

Furthermore, Lin, et al. resolved an X-ray structure of the N-terminal fragment of Pellino2, which lacks the RING-like domain (Lin et al., 2008). They found that the Pellino proteins contain a cryptic phospho-threonine-binding forkhead-associated (FHA) domain at their N-terminal region (Figure 1-8). The FHA domain is known as a modular phospho-serine/threonine recognition motif, through which Pellino proteins interact with phosphorylated IRAK1 (Lin et al., 2008). The FHA domain in Pellino proteins contains an appendage or wing composed of two inserts, which is different to the classical FHA domain (Figure 1-9) (Lin et al., 2008). Pellino proteins are phosphorylated when co-expressed with IRAK1 and this has also been confirmed in *in vitro* kinase assays (Schauvliege et al., 2006; Ordureau et al., 2008). However, a viral form of Pellino, which contains a FHA domain but lacks a complete and functional RING-like domain fails to post-translational modify IRAK1 (Griffin et al., 2011).

Thus, it seems that there is a bi-directional communication between IRAK and Pellinos. Phosphorylation of Pellino by IRAK1 leads to the activation of E3 ligase and the polyubiquitination of both IRAK1 and Pellino. Whilst the polyubiquitylation of Pellino proteins leads to their degradation, this is independent of the proteins RING domain (Butler et al., 2007; Smith et al., 2009). The K63-linked polyubiquitylation of IRAK is proposed to regulate several downstream pathways, such as NF-κB and MAPK cascades (Conze et al., 2008).

Figure 1-8 Structure–function characteristics of mammalian Pellino proteins.

Each Pellino protein has a C-terminal RING-like domain that confers E3 ubiquitin ligase activity and a phosphothreonine-binding FHA domain in its N terminus that might facilitate interaction with phosphorylated IRAK1. The C-terminal regions of Pellino proteins can also interact with TRAF6 and TAK1 and the formation of these complexes, together with Pellino-induced polyubiquitylation of IRAK1.

Adapted from (Moynagh, 2009).

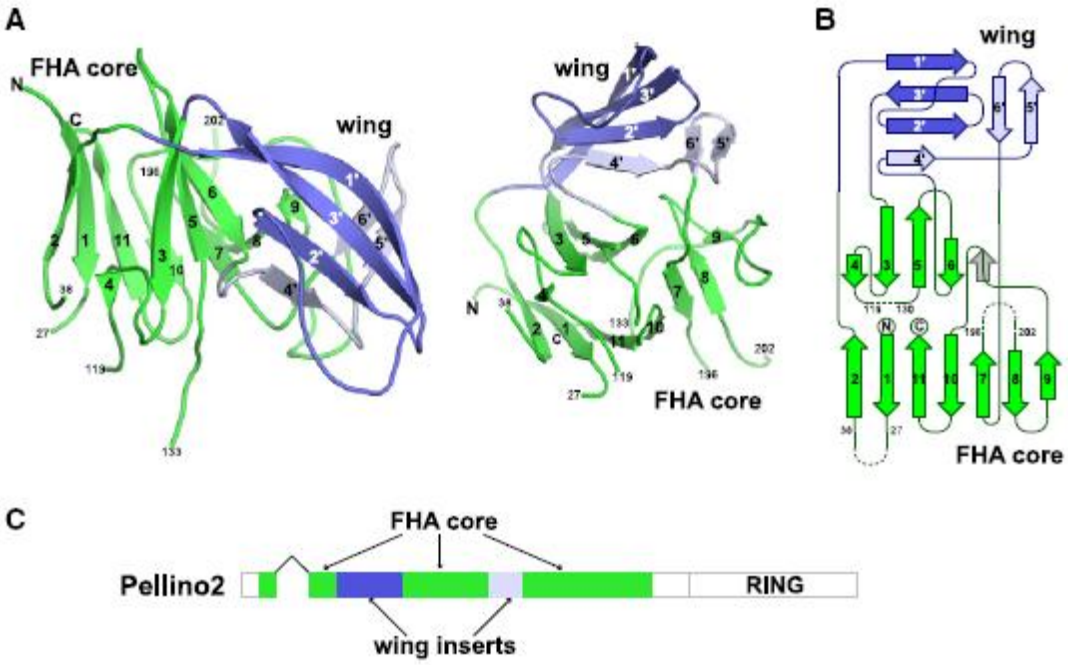

Figure 1-9 The IRAK1-binding region of Pellino2 is an FHA-like domain.

(A) Cartoon views of the Pellino2 structure with the FHA core in green and the non-canonical wing in blue (amino acids 51-98 and 159-184 in dark and light blue, respectively). b strands of the FHA core are numbered 1-11, while those of the wing are 10-60. The N- and C-termini are labeled, as are the amino acids numbers at the beginning and end of each missing loop. (B) Topology diagram of Pellino with the strands colored as in A. Missing loops are shown with dashed lines. The position of b9 in canonical FHA domains is shown in gray. (C) The domain architecture of Pellino2.

Adapted from (Lin et al., 2008)

1.6.1 Pellino1

On the basis of overexpression and RNAi studies, Pellino1 was shown to be involved in IL-1R and MyD88-dependent TLR signalling. Pellino1 was proposed to serve as a scaffolding protein, releasing IRAKs and TRAF6 from the IL-1R and subsequently allowing the protein to interact with TAK1/TAB1/TAB2 complex, and eventually resulting in the activation of NF-κB activation (Jiang et al., 2003). Pellino1 is also subject to regulation and has been shown to be modified by phosphorylation and

ubiquitination (Butler et al., 2007; Smith et al., 2009). Recently studies have also showed that Pellino1 was subject to small-ubiquitin-related-modifier (SUMO) modification (Kim et al., 2011). Furthermore, the inhibitory proteins Smad6 that negatively regulate TGF-β superfamily signalling, also targets Pellino1 and inhibits the formation of the Pellino1-IRAK4-IRAK1-TRAF6 complex. This mediates the inhibitory effects of TGF-β on the proinflammatory IL-1R signalling pathway (Choi et al., 2006). Whilst cell lines studies indicated a role for Pellino1 in IL-1R signalling the generation of Pellino1 knockout mice showed Pellino1 was dispensable for IL-1R signaling (Chang et al., 2009). Studies in Pellino1-deficient mice found that Pellino1 mediated IKK-NF-κB activation and regulated RIP1 ubiquitination in response to LPS and poly(I:C) stimulation. Also the serum concentration of proinflammatory cytokines such as TNF, IL-6, IL-12 was severely attenuated in Pellino1$^{-/-}$ mice after an intraperitoneal injection of LPS or poly(I:C) (Chang et al., 2009). Both transcription of the gene encoding Pellino1 and Pellino1 protein expression increased in response to the stimulation of LPS or poly(I:C) via a TRIF-dependent pathway. Such expression of Pellino1 was also subject to regulation by IKKε/TBK1 (Smith et al., 2011). These studies demonstrated that Pellino1 plays a non-redundant role as an E3 ubiquitin ligase in the TRIF-dependent TLR3 and TLR4 signalling pathway.

1.6.2 Pellino2

The functional role of Pellino2 in IL-1R or TLR signalling remains uncertain. Although overexpression of murine Pellino2 does not enhance the expression of NF-κB-regulated promoters gene, the reduction of Pellino2 expression levels inhibited IL-1 dependent activation of NF-κB-regulated promoters in a MEF cell line (Yu et al., 2002). However, human Pellino2 appears to have no effect on IL-1 or LPS induced NF-κB activation (Liu et al., 2004). Human Pellino2 has been identified as a substrate for IRAK1 and IRAK4. Pellino2 serves a similar function as Pellino1, in that it can

trigger and regulate the translocation of IRAKs from IRAK-TRAF6 complex to the TAK1/TAB1/TAB2 complex. Pellino2 has also been suggested to play a generic role in the transcription machinery (Strelow et al., 2003). Studies have also shown that Pellino2 can drive the activation of ERK1/2 and JNK pathway (Jensen and Whitehead, 2003a). Another study demonstrated that Pellino2 can interact with Bcl10, an intracellular activator (Liu et al., 2004). Bcl10, as a binding partner of Pellino2, is recruited to TLR4 and activates NF-κB in response to LPS. Suppressor of cytokine signalling 3 (SOCS3) blocks the interaction between Bcl10 and Pellino2 and inhibits the downstream activation of NF-κB (Liu et al., 2004). Pellino2 was also identified as one of three genes, Pellino2, IL-8 and ubiquitin-conjugating enzyme E2-UBE2V1, with significantly increased expression between chronic allograft nephropathy and vascular acute rejection using a microarray analysis of 128 genes involved in TLR signaling (Nogueira et al., 2009).

1.6.3 Pellino3

Pellino3 mRNA is expressed in most tissues, whilst the highest expression levels are observed in brain, heart and testis (Jensen and Whitehead, 2003b). Pellino3 proteins can directly interact with IRAK1, TRAF6, TAK1 and NIK (Jensen and Whitehead, 2003b). Although Jensen et al. showed that the overexpression of Pellino3 promoted the activation of JNK and ERK MAPK pathways; Xiao et al. found that the knockdown of the endogenous expression of Pellino3, induced JNK activation in response to IL-1 stimulation (Xiao et al., 2008). In contrast to Pellino1 and Pellino2 that are ineffective in promoting the activation of p38 MAPK, Pellino3 activates this pathway (Butler et al., 2005). Both TRAF6 and TAK1 are key downstream mediators of Pellino3, as p38 MAPK is not activated when co-expressed with their dominant negative counterparts. Also the binding sites for TRAF6 and TAK1 are located at the C-terminus of Pellino3. Pellino3 promotes the activation of MAPK-activated protein

kinase2, which is a p38 substrate, and activates the transcription factor cAMP response element-binding protein (CREB) in a p38 MAPK-dependent manner. Tyrosine residue 44 in Pellino3 is an important functional site for triggering the activation of the p38 MAPK pathway. Although this residue is conserved in all members, it is only required for the interaction between Pellino3 with IRAK1 (Butler et al., 2005).

A recent report has proposed that in response to IL-1, Pellino3 promotes a K63-linked polyubiquitylation of IRAK1, which competes with K48-linked polyubiquitylation at the same Lys134 reside on IRAK1 (Lin et al., 2008). Therefore, it was proposed that Pellino3 inhibits IL-1-induced activation of NF-κB by blocking the degradation of IRAK. However, the role of K48-linked polyubiquitylation in IRAK degradation has been debated, since IL-1-induced degradation of IRAK1 was not blocked by inhibition of the proteolytic activity of the proteasome (Windheim et al., 2008).

Although the exact mechanism underlying the inhibitory effects of Pellino3 on the NF-κB pathway is not completely understood, the proposed negative regulatory role for Pellino3 is still interesting and suggests it as an important regulator in TLR and IL-1R signalling pathways.

To date studies on the role of the Pellino family in innate immunity have been mostly confined to IL1 and TLR pathways with relatively little information available on their role in the TNF pathway. This study addresses this deficit by investigating the role of Pellino3 as a regulator of the TNF signalling pathway.

1.7 Project aims

The specific aims of this project were to:

- probe the role of Pellino3 in TNF-induced cell death
- determine the importance of Pellino3 in regulation of NF-κB and MAPK activation in response to TNF
- define the influence of Pellino3 on TNF-induced formation of DISC
- identify Pellino3-interacting proteins in the TNF pathway
- define the physiological role of Pellino3 in the TNF pathway

CHAPTER TWO: MATERIALS AND METHODS

2.1 MATERIALS

2.1.1 Reagents

Reagents	**Supplier**
Agar	Sigma
Agarose	Promega
Agarose, low melting point	Sigma
Ampicillin	Sigma
APS	Sigma
Bovine serum albumin (BSA)	Sigma
Bradford reagent dye	Bio-Rad
Bromophenol blue	Sigma
Chloroform	Sigma
Clonables™ 2X Ligation Premix	Merck
Coomassie Blue (G250)	Sigma
Cycloheximide (CHX)	Sigma
DAB (3,3'-Diaminobenzidine)	Vector Labs
DAPI (4',6-Diamidino-2-Phenylindole)	Sigma
DEPC (diethylpyrocarbonate)-treated water	Ambion
D-galactosamine (D-Gal)	Sigma
DMEM (Dulbecco's Modified Eagle's medium)	Invitrogen
DMSO (dimethyl sulfoxid)	Sigma
DNA ladder & Loading dye	Promega
dNTPs (deoxyribonucleotide triphosphates)	Promega
DTT (dithiothreitol)	Sigma
E.coli - TOP10 competent cells	Invitrogen
EDTA (ethylenedia~nine tetra-acetic acid)	Sigma
Ethanol	Sigma
Ethidium bromide	Sigma

FBS (fetal bovine serum)	Invitrogen
Formalin solution	Sigma
Glacial acetic acid	Merck
Glycerol	Sigma
Glycine	Sigma
GoTaq® Green Master Mix	Promega
HEPE (hydroxyeicosapentaenoic acid)	Sigma
Hoechst 33342	Sigma
hydrochloric acid (HCl)	Merck
Hydrogen peroxide solution (H_2O_2)	Sigma
Igepal	Sigma
Imidazole	Sigma
Isopropanol	Sigma
IPTG (isopropyl β-D-1 thiogalactopyranoside)	Sigma
Kanamycin	Sigma
Lipofectamine 2000	Invitrogen
Lysogeny broth (LB)	Sigma
Magnesium Chloride	Sigma
Methanol	BDH
Microlon 96-well plates	Greiner
MTT (3-(4,5-dimethylthiazol-2-yl)-2,5-diphenyltetrazolium bromide)	Protech
Ni-NTA (nickel-nitrilotriacetic acid) Resin	Qiagen
NF-κB IRDye Labelled Oligonucleotides	Licor Biosciences
OptiMEM	Invitrogen
PBS (Phosphate buffered saline)	Oxoid
Penicillin / Streptomycin / Glutamine	Invitrogen
PMSF (phenylmethylsulfonyl fluoride)	Sigma
Polybrene	Sigma
Prestained molecular weight marker	Invitrogen
Protease inhibitor mixture	Roche
Protease inhibitor mixture (EDTA free)	Roche
Protein A/G-agarose	Santa Cruz
Protogel	National Diagnostics

Puromycin	Sigma
Random primers	Invitrogen
Restriction enzymes	NewEngland
RNase Zap	Ambion
SDS (sodium dodecyl sulphate)	Sigma
siRNA Pellino3 specific	Ambion
siRNA Lamin a/c	Ambion
Skim milk powder	Sigma
Sodium chloride (NaCl)	Sigma
Sodium hydroxide (NaOH)	Sigma
Sodium orthovanadate (Na_3VO_4)	Sigma
Sodium Phosphate (Na_3PO_4)	Sigma
Sulphuric acid (H_2SO_4)	Sigma
Synthetic oligonucleotides	MWG Biotech
Taq polymerase	Invitrogen
TEMED (N, N, N′, N′-tetramethylethylenediamine)	Sigma
TMB (3, 3', 5, 5'-Tetramethylbenzidine liquid substrate)	Sigma
TNFα	R&D Systems
Tris-base	Sigma
Tris-HCl	Sigma
Trypsin/EDTA	Invitrogen
Tween-20	Sigma
Z-VAD-FMK (benzyloxycarbonyl-valine-alanine-aspartate-fluoromethyl ketone)	Promega.

2.1.2 Kits

Kits	**Supplier**
EMSA (Electophoretic Mobility Shift Assay) Buffer Kit	Licor Biosciences
DeadEnd™ Fluorometric TUNEL System	Promega
GC-RICH PCR system	Roche
M-MLV RT (Reverse Transcriptase) 1st-Strand cDNA Synthesis Kit	Promega
Mouse IL-10 ELISA (Enzyme-Linked Immunosorbent Assay) kit	R&D Systems

Mouse Rantes ELISA kit	R&D Systems
Mouse TNFα ELISA kit	Protech
Plasmid Plus Midi Kit	Qiagen
Plasmid Mini Kit	Qiagen
Qiaquick PCR Purification Kit	Qiagen
Vectastain ABC kit	Vector Laboratories

2.1.3 Antibodies

Antibodies	**Supplier**
β-actin	Sigma
Bcl-x	Cell Signalling
ERK	Cell Signalling
FLAG M2	Sigma
His-HRP (horseradish peroxidase)	Sigma
HA-Tag (6E2)	Cell Signalling
IκB-α	Santa Cruz
JNK	Cell Signalling
Myc-Tag (9B11)	Cell Signalling
P38	Cell Signalling
Pellino3	Santa Cruz
Phosho-ERK	Cell Signalling
Phosho-IκB-α	Cell Signalling
Phosho-JNK	Cell Signalling
Phosho- p38	Cell Signalling
RIP1	Transduction Labs
cleaved caspase-8	Cell Signalling
FADD	ENZO
PARP (Poly-ADP-ribose- polymerase)	Cell Signalling
IKK-β	Cell Signalling
caspase-8	Santa Cruz
cleaved caspase-3	Cell Signalling
Phospho-IKK-α/β	Cell Signalling
Secondary Antibodies：	Supplier
Anti-mouse / rabbit-HRP	Cell Signalling

IRDye 800CW Goat Anti-Rabbit	Licor Biosciences
IRDye 680 Goat Anti-Mouse	Licor Biosciences
IRDye 800CW Donkey Anti-goat	Rockland

2.1.4 Buffers

Buffer	**Composition**
PBS	2.7mM KCl, 1.5mM KH_2PO_4, 137mM NaCl, 8mM Na_2HPO_4, pH 7.4
TBS (Tris buffered saline)	25mM Tris, pH7.4, containing 0.14M NaCl.
Blocking Buffer	1X TBS, 0.1% (v/v) Tween-20 with 5 % w/v nonfat dry milk or 5% w/v BSA
Cell lysis Buffer	20 mM Tris-HCl, pH 7.4, 150 mM NaCl, 0.2% (v/v) Igepal, 10% (w/v) glycerol, 50 mM NaF,1 mM Na_3VO_4, 1 mM DTT, 1 mM PMSF, complete protease inhibitor cocktail (Roche, mini)
EMSA Buffer-A	10 mM HEPES pH 7.9, 10 mM KCl, 1.5 mM $MgCl_2$, shortly before use add: 0.5 mM DTT and 0.5 mM PMSF
EMSA Buffer-C	20 mM HEPES pH 7.9, 420 mM NaCl, 1.5 mM $MgCl_2$, 0.2 mM EDTA, 25% (w/v) glycerol shortly before use add: 0.5 mM PMSF
EMSA Buffer-D	10 mM HEPES pH 7.9, 50 mM KCl, 0.2 mM EDTA, 20% (w/v) glycerol, shortly before use add: 0.5 mM PMSF and 0.5 mM DTT
In Vitro Binding Buffer	20 mM Tris-HCl, pH 7.4, 150 mM NaCl, 0.2% (v/v) Igepal, 10% (w/v) glycerol and complete protease inhibitor cocktail
Laemmli sample buffer (1x Concentrations)	62.5 mM Tris-HCl, pH 6.8, 10% (w/v) glycerol, 2% (w/v) SDS, 0.7 M β-mercaptoethanol , 0.001% (w/v) bromophenol blue
Qiagen native lysis buffer	50 mM $NaH_2PO_4.H_2O$, 300 mM NaCl 10 mM Imidazole, 10mM β-mercaptoethanol

Qiagen native wash Buffer	50 mM $NaH_2PO_4.H_2O$, 300 mM NaCl, 20 mM Imidazole
Qiagen native elution Buffer	37.5 mM NaH_2PO_4, 225mM NaCl, 250 mM Imidazole
SDS running Buffer	25 mM Tris, 192 mM glycine, 0.1% SDS.
SOC medium	2% peptone, 0.5% Yeast extract, 10mM NaCl,
(Super Optimal broth with	2.5mM KCl, 10mM $MgCl_2$, 10mM $MgSO_4$,
Catabolic Repressor medium)	20 mM Glucose
Reagent diluent for ELISA	0.1% (w/v) BSA, 0.05% (v/v) Tween in TBS
Transfer Buffer	25 mM Tris, 192 mM glycine, 20% methanol
TAE (Tris-acetate-EDTA) Buffer	40 mM Tris base, 0.1% (v/v) glacial acetic acid, 1 mM EDTA
TBE	89 mM Tris Base,89 mM Boric Acid,
(Tris-Borate-EDTA) Buffer	2 mM EDTA
TE (Tris-EDTA) buffer	10 mM Tris-HCl, 1 mM EDTA pH 8.0,

2.1.5 Cells

Cells	**Description**
HEK293T	Human embryonic kidney cells
Hela	Human epithelial carcinoma cell line
U373-MG	Human glioblastoma-astrocytoma, epithelial-like cell line
1321N1	Human astrocytoma cell line

2.1.6 Vectors

Vector	**Supplier**
pET-30a (+)	Novagen
pRSETA	Invitrogen
PCMV-HA	Clotech
pcDNA4	Invitrogen
pMSCV (murine stem cell virus)	Clotech

Vector maps of all plasmids are listed in Appendix I.

2.1.7 Animals

Pellino3 deficient mice and their wild-type littermates were bred at the animal facility at the Immunology Institute, National University of Ireland Maynooth. Genotyping was performed by PCR analysis of genomic DNA from ear punches as described in 2.2.1 and genotypes were reconfirmed after the completion of experiments. The mice were housed in standard rodent cages, enriched with cardboard housing and nesting material. The animals were kept at room temperature (22 – 24°C) in a 12hr light/dark cycle (lights on at 8:00 a.m.) with *ad libitum* access to food and water. All mice were used under the guidelines of the Irish Department of Health, and all procedures were approved by the research ethics committee of the National University of Ireland Maynooth.

2.1.8 Gifts

Cell lines:

HEK293T cells - Prof. Douglas T. Golenbock (The University of Massachusetts Medical School, Worcestor, Massachusetts 01605, USA).

Constructs:

Pellino3s-flag was from Xiaoxia Li (Cleveland Clinic).

Myc-RIP1 was from Xin Lin (University of Texas, M.D. Anderson Cancer Center).

HA-RIP1 and CrmA were from JinWoo Kim (Korea Advanced Institute of Science and Technology).

Caspase-8 (C360/A)-myc and FADD-flag were from A. Thorburn (University of Colorado at Denver and Health Sciences Center)

2.2 METHODS

2.2.1 Molecular biological methods

2.2.1.1 Propagation of DNA

2.2.1.1.1 Preparation of DNA from *E. coli*

TOP10 chemically competent *E.coli* was used for propagation of plasmids and for the cloning of ligation reaction products. 100-400ng of plasmid or a ligation reaction product was added to 5µl or 25µl of TOP10 cells, respectively. BL21 competent *E.coli* was used for recombinant protein expression. DNA and the cells were mixed gently with a pipette and incubated on ice for 30min. The plasmids were allowed to enter the bacterial cells by heat shocking the mixture at 42ºC for 1 min. The cells become permeable to allow easy entry of the plasmid and cooling on ice for 2 min makes the cells once again impermeable. The transformed cells were then incubated in 150µl SOC medium at 37ºC on a Exceller E25 shaker at 220 rpm for 1hr. The mix was then plated out on LB agar plates (LB broth with 1.5% (w/v) agar) containing 100µg/ml ampicillin or kanamycin antibiotics. Plates were inverted and incubated overnight at 37ºC. Plates were then stored at 4ºC for up to four weeks.

2.2.1.1.1.1 Small scale preparation of DNA from *E. coli*

2ml LB broth containing ampicillin (50µg/ml) was inoculated with a single transformed *E. coli* colony from an agar plate. The culture was incubated overnight at 37ºC with constant shaking at 220 rpm. Small plasmid preparations were made using the Qiaprep Spin Miniprep kit from Qiagen Inc. The bacterial cells were centrifuged at 7,500 g for 3min and the supernatant was discarded and the plasmid DNA was extracted as outlined in the manufacturer's handbook. DNA was quantified using a Cary spectrophotometer. After diluting the DNA appropriately in TE buffer, the absorbance of the solution was measured at 260nm and 280nm. All samples used had an optical density OD_{260}/OD_{280} ratio in the range of 1.7 to 1.9. Ratios below 1.7 or above 1.9 indicated RNA or protein contamination, respectively. The concentration was calculated according to the following relation: OD_{260}=1 corresponds to 50µg/ml of DNA.

2.2.1.1.1.2 Large-scale preparation of DNA from *E. coli*

A starter culture of LB broth (2ml) containing ampicillin (50µg/ml) was inoculated with a single transformed *E.coli* colony and incubated at 37ºC with shaking at 220 rpm for 6-8 hr. This was then added to a larger volume of LB broth (100ml) containing the relevant antibiotic and incubated at 37ºC overnight with shaking at 220 rpm. Large plasmid preparations were made using the Qiagen high-speed plasmid midi kit from Qiagen. The bacterial cells were centrifuged at 3,000 g for 25 min and the supernatant was discarded and the plasmid DNA was extracted as outlined in the manufacturer's handbook. DNA was quantified as outlined in Section 2.2.1.1.2.1.

2.2.1.1.2 Genomic DNA Extraction

Three week old mice were ear-punched and the tissue placed in sterile tubes.70-100µl DirectPCR Lysis Reagent (Tail) (Viagen Biotech) containing freshly prepared 0.2~0.4 mg/ml Proteinase K was added to the 1.5ml tubes holding the ear punch samples. The tubes were incubated at 55°C for 3hr or until no tissue clumps were observed. Crude lysates were incubated at 85°C for 45 min. Lysates were stored at -20ºC.

2.2.1.2 Isolation of RNA and cDNA Synthesis

2.2.1.2.1 Isolation of total RNA

In order to minimise RNA degradation, a number of precautions were taken throughout the following procedures. All water and salt-based solutions were treated with DEPC (0.2%v/v) and then autoclaved. All plasticware was certified RNase-free. Before commencing, equipment was wiped with "RNase Zap" an RNase decontamination solution. Gloves were worn at all times and regularly changed.

To confirm the suppression of endogenous expression of Pellino 3, cells were seeded at 2 x 10^5 cells/ml in 6-well plates (3ml DMEM/well). Total RNA was extracted from cells using Trizol Reagent as per manufacturer's instructions. The amount of isolated RNA was quantified by measuring the absorbance at wavelengths of 260 nm and 280 nm on a spectrophotometer, where an absorbance of 1 unit at 260 nm is ~ 40µg/ml. Pure RNA preparations have an OD_{260}/OD_{280} ration of 1.6-1.8. Extracted RNA was stored at -80ºC.

2.2.1.2.2 Synthesis of first strand cDNA from messenger RNA (mRNA)

The M-MLV RT 1st-Strand cDNA Synthesis Kit is used for generating full-length first-strand cDNA from total cellular RNA. 1µg of RNA was placed in nuclease-free microcentrifuge tubes and incubated for 10 min at 70ºC. The mixture was then chilled on ice and centrifuged briefly. The following components were then added:

M-MLV RT (200U/µl)	0.1µl
dNTPs (10mM)	1µl
5 x M-MLV Buffer	2µl
$MgCl_2$ (25mM)	2µl
RNasin (40U/µl)	0.25µl
Random Primers (0.5µg/µl)	1µl
Nuclease-Free Water	to 10µl

The reaction mixture was incubated for 10 min at RT allowing the primers to anneal to the RNA. Next, the reaction was incubated at 42°C for 30 min. M-MLV RT was then deactivated by heating to 95^{o}C for 5 min followed by cooling to 4^{o}C for 5 min. Generated cDNA was stored at 4ºC for short-term storage or -20^{o}C for long-term storage.

2.2.1.3 Expression plasmid construction

2.2.1.3.1 PCR Amplification

PCR products were amplified using either cDNA or plasmid DNA as template. The primers were designed based on deposited GenBank sequences. Each forward and reverse primer contained a restriction site, thereby flanking the gene. Proteins were tagged at either the amino- or carboxy-terminus by incorporating the appropriate epitope tag sequence into the forward or reverse primer, respectively (see Appendix I Table I for details of primer sequences, restriction sites used). The GC-RICH PCR System, which contains a mixture of Taq polymerase and Tgo proofreading polymerase, was used for the amplification of PCR products. The standard PCR conditions below were used to amplify the target sequence:

Template (50ng plasmid DNA)	2µl
5X Enzyme Buffer	10µl
GC-Rich Resolution Solution	2.5µl
$MgCl_2$	5µl
Primers (10pmol/µl)	2.5µl each
dNTP mix (10mM each)	4µl
Enzyme mix	1µl
PCR-grade water	to 50µl

Each reaction was initially heated to 94ºC for 5 min. This was followed by 35 cycles of 94ºC for 30 s, 52ºC for 30 s, and 72ºC for 2 min. Samples were then incubated at 72ºC for 10 min and stored at 4ºC if necessary.

2.2.1.3.2 Agarose gel electrophoresis

Agarose gels were prepared by suspending agarose in TAE. This was heated in a microwave until the agarose had completely dissolved, and was then cooled to less than 50ºC. Ethidium bromide (5µg/ml) was added and the agarose poured into the gel tray. Following solidification, agarose gels were covered and electrophoresed in TAE (1X). Samples were mixed with loading dye. Samples were run simultaneously with molecular size markers, with the range of ladder chosen to suit the particular sample size. The voltage at which gels were run depended on the particular application. Nucleic acids were visualised under ultraviolet (UV) light (254nm) and images acquired using the Syngene G box gel documentation system (Frederick, MD, USA).

2.2.1.3.3 Preparation of insert and vector DNA

PCR product was electrophoresed on a 1% low melting TAE agarose gel at 100V for 1h. The gel was placed on an UV transilluminator box and the DNA band of correct size was excised using a scalpel, and placed in a 1.5ml microcentrifuge tube. DNA was extracted from the gel using the QIAquick Gel Extraction Kit, according to the manufacturer's instructions. DNA was eluted in a volume of 40µl and constituted insert for the following cloning procedure.

Both insert DNA and vector were digested overnight at 37ºC with 30U each of the required restriction enzymes, using recommended reaction buffers. DNA was

electrophoresed in a 1% TAE agarose gel, before excision and gel purification using the QIAquick Gel Extraction Kit.

Both insert and vector DNA was electrophoresed in a 1%TAE agarose gel alongside a quanti-ladder in order to gauge the concentration of insert and vector for subsequent ligation reactions.

2.2.1.3.4 Ligation of insert and vector

A ligation reaction was performed with the ratio of insert to vector determined by their concentration and size. 100ng of vector was used and the amount of insert required was calculated as follows:

$$\frac{\text{Quantity of Vector (100ng)} \times \text{Size of Insert} \times 3}{\text{Size of Vector}} = \text{ng Insert}$$

Each ligation reaction consisted of vector DNA, insert DNA, Clonables™ 2X Ligation Premix, and the total volume (5µl) was made up. The reaction was incubated at 16ºC for 20 min. The ligation reaction mix was then used to transform competent *E.coli* cells. Plasmid DNA was then purified from colonies and sequenced by MWG Biotech to confirm the fidelity of PCR amplification and the correct insertion of DNA insert into the vector.

2.2.1.4 PCR-based genotyping

PCR amplification was performed on genomic DNA using GotoTaq DNA polymerase and specific primers to detect heterozygous/homozygous conventional alleles:
2092_25: CCCAACATAGGTGTTTCCTCTCC -
2092_29: GTGCATACACATTCATGCAAGC -
2091_27: GACACGTGTGGAGATAATGAGG -
2091_28: ACCCAGGCACAAGTCAAGC -
control primers:
1260_1: GAGACTCTGGCTACTCATCC -
1260_2: CCTTCAGCAAGAGCTGGGGAC -

Cre transgene Primers:

1011_1: Cre_tot1_ACGACCAAGTGACAGCAATG -

1011_2: Cre_tot2_CTCGACCAGTTTAGTTACCC -

Reaction:

Template	2µl
5 xBuffer	5µl
$MgCl_2$	2µl
Primers (10pmol/µl)	2.5µl each
dNTP mix (10mM each)	1µl
GotoTaq	0.15µl
PCR-grade water	to 25µl

For each target the samples were initially heated to 94°C for 5 min. This was followed by 35 cycles at 95°C for 30s, at 60°C for 30s and at 72°C for 1 min. Samples were then incubated at 72°C for 10 min and stored at 4°C. The PCR products were subjected to electrophoresis on a 2% (w/v) TAE agarose gel, containing 5µg/ml ethidium bromide.

2.2.1.5 Real time PCR

Reverse Transcription was carried out as described in section 2.2.1.2. Primer sequences used to amplify the fragments of the indicated genes are described in the Appendix I Table II.

A 20µl real-time PCR reaction mixture was prepared in each optical tube as following:

Template (50ng plasmid DNA)	2µl
Master Mix (2x)	10µl
Primers (10pmol/µl)	1µl each
PCR-grade water	to 20µl

For each target the samples were initially heated to 95°C for 15 min for predenaturation. This was followed by 40 cycles at 95°C for 30s, at 60°C for 30s and at 72°C for 30s. Integration of the fluorescent SYBR Green into the PCR product was monitored after each annealing step. Amplification of one specific product was confirmed by melt curve analysis where a single melting peak eliminated the possibility of primer-dimer association. For melting curve analysis to be performed the products were heated from

60°C to 95°C after the 40 cycles. The PCR were conducted in a Bio-Rad ICycler real-time PCR instrument. The relative quantification of target genes expression was evaluated using the ΔΔCT method. Crossing Threshold (Oshima et al.), which recorded the cycle when sample fluorescence exceeds a chosen threshold above background fluorescence, was generated by Bio-Rad ICycler software. The ΔCT value was determined by subtracting the HPRT CT value for each sample from the target CT value. Fold change in the relative gene expression of target were determined by calculating the $2^{-\Delta CT}$.

2.2.2 Cell Biological Methods

2.2.2.1 Cell Lines

Hela, HEK293T, U373 and 1321N1 cells were cultured in Dulbecco's modified Eagle's medium supplemented with 10% (v/v) fetal bovine serum, 100μg/ml penicillin G, and 100μg/ml streptomycin. Cells were maintained at 37°C in a humidified atmosphere of 5% CO_2. Cells were passaged every 2 to 3 days using 1% (w/v) Trypsin/EDTA solution in PBS.

2.2.2.2 MEF cells

For the preparation of primary MEFs, Pellino3$^{+/-}$ mice were intercrossed to produce Pellino3$^{+/+}$ and Pellino3$^{-/-}$ embryos. Mouse breeder pairs were set up in the afternoon with one male being set up with two or three virgin 7-8 week old females. Females were checked for copulatory plugs the following morning. If present, this was marked as day +0.5 (or rounded off to day +1). Females, with copulatory plugs, were removed from the male's breeder cages. The remaining females were checked on a daily basis.

E13.5-timed pregnant mice were euthanized according to standard protocols. The uterus (containing the embryos) was cut free from the mouse and placed in a sterile petri dish. Embryos were removed from the uterus one at a time in sterile PBS under sterile conditions in a laminar flow hood. The head and all of the soft tissues from each embryo were removed under a dissecting scope so that only the carcasses were left. Embryo carcasses were minced using small scissors, and then washed with 2-3 times with PBS 2-3 in 15ml conical tubes. Enough trypsin-EDTA solution was added to just

cover each minced carcass. The mixture was then incubated at 37ºC for 15 min. MEF media (10ml) was then added to the conical tubes. The tissue was dissociated into single cells by vigorous pipetting. The digested tissue was passed through a 70µM cell strainer to get rid of un-dissociated tissue clumps. The cells that flowed through the cell strainer were washed once with fresh MEF media, and cells from each embryo were plated to individual 175cm^2 flasks. MEF cells were passaged every 3-4 days or until they were confluent. DNA samples were collected from discarded head or soft tissue for genotyping. It was necessary to dilute the DNA because of the large amount of DNA and the possibility of maternal blood contamination.

2.2.2.3 Transient Transfection

2.2.2.3.1 Transfection of cells for overexpression studies

Cells were seeded at 2x10^5 cells/ml in 6-well plates (3ml DMEM/well). Cells were grown for 24 hr to approximately 70% confluency. For each well of a 6-well plate to be transfected, DNA (amount depending on individual assays as outlined in relevant sections) was diluted in 250µl OptiMEM and mixed gently. 4µl Lipofectamine 2000 was then diluted in 250µl OptiMEM and incubated at room temperature. After 5 min incubation, the diluted DNA was combined with the diluted Lipofectamine 2000, mixed gently, and incubated at room temperature for 20 min. 1ml of medium was removed from each well before adding the DNA-Lipofectamine complexes (500µl).

2.2.2.3.2 Transfection of cells for Knockdown studies

Pellino3-specific siRNA (Sense: 5'-GCACAGCAUCUCGUAUACATT-3'; Antisense: 5'-UGUAUACGAGAUGCUGUGCTG3-') was from Ambion and cells were transfected by Lipfectamine2000 (see section 2.2.2.3) and allowed recover for 48 hr prior to experiments.

2.2.2.4 Lentiviral ShRNA Infection

2.2.2.4.1 Lentiviral production

HEK293T cells were seeded at 2x10^5 cells/ml in 6-well plates (3 ml /well) and grown for 24 hr to approximately 70% confluency. The cells were transfected as described in section 2.2.2.3.1 with a DNA mixture containing packaging plasmid dR89.1 (900ng),

envelope plasmid VSV-G (100ng) and Pellino3-shRNA (1µg). The human Pellino3 shRNA had the following sequence:.

5'GCACTTGCTGATAGCCACTATCCGGGCACTTGCTGATAGCCACTATCTCGA GATAGTGGCTATCAGCAAGTGCTTTTTTG. -3'

A control shRNA was also used in the transfection. It was a non-targeting shRNA vector that can activate the RNA-induced silencing complex and the RNAi pathway, but does not target any human or mouse genes. To remove the transfection reagent, the media was changed 24 hr post-transfection and replaced with fresh high serum (30%) growth media. The cells were then incubated for 24 hr. The media containing lentivirus were harvested 48h post-transfection and transferred to a polypropylene tube for storage at -20°C. The media was replaced with fresh high serum (30%) growth media and the cells were incubated for further 24 hr. The virus was harvested one more time and after the final harvest the packaging cells were discarded.

2.2.2.4.2 Lentiviral infection

Hela, HEK293T, U373 and 1321N1 cells were seeded at $2x10^5$ cells/ml in 6-well plates (3ml/well medium). The cells were left to recover for a few hours and then infected with 600µl of virus-containing conditioned media. Polybrene (8µg/ml) was added to improve transduction efficiency. The plates were incubated at 37ºC. The media was removed 24 hr post-infection and replaced with fresh growth media containing puromycin (10µg/ml) to select for cells transduced with shRNA. The polyclonal population of cells were cultured for one week before suppression of Pellino3 expression was determined. The knockdown efficiency was assessed by immunoblotting of whole cell lysates.

2.2.2.5 Retroviral rescue assay

MSCV plasmid or MSCV-mPellino3 (mP3), MSCV-mP3FHAm or MSCV-mP3Em (1µg) were co-transfected with the packaging vector φ (1µg) into 293T cells. After 48 hr, the retrovirus-containing medium was harvested and used to infect Pellino3-deficient MEFs in 25 cm^2 flasks. The flasks were incubated at 37°C for 48 hr prior to experiments.

2.2.2.6 TUNEL staining and confocal microscopy

Transfected cells were treated as indicated in Figures, then fixed in 4% (w/v) paraformaldehyde for 15 min and stained with TUNEL and Hoechst 33342 using the DeadEndTM fluorometric TUNEL system according to manufacturer's instruction. Confocal images were captured using the X40 objective on the Olympus Fluoview System laser scanning microscope equipped with the appropriate filter sets and analyzed using Photoshop8.0 and SPOT3.5 software (supported by Ilona Dix).

2.2.2.7 MTT assays

Pellino3 knockdown cells were grown in 48-well plates and then stimulated with TNFα (40ng/ml) and CHX (10µg/ml) or CHX alone for indicated times. MTT (5mg/ml) was added to the cells and incubated for 3 hr at 37°C. Media was removed and DMSO added to dissolve the cells. The absorbance of the solubilised material was measured at 540nm using a BioTEK microplate reader and this was used as an index of mitochondrial activity and thus cell viability.

2.2.3 Biochemical methods

2.2.3.1 Western blot analysis

2.2.3.1.1 Preparation of samples

The harvesting of whole cell extracts was carried out at 4ºC. Medium was removed from cells and the cells were then washed once in PBS before adding lysis buffer to each well. The plate was placed on a rocker for 30 min at 4ºC. The lysates were then scraped into 1.5ml microcentrifuge tubes and centrifuged at 12,000 x g for 10 min. The supernatants were removed to new 1.5ml microcentrifuge tubes. Extracts were boiled for 5 min in sample buffer, briefly centrifuged at 4ºC and stored at -20ºC

2.2.3.1.2 SDS-polyacrylamide gel electrophoresis (SDS-PAGE)

Samples and appropriate prestained (26.6-180kDa) protein markers were loaded into separate wells. Electrophoresis was performed at 80V through a 5% SDS polyacrylamide stacking gel and then through a 7-15% SDS polyacrylamide resolving

gel at 120V for 1.5~2 hr. The percentage gel was chosen based on the size of the proteins being electrophoresed.

2.2.3.1.3 Immunoblotting

Following separation by electrophoresis, the proteins were transferred electrophoretically to nitrocellulose membranes in a Hoefer TE 70 Semiphor semi-dry transfer unit at 110mA for 1.25 hr using Whatmann and nitrocellulose pre-soaked in cold transfer buffer for 10 min. Following transfer, non-specific binding was blocked by incubating the nitrocellulose membranes at room temperature for 1 hr (or overnight) in blocking Buffer. The membranes were then incubated at 4ºC overnight with the primary antibodies diluted in TBST containing 5% (w/v) skimmed milk powder or BSA, optimal dilutions of primary as indicated on datasheet. The membranes were subsequently subjected to 3 x 10 min washes in TBST prior to incubation with secondary antibody specific for the primary antibody in question (anti-rabbit or anti-mouse) in TBST containing 5% (w/v) skimmed milk powder for 1hr in the dark at room temperature. The membranes were then washed a further 3 times for 10 min each in TBST in the dark. The immunoreactive bands were detected using Odyssey infrared imaging system from Licor Biosciences, according to the instructions of the manufacturer.

2.2.3.2 Co-immunoprecipitation (CoIP)

2.2.3.2.1 Co-IP analysis of overexpressed proteins

Cells were transfected with Lipofectamine2000 as previously described in section 2.2.2.3 at a 1:1 ratio of expression constructs. Cell extracts were generated as previously described in section 2.2.3.1.1. Cell lysates were initially precleared by incubating with non immune IgG antibody (1µg) and protein A/G-agarose (10µl) for 1hr at 4°C with rocking followed by rapid centrifugation of the agarose beads. Each supernatant was removed to a fresh microcentrifuge tube followed by addition of the appropriate antibody (2µg) and incubated for 24 hr at 4°C with rocking. An aliquot (50µl) of protein A/G agarose was added to each sample and incubated with rocking overnight at 4°C. Samples were added to chilled spin columns and centrifuged at 16,000 g for 1 min. The beads were washed with CoIP lysis buffer (500µl) and subject to re-centrifugation. This step was repeated 3 times. The columns were moved to fresh tubes and 60µl of SDS-

PAGE sample buffer was added to the columns for 20 min at room temperature. Samples were centrifuged at 16,000g for 2 min, to elute immunocomplexes and subsequently boiled at 100ºC for 5 min and analyzed using SDS polyacrylamide gel electrophoresis and Western blotting (section 2.2.3.1).

2.2.3.2.2 Co-IP analysis of endogenous proteins

For DISC complexes analysis, cells were stimulated for various times with TNFα (40ng/ml), CHX (10μg/ml) and Z-VAD-FMK (20μm) and then were lysed for immunoprecipitation and Western immunoblotting analysis as described above.

2.2.3.3 *In vitro* binding assay

2.2.3.3.1 Expression and purification of 6×his-tagged proteins

Plasmid DNA (1μl) was transformed into competent *E .coli* strain BL21 cells as described in section 2.2.1.1. 25ml LB broth, containing the appropriate antibiotics, was inoculated with a single transformed colony and grown overnight at 37°C. 10ml aliquot of this pre-culture was used to inoculate 1L of LB, containing the appropriate antibiotics, and incubated at 37°C up to the logarithmic phase of growth (OD600 reaches 0.6~0.8). Protein expression was then induced by overnight treatment at 15°C with IPTG (100μM). The bacteria were pelleted by centrifugation of 6,000 g for 15 min at 4°C, and resuspended in 25ml native lysis buffer. Three cycles of freeze-thawing and sonication were performed on the lysates to completely lyse the bacteria. The lysates were cleared by centrifugation at 10,000 g for 30 min. 0.8ml Ni-NTA resin was washed three times with wash buffer, then added to the cleared lysates, and incubated at RT for 2 hr with constant rotation. The Lysates-Ni-NTA mixture was loaded into a gravity flow column. Trapped resin was washed three times with 10ml wash buffer. Protein was eluted in 5ml Elution Buffer. Protein purity was determined by SDS-PAGE analysis (with Coomassie Blue G250 staining).

2.2.3.3.2 *In vitro* binding assays

Recombinant myc-tagged Pellino3 proteins (1μg) were initially immunoprecitated in binding buffer using an anti-myc antibody (2μg) and proteinA/G beads (30μl) as above. The beads were washed 5 times with binding buffer and then incubated overnight at 4°C

with lysates (300µl from 6 well plates) from HEK293T cells previously transfected with HA tagged RIP1. Beads were subjected to serial washes with binding buffer followed by centrifugation. Co-precipitated proteins were eluted in SDS-PAGE sample buffer and then subjected to Western blot analysis.

2.2.3.4 EMSA

EMSA was used to detect the presence of DNA-binding proteins in nuclear extracts. NF-κB Infrared Dye labelled oligonucleotides was purchased from Licor Biosciences.

2.2.3.4.1 Preparation of sub-cellular fractions

Following treatment, cells were washed with 1 ml of ice cold PBS and then scraped into hypotonic Buffer-A (1ml). Following centrifugation at 4ºC, (21,000 g for 10 min) the supernatants were removed and the cells were lysed for 10 min on ice in Buffer-A containing 0.1% (w/v) Igepal (20µl). Lysates were centrifuged at 21,000 g for 2 min. The resulting supernatants constituted cytosolic extracts and were stored at -20ºC in fresh microcentrifuge tubes. The remaining pellets were resuspended in 20µl of Buffer-C and incubated on ice for 15 min. Incubations were then centrifuged at 21,000 g for 10 min. The supernatants were then transferred to 75µl of Buffer D. Such samples constituted nuclear extracts. Protein concentrations were determined by the method of Bradford and assayed for NF-κB-DNA binding activity as outlined in the following section.

2.2.3.4.2 EMSA reaction

Nuclear extracts (5µg of protein), generated as described in section 2.2.3.4.1, were incubated with the following reaction mix:

10x Binding Buffer	2µl
Poly (dI-dC)	1µl
25mM DTT	2µl
1% NP40	1µl
1mM $MgCl_2$	1µl
NF-κB IRDye labelled oligonucleotides	1µl
	8µl

Nuclear extracts (5 μg of protein)	…
Water	to 20μl

NF-κB consensus oligonucleotide:

5’ - AGTTGAGGGGACTTTCCCAGGC - 3’

3’ - TCAACTCCCCTGAAAGGGTCCG - 5’

Underlined nucleotides are the binding site

For competition assays, unlabeled oligonucleotides containing the consensus NF-κB were added for 20 min at room temperature, prior to addition of the IRDye labelled oligonucleotides. Incubations were performed in the dark for 1hour at room temperature. Poly (dI-dC) was added to prevent non-specific binding of proteins to the NF-κB, oligonucleotide probe and thereby to reduce background.

2.2.3.4.3 Preparation of native polyacrylamide gel

A native 5% Acrylamide Gel was prepared as follows

H_2O	39ml
10x TBE	2.5ml
30% Polyacrylamide	8.4ml
10% APS	250μl
TEMED	20μl

The components were mixed well while minimizing bubble formation. The gel was poured and allowed polymerize for 30-45 min. The gel was pre-run in 0.5X TBE for 30 min at 90V.

2.2.3.4.4 Electrophoresis

Following incubation of reaction, orange loading dye (2μl) was added and the incubations were then subjected in the dark to electophoresis for 90 min at 90V in a non-denaturing 4% (w/v) polyacrylamide gel. Gels were run in 0.5 x TBE buffer. Gels were then removed from the glass plates and visualised using Odyssey Infrared Imaging System from Licor Biosciences.

2.2.3.5 ELISA

Samples were collected and stored at -20ºC until ELISA analysis. 96-well NUNC "Maxisorb" plates were coated with mouse anti-human IL-8 capture antibody (4µg/ml) and were incubated overnight at room temperature. Plates were washed three times with wash buffer (PBS with 0.05% (v/v) Tween-20) and dried by inverting the plates on tissue paper. Plates were blocked for 1 hr with PBS containing 1% (w/v) BSA. Plates were again washed three times and dried. Samples or standards (100µl) diluted in reagent diluent were added to each well. The concentrations of standards were between 0 and 2000pg/ml. Plates were incubated with samples or standards for 2 hr and then the series of washes was repeated. Detection antibody (100µl) (biotinylated sheep anti-human antibody) diluted in reagent diluent was added to each well (40ng/ml). Again plates were incubated for 2 hr and washed. Streptavidin-HRP conjugate (100µl) was added to each well. The plates were incubated in the dark for 20 min and then the wash step was repeated. 100µl TMB (1.25mM/l) solution was added to each well and again plates were incubated in the dark for no longer than 20 min. 50µl 1 N H_2SO_4 was used to stop the reaction and the OD was measured for each well at 450nm and 590nm using a ELx800TM microplate reader with Gen5 Data Analysis Software. The concentrations of IL-8 in each sample were extrapolated from a standard curve that related the OD of each standard amount to the known concentration. Standard samples were assayed in duplicate to generate the standard curve, while all samples were assayed in triplicate.

2.2.4 Animal experiments

For liver toxicity induced by TNF and D-Gal, age and sex-matched wild type and Pellino3-deficient mice were injected intraperitoneally with TNF (0.0025µg/g body weight) plus D-Gal (0.8mg/g body weight). Mouse survival was monitored within 36 hr, after which no further deaths occurred. Liver samples were collected at 12 hr after injection. Serum samples were obtained at 7 hr after treatment.

2.2.5 Immunohistochemical analysis

The samples of liver tissue were fixed in neutral buffered formalin. Following fixation tissues were paraffin embedded, sectioned at 5µm and stained with haematoxylin and

eosin (H&E). For detection of cleaved caspase-3, sections were deparaffinized and incubated in 0.3% (v/v) H_2O_2 for 30 min for blockade of endogenous peroxidase activity and then blocked with PBS containing 5% (v/v) goat serum and finally incubated with anti-cleaved caspase-3. The Vectastain ABC kit was used according to the manufacturer's specifications for immunoperoxidase systems. Peroxidase activity was visualized with ImmPACT™ DAB (Aragay et al.). The nuclear counterstain was stained by HEMATOXYLIN (Blue). Staining was viewed with an E-800 Eclipse microscope (Nikon).

CHAPTER THREE: RESULTS

TNF is a proinflammatory cytokine that can regulate cell proliferation, differentiation and death. Exposure of cells to TNF can activate the TNFR signalling pathway, inducing cell survival by activating NF-κB or cell death through apoptosis / necroptosis (Scaffidi et al., 1999; Galluzzi and Kroemer, 2008). Binding of TNF to its receptor initiates the formation of complex I, a multi-component complex containing TRADD, RIP1, TRAF2 and TRAF5, which is responsible for mediating the activation of the NF-κB and JNK pathways (Chen and Goeddel, 2002; Hsu et al., 1996). RIP1 plays an essential role in the activation of NF-κB. TNF-induced K63-linked polyubiquitination of RIP1 facilitates the recruitment of the IKK complex by virtue of the ubiquitin-binding domain of IKKγ (Ea et al., 2006). The polyubiquitinated RIP1 also recruits TAK1 via the ubiquitin-binding domains of TAK1-associated proteins termed TABs, thus allowing TAK1 to phosphorylate and activate IKK (Chen, 2005; Ishitani et al., 2003; Wang et al., 2001). NF-κB exists in all cells in a resting state in the cytoplasm and is activated only in response to stimuli. Under resting condition, NF-κB is sequestered in an inactive form by unphosphorylated IκBα. In response to extracellular signals such as TNF, IκBα is phosphorylated by the IKK complex, leading to its ubiquitination and degradation, allowing for NF-κB to translocate into the nucleus and trigger the transcription of a series of target genes (Zandi et al., 1997).

Whilst NF-κB is a key pro-inflammatory transcription factor it can also enhance cell division and inhibit apoptosis in response to harmful stimuli. It is responsible for protecting cells from TNF-induced apoptosis by activating anti-apoptotic genes, such as

XIAP (Eckelman et al., 2006), cIAP1/ cIAP2 (Rothe et al., 1995), and cFLIP (Krueger et al., 2001).

In response to certain stimuli, Complex I is released from TNFR1 and recruits FADD and procaspase-8, to form an "apoptotic complex" (DISC), leading to apoptosis (Micheau and Tschopp, 2003; Wang et al., 2008). The formation of DISC is tightly regulated to keep the balance between survival and death in cells. A series of prosurvival genes under direct NF-κB control, such as cFLIP1, cIAP1, cIAP2, Bcl-x, XIAP (Micheau et al., 2001; Mahoney et al., 2008; Tao et al., 2006; Dutta et al., 2006) can inhibit caspase-8 binding to FADD, blocking the activity of DISC. This inhibition is relieved through either degradation of these prosurvival proteins or termination of the NF-κB transcriptional activity (Wang et al., 1998; Chang et al., 2006; Micheau et al., 2001). The K63 polyubiquitination of RIP1 is a key determining factor in these pathways since its ubiquitination biases the TNF pathway towards activation of NF-κB and the induction of anti-apoptotic genes (Hayden and Ghosh, 2008).

The mammalian Pellino family is comprised of 4 family members, Pellino1, Pellino2 and two spliced variants of Pellino3 (Pellino3s and 3l) (Moynagh, 2009; Schauvliege et al., 2007). Each member of the family contains an N-terminal FHA domain, a phosphothreonine-binding module that facilitates interaction with IRAKs (Lin et al., 2008) and a C-terminal RING-like domain that catalyses K63 polyubiquitination of IRAKs (Butler et al., 2007; Ordureau et al., 2008; Schauvliege et al., 2006). IRAKs are key signalling intermediates the IL-1 and the TLR pathways and thus Pellino proteins are implicated in these signalling cascades. In a previous study, Chang and colleagues identified Pellino1 as an E3 ubiquitin ligase for RIP1 in the TLR3/TLR4 pathways, suggesting that Pellino proteins may be able to regulate TNF signalling. The major focus of this thesis was to investigate whether Pellino3 is involved in TNF signalling pathway and to identify the molecular mechanisms involved.

3.1 Pellino3 knockdown sensitizes cells to the pro-apoptotic effects of TNF.

To investigate the potential role(s) of Pellino3 in regulating TNF signaling, Hela cells, that display stable suppression of Pellino3, were generated using Pellino3-specific shRNA. Pellino3 expression was measured at the mRNA level and this approach confirmed that Pellino3 expression was reduced by 55% in cells selected for stable integration of Pellino3-specific shRNA (Figure 3-1A). TNF is well known to cause cell death in the presence of protein synthesis inhibitors by virtue of the latter preventing the induction of anti-apoptotic proteins. In this study, cells were treated with TNF and CHX, a well known protein synthesis inhibitor, which enhances the sensitivity of tumor cells to the cytotoxic effects of TNF (Vassalli, 1992). The combined treatment of Hela cells with TNF (40ng/ml) and CHX (10μg/ml) caused the cells to become rounded and non-adherent but the number of such cells was greatly increased when Pellino3 expression was suppressed by Pellino3-specific shRNA (Figure 3-1B). To quantify cell viability, an MTT assay was performed. This is a rapid, precise and simple method that measures mitochondrial activity based on the absorbance of the dissolved MTT formazan crystals formed in living cells (Mosmann, 1983). The MTT-based viability assay revealed that the morphological changes, observed in Pellino3 knockdown cells were associated with reduced cell viability. Thus the combined treatment of TNF and CHX caused a 50% reduction in cell viability in Pellino3 knockdown cells, whereas the co-treatment reduced viability by 20% in control cells (Figure 3-1C).

Since TNF can induce cell death via caspase activation as well as by necroptosis, it was necessary to investigate the type of death induced in Pellino3 deficient cells. To this end a FACS-based approach measuring Annexin V staining was conducted. Annexin V can

bind to phosphatidylserine that is exposed on the outer leaflet of the plasma membrane and this is a key feature of early apoptosis (Koopman et al., 1994). Knockdown of Pellino3 expression caused greatly enhanced Annexin V staining of Hela cells when co-treated with TNF and CHX, compared with cells infected with lentivirus containing control shRNA (Figure 3-1D). After exposure with TNF plus CHX the percentage of Pellino3 shRNA-infected cells with positive staining of Annexin V was approximately 45%, while 23% of control cells showed positive staining. There was no difference observed in Annexin V staining of control and Pellino3-knockdown cells that had been exposed to CHX alone. In order to further confirm that the increased cell death in Pellino3-knockdown cells was apoptotic in nature the sensitivity of cell death to Z-VAD-fmk was assessed. The latter has the ability to inhibit apoptotic cell death by inhibiting the upstream activator caspase-8 (Sun et al., 1999). The level of apoptosis in Pellino3-knockdown cells was reduced to control levels of 14% by treatment of cells Z-VAD-fmk further confirming that knockdown of Pellino3 promotes the ability of TNF to induce caspase-dependent apoptosis (Figure 3-1D).

Apoptosis is also associated with the cleavage of a number of intracellular proteins including caspase-8, caspase-3 and PARP. The activation of caspase-8 leads to the generation of the active p18 and p10 subunits, which have the ability to cleave and activate the executioner caspases, such as caspase-3, -6, -7, leading to apoptosis (Muzio et al., 1996). Caspase-3 is cleaved to release the active 17 kD and 12 kD subunits, ultimately eliciting DNA fragmentation and cell shrinkage (Tewari et al., 1995). PARP, which is 113 kDa nuclear chromatin-associated enzyme involved in DNA repair process is also a classical caspase substrate and upon caspase activation is cleaved into two fragments of approximately 89 kD and 24 kD (Margolin et al., 1997). Thus the cleavage status of caspase-8, caspase-3 and PARP was examined in Pellino3 knockdown cells in response to TNF and CHX treatment to further validate the apoptotic nature of the cell

killing in these cells (Figure 3-2). The combined treatment of TNF and CHX caused a time-dependent increase in the levels of cleaved caspase-8, caspase-3 and PARP but the levels were greatly increased in Pellino3 knockdown cells. In combination with the earlier data these findings clearly indicate that reduced Pellino3 expression sensitizes Hela cells to the pro-apoptotic effects of TNF.

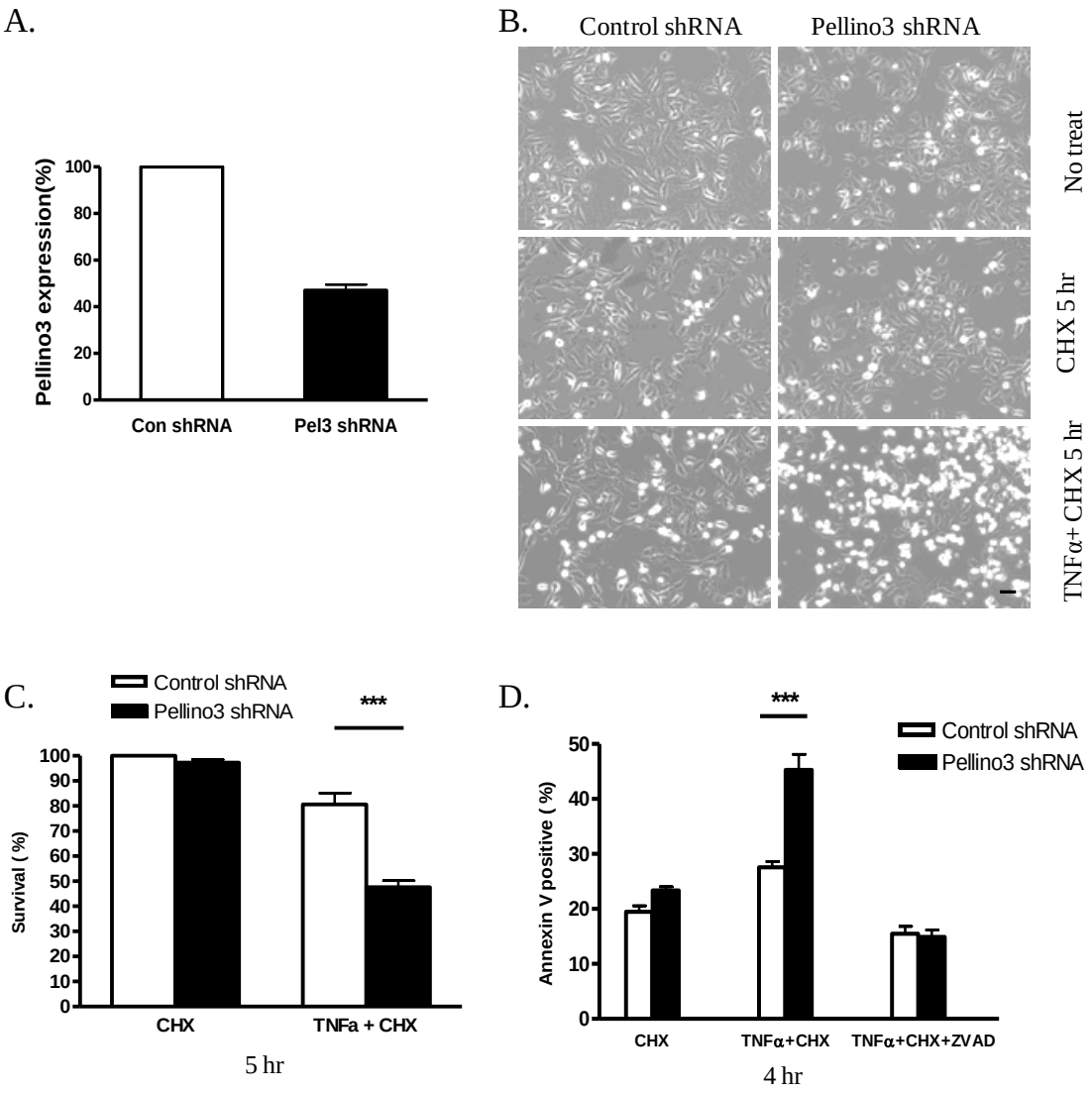

Figure 3-1 Knockdown of Pellino3 expression enhances the pro-apoptotic effects of TNF in Hela cells.

Hela cells were infected with lentivirus containing constructs that encoded control or human Pellino3-specific shRNA. Cells were grown in the presence of puromycin to select for cells showing stable integration of shRNA constructs. (A) RNA was extracted from cells 48 hr post transfection and analysed by quantitative RT-PCR for levels of Pellino3 mRNA. Data are presented relative to cells transfected with lamin A/C-siRNA and represent the means +/- S.D. of 3 independent experiments. (B,C,D) Selected cells were treated in the absence (control) or presence of human TNF (40ng/ml), CHX (10μg/ml) or the caspase inhibitor zVAD-fmk (20μM) for 5 hr or other indicated times. (B) Cells were photographed using a phase contrast microscope (bar 20μm). (C) Cells were analyzed for cell viability using MTT assays with viability expressed relative to control shRNA-infected cells treated with CHX alone. (D) Cells were

analyzed by flow cytometry for percentage of cells staining positive for Annexin V staining. Data represent the mean +/- S.D. of 3 independent experiments. ***p<0.001.

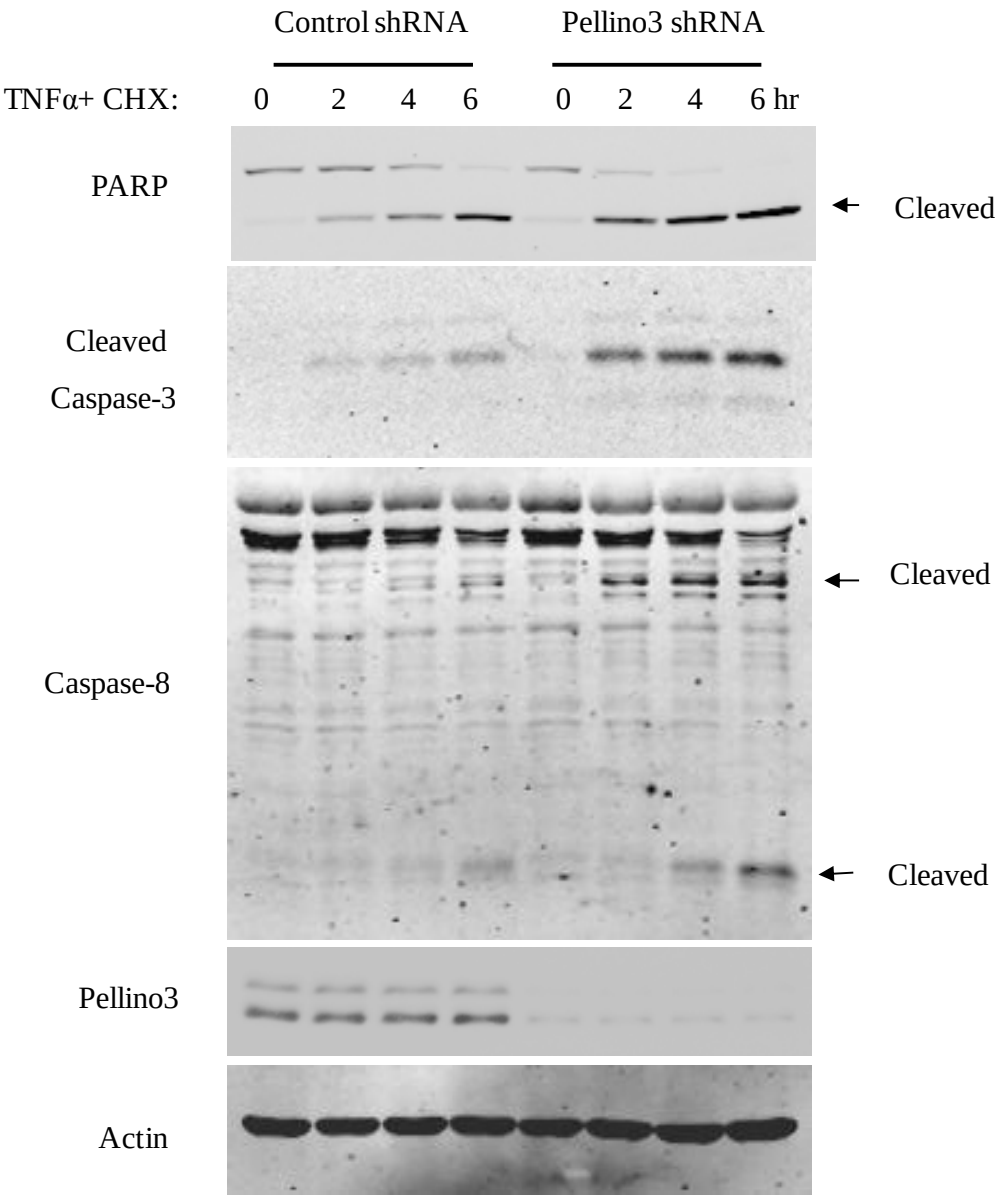

Figure 3-2 Immunoblot analysis of apoptotic marker proteins in Pellino3 knockdown Hela cells.

Hela cells were infected with lentivirus containing constructs that encoded control or human Pellino3-specific shRNA. Cells were grown in the presence of puromycin to select for cells showing stable integration of shRNA constructs. Selected cells were treated in the absence (0) or presence of human TNF (40ng/ml) plus CHX (10μg/ml) for indicated times. Cell lysates were subjected to 10–15% SDS-PAGE and probed by immunoblotting for expression levels of PARP, cleaved caspase-3, caspase-8, Pellino3 and β-actin. Cleaved forms of PARP and caspase-8 are indicated by arrows.

3.2 Suppression of pellino3 enhances TNF-induced apoptosis in a manner independent of NF-κB and MAPK signalling.

After binding to TNFR1, TNF can activate NF-κB, which is a well-known transcription factor that has ability to upregulate anti-apoptotic proteins (Chen and Goeddel, 2002). Activation of the MAPKs, p38 and JNK is also known to regulate apoptosis, while the ERK pathway activity is suppressed by JNK/p38 kinases during apoptosis induction (Junttila et al., 2008). Given such regulatory roles of the NF-κB and MAPK pathways in regulating apoptosis, the effects of Pellino3 knockdown on the ability of TNF to trigger these pathways was next examined in an effort to increase our understanding of the molecular basis to pro-apoptotic effects associated with Pellino3 knockdown. Since the activation of NF-κB requires the prior phosphorylation and degradation of its inhibitory protein IκBα, the levels of IκBα were initially measured as an indirect index of activation of the NF-κB pathway.

In Hela cells infected with Pellino3 shRNA the early phase of TNF-induced degradation of IκBα was still evident, but less IκBα was apparent at the later time points, suggesting that knockdown of Pellino3 may prolong the temporal profile of NF-κB activation (Figure 3-3 A).

In order to directly measure the effects of Pellino3 knockdown on NF-κB activity, nuclear extracts were prepared from cells and assayed by EMSA analysis for binding to fluorescently labelled oligonucleotides containing the NF-κB consensus motif. Basal NF-κB-DNA complexes were present in extracts from unstimulated cells while a complex of slower electrophoretic mobility was evident in extracts from TNF-stimulated cells (Figure 3-3B). Suppression of endogenous Pellino3 with shRNA led to an increase in the formation of the upper complexes following TNF stimulation,

compared to control shRNA. The enhanced levels were apparent at 25 min post TNF stimulation but the activation of NF-κB in response to TNF was more sustained in nature, with the activation still much higher at 60 min post TNF stimulation in cells infected with Pellino3 shRNA. NF-κB-DNA complexes were judged to be specific based on their sensitivity to the unlabelled oligoncleotide containing the NF-κB binding motif (see first lane in Figure 3-3B). The EMSA analysis in conjunction with the IκBα analysis is consistent with a role for Pellino3 in terminating TNF-induced activation of NF-κB.

The effect of Pellino3 knockdown on TNF-induced MAPK activation was next examined. Exposure of Hela cells to TNF caused increased phosphorylation of JNK, P38 and ERK that peaked by 15-30 min in both control and Pellino3 knockdown Hela cells (Figure 3-4). The TNF-induced stimulation of ERK1/2 affected predominantly the p44 isoform. However, the phosphorylation of JNK and P38 induced by TNF was slightly attenuated by Pellino3 knockdown. There was a very small effect on the phosphorylation of ERK comparing control and Pellino3 knockdown cells. Knockdown of Pellino3 had no effect on total levels of these kinases. These effects of Pellino3 on the MAPK pathway are in agreement with the previous report that Pellino 3 activated p38 MAPK in a TRAF6 and TAK-1 dependent manner (Butler et al., 2005).

Given that low NF-κB activity and increased activation of MAPK signalling tends to be associated with pro-apoptotic effects and Pellino3 knockdown has the opposing effects on these pathways the present data suggest that the increased pro-apoptotic capacity of TNF under conditions of reduced Pellino3 are unlikely to be secondary to effects on the NF-κB and MAPK pathways.

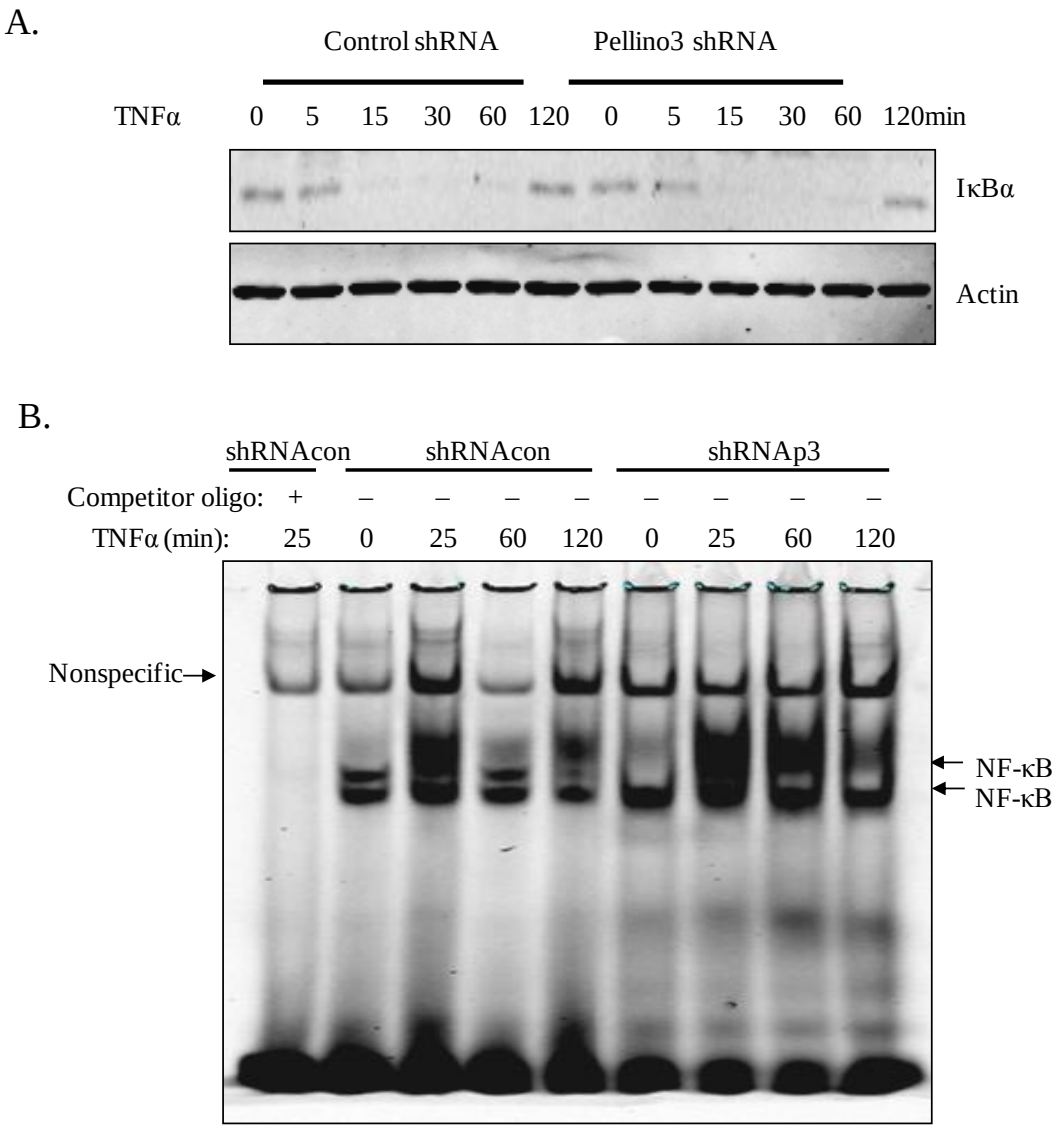

Figure 3-3 Effects of Pellino3 knockdown on TNF-induced activation of NF-κB in Hela cells

Hela cells were infected with lentivirus containing constructs that encoded control or human Pellino3-specific shRNA. Cells were grown in the presence of puromycin to select for cells showing stable integration of shRNA constructs. Selected cells were treated in the absence (0) or presence of human TNF (40ng/ml) for indicated times. (A) Cell lysates were prepared and immunoblotted for expression level of IκBα. Lysates were also probed for levels of β-actin to act as loading controls. (B) Nuclear extracts were prepared and subsequently incubated with an IR-labelled oligonucleotide containing an NF-κB-binding motif and separated by native PAGE. The arrows indicate the mobility of basal and TNF induced NF-κB-DNA complexes. The specificity of the NF-κB-DNA binding reaction was confirmed by the absence of the complexes when the binding reaction is performed in the presence of the unlabelled (competitor) oligonucleotide.

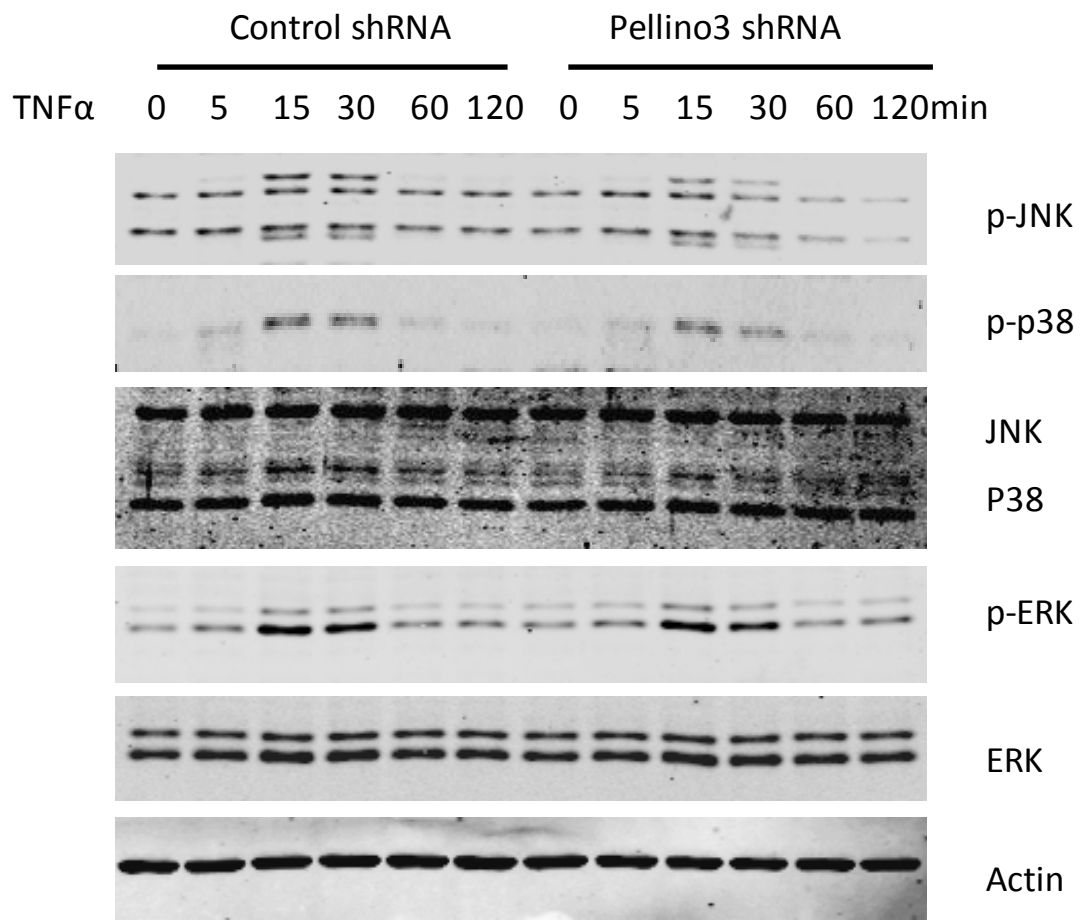

Figure 3-4 Effects of Pellino3 knockdown on TNF-induced activation of MAPKs in Hela cells.

Hela cells were infected with lentivirus containing constructs that encoded control or human Pellino3-specific shRNA. Cells were grown in the presence of puromycin to select for cells showing stable integration of shRNA constructs. Selected cells were treated in the absence (0) or presence of human TNF (40ng/ml) for indicated times. Cell lysates were prepared and immunoblotted for phosphorylated levels of JNK (p-JNK), P38 (p-P38), ERK (p-ERK) and total levels of JNK, P38 and ERK. Lysates were also probed for levels of β-actin to act as loading controls.

3.3 Role of Pellino3 in TNF-induced apoptosis in various cell types

The data above demonstrate that the suppression of Pellino3 expression hyposensitized Hela cells to the pro-apoptotic effects of TNF. In order to assess if such effects of suppressed Pellino3 expression were cell-type dependent similar studies were performed in three additional human cell lines (U373, 1321N1 and HEK293T). Human U373 MG astrocytoma cell line has been extensively used as a model system for the study of the activation of astrocytes by cytokines, particularly by IL-1β and TNF (Lieb et al., 1996; Machein et al., 1995). Human astrocytoma 1321N1 cells are widely used as a model system for characterizing intracellular signaling pathways and receptor-mediated responses (Aragay et al., 1995). HEK293T cells, a transformed cell line derived from human embryonic kidney preparations, are commonly used in cell biology research, such as a model for examining a transfected receptor, a transient expression host or a vehicle for the expression of recombinant proteins (Graham et al., 1977; Thomas and Smart, 2005).

3.3.1 Suppression of Pellino3 expression sensitizes U373 and 1321N1 cells to TNF-induced apoptosis

The human cell line U373 was initially used to evaluate if the regulatory effects of Pellino3 on the TNF pathway extend beyond Hela cells. In keeping with the findings from Hela cells, the same effects were apparent in that suppression of Pellino3 expression in U373 lead to increased cell death (Figure 3-5), reduced cell viability (Figure 3-6 A) and levels of cleaved PARP, caspase-3 and caspase-8 in response to TNF and CHX (Figure 3-6 B). Again these pro-apoptotic effects of Pellino3 knockdown appear to be independent of targeting of the NF-κB and MAPK pathways since Pellino3 knockdown in U373 cells lead to an increase in the TNF-induced degradation of IκBα

and a slight decrease in the phosphorylation of JNK and P38 in response to TNF (Figure 3-7). The effect on phosphorylation of ERK was very small (Figure 3-7). These effects of Pellino3 knockdown on TNF signalling were also mirrored in the 1321N1 astrocytoma in that suppressed expression of Pellino3 lead to greater cell rounding and detachment (Figure 3-8), reduced cell viability and increased PARP/caspase cleavage (Figure 3-9), prolonged degradation of IκBα and modest inhibitory effects on TNF-induced activation of the MAPK pathways (Figure 3-10). Such uniform findings across the Hela, U373 and 1321N1 cell lines verify that the observed specific role of Pellino3 knockdown in sensitizing cells to the pro-apoptotic effects of TNF is not a cell-type-specific phenomenon and strongly supports a widespread role for Pellino3 in the TNF signalling pathway.

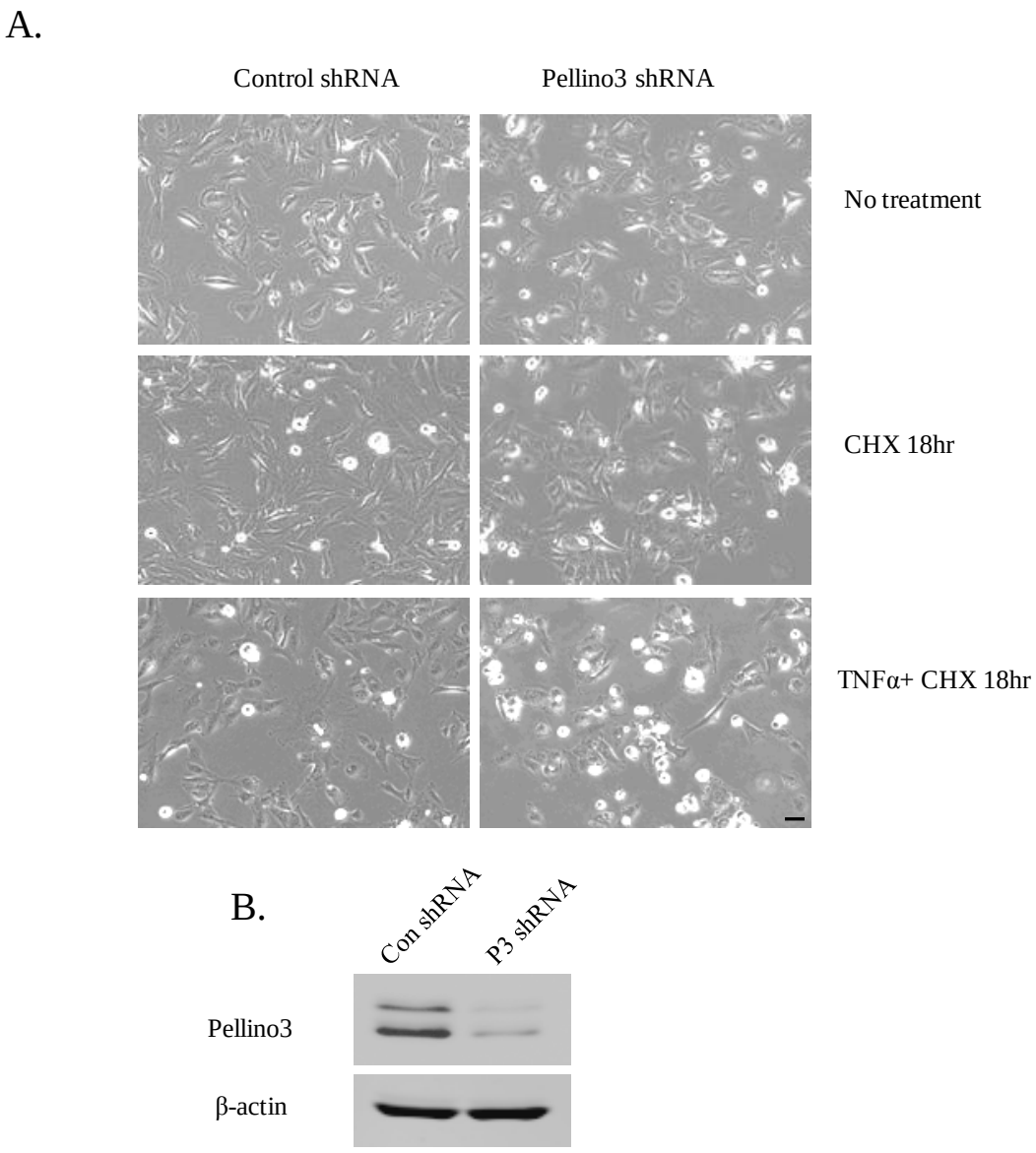

Figure 3-5 Knockdown of Pellino3 causes TNF-induced apoptosis in U373 cell

U373 cells were infected with lentivirus containing constructs that encoded control or human Pellino3-specific shRNA. Cells were grown in the presence of puromycin to select for cells showing stable integration of shRNA constructs. (A) Selected cells were treated in the absence (control) or presence of human TNF (40ng/ml) plus CHX (10μg/ml) for 18 hr. Cells were photographed using a phase contrast microscope (bar 20μm). (B) Immunoblot analysis demonstrating efficacy of Pellino3 protein knockdown (with β-actin as a loading control) is also shown.

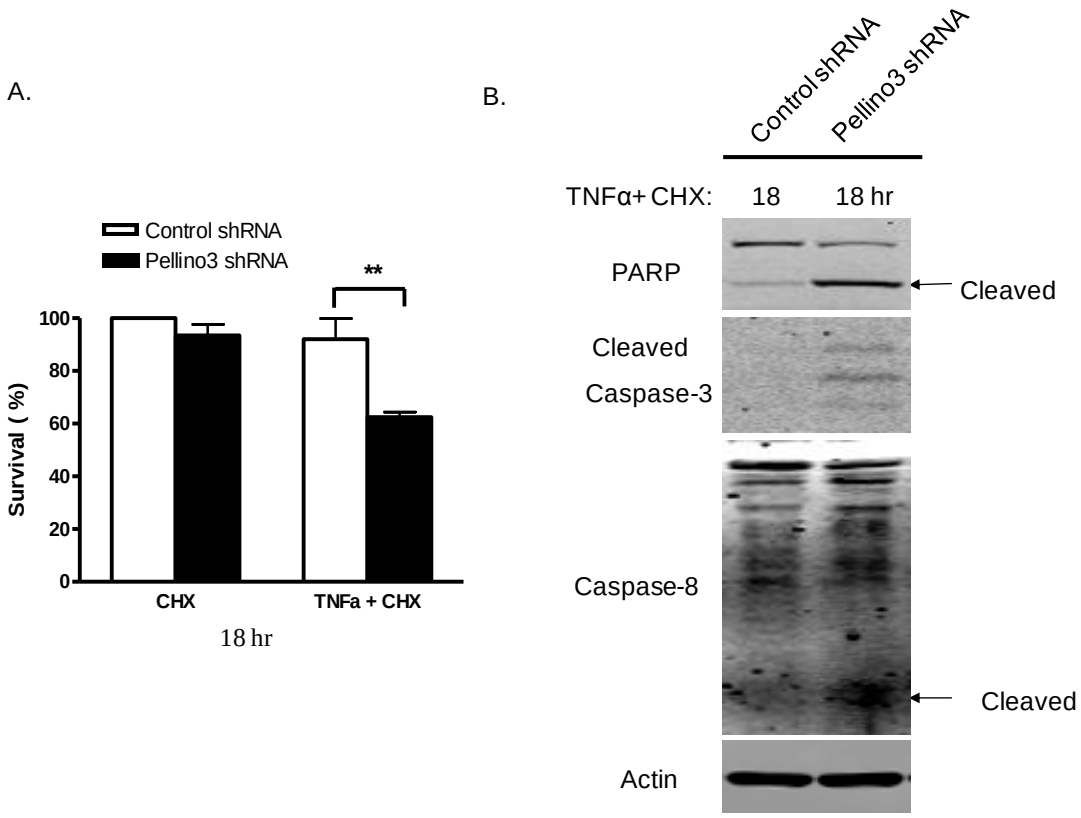

Figure 3-6 Knockdown of Pellino3 causes TNF-induced apoptosis in U373 cell was measured by MTT assay and Western blot

U373 cells were infected with lentivirus containing constructs that encoded control or human Pellino3-specific shRNA. Cells were grown in the presence of puromycin to select for cells showing stable integration of shRNA constructs. Selected cells were treated in the absence (control) or presence of human TNF (40ng/ml) plus CHX (10μg/ml) for 18 hr. (A) Cells were analyzed for cell viability using MTT assays with viability expressed relative to control shRNA-infected cells treated with CHX alone. Data represent the mean +/- S.D. of 3 independent experiments. ** $p<0.01$. (B) Cell lysates were probed by immunoblotting for expression levels of PARP, caspase-3, caspase-8 and β-actin. Cleaved forms of PARP and caspase-8 are indicated by arrows.

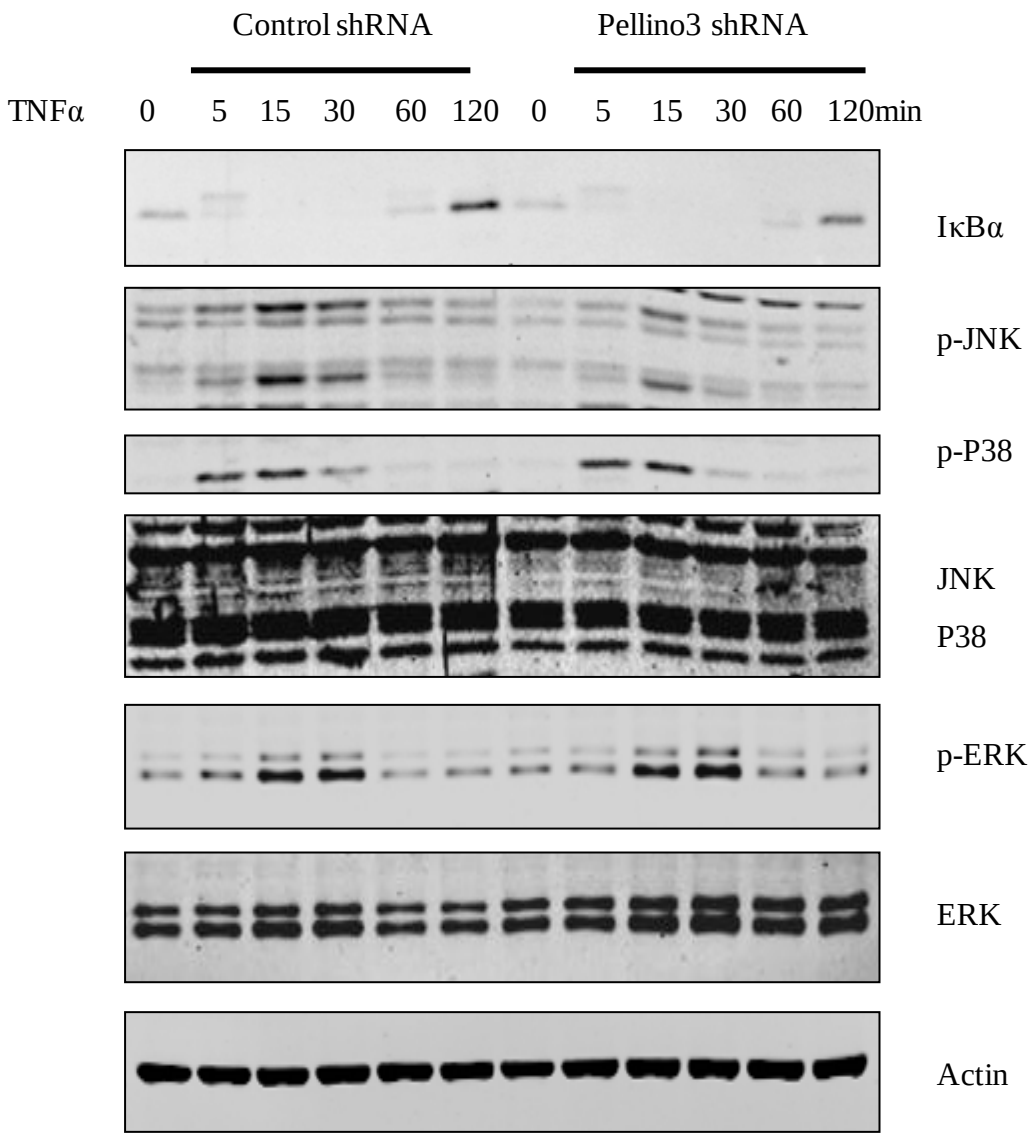

Figure 3-7 Pellino3 attenuates apoptosis in U373 cells independent of NF-κB and MAPK signalling.

U373 cells were infected with lentivirus containing constructs that encoded control or human Pellino3-specific shRNA. Cells were grown in the presence of puromycin to select for cells showing stable integration of shRNA constructs. Selected cells were treated in the absence (0) or presence of human TNF (50ng/ml) for indicated times. Cell lysates were prepared and immunoblotted for phosphorylated levels of JNK (p-JNK), P38 (p-P38), ERK (p-ERK) and total levels of IκBα, JNK, P38 and ERK. Lysates were also probed for levels of β-actin to act as loading controls.

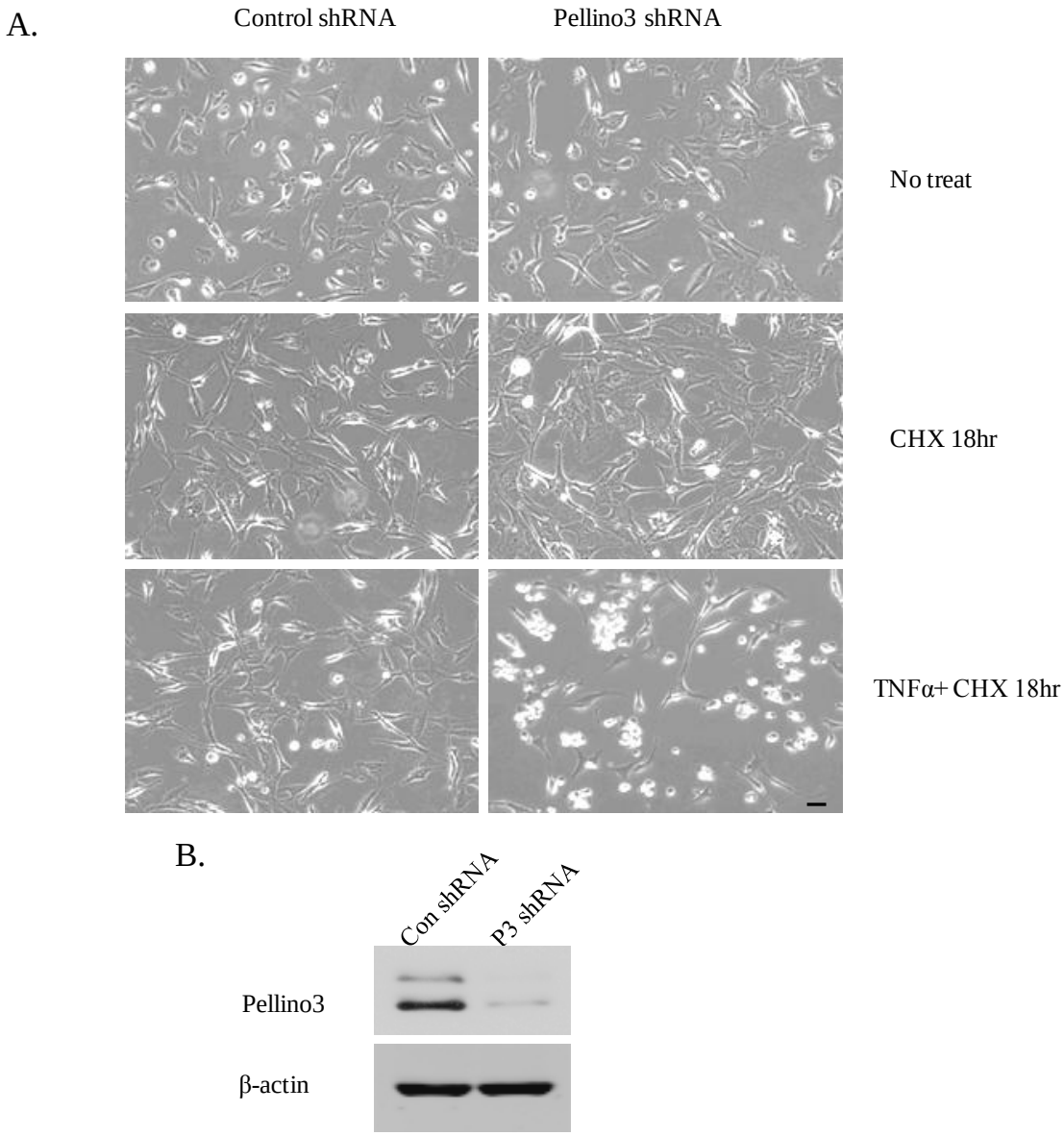

Figure 3-8 Knockdown of Pellino3 causes TNF-induced apoptosis in 1321N1 cell

1321N1 cells were infected with lentivirus containing constructs that encoded control or human Pellino3-specific shRNA. Cells were grown in the presence of puromycin to select for cells showing stable integration of shRNA constructs. Selected cells were treated in the absence (control) or presence of human TNF (40ng/ml) plus CHX (10μg/ml) for 18 hr. (A) Cells were photographed using a phase contrast microscope (bar 20μm). (B) Immunoblot analysis demonstrating efficacy of Pellino3 protein knockdown (with β-actin as a loading control) is also shown.

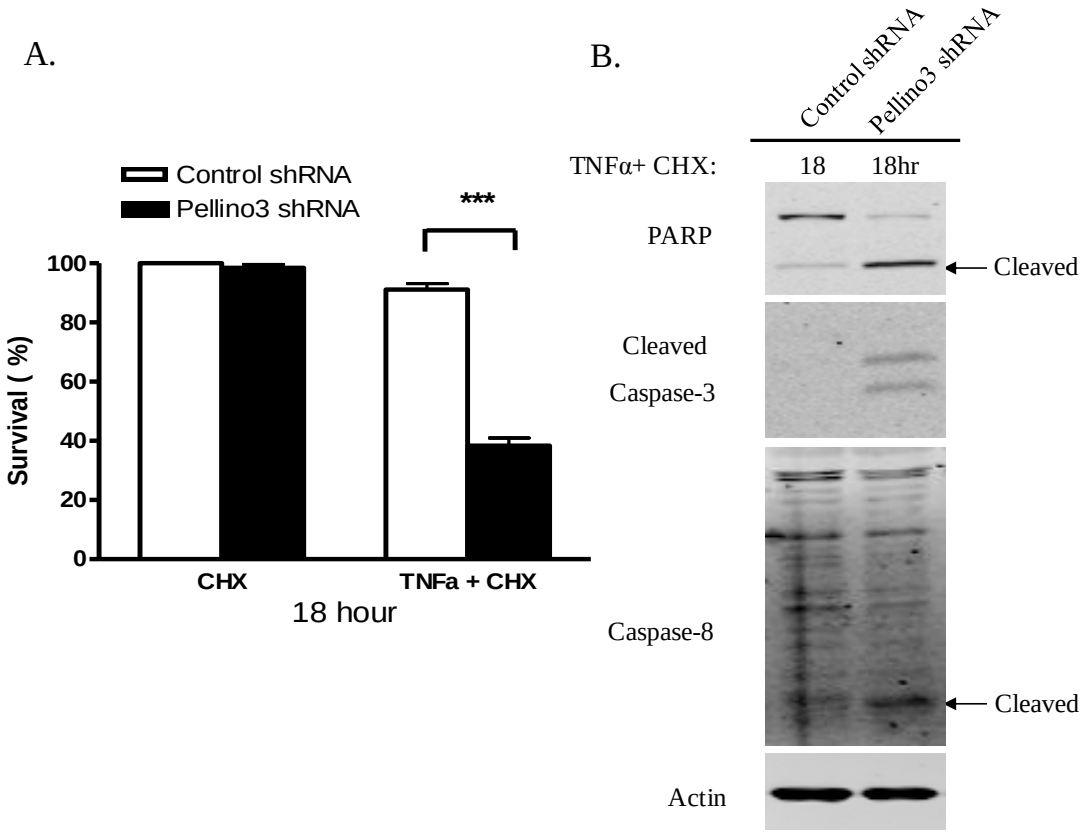

Figure 3-9 Knockdown of Pellino3 causes TNF-induced apoptosis in 1321N1 cell was measured by MTT assay and Western blot

1321N1 cells were infected with lentivirus containing constructs that encoded control or human Pellino3-specific shRNA. Cells were grown in the presence of puromycin to select for cells showing stable integration of shRNA constructs. Selected cells were treated in the absence (control) or presence of human TNF (40ng/ml) plus CHX (10μg/ml) for 18 hr. (A) Cells were analyzed for cell viability using MTT assays with viability expressed relative to control shRNA-infected cells treated with CHX alone. Data represent the mean +/- S.D. of 3 independent experiments. ***$p<0.001$. (B) Cell lysates were probed by immunoblotting for expression levels of PARP, caspase-3, caspase-8 and β-actin. Cleaved forms of PARP and caspase-8 are indicated by arrows.

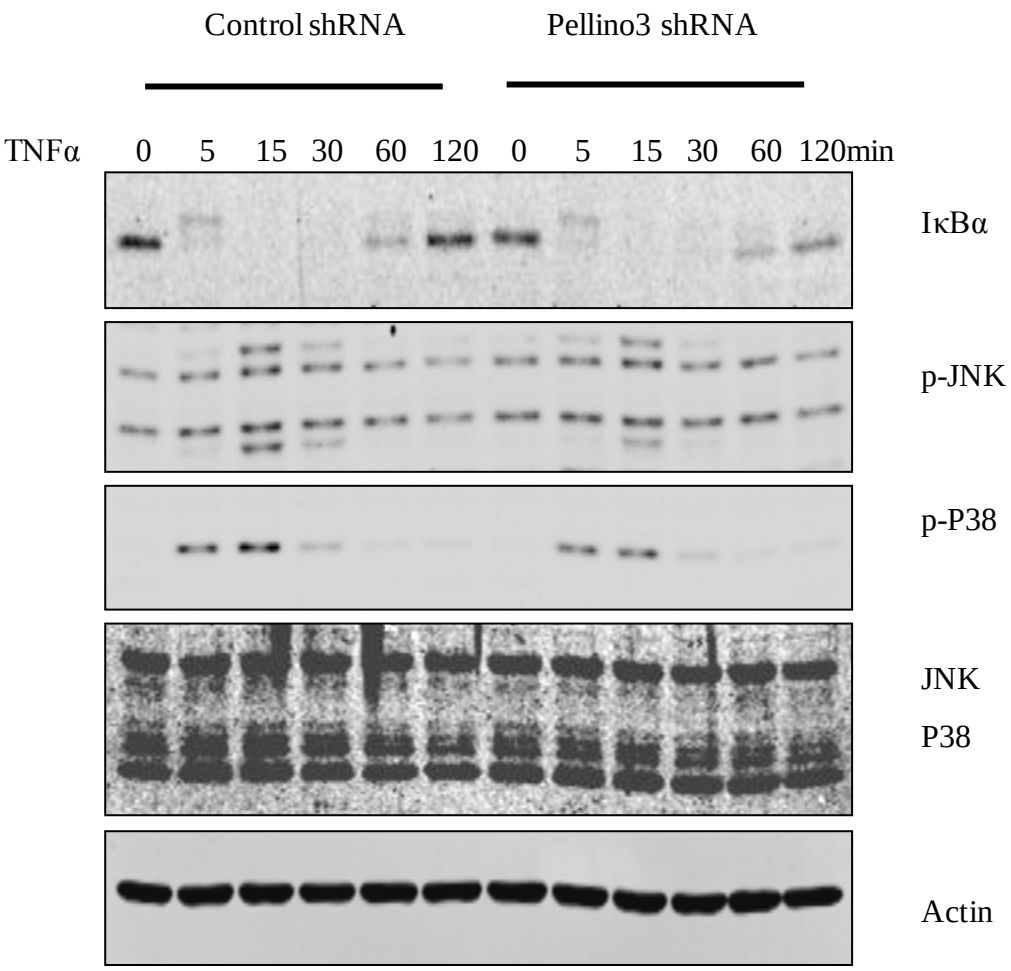

Figure 3-10 Pellino3 attenuates apoptosis in 1321N1 cells independent of NF-κB and MAPK signalling.

1321N1 cells were infected with lentivirus containing constructs that encoded control or human Pellino3-specific shRNA. Cells were grown in the presence of puromycin to select for cells showing stable integration of shRNA constructs. Selected cells were treated in the absence (0) or presence of human TNF (40ng/ml) for indicated times. Cell lysates were prepared and immunoblotted for phosphorylated levels of JNK (p-JNK), P38 (p-P38), ERK (p-ERK) and total levels of IκBα, JNK, P38 and ERK. Lysates were also probed for levels of β-actin to act as loading controls.

3.3.2 Knockdown of Pellino3 causes TNF-induced apoptosis in HEK293T cells

To further validate the above conclusion that Pellino3 knockdown enhanced TNF-induced apoptosis HEK293T cells was used to demonstrate that the independent approaches of employing shRNA expression constructs or synthesized siRNAs to suppress Pellino3 expression manifested the same findings in terms of increasing sensitivity of cells to the pro-apoptotic effects of TNF. Suppression of Pellino3 by shRNA increased cleavage of PARP, caspase-3 and caspase-8 after TNF plus CHX treatment (Figure 3-11A). After exposure with TNF plus CHX the percentage of apoptotic cells was approximately 30% in Pellino3 shRNA-infected cells, while in control shRNA-infected cells the percentage of apoptotic cells was only 22%. Upon treatment with CHX alone or TNF plus CHX as well as z-VAD-fmk, there was no observable difference in the percentages of apoptotic cells (Figure 3-11B). The shRNA suppression of endogenous Pellino3 expression in HEK293T was evidenced by immunoblot analysis (Figure 3-11C). HEK293T cells were also transfected with control siRNA or Pellino3-specific siRNA and stimulated with TNF (50ng/ml) for 18 hr. TUNEL staining experiments demonstrated a basal level of apoptosis in Pellino3 knockdown cells with a strong increase after exposure to TNF, whilst only a few positive cells were observed in control cells (Figure 3-12A). The siRNA-mediated suppression of endogenous Pellino3 expression in HEK293T is evidenced by Western blot analysis (Figure 3-12B).

As was the case with Hela, knockdown of Pellino3 delayed the resurgence of IκBα. To address this in more detail, cell lysates were also probed for the phosphorylation status of the upstream IκB kinases, IKKα and IKKβ. IKK is the major activator of NF-κB. The activated IKK phosphorylates IκBα, leading to IκBα ubiquitination and its degradation by the 26S proteasome (Karin, 1999). Cells transfected with Pellino3 siRNA showed a

stronger and more prolonged TNF-induced phosphorylation of IKKα/β□□Figure 3-13). As phosphorylation of IKK kinases is important for downstream signalling and activation of NF-κB, this further proves that Pellino3 acts as a negative regulator of NF-κB.

Phosphorylation of JNK and P38 induced by TNF in HEK293T cells were also attenuated by Pellino3 knockdown and there was a very small effect on phosphorylation of ERK comparing control and Pellino3 knockdown cells, whilst having no effects on total levels of these kinases (Figure 3-14).

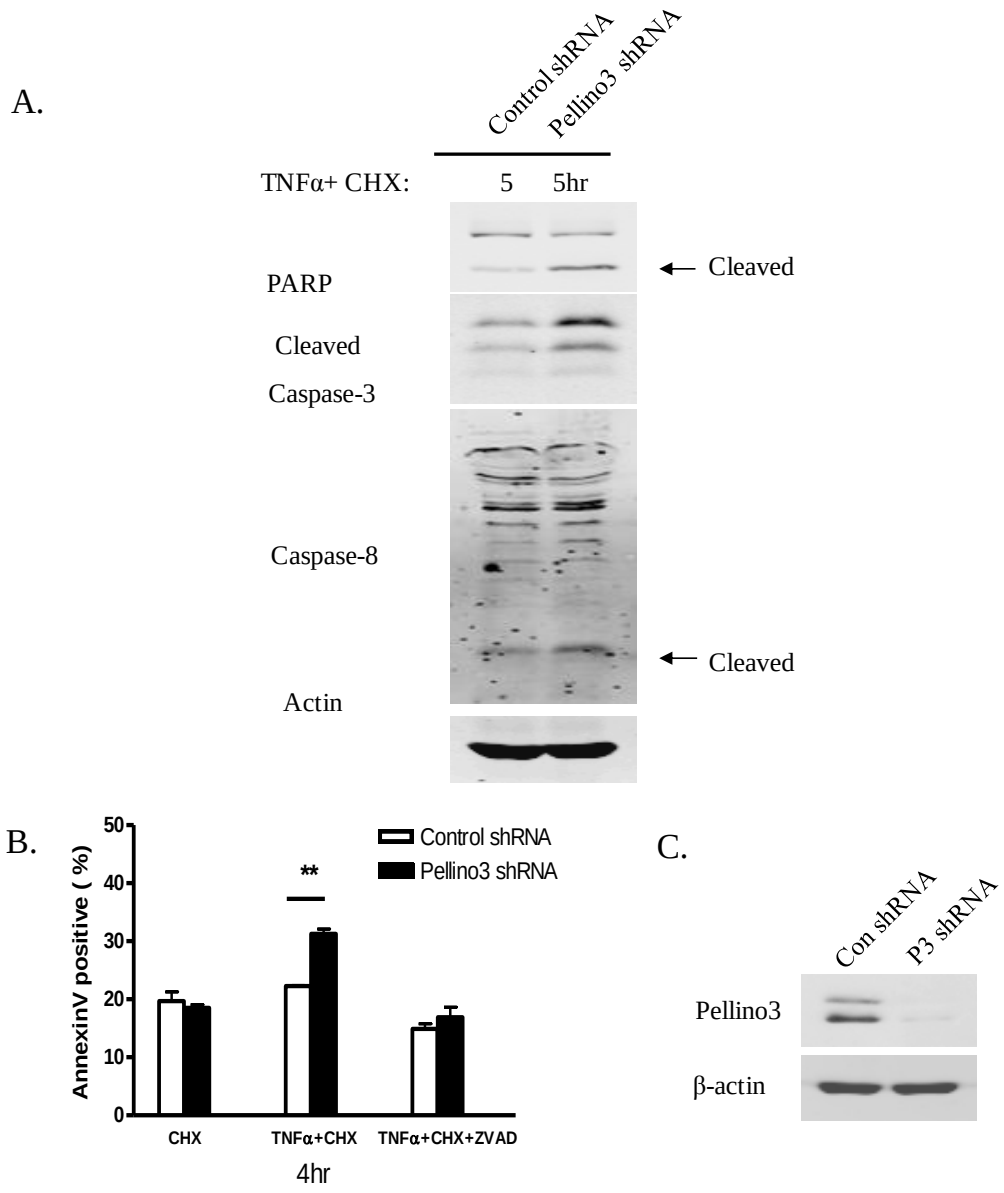

Figure 3-11 Knockdown of Pellino3 by shRNA causes TNF-induced apoptosis in HEK293T cells

HEK293T cells were infected with lentivirus containing constructs that encoded control or human Pellino3-specific shRNA. Cells were grown in the presence of puromycin to select for cells showing stable integration of shRNA constructs. Selected cells were treated in the absence (control) or presence of human TNF (50ng/ml), CHX (10μg/ml) or zVAD-fmk (20μM) for indicated times. (A) Cell lysates were probed by immunoblotting for expression levels of PARP, caspase-3, caspase-8 and β-actin. Cleaved forms of PARP and caspase-8 are indicated by arrows. (B) Cells were analyzed by flow cytometry for percentage of cells staining positive for Annexin V staining. Data represent the mean +/- S.D. of 3 independent experiments; **$p<0.01$. (C) Immunoblot analysis demonstrating efficacy of Pellino3 protein knockdown (with β-actin as loading control) is also shown.

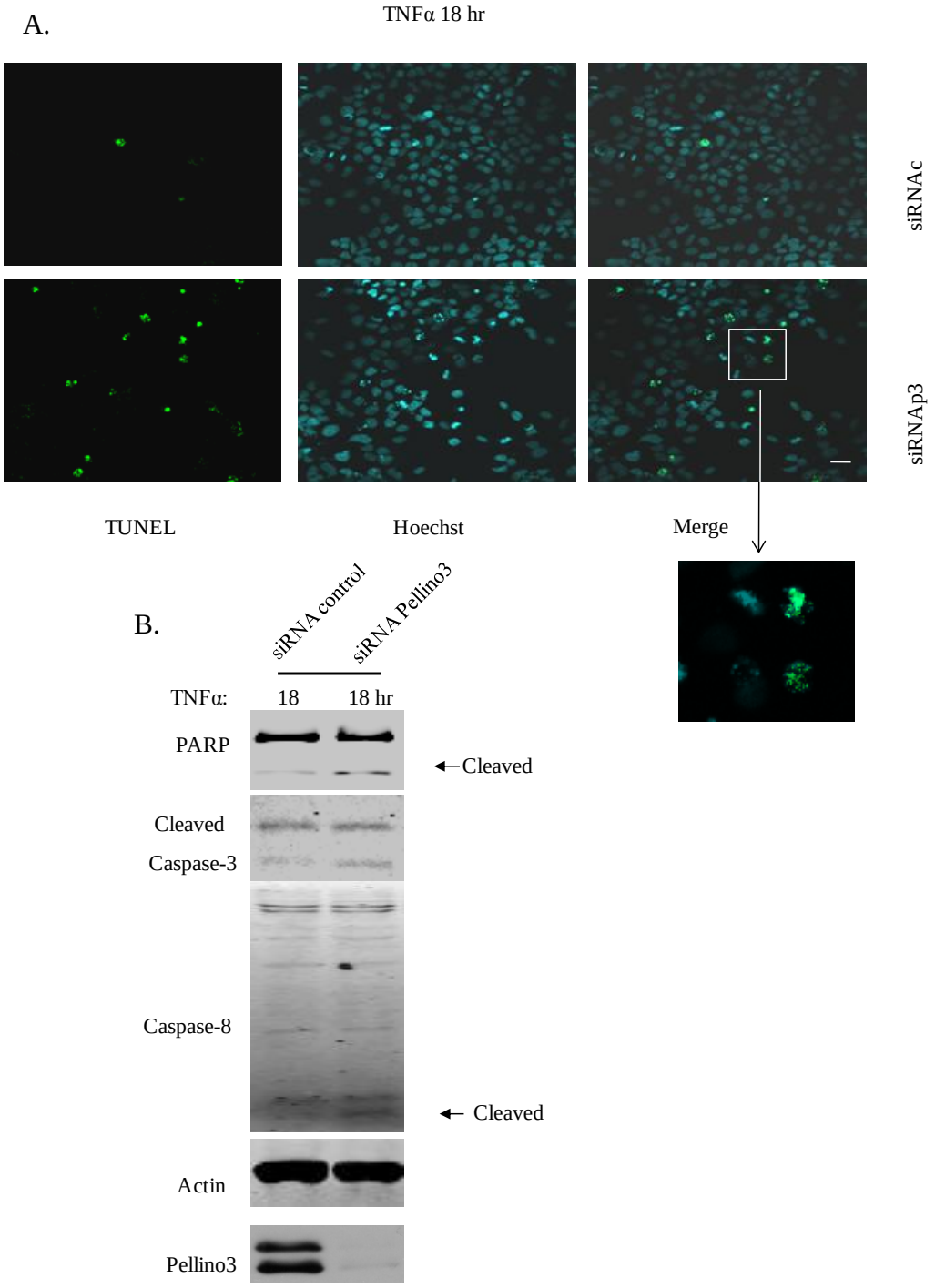

Figure 3-12 Knockdown of Pellino3 by siRNA causes TNF-induced apoptosis in HEK293T cells

HEK293T cells were transfected with control or Pellino3-specific siRNA. Cells were treated with TNF (50ng/ml) for 18 hr. (A) Cells were stained by TUNEL and Hoechst and subjected to confocal microscopy. Bar 20μm. (B) Cell lysates were probed by immunoblotting for expression levels of PARP, caspase-3, caspase-8, Pellino3 and β-actin. Cleaved forms of PARP and caspase-8 are indicated by arrows.

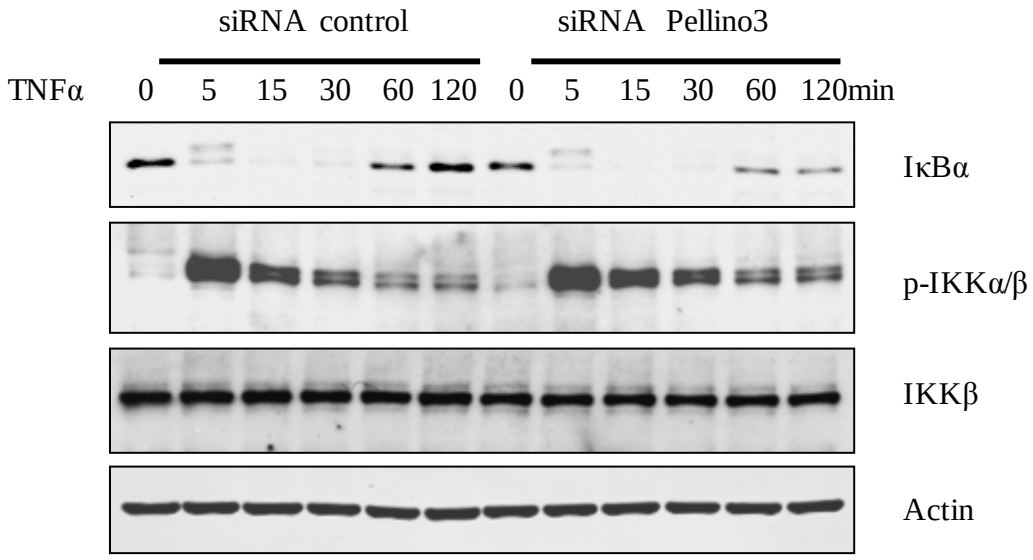

Figure 3-13 Effects of Pellino3 knockdown on TNF-induced activation of NF-κB in HEK293T cells.

HEK293T cells were transfected with control or Pellino3-specific siRNA and then treated with TNF (50ng/ml) for 18 hr. cells were treated in the absence (0) or presence of human TNF (50ng/ml) for indicated times. Cell lysates were prepared and immunoblotted for phosphorylated levels of IKKα/β (p-IKKα/β) and total levels of IκBα, IKKβ. Lysates were also probed for levels of β-actin to act as loading controls.

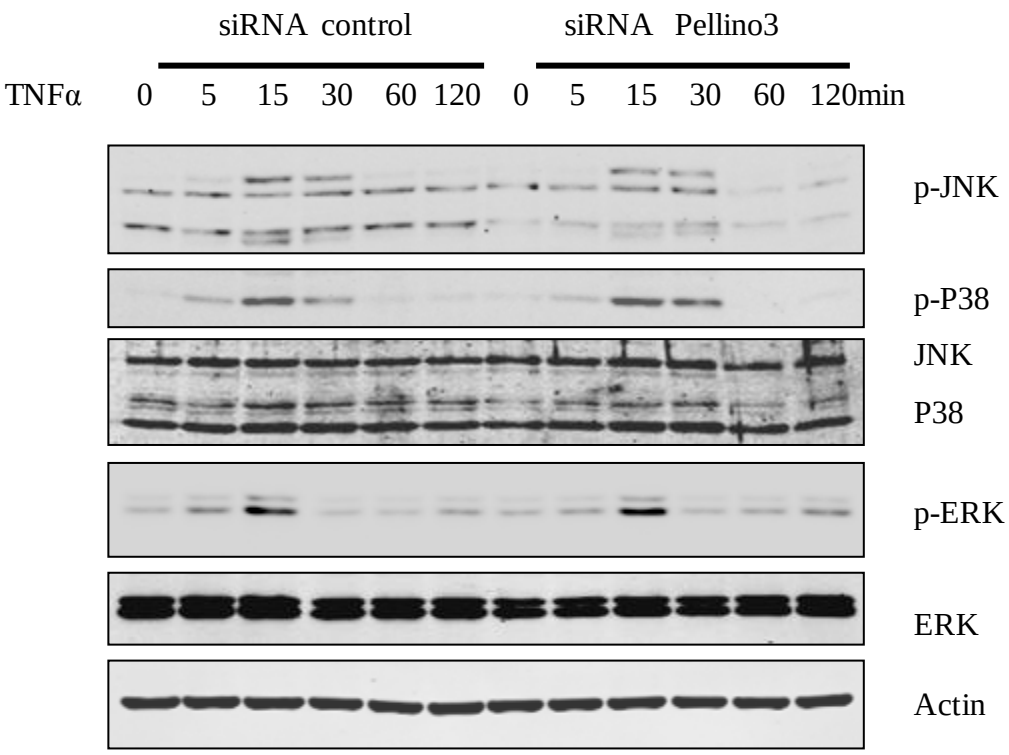

Figure 3-14 Effects of Pellino3 knockdown on TNF-induced activation of MAPKs in HEK293T cells.

HEK293T cells were transfected with control or Pellino3-specific siRNA and then treated with TNF (50ng/ml) for 18 hr. cells were treated in the absence (0) or presence of human TNF (50ng/ml) for indicated times. Cell lysates were prepared and immunoblotted for phosphorylated levels of JNK (p-JNK), P38 (p-P38), ERK (p-ERK) and total levels of JNK, P38 and ERK. Lysates were also probed for levels of β-actin to act as loading controls.

3.4 Pellino3 is involved in DISC formation

Given that the proapoptotic effects of Pellino3 knockdown can not be attributed to inhibition of NF-κB or activation of MAPKs, the direct effects of knockdown on the apoptotic pathway were examined. TNF-induced apoptosis is known to proceed through the recruitment of proteins such as TRADD, TRAF2, RIP1, caspase-8 and FADD to form a complex named DISC, which together serve as a cell death checkpoint control in TNF-sensitive cells (Micheau and Tschopp, 2003). The role of Pellino3 in DISC formation was next determined.

3.4.1 Loss of Pellino3 facilitates the formation of DISC

The importance of Pellino3 in DISC formation was evaluated by measuring the interaction of DISC components, in response to TNF, in Hela cells infected with Pellino3 specific shRNA. Hela cells infected with Pellino3 or control shRNA were treated with TNF plus CHX as well as z-VAD-FMK for 2 or 5 hr. Cells were lysed and subjected to immunoprecipitation using an anti-caspase-8 antibody. Expression of RIP1 and FADD in the whole cell lysates were examined by Western blotting. Co-immunoprecipitation studies on the endogenous signalling proteins confirmed previous reports that TNF promotes time-dependent interaction of caspase-8 with FADD and RIP1 to form DISC in Hela cells (Figure 3-15) (Kundu, 2009). Upon TNF treatment, FADD and RIP1 formed a complex with caspase-8 at 5 hr in control cells but the levels of FADD and RIP1 that co-precipitated with caspase-8 were increased in Pellino3 knockdown cells. Furthermore the interaction of caspase-8 and FADD was apparent at earlier times. The marked enhancement of FADD recruitment to caspase-8 was also confirmed in Pellino3 knockdown in HEK293T cells. The effect of knockdown of Pellino3 by siRNA on the recruitment of FADD to caspase-8 was examined at 2 or 5 hr

after stimulated with TNF plus CHX as well as z-VAD-FMK and again increased DISC formation was observed in Pellino3 knockdown cells (Figure 3-16).

Collectively, these data imply that Pellino3 regulates the interaction of RIP1 and FADD with caspase-8 upon TNF stimulation.

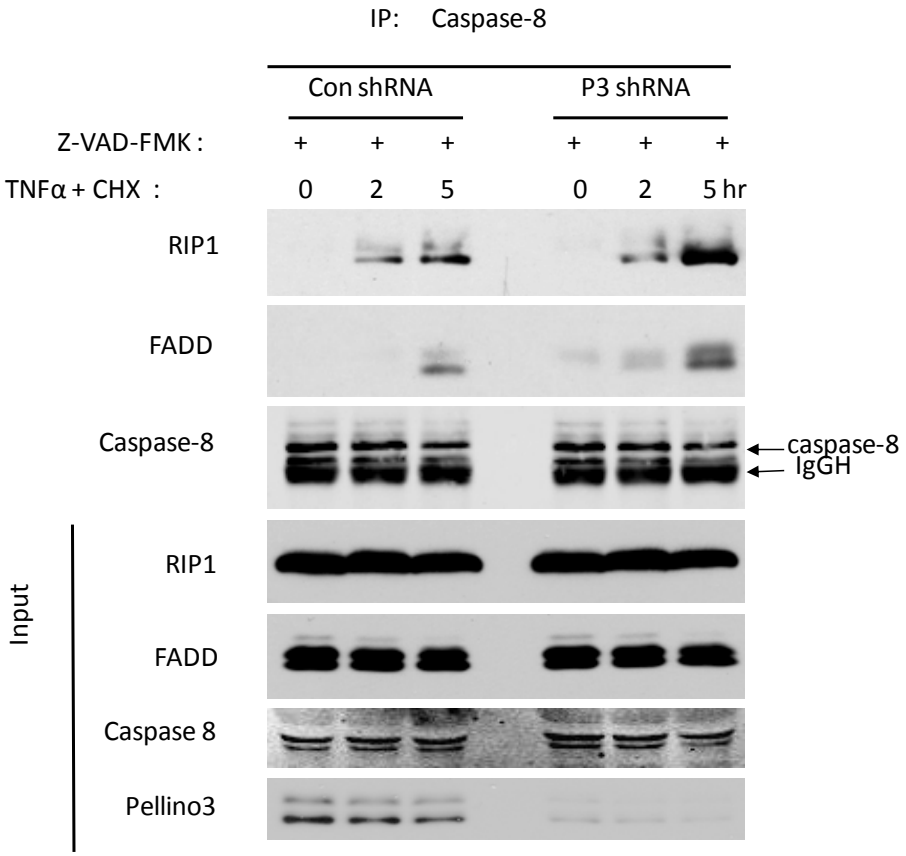

Figure 3-15 Knockdown Pellino3 by shRNA facilitates the formation of DISC in Hela cells.

Hela cells were infected with lentivirus containing constructs that encoded control or human Pellino3-specific shRNA. Cells were grown in the presence of puromycin to select for cells showing stable integration of shRNA constructs. Selected cells were treated in the absence (control) or presence of human TNF (40ng/ml) plus CHX (10μg/ml) for indicated times. In addition to the indicated treatments all cells were treated with zVAD-fmk to prevent activation of caspase-8 and cell death. Cell lysates were immunoprecipitated with anti-caspase-8 antibody and immunoprecipitates were subsequently analyzed for co-precipitated RIP1, FADD and caspase-8 by Western blotting. The expression levels of RIP1, FADD, caspase-8 and Pellino3 in whole cell lysates (‘input’) were also assessed by Western blotting.

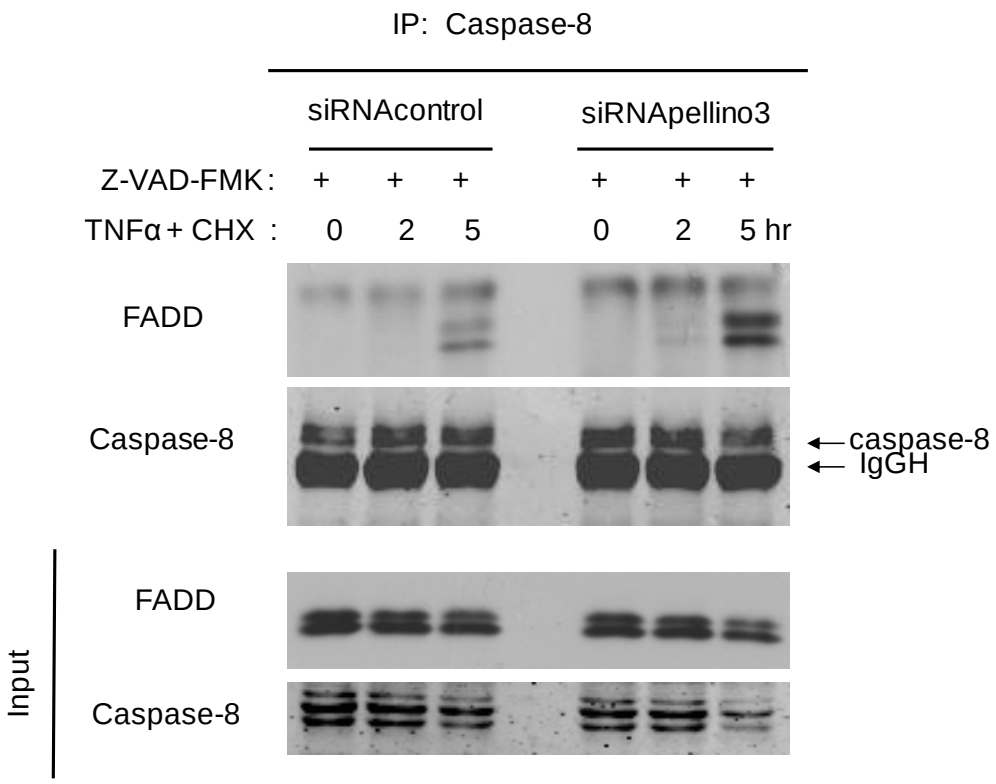

Figure 3-16 Knockdown Pellino3 by siRNA promotes the recruitment of FADD to caspase-8 in HEK293T cells

HEK293T cells were transfected with control or Pellino3-specific siRNA and then treated with human TNF (50ng/ml), CHX (10μg/ml) and zVAD-fmk (20mM) for indicated times. Cell lysates were immunoprecipitated with anti-caspase-8 antibody and immunoprecipitates were subsequently assayed for co-precipitated FADD and caspase-8 by Western blotting. The expression levels of FADD and caspase-8 in whole cell lysates ('input') were also assessed by Western blotting.

3.4.2 Pellino3 interacts specifically with RIP1

RIP1 acts as a central signalling molecule in the TNF pathway by regulating the activation of the NF-κB and MAPKs pathways as well as the induction of apoptosis or necroptosis (Festjens et al., 2006; Holler et al., 2000; Kelliher et al., 1998). RIP1 consists of a C-terminal DD, which can be recruited to several death receptors and interacts with FADD, a RHIM, which can be recruited to TRIF and interacts with RIP3 ((Stanger et al., 1995; Sun et al., 2002). Ubiquitination and deubiquitination of RIP1 play important roles in the regulation of TNF–induced NF-κB activation (Bertrand et al., 2008; Wertz and Dixit, 2010).

Given the importance of RIP1 in TNF signalling, coupled to the recent report of Pellino1 acting as an E3 ubiquitin ligase for RIP1 (Chang et al., 2009), the latter was examined as a potential target for Pellino3. Therefore an immunoprecipitation assay was performed to explore the possible interactions between Pellino3 and RIP1 after transient transfection in HEK293T cells. HA-tagged RIP1 was coexpressed with myc-tagged Pellino3s or Pellino3l, immunoprecipated with anti-myc antibodies and the subsequent precipitate was analyzed for the presence of HA-tagged RIP1 by anti-HA Western blotting. As shown in Figure 3-17A, RIP1 indeed precipitates with both Pellino3s and Pellino3l. The reciprocal coimmunoprecipitation assay (anti-HA immunoprecipitation followed by anti-myc Western blotting) also showed a positive *in vivo* interaction between Pellino3 and RIP1 (Figure 3-17B).

To investigate whether or not Pellino3 directly binds to RIP1, an *in vitro* binding assay was performed. Purified recombinant forms of Pellino3s and 3l were shown to be each capable of pulling down *in vitro* translated RIP1 from lysates of HEK293T cells (Figure 3-17C). RIP1 does not bind to the beads alone.

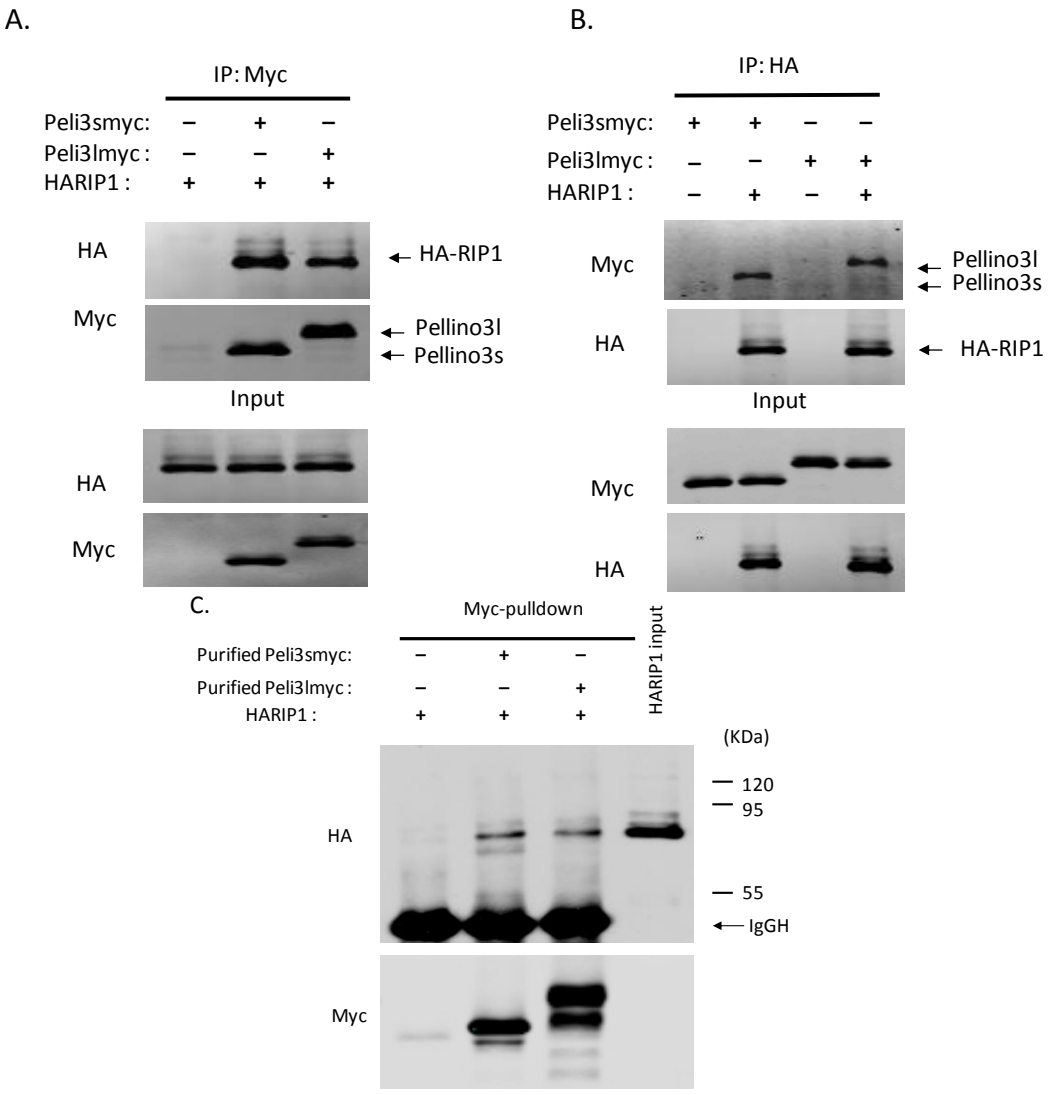

Figure 3-17 : Pellino3 interacts with RIP1.

(A, B) HEK293T cells were co-transfected with indicated combinations of constructs encoding HA-tagged RIP1 and myc-tagged Pellino3s or Pellino3l. The caspase inhibitor CrmA was also trasfected to prevent caspase induced cleavage of RIP1 and consequently cell apoptosis . (A) Cell lysates were immunoprecipitated (IP) using anti-myc antibody, followed by immunoblotting using anti-HA for RIP1. (B) Reciprocal coimmunoprecipitation assays were performed using anti-HA antibody followed by immunoblotting using anti-myc antibody for Pellino3. RIP1, Pellino3 and the precipitated IgG heavy chain (IgGH) are indicated by arrows. (C) Purified myc-tagged Pellino3s, Pellino3l, was immunoprecipitated with anti-myc antibody and then incubated with HEK293T cell lysates from cells previously transfected with HA-tagged RIP1. Samples were then precipitated (myc-pulldown) and analysed by immunoblotting using anti-myc and -HA antibodies. Input HA-RIP1 protein is shown at right.

3.4.3 Pellino3 interacts directly with the caspase domain of caspase-8

Pellino3 was next assessed for its ability to interact with another component of the DISC, caspase-8. The co-expression of HA-tagged pro-caspase-8 (with a mutation to prevent autocleavage) with myc-tagged Pellino3s or Pellino3l followed by co-immunoprecipitation analysis demonstrated that Pellino3 proteins and pro-caspase-8 were reciprocally co-immunoprecipitated (Figure 3-18).

The interaction between Pellino3 and procaspase-8 is direct in nature since purified recombinant forms of both proteins interact with each other *in vitro* (Figure 3-19).

To map the interaction regions between procaspase-8 and Pellino3 proteins the interaction of Pellino3 with various caspase-8 mutants was evaluated. Procaspase-8 contains two death effector domains (DEDa and DEDb) in its N-terminal pro-domain (residues 1-194) and a C-terminal region (residues 195-479) that encodes the catalytic large (p18) and small subunits (p10) (Fan et al., 2005). The DED is a protein interaction domain that plays a critical role for caspase-8 dimerization and for its interaction with FADD. Schematic illustration of Procaspase-8 and its truncated constructs is shown on Figure 3-20A. Expression constructs encoding procaspase-8, DEDa / DEDb and caspase regions of caspase-8 were co-expressed with Pellino3s in HEK293T cells. Procaspase-8 and its caspase region were shown to interact with Pellino3 using co-immunoprecipitation analysis whereas there was no such interaction between the DEDa/DEDb domain and Pellino3 (Figure 3-20B). The interaction of the caspase domain with Pellino3 was proven to be direct in nature by showing that purified recombinant forms of the caspase domain interacts with Pellino3 *in vitro* (Figure 3-21), whereas the DED domain fails to interact with Pellino3 (Figure 3-22).

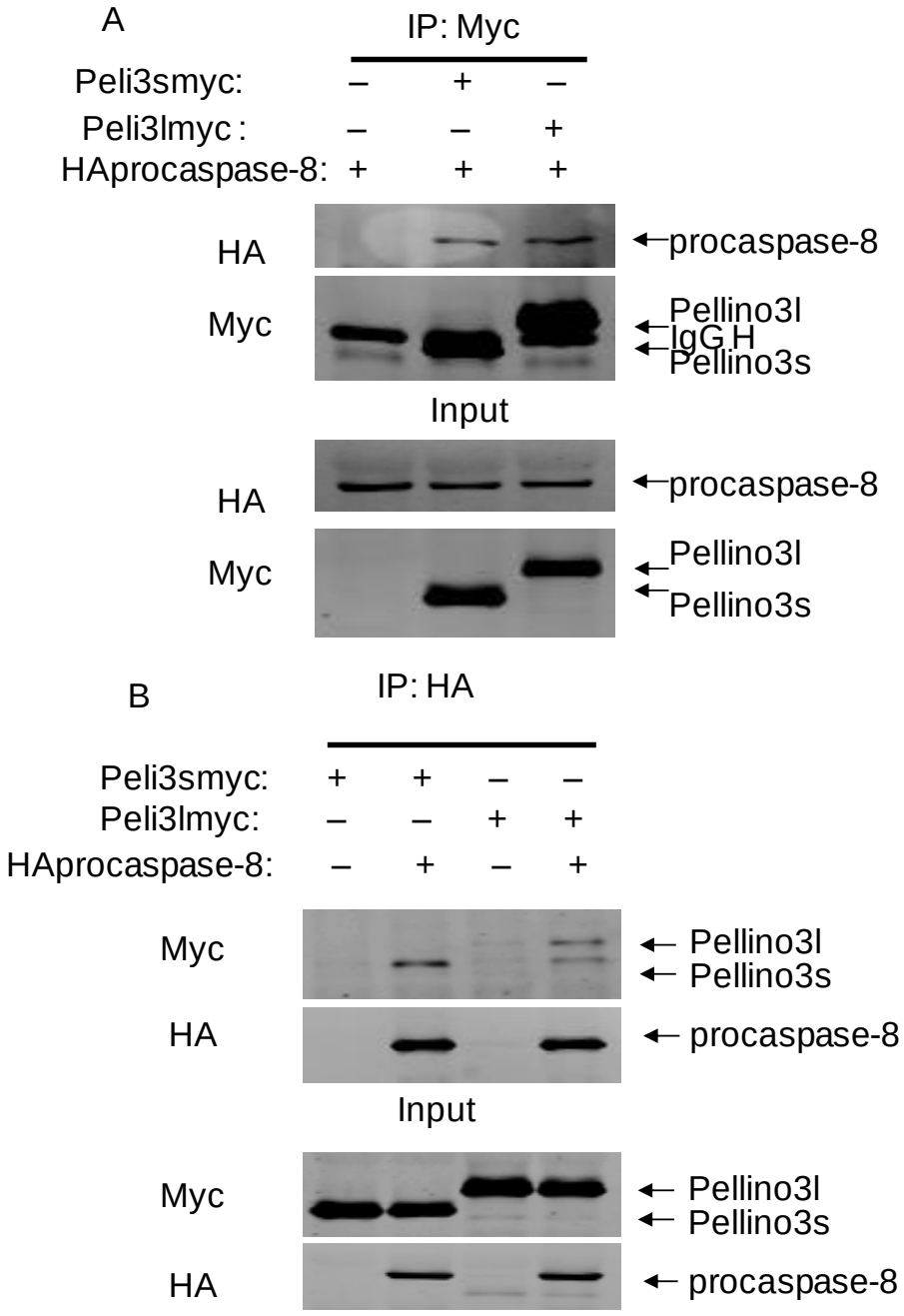

Figure 3-18 Pellino3 co-immunoprecipitates with caspase-8.

HEK293T cells were co-transfected with indicated combinations of constructs encoding HA-tagged procaspase-8 and myc-tagged Pellino3s or Pellino3l. (A) Cell lysates were immunoprecipitated (IP) using anti-myc antibody, followed by immunoblotting using anti-HA for procaspase-8. (B) Reciprocal coimmunoprecipitation assays were performed using anti-HA antibody followed by immunoblotting using anti-myc antibody for Pellino3.

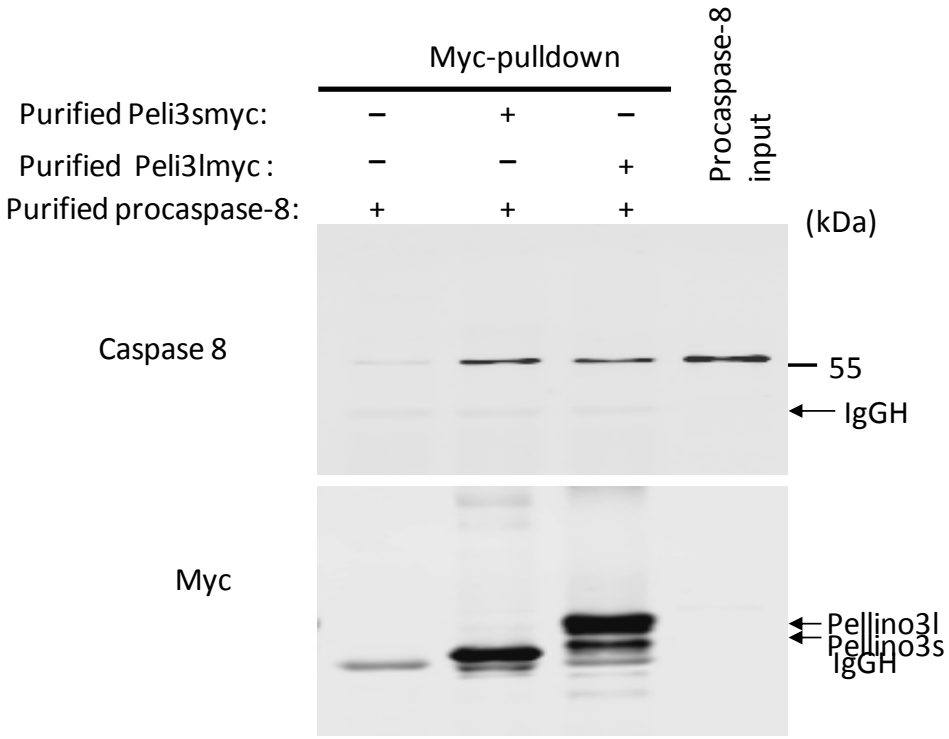

Figure 3-19 Pellino3 interacts directly with caspase-8.

Purified myc-tagged Pellino3s or Pellino3l was immunoprecipitated with anti-myc antibody and then incubated with purified procaspase-8 protein. Samples were then precipitated (myc-pulldown) and analysed by immunoblotting using anti-myc or –caspase-8 antibodies. Input procaspase-8 protein is shown at right.

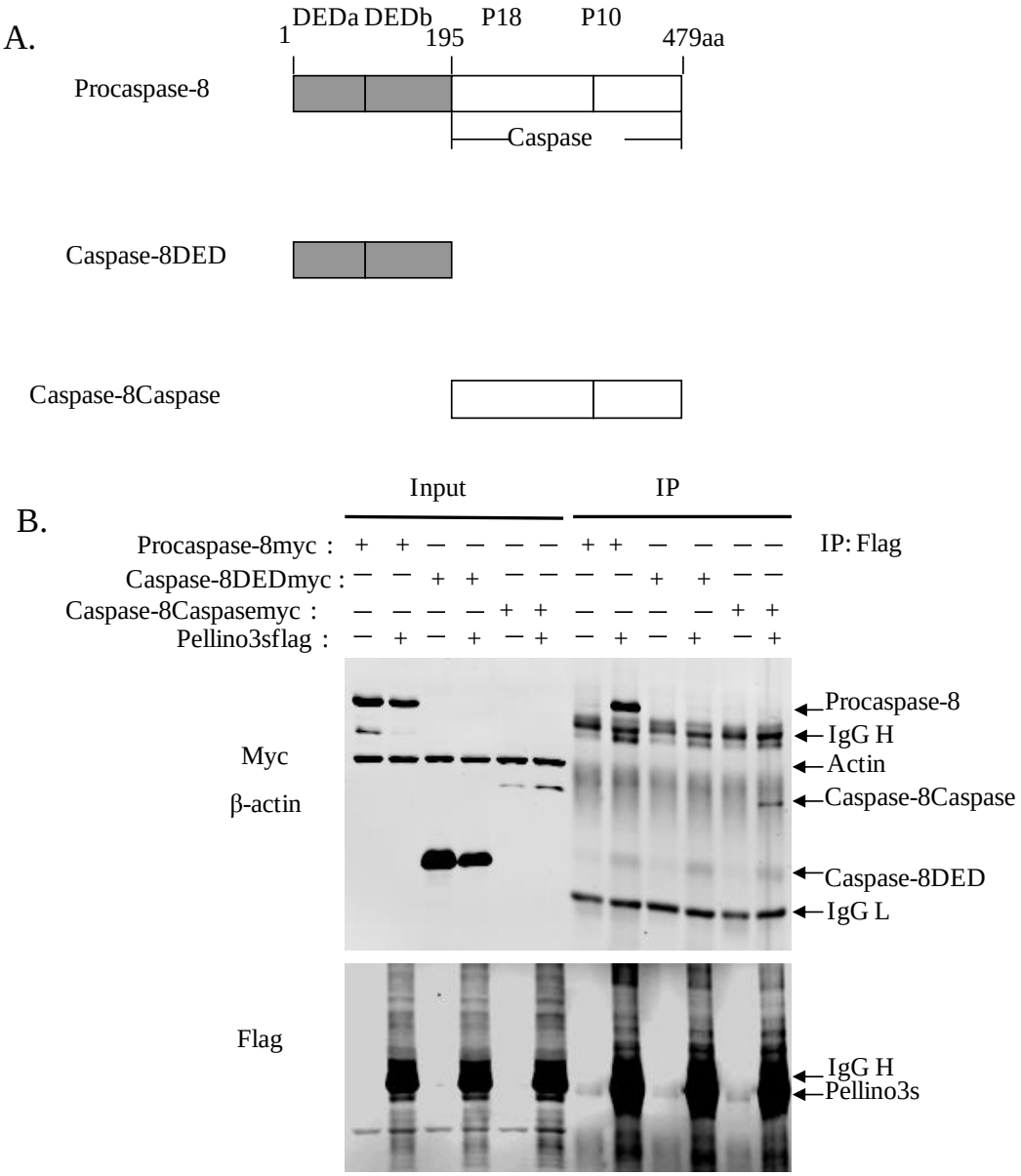

Figure 3-20 Pellino3 interacts with caspase-8 via its caspase domain in HEK293T cells.

(A) Procaspase-8 and its truncated constructs, caspase-8 DED domain (residues 1-194), caspase-8-caspase domain (residues 195-479) were chematic illustrated. (B) HEK293T cells were co-transfected with the indicated combinations of constructs encoding myc-tagged procaspase-8, caspase-8 DED domain, caspase-8-caspase domain and flag-tagged Pellino3s. Cell lysates were immunoprecipitated (IP) using an anti-flag antibody, followed by immunoblotting using anti-myc, -flag or –β-actin antibodies.

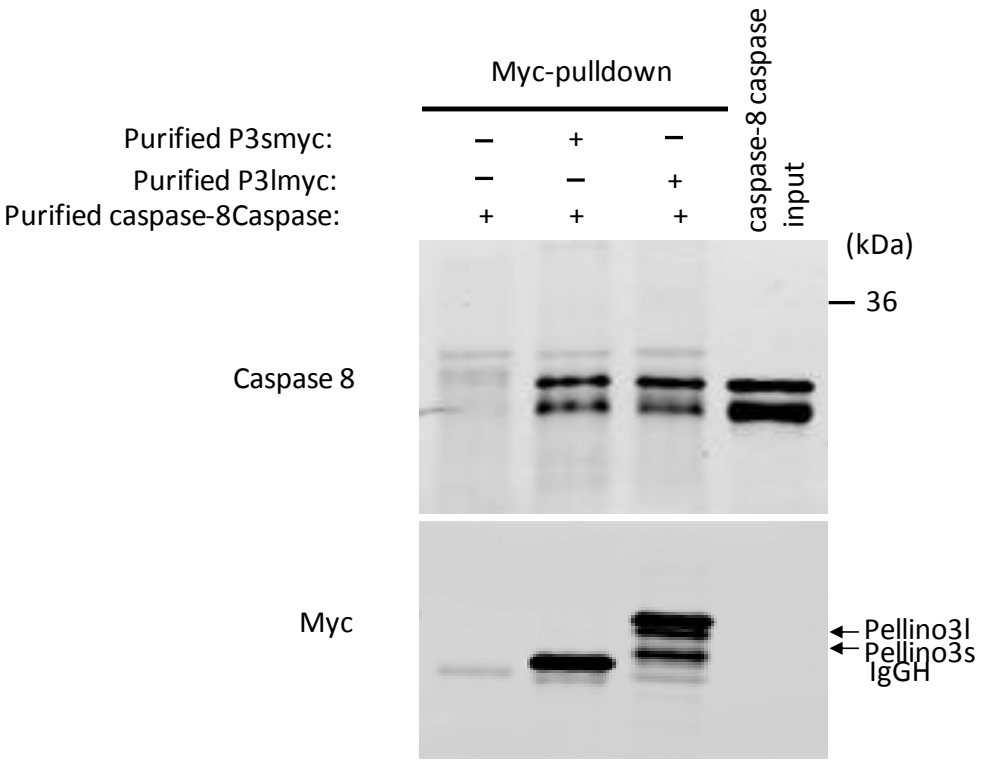

Figure 3-21 Pellino3 interacts directly with caspase-8 via its caspase domain.

Purified myc-tagged Pellino3s or Pellino3l was immunoprecipitated with anti-myc antibody and then incubated with purified caspase-8 caspase domain. Samples were then precipitated (myc-pulldown) and analysed by immunoblotting using anti-myc or –caspase-8 antibodies. Samples of recombinant Pellino proteins and caspase-8 caspase domain, prior to immunoprecipitation (Input), were similarly analysed by immunoblotting. The mobility of each protein, including the precipitated IgG heavy chain (IgGH), is indicated by an arrow.

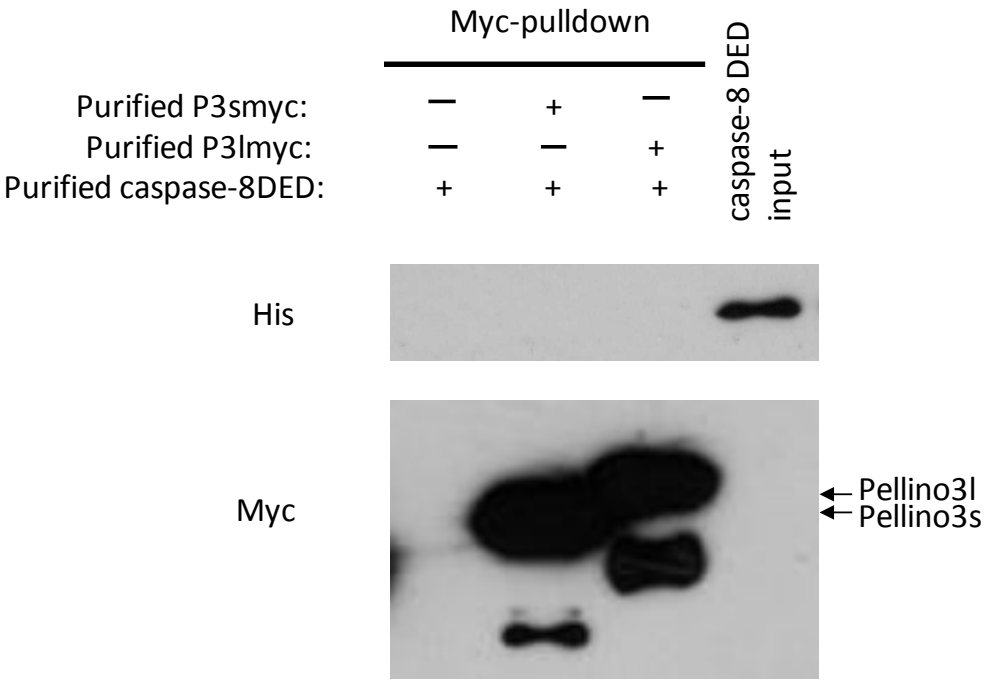

Figure 3-22 Pellino3 does not interacts with caspase-8 DED domain in vitro.

Purified myc-tagged Pellino3s or Pellino3l was immunoprecipitated with anti-myc antibody and then incubated with purified caspase-8 DED domain. Samples were then precipitated (myc-pulldown) and analysed by immunoblotting using anti-His-HRP antibody.

3.4.4 Pellino3 does not interact with FADD

FADD, a 26 kD cytoplasmic protein, contains two interaction motifs: a DD that associates with the DD-containing apoptosis signalling proteins, such as RIP1, and a DED that interacts with a homologous DED in procaspase-8 or procaspase-10 (Boldin et al., 1995; Jeong et al., 1999). It is well-established that FADD plays a role as a mediator of apoptosis (Wilson et al., 2009; Yeh et al., 1998; Zhang et al., 1998). In response to stimulation of TNF, FADD is rapidly recruited to RIP1 through its DD. The interaction of FADD and RIP1 unmasks the DED domain of FADD, allowing the

recruitment of subsequent caspases and thereby activating a cysteine protease cascade leading to cell death (Muzio et al., 1996).

Expression constructs encoding Flag-FADD were co-expressed with Pellino3s in HEK293T cells. Co-immunoprecipitation analysis showed that there was no interaction between FADD and Pellino3 (Figure 3-23).

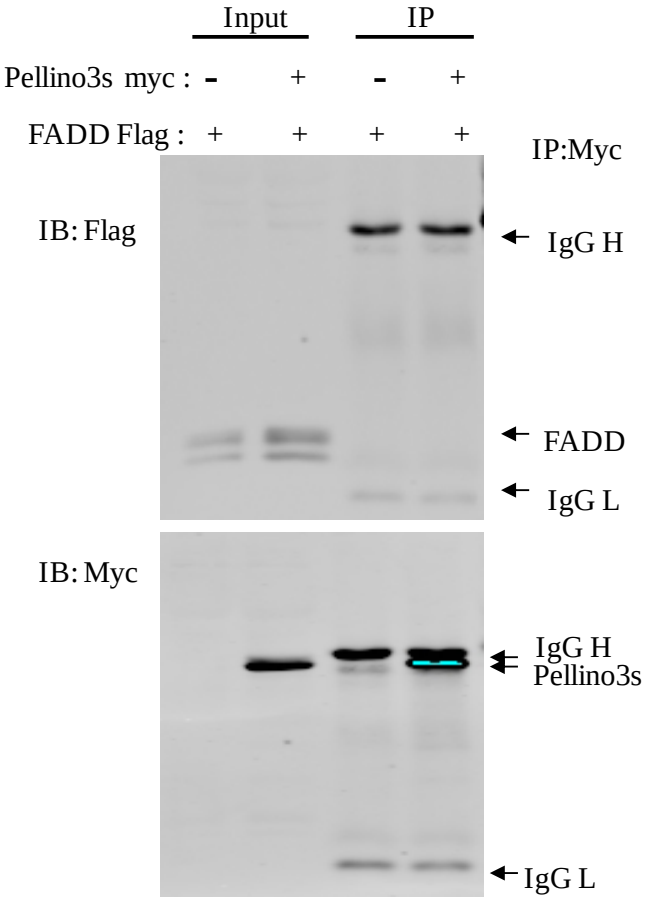

Figure 3-23 Pellino3 does not interact with FADD.

HEK293T cells were co-transfected with indicated combinations of constructs encoding Flag-tagged FADD and myc-tagged Pellino3s. Cell lysates were immunoprecipitated (IP) using anti-myc antibody, followed by immunoblotting using anti-Flag for FADD.

3.5 The FHA domain of Pellino3 mediates its capacity for regulating DISC formation

Pellino proteins contain an N-terminal cryptic phospho-threonine-binding FHA domain that facilitates interaction with phosphorylated IRAK1 (Lin et al., 2008) and a C-terminal RING-like domain that catalyses K63 polyubiquitination of IRAKs (Butler et al., 2007; Ordureau et al., 2008; Schauvliege et al., 2006).

The functional contributions of the different domains of Pellino3 to its regulatory effects on TNF signalling were next assessed. This was addressed by experiments that aimed to rescue the phenotypic effects of Pellino3 knockdown on TNF signalling in HEK293T cells, using various forms of Pellino3. A series of mutants were generated: firstly, FHA domain mutants in which arginine (R) and serine (S) were mutated to alanine (A) at residues 155 and 185 in Pellino3l and residues 131 and 161 in Pellino3s, respectively (Figure 3-24A), and secondly RING domain mutants in which the cysteine (C) residues 384 and 387 in Pellino3l and residues 360 and 363 in Pellino3s were mutated to alanine (A), respectively (Figure 3-24B).

Wild-type or mutant forms of myc tagged Pellino3 were introduced into Pellino3 shRNA-infected HEK293T cells. TNF-induced apoptosis was tested by FACS and Western blotting. These experiments revealed that wild-type Pellino3 protected Pellino3 deficient cells from TNF-induced apoptosis, indicating that both spliced forms can temper the pro-apoptotic signalling of TNF. Intriguingly forms of Pellino3, containing mutations in their RING-like domain inhibited the ability of TNF to promote increased Annexin V staining and cleavage of PARP and caspase-3 in Pellino3 knockdown cells. By contrast, FHA domain mutants of Pellino3 (Pellino3 FHAm) failed to mimic their wild type counterparts in rescuing the pro-apoptotic effects of TNF (Figure 3-25). At 24

hr post-transfection, cells were treated with TNF plus CHX for another 5 hr before cell viability analysis. As shown in Figure 3-25A, overexpression of wild-type and RING domain mutants of Pellino3 enhanced cell viability compared with control cells (EV: 37%). In contrast, Pellino3-FHA mutants failed to inhibit the TNF-induced increases in Annexin V staining. Western blot analysis further showed that the expression of Pellino3 FHA mutants failed to rescue the increase cleavage of PARP and caspase-3 that was observed in response to Pellino3 knockdown (Figure 3-25B). In contrast, wild-type Pellino3 and RING domain mutants of Pellino3 successfully reduced caspase-3 and PARP cleavage. These data suggest a dispensable role for the RING-like domain of Pellino3 in manifesting its regulatory effects on TNF signalling. In contrast the FHA domain is of crucial importance.

To determine whether Pellino3's FHA domain mediates Pellino3's capacity to regulate DISC formation and whether it regulates the association of DISC proteins, wild-type or mutant forms of myc-tagged Pellino3 were introduced into Pellino3 shRNA infected HEK293T cells. Cells were treated with TNF plus CHX for 5 hr with the presence of zVAD-fmk to prevent activation of caspase-8 and cell death. The associated proteins in the lysates were pulled down with anti-caspase-8 antibody. The expression of RIP1 and FADD in immunoprecipitates and cell lysates were analyzed by Western blotting. Wild-type Pellino3s blocked the recruitment of endogenous FADD to caspase-8 and attenuated the interaction between RIP1 and caspase-8. The E3 mutant showed very similar ability like its wild type counterpart. However, introduction of the FHA mutant Pellino3s did not affect the interaction between FADD and caspase-8 or RIP1 and caspase-8 (Figure 3-26). This rescue experiment was also performed with Pellino3l and its mutants and equivalent results were apparent (Figure 3-27), suggesting both forms of Pellino3 can control TNF-induced apoptosis by regulating the formation of DISC.

These findings also indicate a critical role for the FHA domain of Pellino3 proteins in counter-regulating the pro-apoptotic proclivity of TNF signalling.

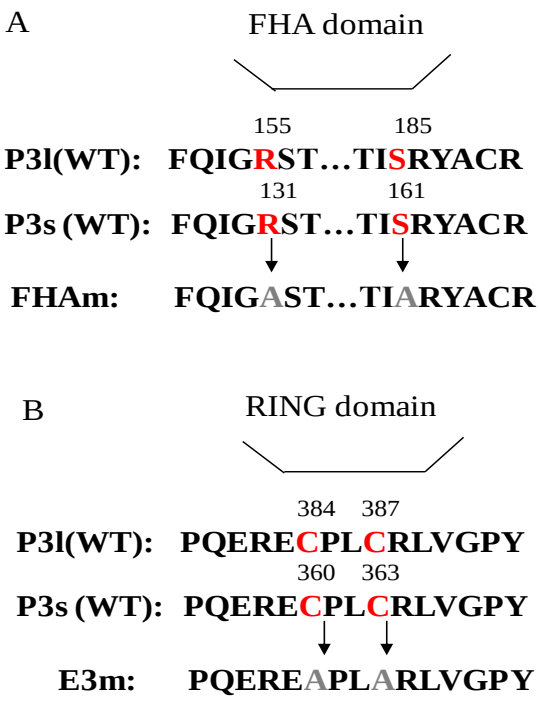

Figure 3-24 Mutational analysis of Pellino3.

(A) Partial nucleotide sequence of Pellino3 from the wild-type (upper panel) and FHA mutated (lower panel) alleles. The mutations are indicated by an arrow. (B) Partial nucleotide sequence of Pellino3 from the wild-type (upper panel) and RING mutated (lower panel) alleles. The mutations are indicated by an arrow.

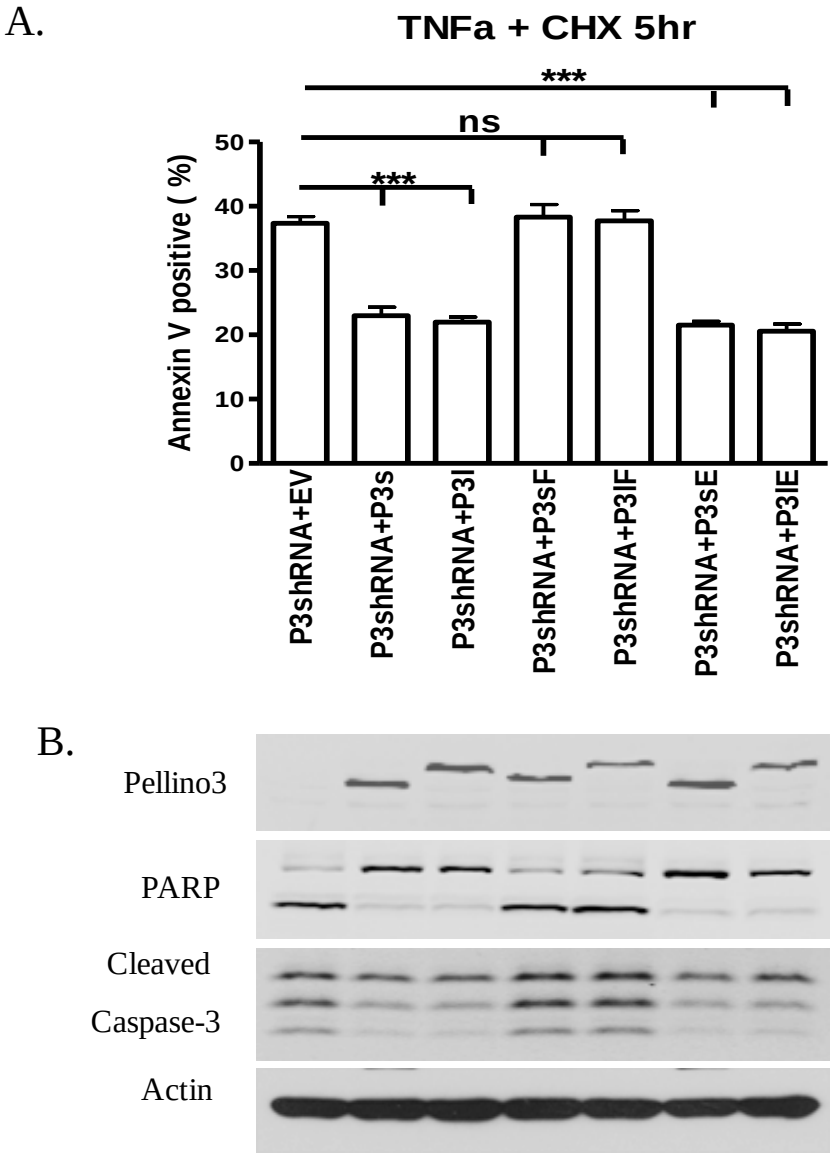

Figure 3-25 Wild type and RING mutants of Pellino3 rescue cells from TNF-induced apoptosis but FHA mutants are ineffective.

HEK293T cells, previously transfected with an expression construct encoding Pellino3-specific shRNA, were transfected with pcDNA3.1 empty vector (EV) or pcDNA3.1 encoding myc-tagged Pellino3s, Pellino3l, Pellino3sFHAm, Pellino3lFHAm, Pellino3sE3m or Pellino3lE3m. Transfected cells were treated with human TNF (40ng/ml) and CHX (10 μg/ml) for 5 hr. (A) Cells were analyzed by flow cytometry for percentage of cells staining positive for Annexin V staining. Data represent the mean +/- S.D. of 3 independent experiments; ***$p<0.001$. (B) The expression levels of Pellino3, PARP, cleaved caspase-3 and β-actin were measured in cell lysates by Western blotting.

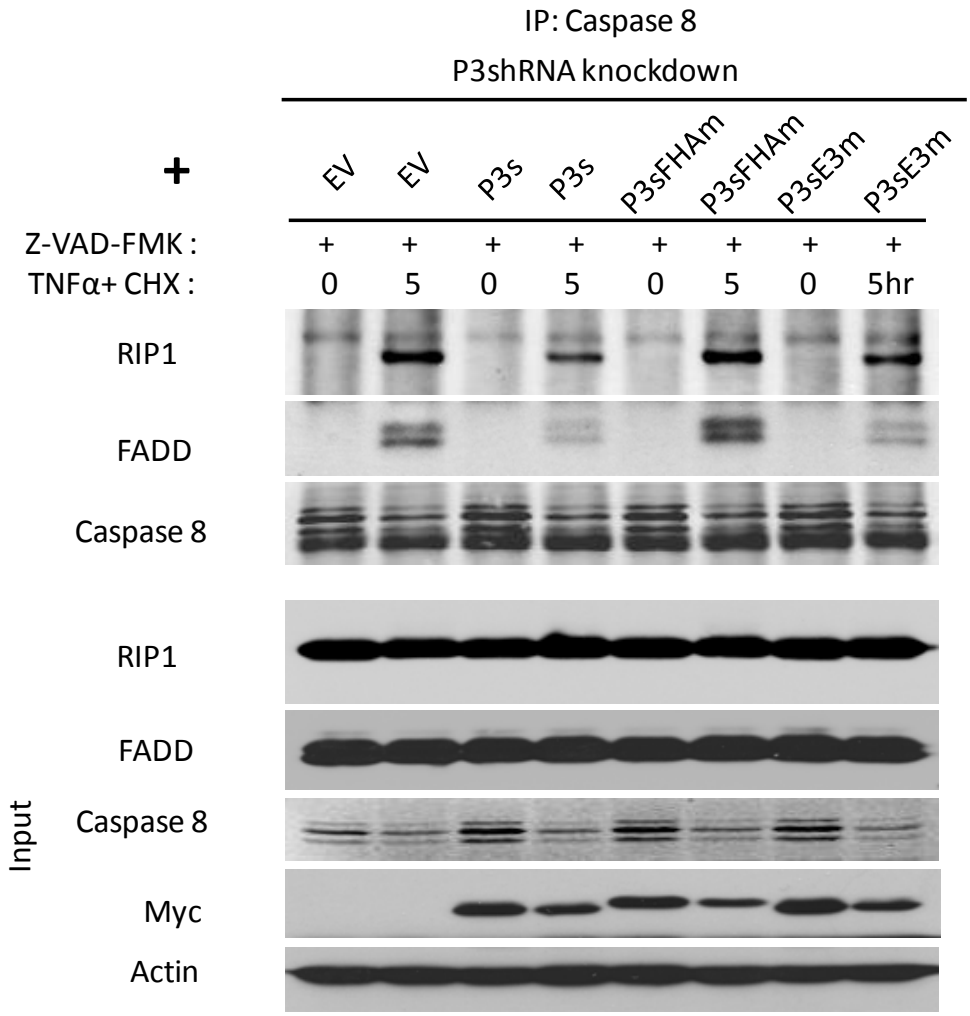

Figure 3-26 Wild type and RING mutants of Pellino3s inhibit TNF-induced formation of DISC.

HEK293T cells, previously transfected with an expression construct encoding Pellino3-specific shRNA, were transfected with pcDNA3.1 empty vector (EV) or pcDNA3.1 encoding myc-tagged Pellino3s, Pellino3sFHAm or Pellino3sE3m. In addition to the indicated treatments with TNF and CHX (above) cells were also treated with zVAD-fmk to prevent activation of caspase-8 and cell death. Cell lysates were immunoprecipitated with an anti-caspase-8 antibody and immunoprecipitates were subsequently analyzed for co-precipitated RIP1, FADD and caspase-8 by Western blotting. The expression levels of RIP1, FADD, caspase-8, Pellino3 and β-actin were measured in whole cell lysates ('input') by Western blotting.

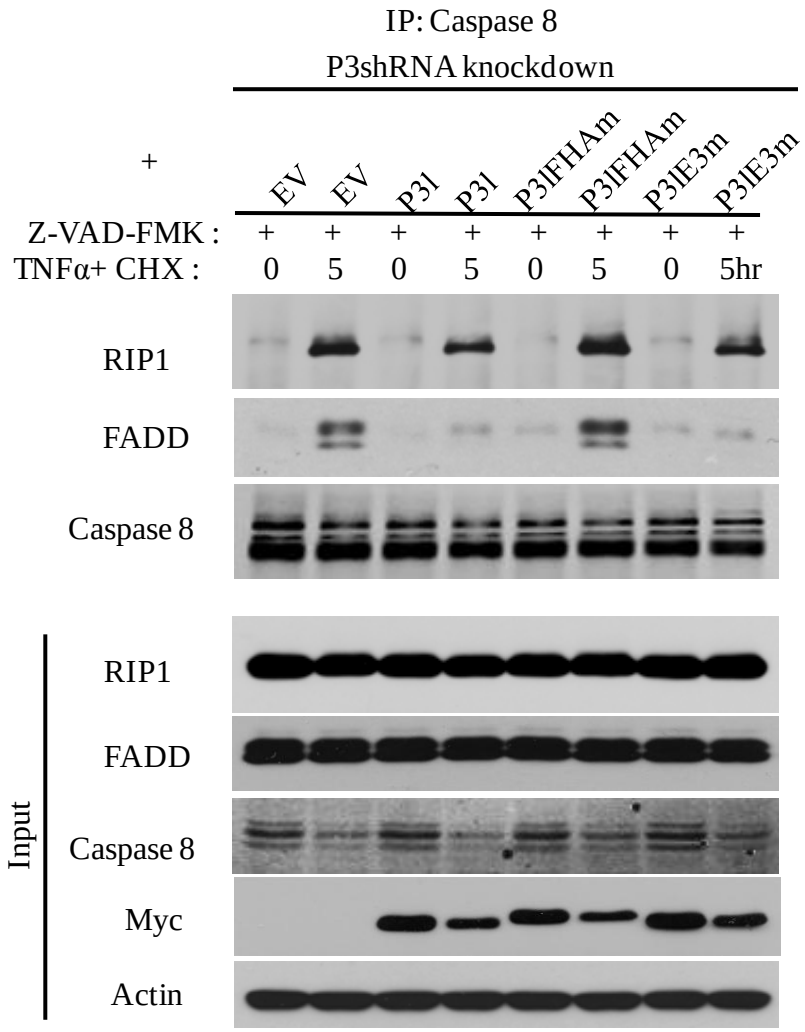

Figure 3-27 Wild type and RING mutants of Pellino3l inhibit TNF-induced formation of DISC.

HEK293T cells, previously transfected with an expression construct encoding Pellino3-specific shRNA, were transfected with pcDNA3.1 empty vector (EV) or pcDNA3.1 encoding myc-tagged Pellino3l, Pellino3lFHAm or Pellino3lE3m. In addition to the indicated treatments with TNF and CHX (above) cells were also treated with zVAD-fmk to prevent activation of caspase-8 and cell death. Cell lysates were immunoprecipitated with an anti-caspase-8 antibody and immunoprecipitates were subsequently analyzed for co-precipitated RIP1, FADD and caspase-8 by Western blotting. The expression levels of RIP1, FADD, caspase-8, Pellino3 and β-actin were measured in whole cell lysates (‘input’) by Western blotting.

Given the ability of Pellino3 to regulate TNF-induced DISC formation, the dynamics of interactions between Pellino3 and the components of DISC were assessed in response to TNF.

Co-immunopreciptiation analyses demonstrated that TNF promoted a strong and time-dependent interaction between endogenous RIP1 and Pellino3s (Figure 3-28 left panels) or Pellino3l (Figure 3-28 right panels). The recruitment of RIP1 to wild type Pellino3 was detectable following TNF stimulation within 2 hr. In contrast, TNF fails to drive the interaction of RIP1 with mutants of Pellino3 that lack a fully functional FHA domain (Figure 3-29). However the introduction of mutations in the RING-like domain of Pellino3s and Pellino3l failed to affect their associations with RIP1 or caspase-8 (Figure 3-30) excluding a role for this domain in facilitating such interactions. This is consistent with the lack of importance of the RING-like domain in mediating the regulatory effects of Pellino3 on TNF signalling.

Interestingly both spliced forms of Pellino3 interacted with endogenous caspase-8 in unstimulated cells and treatment with TNF failed to further enhance this interaction (Figure 3-28). Furthermore neither form of Pellino3 showed association with FADD irrespective of the absence or presence of TNF (third panel of Figure 3-28) and this is consistent with co-immunoprecipitation analysis with overexpressed proteins (Figure 3-23). The FHA mutants showed constitutive binding to caspase-8 (second panel of Figure 3-29) suggesting that the FHA domain is important for RIP1 binding but dispensable for caspase-8 binding.

These findings suggest a critical role for the FHA domain in facilitating the regulatory effects of Pellino3 on TNF signalling by targeting of RIP1 in response to TNF stimulation.

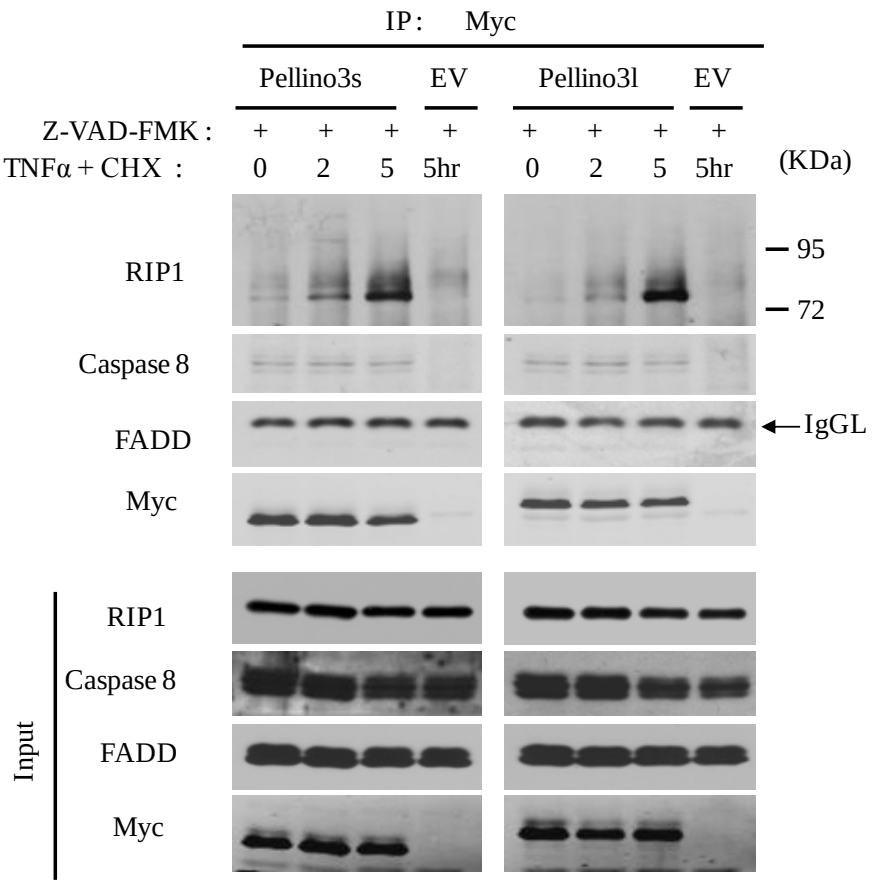

Figure 3-28 Pellino3 recruits RIP1 in response to TNF.

HEK293T cells were transfected with an empty vector (EV) or expression constructs encoding myc-taggged Pellino3s or Pellino3l. Cells were then treated in the absence or presence of TNF (50ng/ml) and CHX (10μg/ml) for indicated times. Cells were also treated with the pan-caspase inhibitor: zVAD-fmk (20μM) to prevent full activation of caspase-8 and cell death. Cell lysates were immunoprecipitated with an anti-myc antibody and immunoprecipitates were subsequently co-precipitated RIP1, caspase-8, FADD and myc-tagged Pellino proteins by Western blotting. The precipitated IgG light chain (IgGL) is indicated by an arrow. The expression levels of RIP1, caspase-8, FADD and myc-tagged Pellino proteins were measured in whole cell lysates (‘input’) by Western blotting.

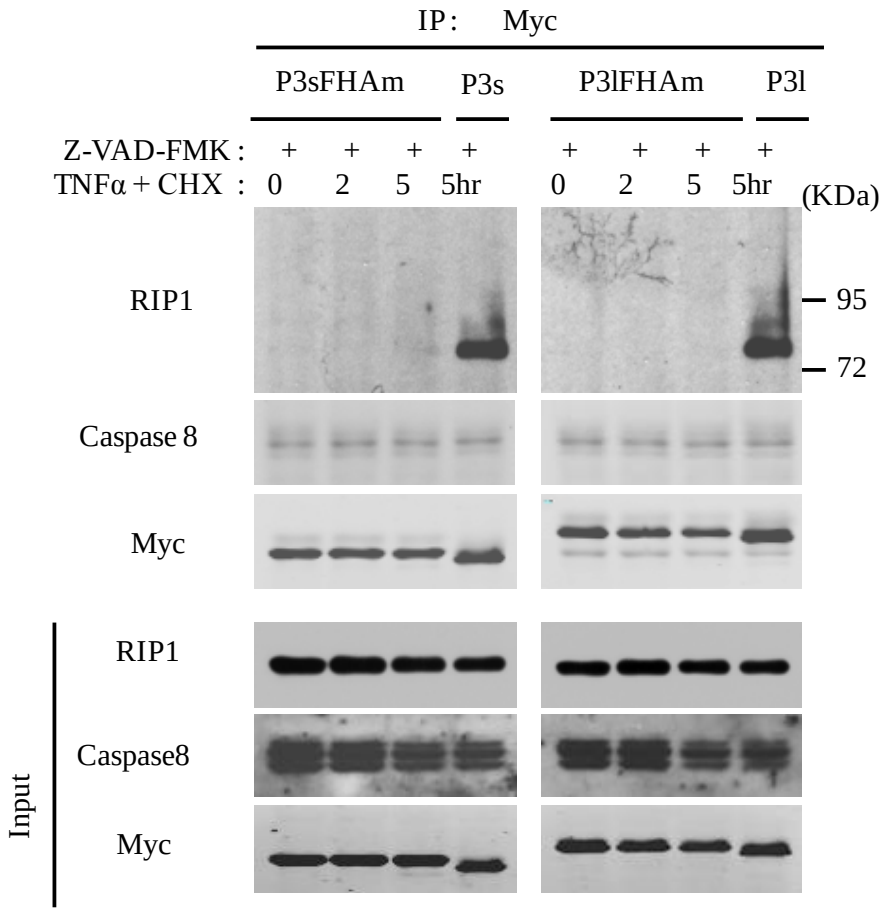

Figure 3-29 The FHA domain of Pellino3 is important for mediating its interaction with RIP1 in response to TNF.

HEK293T cells were transfected with an empty vector (EV) or expression constructs encoding FHA domain mutant forms of Pellino3s (P3sFHAm) or Pellino3l (P3lFHAm). Cells were then treated in the absence or presence of TNF (50ng/ml) and CHX (10μg/ml) for indicated times. Cells were also treated with the pan-caspase inhibitor: zVAD-fmk (20μM) to prevent full activation of caspase-8 and cell death. Cell lysates were immunoprecipitated with an anti-myc antibody and immunoprecipitates were subsequently co-precipitated RIP1, caspase-8, FADD and myc-tagged Pellino proteins by Western blotting. The precipitated IgG light chain (IgGL) is indicated by an arrow. The expression levels of RIP1, caspase-8, FADD and myc-tagged Pellino proteins were measured in whole cell lysates ('input') by Western blotting.

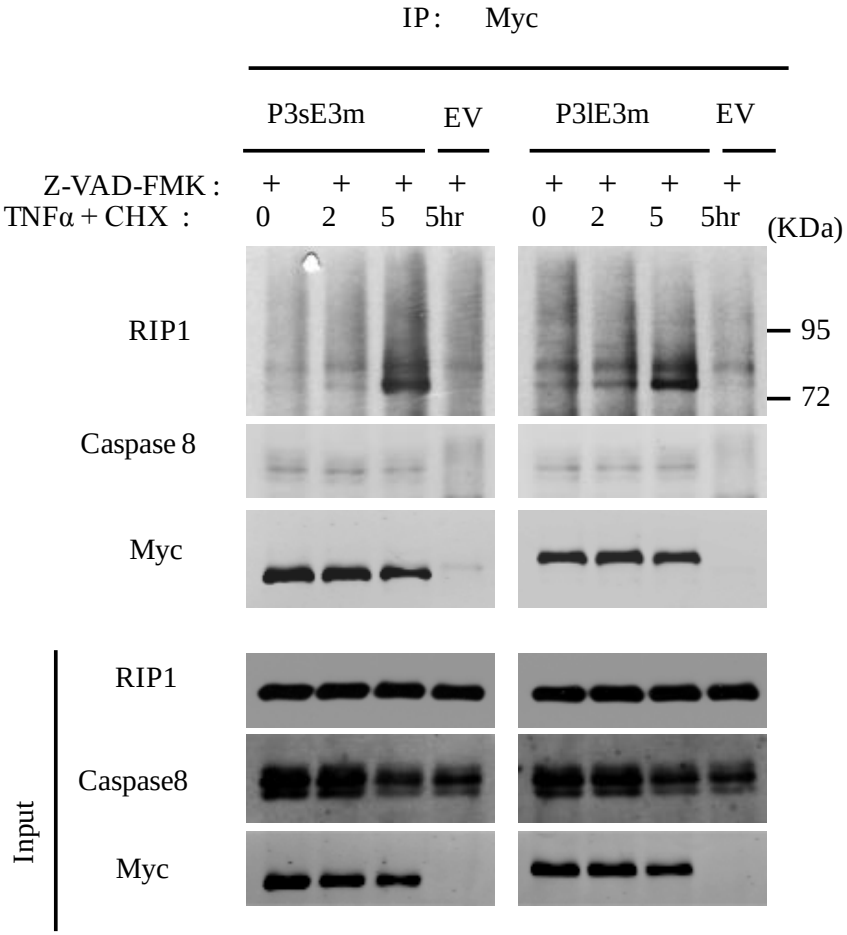

Figure 3-30 The RING-like domain of Pellino3 is dispensable for mediating its interaction with RIP1 in response to TNF.

HEK293T cells were transfected with an empty vector (EV) or expression constructs encoding RING-like domain mutant forms of Pellino3s (P3sE3m) or Pellino3l (P3lE3m). Cells were then treated in the absence or presence of TNF (50ng/ml) and CHX (10μg/ml) for indicated times. Cells were also treated with the pan-caspase inhibitor: zVAD-fmk (20μM) to prevent full activation of caspase-8 and cell death. Cell lysates were immunoprecipitated with an anti-myc antibody and immunoprecipitates were subsequently co-precipitated RIP1, caspase-8, FADD and myc-tagged Pellino proteins by Western blotting. The precipitated IgG light chain (IgGL) is indicated by an arrow. The expression levels of RIP1, caspase-8, FADD and myc-tagged Pellino proteins were measured in whole cell lysates ('input') by Western blotting.

Since the targeting of RIP1 by Pellino3 may act as a key contributing mechanism to the regulatory effects of the latter on the TNF pathway, the Pellino3-RIP1 interaction was further characterized. The FHA mutants of both Pellino3 proteins were compared with their wild type counterparts in terms of their capacity to interact with RIP1 using co-immunoprecipitation assay (Figure 3-31). The result demonstrates that the co-expression of either Pellino3s or Pellino3l with RIP1 leads to strong Pellino3-RIP1 interaction but point mutations in the FHA domains of both forms of Pellino3 leads to dramatic decreases in the levels of this Pellino3-RIP1 interaction, supporting a model where the FHA domain of Pellino3 facilitates its direct interaction with RIP1.

The reduced interaction is also evident in direct binding assays *in vitro* in which purified recombinant forms of the FHA mutants of Pellino3 failed to match their wild type counterparts in pulling down RIP1 from cell lysates (Figure 3-32). These findings support a model where Pellino3, via its FHA domain, directly targets RIP1 and so regulates DISC formation and ultimately apoptosis in response to TNF.

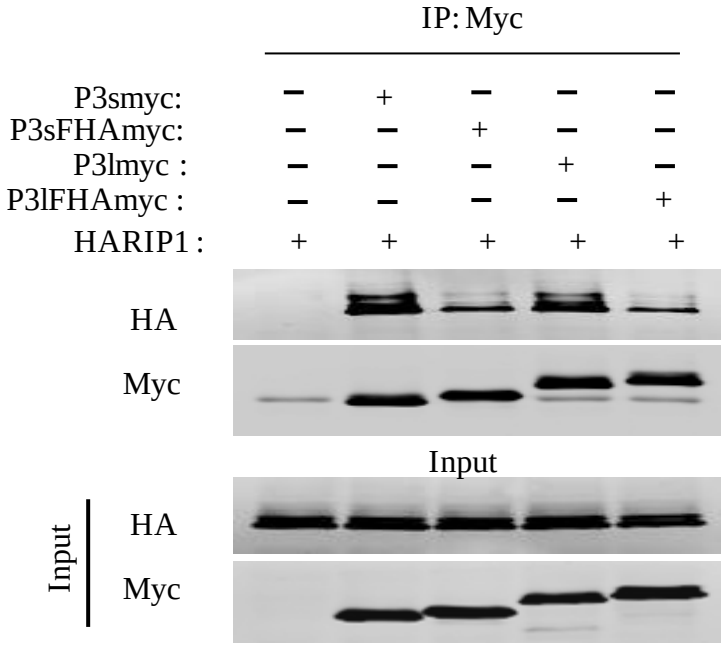

Figure 3-31 FHA domain of Pellino3 is required for its in vivo interaction with RIP1.

HEK293T cells were co-transfected with indicated combinations of constructs encoding HA-tagged RIP1 and myc-tagged Pellino3s or Pellino3l or their corresponding FHA mutants as described above. Such transfections also included co-expression of the caspase inhibitor CrmA to prevent caspase induced cleavage of RIP1 and cell apoptosis. Cell lysates were immunoprecipitated (IP) using an anti-myc antibody followed by immunoblotting using anti-HA or -myc antibodies. Cell lysates, prior to immunoprecipitation (Input), were similarly analysed by immunoblotting.

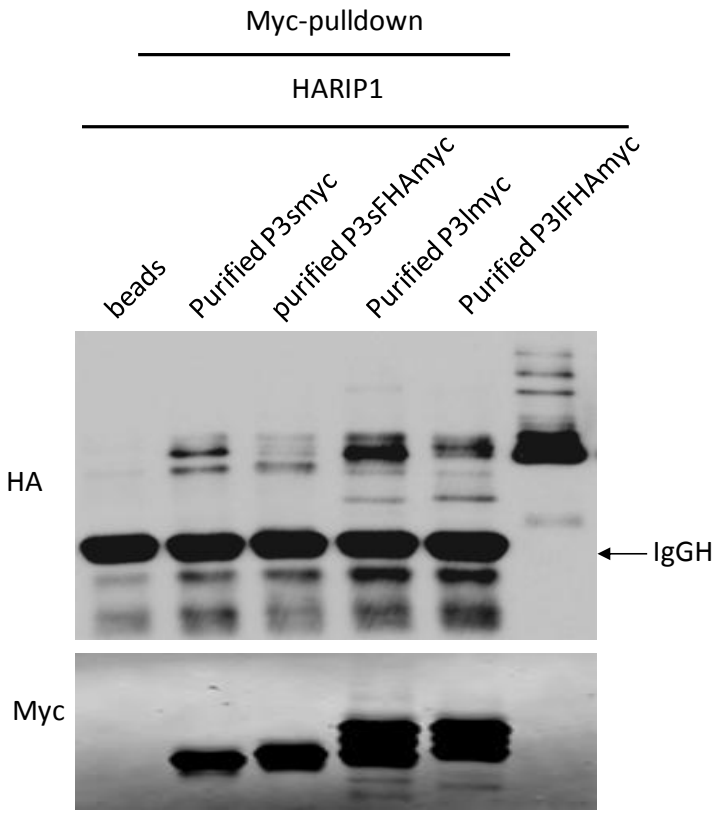

Figure 3-32 FHA domain of Pellino3 is required for its direct interaction with RIP1 in vitro.

Purified myc-tagged Pellino3s, Pellino3l or their FHA mutant counterparts were immunoprecipitated with an anti-myc antibody and then incubated with HEK293T cell lysates from cells previously transfected with HA-tagged RIP1. Samples were then precipitated (myc-pulldown) and analysed by immunoblotting using anti-HA or -myc antibodies. A cell lysate (prior to immunopreciptation (input)) from HEK293T cells previously transfected with HA-tagged RIP1 was also subjected to similar Western blot analysis.

3.6 Studies on Pellino3 knockout mice

3.6.1 Generation and genotyping Pellino3 knockout mice

In order to define the physiological relevance of the above findings and the role of Pellino3 in TNF signalling, Pellino3-deficient mice were generated with a floxed Pellino3 allele according to the strategy outlined in Figure 3-33. A mouse strain in which the Pellino3 gene was flanked by loxP sites was generated by Taconic Artemis using its proprietary technology. Briefly a targeting vector was constructed in which exon3 of the *Pellino3* gene was flanked by loxP sites and the positive selection marker (Puro) was inserted into intron 2. The targeting vector was generated using BAC clones from the C57BL/6J RPCI-23 BAC library and transfected into the Taconic Artemis C57BL/6N Tac ES cell line. Homologous recombinant clones were isolated using positive (Puromycin resistance) and negative (Thymidine kinase - Tk) selections and these were used for the generation of chimeric mice by blastocyst injection. Highly chimeric males were mated with C57BL/6 females and heterozygous offspring were identified by Southern blotting. To generate constitutive Pellino3-deficient mice, mice that were heterozygous for the targeted allele were bred with mice containing Cre recombinase regulated by the ROSA26 locus (C57BL/6-*Gt(ROSA)26Sor*^{tm}*16*$^{(Hasan\ et\ al.)Arte}$). This results in the deletion of exon 3 and loss of function of the Pellino3 gene by generating a frameshift in all downstream exons. The Cre transgene was subsequently removed by breeding the resulting Pellino3$^{+/-}$ mice with C57BL/6 mice during colony expansion. Mice were genotyped by PCR analysis of DNA isolated from ear punches.

Genotyping was performed using the PCR strategies described in chapter 2.2.1.4. An example of a typical gel picture of Pellino3 genotyping PCR is given in Figure 3-34. Genotyping PCR was performed to detect heterozygous/homozygous conventional

alleles (Figure 3-34 upper). A large internal control (585 bp) was amplified in each reaction. Genotypes that are homozygous or heterozygous support amplification as detected by the presence of a 370 bp band, whereas genotypes that are wild type do not support amplification. Genotyping PCR was also to detect heterozygous/homozygous conditional and wild type alleles (Figure 3-34 lower). Genotypes that are wild type or heterozygous support amplification as detected by presence of a 210 bp band, whereas genotypes that are homozygous fail to show an amplified fragment.

Confirmation of gene disruption was performed by RT–PCR and Real-time PCR. Primers that are specific to exon 3 of the murine Pellino3 gene were used to amplify Pellino3 mRNA, isolated from MEFs, in semi-quantitative (

Figure 3-35A) and real time RT-PCR (

Figure 3-35B). These studies demonstrated that Pellino3 mRNA expression was absent in Pellino3$^{-/-}$ mice.

To determine the effect of the Pellino3 knockout on expression of Pellino3 protein, Cell lysates were prepared from both WT and homozygous Pellino3 MEFs and subjected to Western blotting. Probing with an polyclonal anti-Pellino3 antibody revealed a Pellino3 protein of about 50 kDa in MEFs from wild-type embryo and this is absent in MEFs from Pellino3-deficient embryo (Figure 3-36).

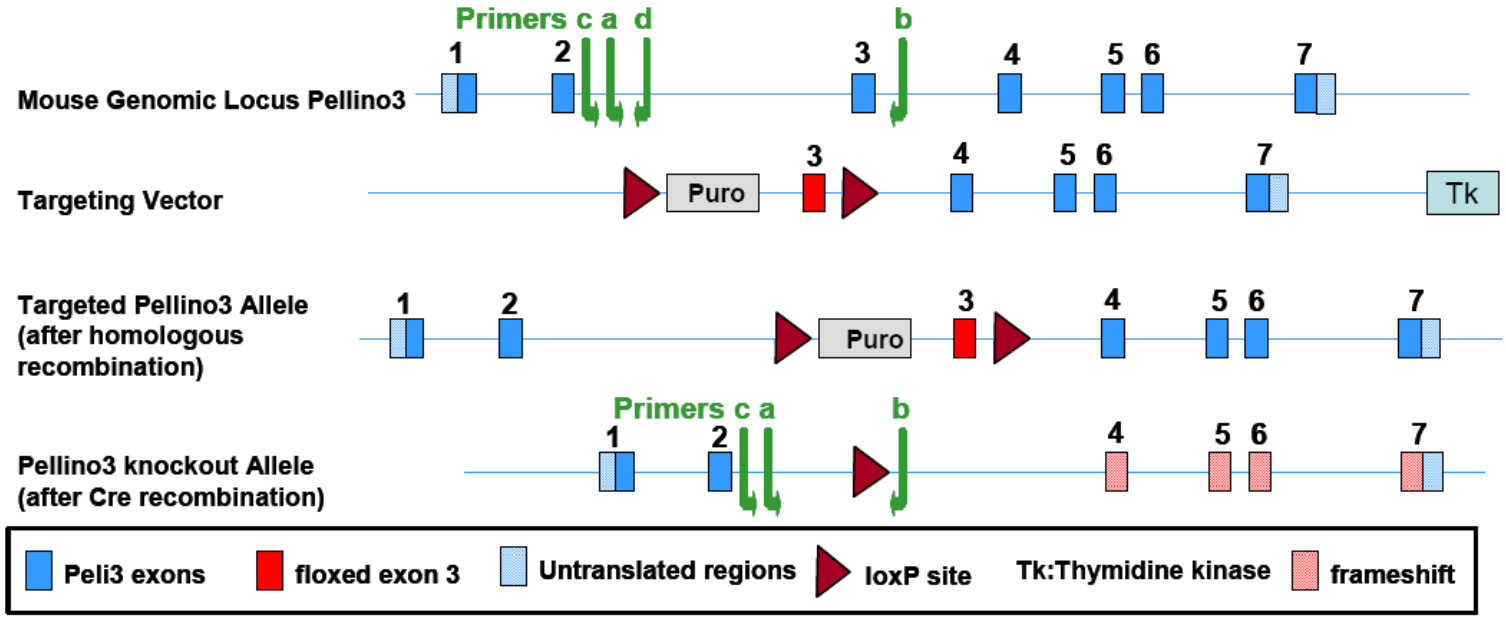

Figure 3-33 Generation of Pellino3 knockout mice.

Diagram shows:the mouse Pellino3 gene; the Pellino3 targeting vector containing exon3 flanked by loxP sites, the postive selection marker (Puro) inserted into intron 2 and a downstream Thymidine Kinase (TK) gene; the targeted Pellino3 allele; and the Pellino3 knockout allele after Cre recombination. Homologous recombinants in ES cells were isolated by Puro selection and used for blastocyst injection. Mice that were heterozygous for the targeted allele were bred with mice containing Cre recombinase regulated by the ROSA26 locus thus generating constitutive Pellino3-deficient mice in which deletion of exon 3 results in loss of function of the Pellino3 gene by generating a frameshift in all downstream exons. Exons are numbered and regions targeted by genotyping primers are also indicated.

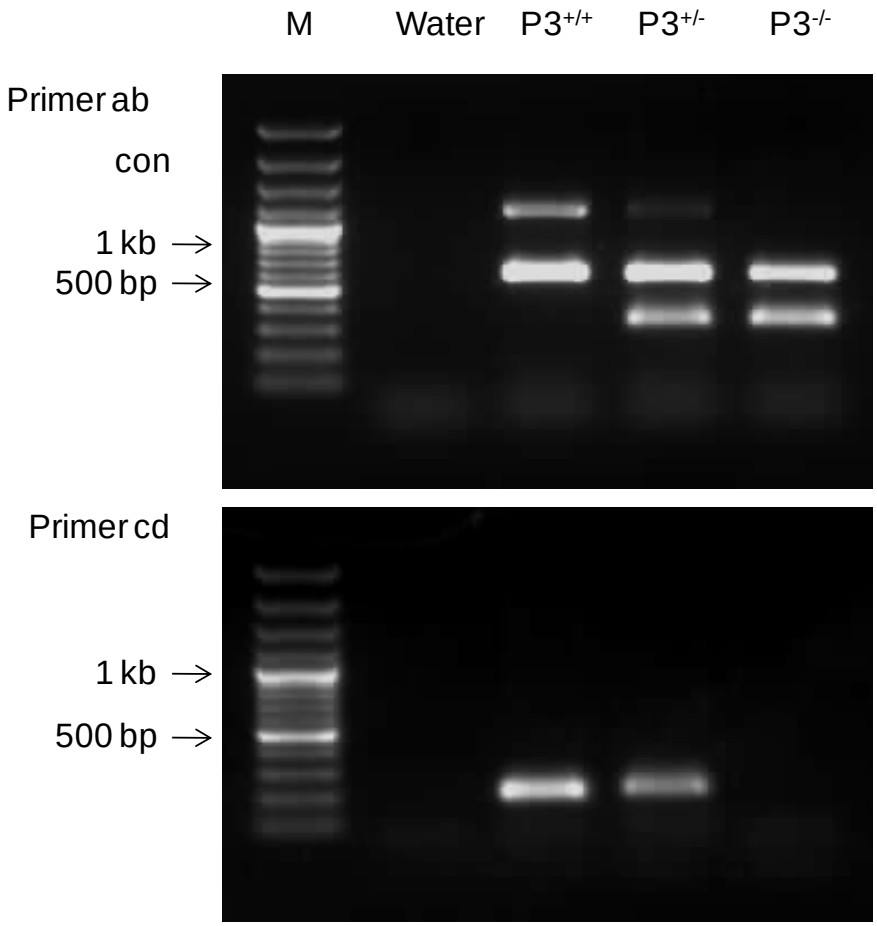

Figure 3-34 Identification of genotypes by PCR.

Genotyping was performed by PCR on genomic DNA from ear punches. Primers a and b differentiate the wild type allele (Pellino3$^{+/+}$) from the Pellino3 knockout allele in heterozygous (Pellino3$^{+/-}$) and homozygous (Pellino3$^{-/-}$) mice based on different fragment size where primers c and d amplify a fragment from the WT allele but not the knockout allele. Water was used as negative control for the PCR reaction.

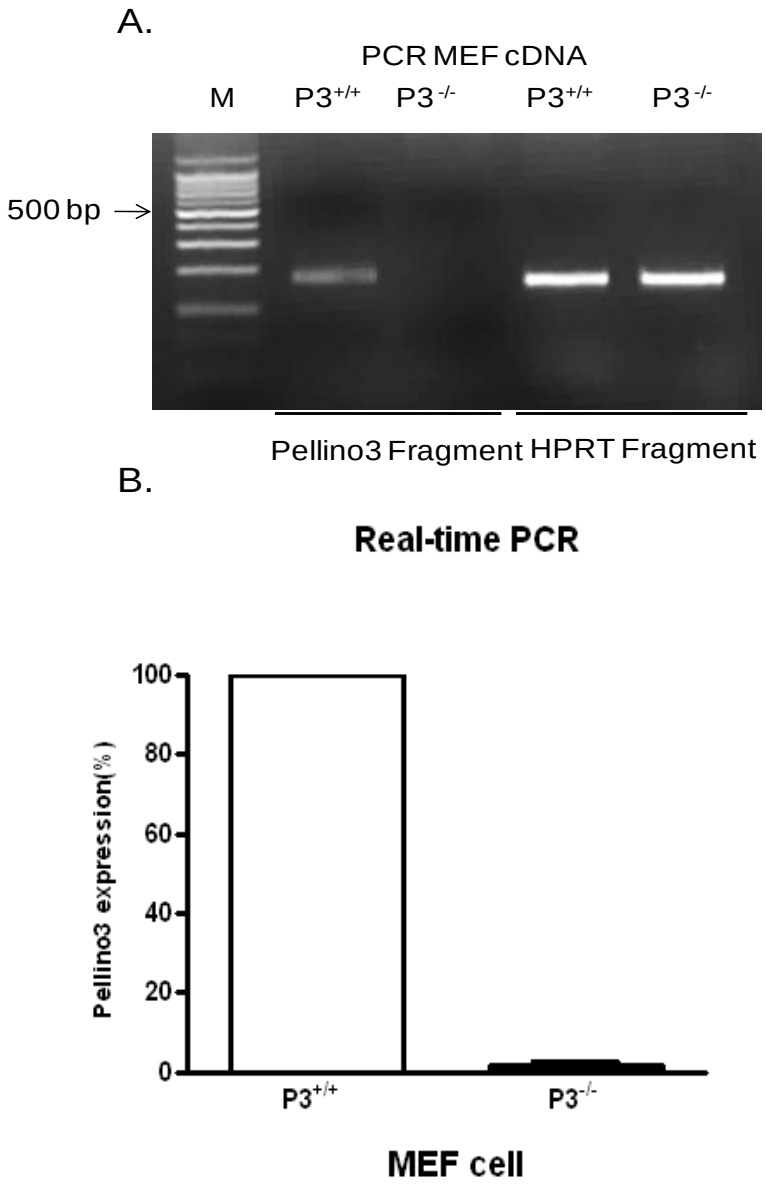

Figure 3-35 Expression level of Pellino3 mRNA in Pellino3 knockout mice.

MEFs were isolated from Pellino3$^{+/+}$ and Pellino3$^{-/-}$ embryos. (A) cDNA was prepared and semi-quantitative RT-PCR was used with specific primers to amplify exon 3 of Pellino3 or a region of the housekeeping gene HPRT. (B) Real time RT-PCR was used to quantify the levels of Pellino3 mRNA expression.

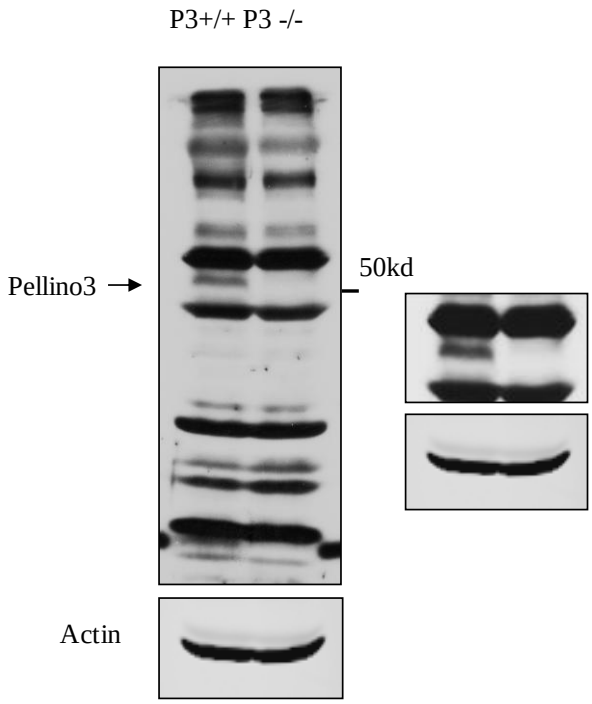

Figure 3-36 Expression level of Pellino3 Protein in Pellino3 knockout mice.

MEFs were isolated from Pellino3$^{+/+}$ and Pellino3$^{-/-}$ embryos. Cell lysates were prepared and subjected to Western blotting using anti-Pellino3 or anti-β-actin antibodies.

3.6.2 Phenotype of Pellino3-deficient mice

Both heterozygous and homozygous Pellino3-deficient mice were viable. Mating of heterozygous animals fed on standard mouse chow produced offspring with the 1:1.48:0.7 proportions of wild-type: heterozygous: homozygous mutant (n = 88:120:62) at 21 days of age (Figure 3-37A). When two heterozygous mice are bred together, 25% of pups derived from these matings should be homozygous. This is the expected Mendelian ratio, which is followed by most knockout mouse descriptions, such as XIAP-deficient mice (Harlin et al., 2001). However, genetic ablation of some genes alters the embryo survival capacity, thus resulting in the birth of fewer homozygous mutant mice than expected (or none), such as caspase-8-deficient mice (Sakamaki et al., 2002). The proportions for heterozygous: homozygous mutant offspring of Pellino3

were lower than the expected Mendelian ratios, suggesting that there could be fetal loss of heterozygous and homozygous mutant Pellino3 mice during gestation.

The heterozygous and homozygous mice grew normally and appeared healthy. Body weights of offspring were measured at 7 (male) or 8 (female) weeks of age. There was no significant difference in body weight between wild-type and heterozygous mice, whereas body weights of homozygous knockout mice were both significantly less than those of wild-type and heterozygous animals (Figure 3-37B and C).

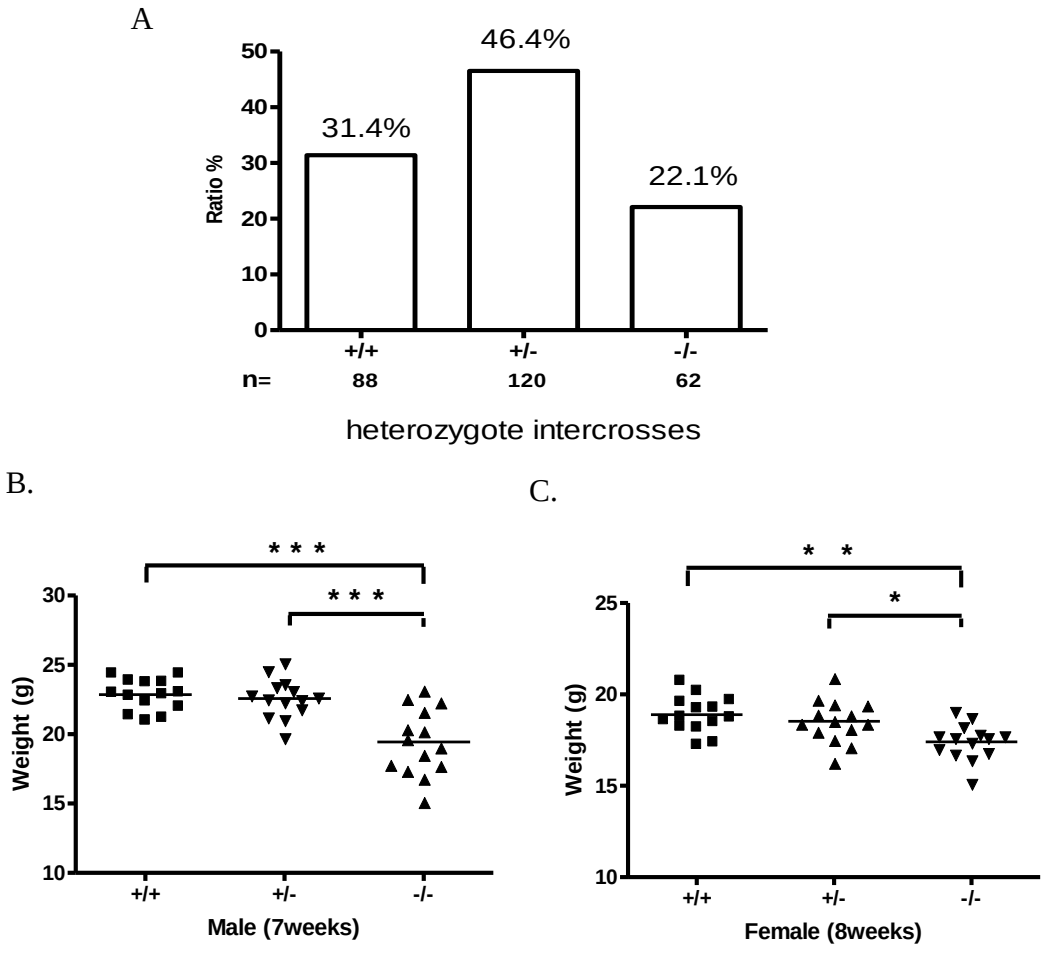

Figure 3-37 Phenotype of Pellino3 knockout mice.

(A) Numbers and percentages of pups of the indicated genotypes obtained from Pellino3 heterozygote intercrosses. (B,C) Weights of 7 week-old male mice (B) and 8 week-old female mice (C) from the breeding of Pellino3$^{+/-}$ mice. Horizontal bars indicate mean weights for each genotype. ***p<0.001, **p<0.01,*p<0.05, n=14.

3.6.3 Cells from Pellino3-deficient mice show increased sensitivity to the pro-apoptotic effects of TNF.

MEFs from Pellino3$^{+/+}$ and Pellino3$^{-/-}$ mice were thus used to assess the effects of Pellino3 deficiency on TNF signalling. WT and homogenous MEF cells were stimulated with TNF (40ng/ml) plus CHX (10μg/ml) for 10 hr. Co-stimulation of these cells with TNF and CHX caused the cells to become rounded and non-adherent but such phenotypic changes were much more apparent in MEFs from Pellino3$^{-/-}$ embryos relative to their wildtype control cells (Figure 3-38A). As measured by Annexin V, TNF plus CHX killed approximately 40% of Pellino3 deficient cells, compared to only 24% of control cells (Figure 3-38B), whilst there was no difference when cells were treated with CHX alone. Absence of Pellino3 also caused increased cleavage of PARP, caspase-3 after TNF plus CHX treatment (Figure 3-38C).

To further confirm the regulatory effects of Pellino3 on the TNF signalling pathway, rescue experiments were performed in Pellino3$^{-/-}$ MEFs using retroviruses. An MSCV-based construct containing the Pellino3 coding sequence was generated by PCR. This construct contained the entire coding sequence of Pellino3, followed by an internal ribosomal entry sequence (IRES) to allow for GFP expression. Pellino3$^{-/-}$ MEFs were infected with MSCV, lacking (retrovirus) or containing the myc-tagged murine Pellino3 gene and then apoptosis was induced by treatment of TNF and CHX. Control cells were transfected with the empty vector (retrovirus), and high cell death was observed. In contrast, expression of Pellino3 successfully rescued Pellino3$^{-/-}$ MEFs from TNF-induced apoptosis (Figure 3-39A). Total percent of apoptotic cells decreased from 45% in the control cells to 25% with Pellino3 expression, as measured by Annexin V-FITC staining (Figure 3-39B). Expression of Pellino3 also attenuated the cleavage of caspase-3 and PARP in Pellino3-deficient MEFs (Figure 3-39C). These

results clearly demonstrate that Pellino3 acts as an anti-apoptotic factor in TNF-induced apoptosis.

Similar to the results from cell lines, knockout of Pellino3 delayed the resurgence of IκBα and increased levels of phosphorylation IκBα (Figure 3-40A). Activation of NF-κB in Pellino3 deficient MEFs was confirmed using EMSA. Interestingly, even Pellino3 heterozygous MEFs induced activation of NF-κB after TNF treatment (Figure 3-40B). Knockout of Pellino3 also attenuated activation of JNK and P38, and to some extent increased activation of ERK (Figure 3-41). The stimulatory effects of Pellino3 deficiency on NF-κB was further confirmed by increased TNF-induced expression of the NF-κB-responsive gene IL-6 in Pellino3$^{-/-}$ MEFs (Figure 3-42) and thus Pellino3 may also regulate inflammatory signalling.

To further evaluate the effect of Pellino3 deficiency in TNF signalling, basal and TNF-induced expression levels of several antiapoptotic proteins mediated by NF-κB or MAPKs, such as A20, c-FLIP and Bcl-x, were examined on mRNA level or protein level. Treatment of MEFs with TNF for 5 hours, resulted in induction of A20 mRNA, as determined by quantitative real-time PCR analysis. TNF-induced A20 mRNA levels were significantly increased in Pellino3$^{-/-}$ MEFs (Figure 3-43A), suggesting that Pellino3 attenuates A20 transcription. Since A20 has been described to terminate TLR-mediated NF-κB up-regulation (Wertz et al., 2004), the inhibition of A20 by Pellino3 may alter the duration and the extent of the NF-κB activity. cFLIP has the ability to form heterodimers with procaspase-8 and inhibit its full activation, preventing apoptosis (Krueger et al., 2001; Geserick et al., 2008). Transcription of c-FLIP in response to TNF stimulation was slightly up regulated in Pellino3$^{-/-}$ MEFs (Figure 3-43B). Bcl-x has the ability to bind to pro-apoptotic proteins and is associated with apoptosis resistance (Jourdan et al., 2000; Boise et al., 1993). The protein levels of Bcl-x remained unchanged during TNF treatment in Pellino3$^{-/-}$ MEFs (Figure 3-43C).

These findings, in support of the data obtained from cell lines, provide strong evidence that Pellino3 play a key role in regulating apoptosis in response to TNF. Furthemore the underlying mechanism appears to be independent of regulatory effects on NF-κB or the expression of anti-apoptotic proteins.

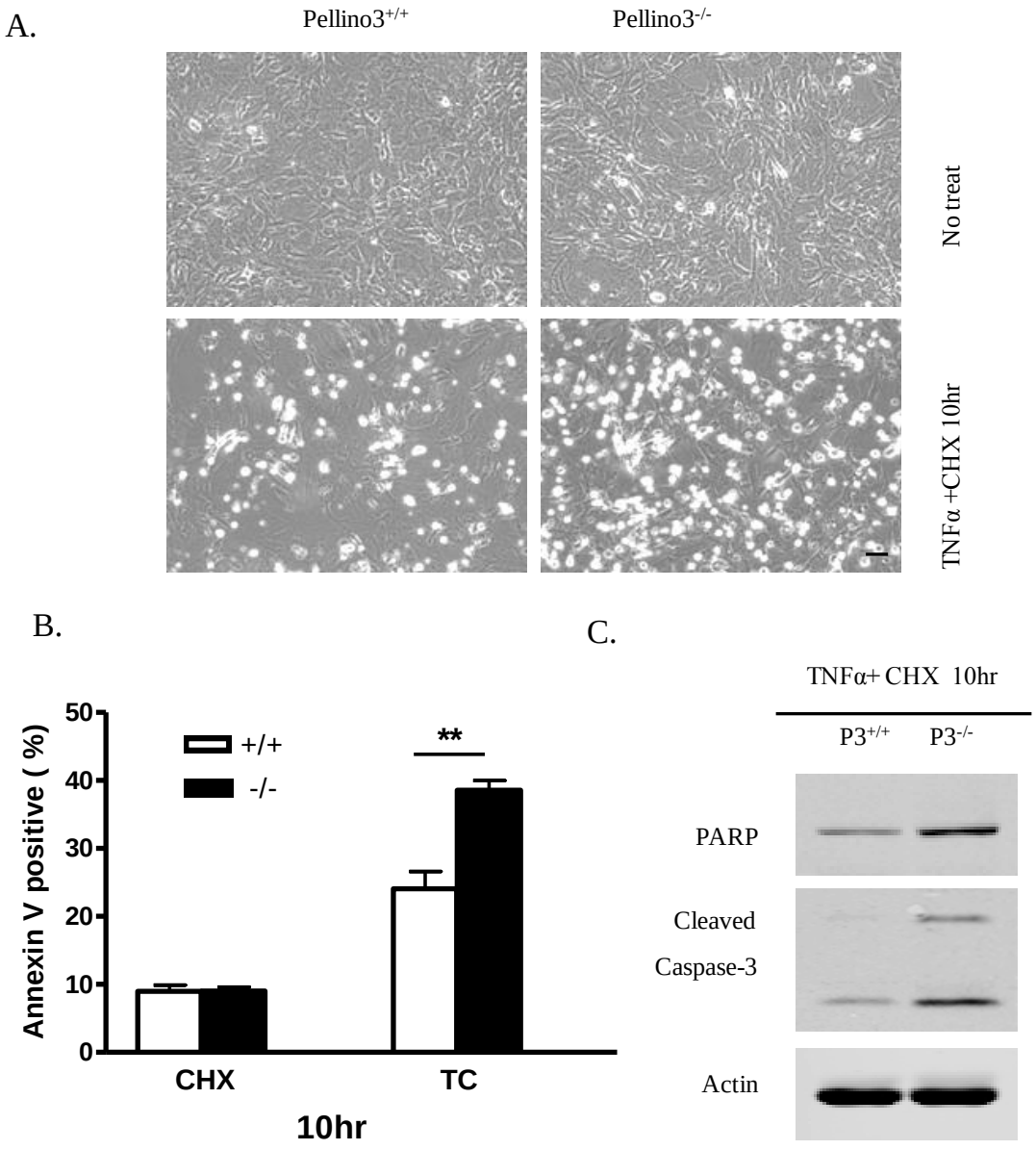

Figure 3-38 Genetic Knockout of Pellino3 promotes TNF-induced apoptosis in MEFs

MEFs were isolated from Pellino3$^{+/+}$ and Pellino3$^{-/-}$ embryos and treated in the absence (control) or presence of murine TNF (20ng/ml) plus CHX (10μg/ml) for 10 hr. (A) Cells were photographed using a phase contrast microscope (bar 20μm). (B) Cells were analyzed by flow cytometry for percentage of cells staining positive for

Annexin V. Data represent the mean +/- S.D. of 3 independent experiments. (C) Cell lysates were probed by immunoblotting for expression levels of PARP, caspase-3 and β-actin.

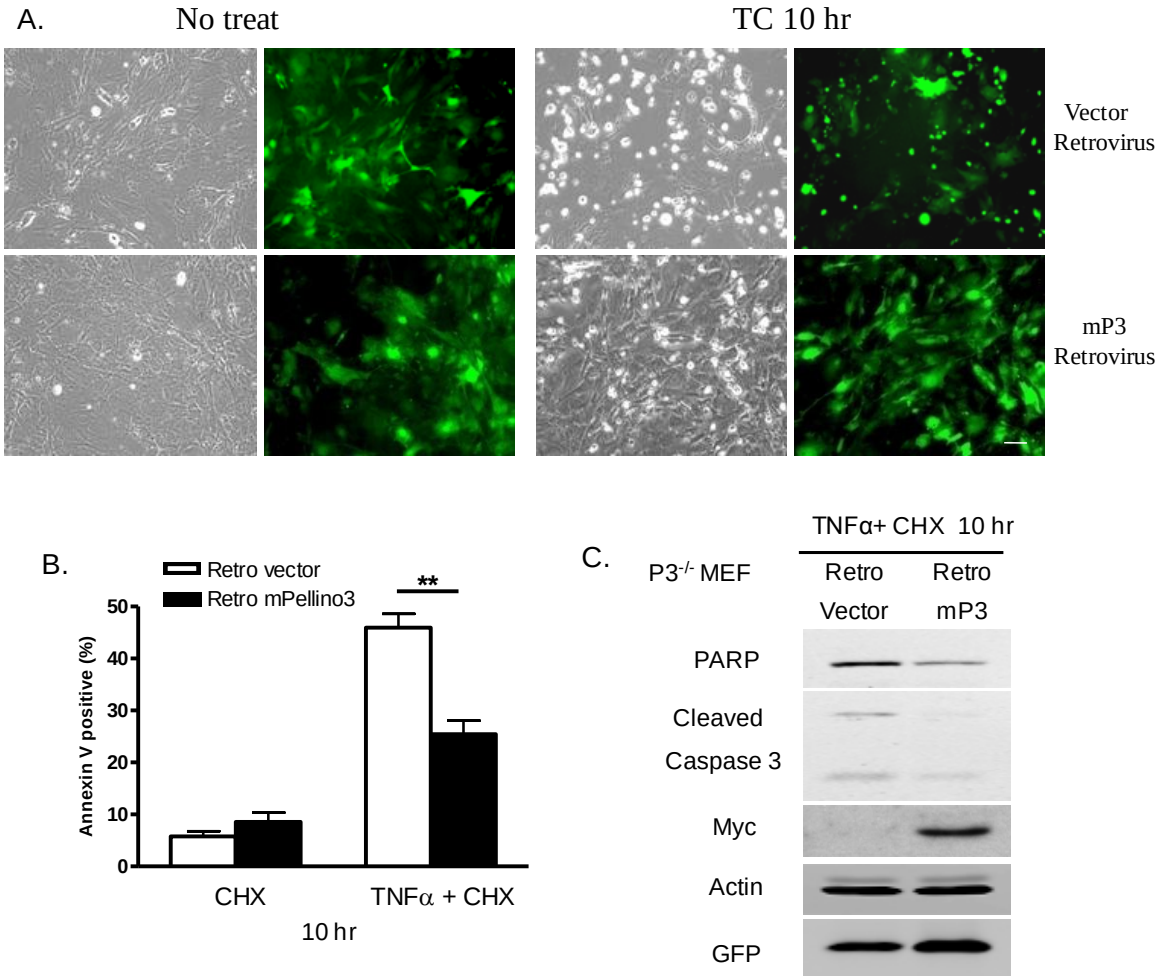

Figure 3-39 Pellino3 rescues Pellino3$^{-/-}$ MEFs from TNF-induced apoptosis.

MEFs, from Pellino3$^{-/-}$ embryos, were retrovirally infected with MSCV, lacking (retrovirus) or containing the myc-tagged murine Pellino3 gene (mPellino3 retrovirus). Infected cells were treated in the absence (control) or presence of human TNF (40ng/ml) and CHX (10μg/ml) for 10 hr. (A) Cells were photographed using a phase contrast microscope (bar 20μm) or (B) viewed by fluorescent microscopy to detect infected cells based on expression of MSCV-encoded GFP. The mean +/- S.D. of 3 independent experiments; **p<0.01. or (C) Cell lysates were probed by immunoblotting for expression levels of PARP, caspase-3, myc, β-actin and GFP.

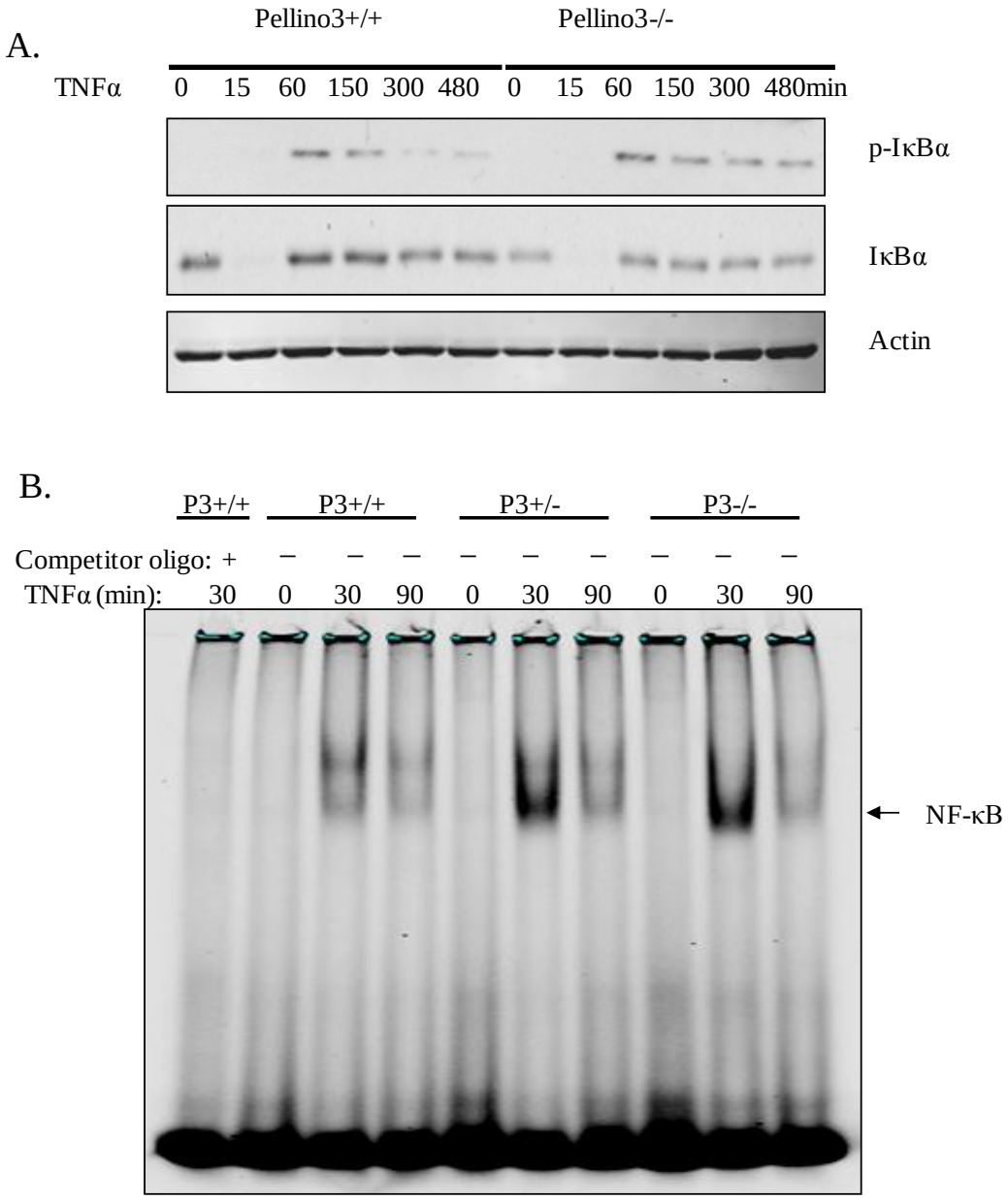

Figure 3-40 Loss of Pellino3 enhances TNF-induced activation of NF-κB in MEFs.

(A) MEFs were isolated from Pellino3$^{+/+}$ and Pellino3$^{-/-}$ embryos and treated in the absence (0) or presence of murine TNF (20ng/ml) for indicated times. Cell lysates were prepared and immunoblotted for phosphorylated levels of IκBα (p-IκBα) and total levels of IκBα. Lysates were also probed for levels of β-actin to act as loading controls. (B) MEFs were isolated from Pellino3$^{+/+}$, Peli3$^{+/-}$ and Pellino3$^{-/-}$ embryos and treated in the absence (0) or presence of murine TNF (50ng/ml) for indicated times. Nuclear extracts were prepared and subsequently incubated with an IR-labelled oligonucleotide containing an NF-κB-binding motif and separated by native PAGE. The arrows indicate the mobility of basal and TNF induced NF-κB-DNA complexes. The specificity of the NF-κB-DNA binding reaction was confirmed by the absence of the complexes when the binding reaction is performed in the presence of the unlabelled (competitor) oligonucleotide.

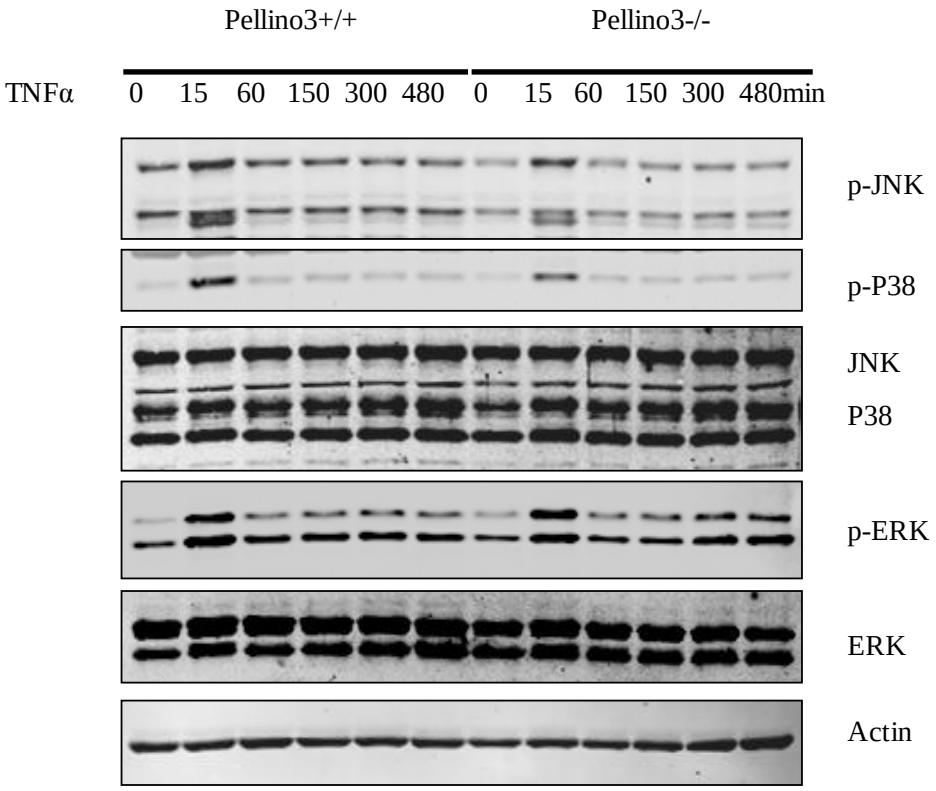

Figure 3-41 Effects of Pellino3 knockout on TNF-induced activation of MAPKs in MEFs

MEFs were isolated from Pellino3$^{+/+}$ and Pellino3$^{-/-}$ embryos and treated in the absence (0) or presence of murine TNF (20ng/ml) for indicated times. Cell lysates were prepared and immunoblotted for phosphorylated levels of JNK (p-JNK), P38 (p-P38), ERK (p-ERK) and total levels of JNK, P38 and ERK. Lysates were also probed for levels of β-actin to act as loading controls.

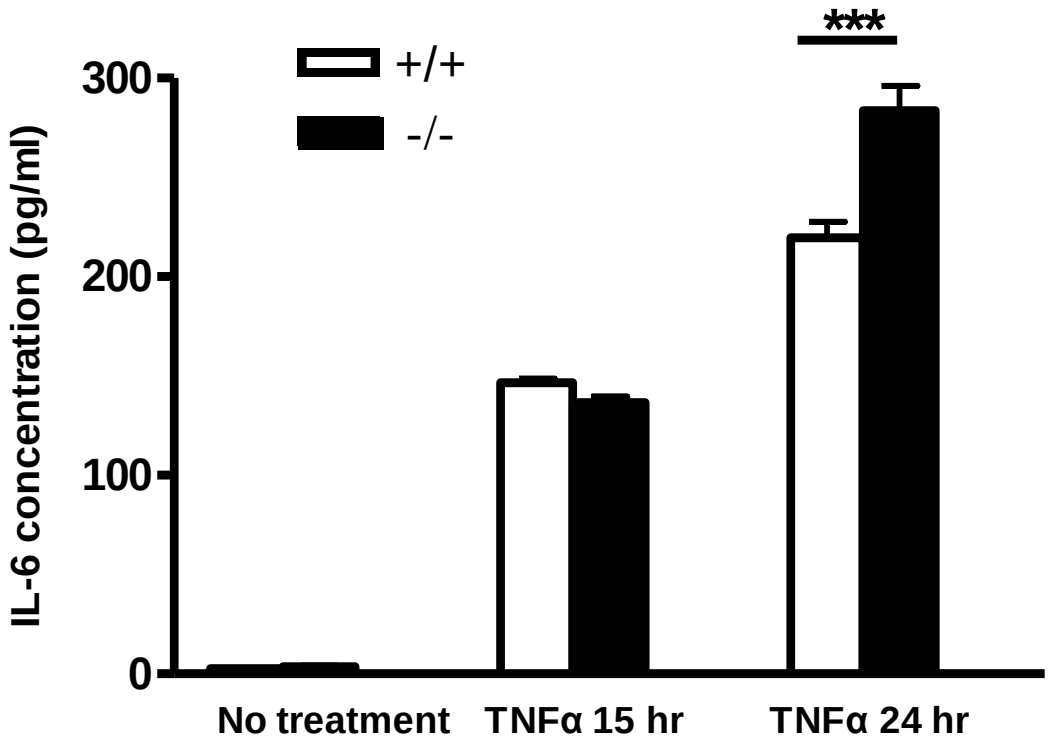

Figure 3-42 Effects of Pellino3 deficiency on TNF-induced expression of IL-6.

MEFs were isolated from Pellino3$^{+/+}$ and Pellino3$^{-/-}$ embryos and treated in the absence (control) or presence of murine TNF (20ng/ml) for the indicated time periods. Conditioned media from treated cells were assayed for levels of IL-6 by ELISA. Data represent the mean +/- S.D. of 3 independent experiments; *** $P < 0.001$.

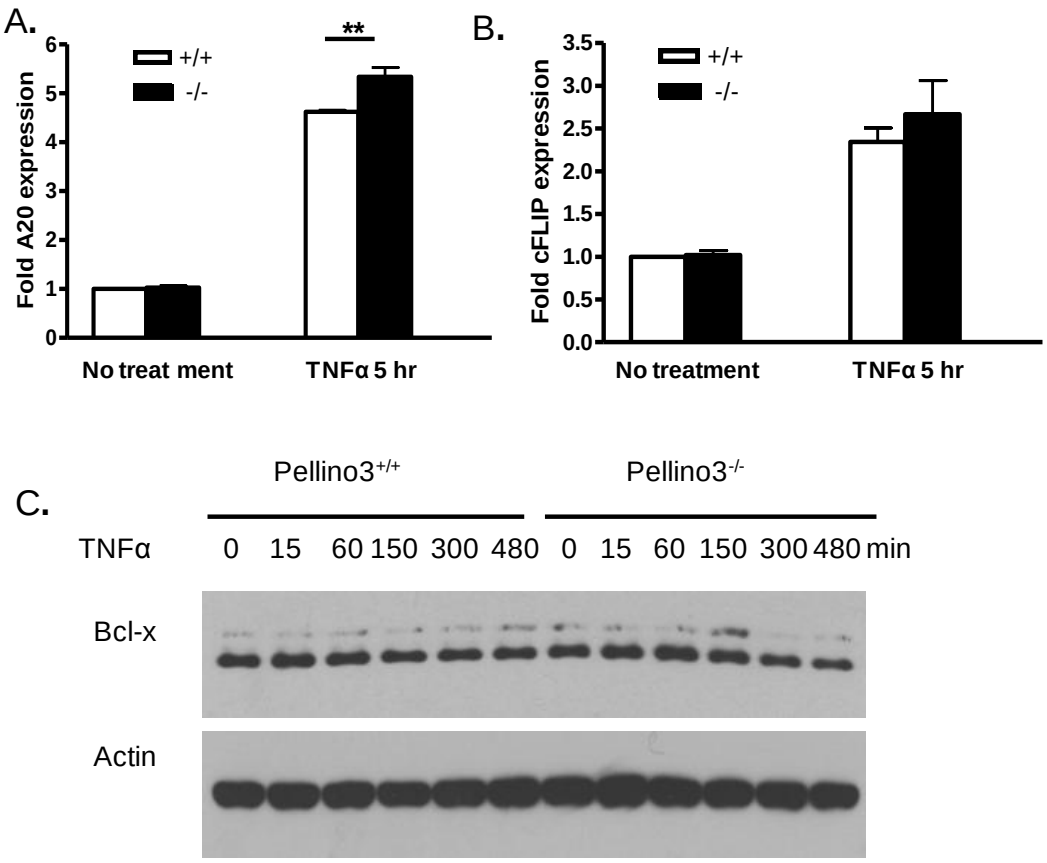

Figure 3-43 Effects of Pellino3 deficiency on expression of anti-apoptotic proteins in response to TNF.

MEFs were isolated from Pellino3$^{+/+}$ and Pellino3$^{-/-}$ embryos and treated in the absence (control) or presence of murine TNF (20ng/ml) for the indicated time periods. (A,B) mRNA expression levels of A20 (A) and cFLIP (B) were measured by quantitative RT-PCR and expressed relative to expression levels in unstimulated Pellino3$^{+/+}$ MEFs. Data represent the mean +/- S.D. of 3 independent experiments; **p<0.01. (C) Cell lysates were probed by immunoblotting for expression levels of Bcl-x and β-actin.

3.6.4 Pellino3 confers protection against hepatoxicity and lethality in response to in vivo administration of TNF.

In order to define the *in vivo* role of Pellino3 in the context of the cytotoxic effects of TNF the well established liver injury model was employed in which the hepatotoxic agent D-gal sensitizes mice to the lethal effects of low doses of TNF. In this model mice die due to acute hepatitis, which is characterized by leukocyte influx, apoptosis, and secondary necrosis (Decker and Keppler, 1974). Mice usually start dying after 6 or 8 hr after injection with a combination of TNF (10µg/kg body weight) and D-Gal (0.8g/kg body weight) (Nagaki et al., 1999 ; Van Molle et al., 1997).

In this study, Pellino3 homozygous mice and their wild type counterparts were injected intraperitoneally with a combination of D-Gal (0.8g/kg body weight) and low dose of murine TNF (2.5µg/kg body weight) or D-Gal alone. The animals were observed during the next 36 hr, after which no further deaths occurred. The survival rate clearly showed that Pellino3 knockout mice were much more sensitive to TNF/D-Gal compared with their WT counterparts (Figure 3-44 A). 5 of 11 (45%) Pellino3 knockout mice died in 12 hr after being challenged, while all remaining knockout mice died within 24 hr. The administration of D-gal alone had no affect on the survival of Pellino3$^{+/+}$ or Pellino3$^{-/-}$ mice (Figure 3-44 B).

Given that hepatoxicity is the key contributing factor to the lethal effects in this model, liver tissue was examined from the different mouse cohorts. Indeed, the livers of Pellino3 knockout mice after TNF/D-Gal challenge displayed widespread hemorrhage whereas no such effects were apparent in Pellino3-deficient that had not been challenged with TNF or in wild type control mice irrespective of the administration regime (Figure 3-45).

Co-administration of D-Gal and TNF to Pellino3$^{+/+}$ mice lead to widespread swelling of hepatocytes due to microvesicular vacuolation and fine granulation of the cytoplasm leading to compression of sinus structures. This is typical of an adaptive cell response to injury coupled with proliferation of hepatic drug metabolizing enzymes as a result of D-gal treatment. In contrast, the same co-administration protocol in Pellino3$^{-/-}$ mice led to widspread hepatotoxicity with marked disruption of hepatocyte cord structures and part replacement by red blood cells. Individual hepatocytes were swollen with many cells containing karyorrhectic (fragmented) nuclei. Immunohistologic analysis of the activation of caspase-3 using an antibody that recognizes only the active caspase-3 p17 subunit was performed to evaluate the apoptosis induced by TNF/D-Gal. TNF/D-gal induced massive caspase-3 activation in Pellino3 knockout liver but only a few in the wild-type counterparts (Figure 3-46). In support of these immunohistochemistry data, Western immunoblot revealed a significant activation of caspase-8 and caspase-3 in the Pellino3$^{-/-}$ livers at 12 hr after TNF/D-Gal injection (Figure 3-47). These data provide very strong evidence for a critical physiological role for Pellino3 in regulating the potential toxic effects of TNF.

Cytokines are potential effector molecules that modulate and regulate immune responses (Strieter et al., 1996). During inflammatory responses, IL-6 is produced to regulate the development of Th 17 cells and the acute phase response (Yoshimura et al., 2009). IL-10 regulates differentiation and proliferation of multiple immune cells (Asadullah et al., 2003). RANTES is chemotactic for T cells, eosinophils, and basophils and plays an active role in recruiting leukocytes into inflammatory sites (Taub et al., 1996). TNF regulates leukocyte activation and infiltration, macrophage activation and triggering T-lymphocyte responses within tissues (Jap and Chee, 2008). To investigate the role of the immune response in TNF/D-Gal-induced apoptosis, the levels of IL-6 (Figure 3-48A), IL-10 (Figure 3-48B), RANTES (Figure 3-48C) and TNF (Figure 3-48D) cytokines were measured by ELISA. TNF/D-Gal caused only very modest increases in serum concentrations of all of the cytokines in Pellino3

knockout mice compared with wild type mice. There was no statistically significant difference found. Thus the death caused by TNF/D-Gal exposure in Pellino3 knockout mice is not due to the excessive and uncontrolled production of inflammatory mediators and pro-inflammatory cytokines.

In conjunction with the earlier cell-based approaches these *in vivo* findings now provide unequivocal support for Pellino3 acting as a novel player in TNF biology. The high sensitivity of Pellino3$^{-/-}$ mice to the lethal effects of TNF clearly promotes Pellino3 as a crucial factor in determining whether cells survive or die in response to TNF challenge.

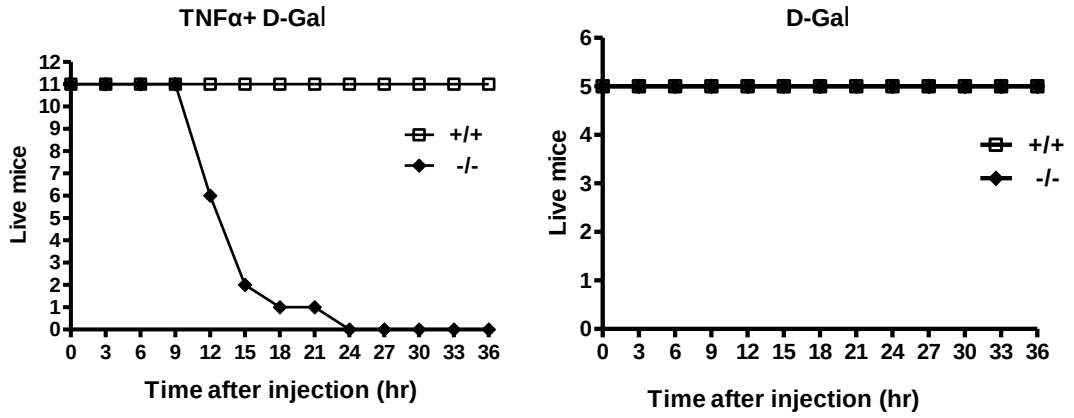

Figure 3-44 Loss of Pellino3 in mice leads to increased hepatoxicity and lethality in response to in vivo administration of TNF.

Age- and sex-matched Pellino3$^{+/+}$ and Pellino3$^{-/-}$ mice were injected intraperitoneally with 2.5 µg TNF plus 0.8g D-Gal per kg body weight (n=11) or D-Gal alone (n=5). Survival was monitored every hour for 36 hr. (A) Survival curves of mice injected with TNF plus D-Gal. (B) Survival curves of mice injected with D-Gal alone.

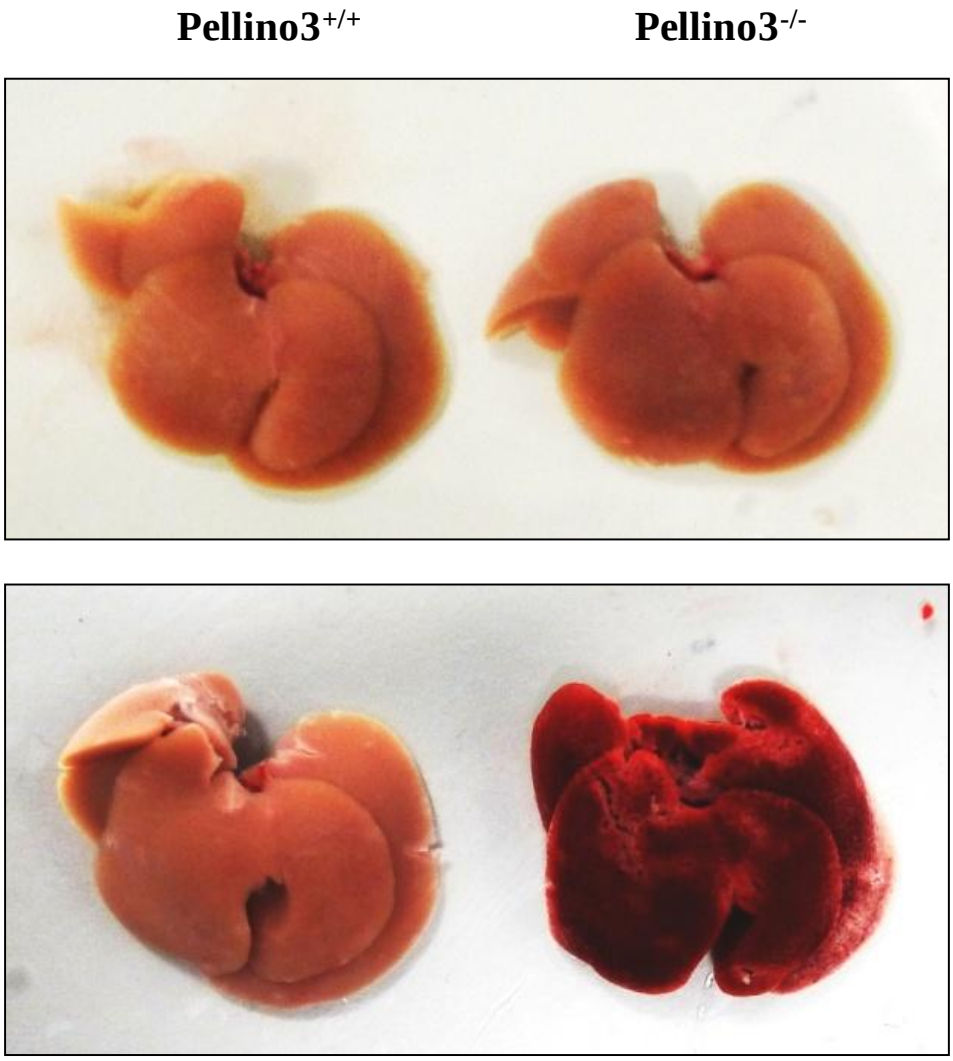

Figure 3-45 Liver tissues after injection of TNF and D-Gal

Age- and sex-matched Pellino3$^{+/+}$ and Pellino3$^{-/-}$ mice were injected intraperitoneally with 2.5μg TNF plus 0.8g D-Gal per kg body weight or D-Gal alone. Liver tissues were collected and photographed at 12 hr after injection.

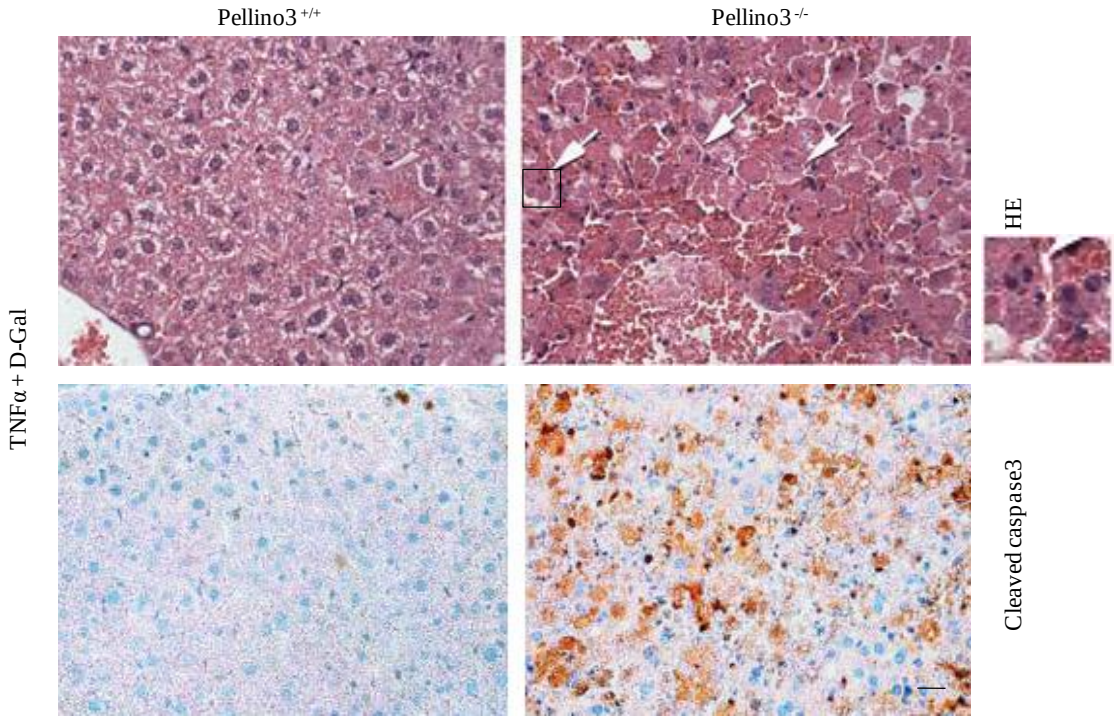

Figure 3-46 Loss of Pellino3 sensitizes liver cells to TNF/ D-Gal-induced apoptosis

Age- and sex-matched Pellino3$^{+/+}$ and Pellino3$^{-/-}$ mice were injected intraperitoneally with TNF and D-Gal or D-Gal alone. Hepatic tissue was collected 12 hr after injection, sectioned and subjected to histological analysis using Haematoxylin and eosin (H&E) staining and immunohistochemistry using anti-cleaved caspase-3 antibody. (bar 20μm).The white arrows indicate cells with fragmented nuclei.

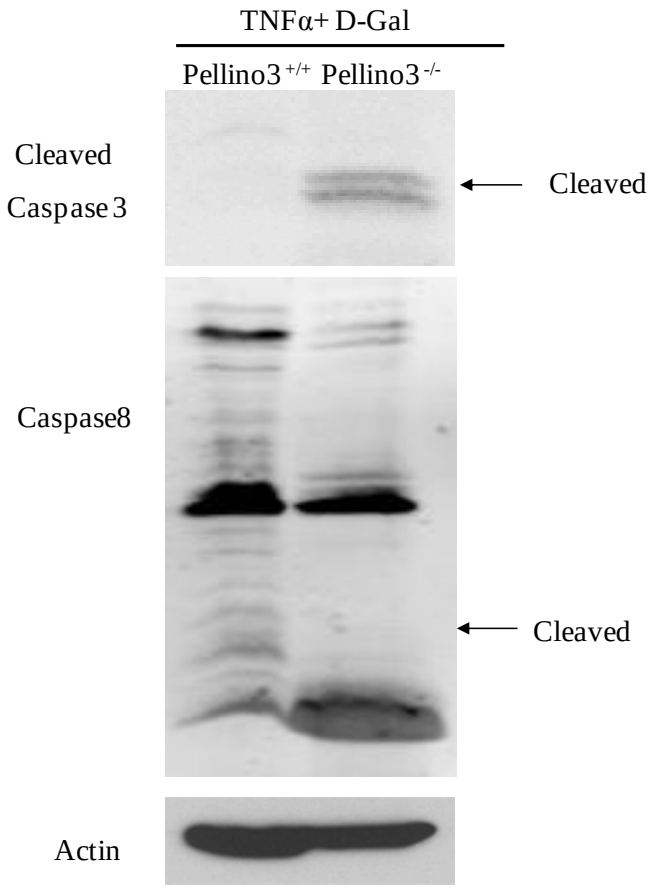

Figure 3-47 Pellino3 deficiency leads to increased apoptotic markers in hepatic tissue in response to TNF/ D-Gal

Age- and sex-matched Pellino3$^{+/+}$ and Pellino3$^{-/-}$ mice were injected intraperitoneally with TNF and D-Gal or D-Gal alone. Cell lysates were generated from hepatic tissue 12 hr post injection and probed by immunoblotting for levels of cleaved caspase-3, caspase-8, mPellino3 and β-actin.

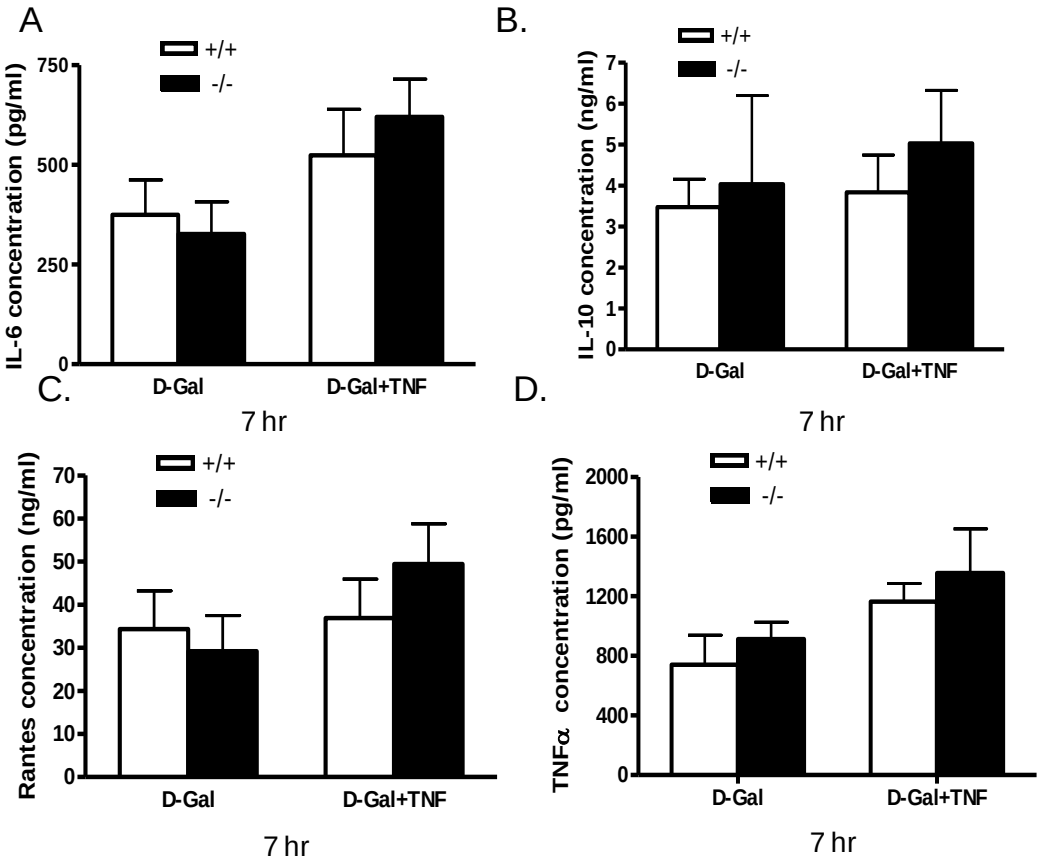

Figure 3-48 Proinflammatory cytokine levels after TNF/Gal injection.

Age- and sex-matched Pellino3$^{+/+}$ and Pellino3$^{-/-}$ mice were injected intraperitoneally with TNF and D-Gal or D-Gal alone. Blood samples are taken from mice 7 hr after injection and serum assayed by ELISA or levels of IL-6 (A), IL-10 (B), Rantes (C) and TNF (D) . Data represent the mean +/- S.D. of 4 independent experiments.

CHAPTER FOUR: DISCUSSION

TNF is a proinflammatory cytokine that regulates multiple cellular processes, such as apoptosis, proliferation and inflammation (Wajant et al., 2003). Inappropriate production of TNF or sustained activation of TNF signalling has been correlated to the pathogenesis of many human diseases, including cancer, sepsis, diabetes and autoimmune diseases (Aggarwal, 2003). Understanding the signal transduction mechanisms involved in regulating the TNF pathway has created opportunities in identifying novel targets, which may be useful in therapeutic treating inflammatory disorders. The aim of this study was to investigate the potential role of Pellino3 in the regulation of the TNF signalling.

4.1 Pellino3 is a key regulator of TNF-induced apoptosis

While using a siRNA or shRNA-based targeting strategy to suppress the endogenous expression of Pellino3, a significant increase in sensitivity to TNF-induced cell death was observed in various cell lines, including Hela, HEK293T, 1321N1 and U373. In order to define the physiological relevance of the role of Pellino3 in TNF signalling, Pellino3-deficient mice were generated. Consistent with observations obtained from human cell lines, cells from Pellino3-deficient mice are much more sensitive to TNF-induced apoptosis, compared to their wild type control cells, demonstrating that the role for Pellino3 in regulating TNF-induced cell death is not a cell line-specific phenomenon. Instead Pellino3 appears to play a widespread role in regulating cell survival in response to TNF. Although TNF has been identified as a potent inducer of

apoptotic cell death, it has also been shown to contribute to necrosis (Denecker et al., 2001; Fiers et al., 1995). However Pellino3 seems to regulate the pro-apoptotic effects of TNF based on the use of apoptotic markers. Thus knockdown or deficiency in Pellino3 expression lead to increased Annexin V staining, a key signatute of apoptosis. Furthermore, this event could be efficiently blocked by the pan-caspase inhibitor zVAD-fmk, indicating that TNF induced a caspase-dependent apoptosis in Pellino3 deficient cells. In addition, during apoptosis, members of the caspase protease family are activated, leading cells to undergo rapid death (Kumar, 1995; Yuan et al., 1993). Cleaved caspase-8, cleaved caspase-3 and PARP are typical markers for the detection of apoptotic cells (Muzio et al., 1996; Tewari et al., 1995; Margolin et al., 1997). In this study, cleavage of caspase-3, caspase-8 and PARP were also measured to confirm that apoptosis was occurring, and in keeping with the other markers of apoptosis, Pellino3 deficiency resulted in increased levels of cleaved forms of these proteins in response to TNF.

In order to ensure that the greater pro-apoptotic effects of TNF in Pellino3 knockdown or knockout cells were due specifically to Pellino3 deficiency, rescue experiments were performed. Introduction of the expression construct encoding Pellino3s or Pellino3l could efficiently prevent the TNF-induced apoptosis in Pellino3 deficiency HEK293T cells. This was demonstrated by reduced Annexin V staining and cleavage of PARP and caspase-3, indicating that both spliced forms can temper the pro-apoptotic signalling of TNF. Moreover, a murine Pellino3 expression construct also rescued Pellino3$^{-/-}$ deficient MEFs from undergoing apoptosis in response to TNF stimulation.

Based on these various approaches spanning cell lines to genetic models this study provides very strong support for a key role for Pellino3 in regulating TNF-induced apoptosis.

4.2 The regulatory effects of Pellino3 in apoptosis are not due to modulation of the NF-κB/ MAPK pathways

In most cell types, aberrant TNF signalling tend to activate the oncogenic and pro-inflammatory signalling pathways, such as NF-κB and MAPKs which exert positive effects on cell survival and proliferation rather than triggering apoptosis (Varfolomeev et al., 1996). Most cell types are resistant to apoptosis induced by TNF, unless the cells are treated with a sensitising agent, such as protein synthesis inhibitor, cycloheximide (CHX). This results in the disruption in the balance between cell survival and death and instructs cells to undergo apoptosis (Vassalli, 1992). This is mainly due to blockade of induction of NF-κB responsive anti-apoptotic genes. Given the key counter-regulatory role of NF-κB in controlling the apoptotic arm of the TNF signalling pathway it was essential to explore if the effects of Pellino3 deficiency on TNF-induced apoptois could have an underlying basis in dysregulation of the NF-κB pathway. This was especially relevant in the context of an increasing literature exploring the regulatory importance of the Pellino family in the NF-κB pathway.

Published transfection studies with cell-line models suggest that Pellino1 and Pellino2 have the ability to activate NF-κB in IL-1 signalling (Jiang et al., 2003; Yu et al., 2002). However, the suggestion that Pellino1 plays a positive role on NF-κB activation in response to IL-1 has been challenged with findings from Pellino1 deficient mice. A study on Pellino1$^{-/-}$ MEFs showed that the genetic deficiency of Pellino1 had no effect on the ability of IL-1 to promote activation of NF-κB (Chang et al., 2009). However the latter study also demonstrated that deficiency in Pellino1 attenuated the activation of NF-κB in MEFs and splenocytes in response to TLR3 and TLR4 stimulation. A mechanistic explanation was provided by Pellino1 acting as a ubiquitin E3 ligase for RIP1 thus catalysing ubiquitination of the latter and facilitating TRIF-dependent TLR3/4-induced activation of NF-κB. This demonstrates that the

function of Pellino1 in terms of regulating activation of NF-κB may be stimulus dependent. Indeed Pellino1 has been recently shown to inhibit T cell activation by negatively regulating the NF-κB subunit c-Rel (Chang et al., 2011). In the latter study Pellino1 was shown to ubiquitnate c-Rel thus promoting its degradation and downregulating T cell activation, a key part of the tolerance to self antigens. This raises the intriguing contrast of Pellino1 acting to positively regulate NF-κB activation in the TLR3/4 pathways whereas it negatively regulates the activation of NF-κB by CD28/T cell receptor co-stimulation in T cells (Moynagh, 2011). Interestingly a report has also suggested that Pellino3 may play a negative regulatory role with respect to NF-κB (Xiao et al., 2008). Using cell line models the authors propose that Pellino3 inhibits IL-1-induced activation of NF-κB by catalysing K63-linked IRAK polyubiquitylation and this competes with K48-linked IRAK polyubiquitylation for the same ubiquitylation site, Lys134 and blocks IRAK degradation. Xiao et al propose that degradation of IRAK is required for NF-κB activation but this model lacks some clarity (Moynagh, 2009). Indeed various reports question the importance of IRAK-degradation in the NF-κB pathway especially given the findings that the polyubiquitination of Lys134 on IRAK is not essential for IL-1 signalling (Conze et al., 2008; Windheim et al., 2008).

Whilst the role of Pellino1 in TNF signalling was not explored in Pellino1-deficient mice (Chang et al., 2009), earlier studies using gene knockdown technology in cell lines reported that Pellino1 and Pellino2 fail to play a role in TNF-induced activation of NF-κB (Jiang et al., 2003; Yu et al., 2002). However until the present study the role of Pellino3 in regulating TNF-induced activation of NF-κB activation had not been explored and we were also keen to examine its potential role in this pathway as a means to explain its modulatory effects on TNF-induced apoptosis.

The activation of NF-κB is dependent on the phosphorylation and degradation of its inhibitory IκB proteins. The phosphorylation of the IκB is initiated through the IKK

complex, which consist of two catalytic subunits IKKα and IKKβ and the regulatory subunit IKKγ (DiDonato et al., 1997; Mercurio et al., 1997; Regnier et al., 1997). In this study, the deficiency of Pellino3 increased TNF-induced NF-κB signalling events, including phosphorylation of IKKα/β, phosphorylation of IκBα and degradation of IκBα. Moreover, EMSA data obtained direct evidence that Pellino3 negatively regulated NF-κB activation in TNF signalling pathway. This is consistent with a previous report indicating that Pellino3 may negatively regulate IL-1 induced activation of NF-κB (Xiao et al., 2008). Since NF-κB tends to be regarded as a pro-survival transcription factor, the increased activation of NF-κB in response to TNF under conditions of Pellino3 deficiency or knockdown, tends to exclude a role for NF-κB in mediating the pro-apoptotic effects following suppressed Pellino3 expression.

Although Pellino1 has no effect on any of the MAPK pathways and Pellino2 drives activation of the ERK1/2 and JNK pathways, Pellino3 has been shown to have the ability to promote the activation of p38 MAPK, which induces cell death in some cell lines (Butler et al., 2005; Jensen and Whitehead, 2003a). Similar to the positive role for Pellino3 in mediating IL-1 –induced activation of p38 MAPK (Butler et al., 2005), the present findings also suggest a mediatory role for Pellino3 in facilitating TNF-induced activation of p38 MAPK and JNK. Since p38 and JNK activity is thought to promote apoptosis (Horstmann et al., 1998; Tang et al., 2001), the decreased phosphorylation levels of p38 and JNK that were observed in response to TNF in Pellino3 deficient cells argues against a role for these MAPK pathways in mediating the pro-apoptotic effects associated with Pellino3 deficiency.

Moreover, expression of several anti-apoptotic proteins associated with NF-κB or MAPK pathway were also tested at the mRNA and protein levels. Elevated mRNA levels of A20 and cFLIP were observed in response to TNF treatment and such expression was not compromised in the absence of Pellino3 and this is consistent with the strong activation of NF-κB under these conditions. The lack of a role for the NF-

κB pathway in underlying the pro-apoptotic effects of TNF under conditions of low or absent Pellino3 expression argued for an analysis of a direct role for Pellino3 in regulating the apoptotic arm of the TNF pathway.

4.3 Pellino3 is a regulator of DISC formation

Upon TNF stimuli, TNFR trimerisates and recruits many effector proteins, such as TRADD, TRAF2, TRAF5 and RIP1 to form a complex referred as complex I (Chen and Goeddel, 2002). RIP1 is a key in determining the cells' fate to live or die. RIP1 can activate NF-κB by recruiting the IKK complex to TNF-R1, which is dependent on the TNF-induced K63-linked polyubiquitin of RIP1, thus facilitating the recruitment of the IKK complex (Meylan et al., 2004; Ting et al., 1996; Ea et al., 2006). RIP1 can also recruit FADD via a homotypic DD-DD interaction, forming a new complex, named complex II. The new complex subsequently activates procaspase-8 and initiates cell apoptosis. Given that Pellino3 has anti-apoptotic activity, and Pellino1 has showed its ability to interact with and ubiquitinate RIP1 (Chang et al., 2009), which is a key component of DISC, it was conceivable that Pellino3 may affect the formation of DISC. The interactions between Pellino3 and the core components of DISC, RIP1, FADD and caspase-8 were also examined. Pellino3 and RIP1 indeed formed a stable complex, which was detected by coimmunoprecipitation assay. *In vitro* binding assays also showed that Pellino3 bound directly to RIP1. Interestingly, Pellino3 does not affect RIP1 ubiquitination (data not shown), and this contrasts with the ability of Pellino1 to act as an ubiquitin E3 ligase for RIP1 (Chang et al., 2009). This demonstrates the non-redundant nature of members of the Pellino family.

Coimmunoprecipitation assays and *in vitro* binding assays also showed that Pellino3 directly interacts with caspase-8. Procaspase-8 contains a C-terminal catalytic domain and two DEDs in its N-terminal, which interact with a homologous DED on FADD

(Cryns and Yuan, 1998). After complex II formation, caspase-8 is slowly activated. While the catalytic domain of caspase-8 stays in the complex, the active p20/p18 domain is released to cytosol (Jin and El-Deiry, 2006). Our studies show that Pellino3 interacts with the catalytic domain of caspase-8, not the DED domain, indicating that after Caspase-8 activation Pellino3 may still stay in the complex and play a further role. Moreover, Pellino3 does not bind to FADD. The ability of Pellino3 to interact with endogenous RIP1, procaspase-8 and FADD in the presence of TNF were also assessed. Overexpressed Pellino3 is constitutively associated with procaspase-8, and after TNF stimulation Pellino3 is recruited to RIP1, and thus brings the latter into close proximity with procaspase-8. Pellino3 has no interaction with endogenous FADD, which is consistent with the coimmunoprecipitation results. However, the suppressed expression of Pellino3 resulted in greater levels of RIP1 and FADD interacting with caspase-8 and as such the increased DISC formation is consistent with the greater pro-apoptotic effects of TNF in cells where Pellino3 expression is suppressed. Collectively, these data demonstrate that Pellino3 plays a key role in regulating DISC formation and apoptosis in response to TNF.

Recent studies have reported that A20 binding and inhibitor of NF-κB (ABIN-1) and ubiquitously expressed transcript-V1 (UXT-V1) have the ability to protect cells against TNF-induced apoptosis. ABIN-1 functions through inhibiting caspase-8 recruitment to FADD, preventing caspase-8 cleavage and programmed cell death (Oshima et al., 2009). UXT-V1 plays its role by binding to TRAF2 and preventing the TRAF2-RIP-TRADD complex from recruiting FADD and caspase-8 (Huang et al., 2011). Pellino3 may work through a mechanism that is similar to that used by ABIN-1. However, ABIN-1's anti-apoptotic activity requires its ubiquitin sensing activity (Oshima et al., 2009). Although Pellino3 contains a RING like motif and possess E3 ubiquitin ligase activity (Butler et al., 2007), the present study shows that regulatory effects of Pellino3 in the TNF pathway are not dependent on its E3 ligase activity.

4.4 Pellino3 targets RIP1 in a FHA domain-dependent manner

All Pellino proteins contain a C-terminal RING-like domain and an N-terminal FHA domain. The first functional motif identified in Pellino proteins was the RING-like domain. Proteins containing RING domains possess a ubiquitin ligase activity that catalyses the transfer of ubiquitin chains from E2 ubiquitin conjugating enzymes to the target substrates (Deshaies and Joazeiro, 2009). Pellino proteins have been shown to have both K63 and K48 E3 ligase activities. They interact with IRAK with the latter being capable of inducing phosphorylaton and increasing the E3 ligase activity of the Pellinos ultimately resulting in increased polyubiquitination of IRAK (Butler et al., 2007; Ordureau et al., 2008). RIP1 acts in an equivalent capacity to IRAK-1 in the TNF pathway and thus it was intriguing that Pellino1 can also bind and ubiquitinate RIP1. However our study shows no evidence that Pellino3 is involved in regulating RIP1 ubiquitination. Also the RING mutant of Pellino3 was still able to interact with RIP1 (in related research of this study), suggesting the regulatory effects of Pellino3 on DISC formation and apoptosis are independent of its E3 catalytic activity. The FHA domain is a phosphopeptide recognition domain, found in many regulatory proteins which play a role in the checkpoint and DNA-damage response (Durocher et al., 2000). Lin et al. discovered that Pellino2 binds to the phosphorylated forms of IRAK through their FHA domain and targets them for ubiquitinylation (Lin et al., 2008). As RIP1 is a distant relative to the IRAK family (Dardick and Ronald, 2006) and upon TNF treatment, RIP1 undergoes autophosphorylation and ubiquitination (Lee et al., 2004), this suggested that the FHA domain might play a role in RIP1-Pellino3 interaction. Coimmunoprecipitation assays and *in vitro* binding assays showed that the FHA domain of Pellino3 is required for its binding to RIP1. Furthermore, the FHA domain of Pellino3 is crucial for its anti-apoptotic activity. This at least demonstrates a critical role for the FHA domain in Pellino3 biology. However the questions remains as to the functional relevance of the RING-like

domain of Pellino3. Given its highly conserved nature and preservation through evolution it is likely to be of fundamental importance but it remains to be delineated.

4.5 In vivo animal studies

As mentioned in 4.1, Pellino3-deficient mice were generated to further investigate the function of Pellino3 in vivo. The Pellino3 homozygous knockout mice were viable, and their general condition did not reveal gross abnormalities with the exception of a reduced body weight. The proportions for heterozygous and homozygous mutant pups are slightly lower than the expected Mendelian ratio. Foetal loss of Pellino3 mutant mice suggests that Pellino3 may play a role in embryo development or fertilization and it is interesting to speculate that this may be related to the increased propensity of cells to undergo apoptosis when Pellino3 expression is reduced or absent. Furthermore, Pellino3-deficient mice showed a greatly increased susceptibility to the lethal effects of TNF and this was associated with increased severity of TNF-induced hepatotoxicity. This finding provides strong physiological evidence to support the previous *in vitro* studies that loss of Pellino3 greatly increases the proclivity of TNF to induce apoptosis.

4.6 Concluding Remarks

In summary, the present findings highlight Pellino3 as a new player in the TNF signalling pathway, and strongly indicate that it may play an important role in determining whether a cell survives or dies in response to TNF. Pellino3 directly interacts with the DISC components, RIP1 and caspase-8. Knockdown or genetic deficiency of Pellino3 sensitises cells to TNF-induced apoptosis, which is

independent of NF-κB or MAPK signalling. Instead the loss of Pellino3 leads to increased DISC formation in response to TNF. Interestingly, the regulatory effects of Pellino3 on RIP1 are independent of its well-known E3 ligase activity. Instead the N-terminal FHA domain of Pellino3 is crucially important in facilitating its interaction with RIP1 and the regulation of TNF-induced DISC formation. The FHA domain is a phosphothreonine-binding module, and the identification of potential recognition sites on RIP1 for the FHA domain of Pellino3 will add greatly to our understanding of the TNF signalling pathway. Pellino3-deficient mice also show a greatly increased sensitivity to TNF-induced hepatotoxicity and ultimate lethality, thus emphasising the crucial physiological role of Pellino3 in determining cell's fate in response TNF challenge.

The role of Pellino3 in the regulation of the formation of FADD-RIP1-caspase-8 complexes independently of death receptor signalling may also be interesting to explore. Recent reports described a cytosolic death-inducing FADD-caspase-8-RIP1 complex that forms independently of death receptor activation but in response to intracellular stress (Feoktistova et al., 2011; Tenev et al., 2011). To differentiate it from complex II, the "Ripoptosome" was coined to define a complex that forms spontaneously in response to depletion of cIAPs by IAP antagonists or the genotoxic compound etoposide. It will be interesting to explore the potential of Pellino3 to regulate Ripoptosome formation and cell death pathways in response to such intracellular cues and stress. The role of Pellino3 during TNF-induced apoptosis is presented in Figure 4-1.

The present study also adds to a growing appreciation of the diverse functions of the Pellino family in immune signalling pathways. To date most studies focused on Pellino proteins as regulators of IL-1 and TLR signalling, this study extends their roles beyond these pathways. Interestingly a very recent report has described Pellino1 as an important regulator of T cell activation and self tolerance (Chang et al., 2011).

Such findings, in conjunction with the present study, add to an increasing appreciation of the importance of the Pellino family in a variety of signalling pathways in the innate and adaptive immune systems.

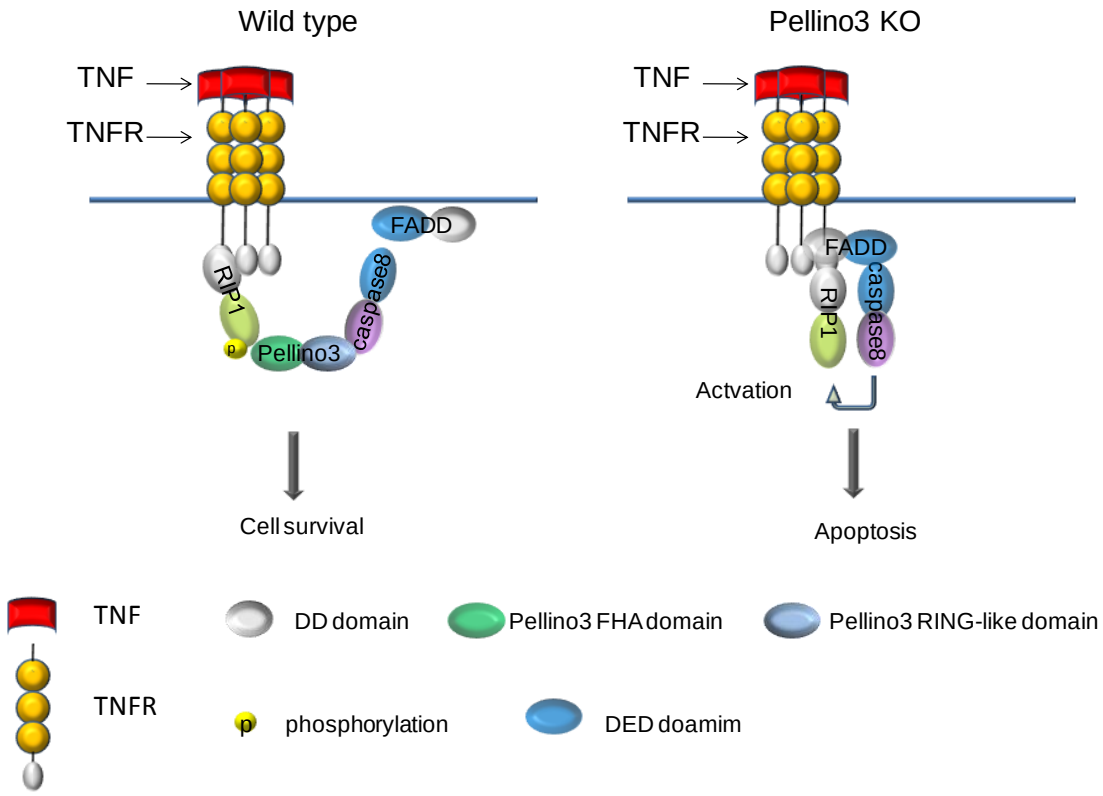

Figure 4-1 The role of Pellino3 during TNF-induced apoptosis.

Pellino3 blocks recruitment of FADD in the DISC. Pellino3 directly interacts with the DISC components, RIP1 and caspase-8. The FHA domain of Pellino3 is crucial in facilitating its interaction with RIP1 and the regulation of TNF-induced DISC formation. The loss of Pellino3 leads to increased DISC formation in response to TNF.

BIBLIOGRAGHY

Aggarwal, B.B. (2003). Signalling pathways of the TNF superfamily: a double-edged sword. Nat Rev Immunol *3*, 745-756.

Akira, S., and Takeda, K. (2004). Toll-like receptor signalling. Nat Rev Immunol *4*, 499-511.

Aksentijevich, I., Masters, S.L., Ferguson, P.J., Dancey, P., Frenkel, J., van Royen-Kerkhoff, A., Laxer, R., Tedgard, U., Cowen, E.W., Pham, T.H., *et al.* (2009). An autoinflammatory disease with deficiency of the interleukin-1-receptor antagonist. N Engl J Med *360*, 2426-2437.

Alexopoulou, L., Holt, A.C., Medzhitov, R., and Flavell, R.A. (2001). Recognition of double-stranded RNA and activation of NF-kappaB by Toll-like receptor 3. Nature *413*, 732-738.

Alkalay, I., Yaron, A., Hatzubai, A., Orian, A., Ciechanover, A., and Ben-Neriah, Y. (1995). Stimulation-dependent I kappa B alpha phosphorylation marks the NF-kappa B inhibitor for degradation via the ubiquitin-proteasome pathway. Proc Natl Acad Sci U S A *92*, 10599-10603.

Amati, L., Pepe, M., Passeri, M.E., Mastronardi, M.L., Jirillo, E., and Covelli, V. (2006). Toll-like receptor signaling mechanisms involved in dendritic cell activation: potential therapeutic control of T cell polarization. Curr Pharm Des *12*, 4247-4254.

Aragay, A.M., Collins, L.R., Post, G.R., Watson, A.J., Feramisco, J.R., Brown, J.H., and Simon, M.I. (1995). G12 requirement for thrombin-stimulated gene expression and DNA synthesis in 1321N1 astrocytoma cells. J Biol Chem *270*, 20073-20077.

Ardley, H.C., and Robinson, P.A. (2005). E3 ubiquitin ligases. Essays Biochem *41*, 15-30.

Asadullah, K., Sterry, W., and Volk, H.D. (2003). Interleukin-10 therapy--review of a new approach. Pharmacol Rev *55*, 241-269.

Ashkenazi, A., and Dixit, V.M. (1998). Death receptors: signaling and modulation. Science *281*, 1305-1308.

Baboshina, O.V., and Haas, A.L. (1996). Novel multiubiquitin chain linkages catalyzed by the conjugating enzymes E2EPF and RAD6 are recognized by 26 S proteasome subunit 5. J Biol Chem *271*, 2823-2831.

Bagchi, A., Herrup, E.A., Warren, H.S., Trigilio, J., Shin, H.S., Valentine, C., and Hellman, J. (2007). MyD88-dependent and MyD88-independent pathways in synergy, priming, and tolerance between TLR agonists. J Immunol *178*, 1164-1171.

Bandman, O., Coleman, R.T., Loring, J.F., Seilhamer, J.J., and Cocks, B.G. (2002). Complexity of inflammatory responses in endothelial cells and vascular smooth muscle cells determined by microarray analysis. Ann N Y Acad Sci *975*, 77-90.

Banner, D.W., D'Arcy, A., Janes, W., Gentz, R., Schoenfeld, H.J., Broger, C., Loetscher, H., and Lesslauer, W. (1993). Crystal structure of the soluble human 55 kd TNF receptor-human TNF beta complex: implications for TNF receptor activation. Cell *73*, 431-445.

Barnes, B.J., Field, A.E., and Pitha-Rowe, P.M. (2003). Virus-induced heterodimer formation between IRF-5 and IRF-7 modulates assembly of the IFNA enhanceosome in vivo and transcriptional activity of IFNA genes. J Biol Chem *278*, 16630-16641.

Bertrand, M.J., Milutinovic, S., Dickson, K.M., Ho, W.C., Boudreault, A., Durkin, J., Gillard, J.W., Jaquith, J.B., Morris, S.J., and Barker, P.A. (2008). cIAP1 and cIAP2 facilitate cancer cell survival by functioning as E3 ligases that promote RIP1 ubiquitination. Mol Cell *30*, 689-700.

Boise, L.H., Gonzalez-Garcia, M., Postema, C.E., Ding, L., Lindsten, T., Turka, L.A., Mao, X., Nunez, G., and Thompson, C.B. (1993). bcl-x, a bcl-2-related gene that functions as a dominant regulator of apoptotic cell death. Cell *74*, 597-608.

Boldin, M.P., Varfolomeev, E.E., Pancer, Z., Mett, I.L., Camonis, J.H., and Wallach, D. (1995). A novel protein that interacts with the death domain of Fas/APO1 contains a sequence motif related to the death domain. J Biol Chem *270*, 7795-7798.

Brissoni, B., Agostini, L., Kropf, M., Martinon, F., Swoboda, V., Lippens, S., Everett, H., Aebi, N., Janssens, S., Meylan, E., *et al.* (2006). Intracellular trafficking of interleukin-1 receptor I requires Tollip. Curr Biol *16*, 2265-2270.

Bulut, Y., Faure, E., Thomas, L., Karahashi, H., Michelsen, K.S., Equils, O., Morrison, S.G., Morrison, R.P., and Arditi, M. (2002). Chlamydial heat shock protein 60 activates macrophages and endothelial cells through Toll-like receptor 4 and MD2 in a MyD88-dependent pathway. J Immunol *168*, 1435-1440.

Butler, M.P., Hanly, J.A., and Moynagh, P.N. (2005). Pellino3 is a novel upstream regulator of p38 MAPK and activates CREB in a p38-dependent manner. J Biol Chem *280*, 27759-27768.

Butler, M.P., Hanly, J.A., and Moynagh, P.N. (2007). Kinase-active interleukin-1 receptor-associated kinases promote polyubiquitination and degradation of the Pellino family: direct evidence for PELLINO proteins being ubiquitin-protein isopeptide ligases. J Biol Chem *282*, 29729-29737.

Chang, L., Kamata, H., Solinas, G., Luo, J.L., Maeda, S., Venuprasad, K., Liu, Y.C., and Karin, M. (2006). The E3 ubiquitin ligase itch couples JNK activation to TNFalpha-induced cell death by inducing c-FLIP(L) turnover. Cell *124*, 601-613.

Chang, M., Jin, W., Chang, J.H., Xiao, Y., Brittain, G.C., Yu, J., Zhou, X., Wang, Y.H., Cheng, X., Li, P., *et al.* (2011). The ubiquitin ligase Peli1 negatively regulates T cell activation and prevents autoimmunity. Nat Immunol *12*, 1002-1009.

Chang, M., Jin, W., and Sun, S.C. (2009). Peli1 facilitates TRIF-dependent Toll-like receptor signaling and proinflammatory cytokine production. Nat Immunol *10*, 1089-1095.

Chen, G., and Goeddel, D.V. (2002). TNF-R1 signaling: a beautiful pathway. Science *296*, 1634-1635.

Chen, Z., Gibson, T.B., Robinson, F., Silvestro, L., Pearson, G., Xu, B., Wright, A., Vanderbilt, C., and Cobb, M.H. (2001). MAP kinases. Chem Rev *101*, 2449-2476.

Cho, Y.S., Challa, S., Moquin, D., Genga, R., Ray, T.D., Guildford, M., and Chan, F.K. (2009). Phosphorylation-driven assembly of the RIP1-RIP3 complex regulates programmed necrosis and virus-induced inflammation. Cell *137*, 1112-1123.

Choi, K.C., Lee, Y.S., Lim, S., Choi, H.K., Lee, C.H., Lee, E.K., Hong, S., Kim, I.H., Kim, S.J., and Park, S.H. (2006). Smad6 negatively regulates interleukin 1-receptor-Toll-like receptor signaling through direct interaction with the adaptor Pellino-1. Nat Immunol *7*, 1057-1065.

Clark, R., and Kupper, T. (2005). Old meets new: the interaction between innate and adaptive immunity. J Invest Dermatol *125*, 629-637.

Cohen, P. (1992). Signal integration at the level of protein kinases, protein phosphatases and their substrates. Trends Biochem Sci *17*, 408-413.

Conze, D.B., Wu, C.J., Thomas, J.A., Landstrom, A., and Ashwell, J.D. (2008). Lys63-linked polyubiquitination of IRAK-1 is required for interleukin-1 receptor- and toll-like receptor-mediated NF-kappaB activation. Mol Cell Biol *28*, 3538-3547.

Cryns, V., and Yuan, J. (1998). Proteases to die for. Genes Dev *12*, 1551-1570.

Cusson-Hermance, N., Khurana, S., Lee, T.H., Fitzgerald, K.A., and Kelliher, M.A. (2005). Rip1 mediates the Trif-dependent toll-like receptor 3- and 4-induced NF-{kappa}B activation but does not contribute to interferon regulatory factor 3 activation. J Biol Chem *280*, 36560-36566.

da Silva Correia, J., Soldau, K., Christen, U., Tobias, P.S., and Ulevitch, R.J. (2001). Lipopolysaccharide is in close proximity to each of the proteins in its membrane receptor complex. transfer from CD14 to TLR4 and MD-2. J Biol Chem *276*, 21129-21135.

Dardick, C., and Ronald, P. (2006). Plant and animal pathogen recognition receptors signal through non-RD kinases. PLoS Pathog *2*, e2.

Datta, R., Oki, E., Endo, K., Biedermann, V., Ren, J., and Kufe, D. (2000). XIAP regulates DNA damage-induced apoptosis downstream of caspase-9 cleavage. J Biol Chem *275*, 31733-31738.

Decker, K., and Keppler, D. (1974). Galactosamine hepatitis: key role of the nucleotide deficiency period in the pathogenesis of cell injury and cell death. Rev Physiol Biochem Pharmacol, 77-106.

Declercq, W., Van Herreweghe, Franky, Berghe, Tom Vanden, and Vandenabeele, Peter (2009). Death Receptor ‐ induced Necroptosis. eLS John Wiley & Sons Ltd, Chichester http://wwwelsnet [doi: 101002/9780470015902a0021566] *Dec 2009*.

Degterev, A., Hitomi, J., Germscheid, M., Ch'en, I.L., Korkina, O., Teng, X., Abbott, D., Cuny, G.D., Yuan, C., Wagner, G., *et al.* (2008). Identification of RIP1 kinase as a specific cellular target of necrostatins. Nat Chem Biol *4*, 313-321.

Degterev, A., Huang, Z., Boyce, M., Li, Y., Jagtap, P., Mizushima, N., Cuny, G.D., Mitchison, T.J., Moskowitz, M.A., and Yuan, J. (2005). Chemical inhibitor of nonapoptotic cell death with therapeutic potential for ischemic brain injury. Nat Chem Biol *1*, 112-119.

Dejardin, E. (2006). The alternative NF-kappaB pathway from biochemistry to biology: pitfalls and promises for future drug development. Biochem Pharmacol *72*, 1161-1179.

Demaria, O., Pagni, P.P., Traub, S., de Gassart, A., Branzk, N., Murphy, A.J., Valenzuela, D.M., Yancopoulos, G.D., Flavell, R.A., and Alexopoulou, L. (2010). TLR8 deficiency leads to autoimmunity in mice. J Clin Invest *120*, 3651-3662.

Denecker, G., Vercammen, D., Declercq, W., and Vandenabeele, P. (2001). Apoptotic and necrotic cell death induced by death domain receptors. Cell Mol Life Sci *58*, 356-370.

Deng, L., Wang, C., Spencer, E., Yang, L., Braun, A., You, J., Slaughter, C., Pickart, C., and Chen, Z.J. (2000). Activation of the IkappaB kinase complex by TRAF6 requires a dimeric ubiquitin-conjugating enzyme complex and a unique polyubiquitin chain. Cell *103*, 351-361.

Deshaies, R.J., and Joazeiro, C.A. (2009). RING domain E3 ubiquitin ligases. Annu Rev Biochem *78*, 399-434.

Diebold, S.S., Kaisho, T., Hemmi, H., Akira, S., and Reis e Sousa, C. (2004). Innate antiviral responses by means of TLR7-mediated recognition of single-stranded RNA. Science *303*, 1529-1531.

Dinarello, C.A. (1996). Biologic basis for interleukin-1 in disease. Blood *87*, 2095-2147.

Dinarello, C.A. (2011). Interleukin-1 in the pathogenesis and treatment of inflammatory diseases. Blood *117*, 3720-3732.

Du, X., Poltorak, A., Wei, Y.G., and Beutler, B. (2000). Three novel mammalian Toll-like receptors: gene structure, expression, and evolution. Eur Cytokine Netw *11*, 362-371.

Dunne, A., and O'Neill, L.A. (2003). The interleukin-1 receptor/Toll-like receptor superfamily: signal transduction during inflammation and host defense. Sci STKE *2003*, re3.

Durocher, D., Taylor, I.A., Sarbassova, D., Haire, L.F., Westcott, S.L., Jackson, S.P., Smerdon, S.J., and Yaffe, M.B. (2000). The molecular basis of FHA domain:phosphopeptide binding specificity and implications for phospho-dependent signaling mechanisms. Mol Cell *6*, 1169-1182.

Dutta, J., Fan, Y., Gupta, N., Fan, G., and Gelinas, C. (2006). Current insights into the regulation of programmed cell death by NF-kappaB. Oncogene *25*, 6800-6816.

Ea, C.K., Deng, L., Xia, Z.P., Pineda, G., and Chen, Z.J. (2006). Activation of IKK by TNFalpha requires site-specific ubiquitination of RIP1 and polyubiquitin binding by NEMO. Mol Cell *22*, 245-257.

Eckelman, B.P., Salvesen, G.S., and Scott, F.L. (2006). Human inhibitor of apoptosis proteins: why XIAP is the black sheep of the family. EMBO Rep *7*, 988-994.

Enesa, K., Zakkar, M., Chaudhury, H., Luong le, A., Rawlinson, L., Mason, J.C., Haskard, D.O., Dean, J.L., and Evans, P.C. (2008). NF-kappaB suppression by the deubiquitinating enzyme Cezanne: a novel negative feedback loop in pro-inflammatory signaling. J Biol Chem *283*, 7036-7045.

Fan, T.J., Han, L.H., Cong, R.S., and Liang, J. (2005). Caspase family proteases and apoptosis. Acta Biochim Biophys Sin (Shanghai) *37*, 719-727.

Feoktistova, M., Geserick, P., Kellert, B., Dimitrova, D.P., Langlais, C., Hupe, M., Cain, K., MacFarlane, M., Hacker, G., and Leverkus, M. (2011). cIAPs block Ripoptosome formation, a RIP1/caspase-8 containing intracellular cell death complex differentially regulated by cFLIP isoforms. Mol Cell *43*, 449-463.

Festjens, N., Vanden Berghe, T., and Vandenabeele, P. (2006). Necrosis, a well-orchestrated form of cell demise: signalling cascades, important mediators and concomitant immune response. Biochim Biophys Acta *1757*, 1371-1387.

Field, A.K., Tytell, A.A., Lampson, G.P., and Hilleman, M.R. (1967). Inducers of interferon and host resistance. II. Multistranded synthetic polynucleotide complexes. Proc Natl Acad Sci U S A *58*, 1004-1010.

Fiers, W., Beyaert, R., Boone, E., Cornelis, S., Declercq, W., Decoster, E., Denecker, G., Depuydt, B., De Valck, D., De Wilde, G., *et al.* (1995). TNF-induced intracellular

signaling leading to gene induction or to cytotoxicity by necrosis or by apoptosis. J Inflamm *47*, 67-75.

Fitzgerald, K.A., Rowe, D.C., Barnes, B.J., Caffrey, D.R., Visintin, A., Latz, E., Monks, B., Pitha, P.M., and Golenbock, D.T. (2003). LPS-TLR4 signaling to IRF-3/7 and NF-kappaB involves the toll adapters TRAM and TRIF. J Exp Med *198*, 1043-1055.

Foster, S.L., Hargreaves, D.C., and Medzhitov, R. (2007). Gene-specific control of inflammation by TLR-induced chromatin modifications. Nature *447*, 972-978.

Gaestel, M., Kotlyarov, A., and Kracht, M. (2009). Targeting innate immunity protein kinase signalling in inflammation. Nat Rev Drug Discov *8*, 480-499.

Galluzzi, L., and Kroemer, G. (2008). Necroptosis: a specialized pathway of programmed necrosis. Cell *135*, 1161-1163.

Gaur, U., and Aggarwal, B.B. (2003). Regulation of proliferation, survival and apoptosis by members of the TNF superfamily. Biochem Pharmacol *66*, 1403-1408.

Gauzzi, M.C., Del Corno, M., and Gessani, S. (2010). Dissecting TLR3 signalling in dendritic cells. Immunobiology *215*, 713-723.

Geserick, P., Drewniok, C., Hupe, M., Haas, T.L., Diessenbacher, P., Sprick, M.R., Schon, M.P., Henkler, F., Gollnick, H., Walczak, H., *et al.* (2008). Suppression of cFLIP is sufficient to sensitize human melanoma cells to TRAIL- and CD95L-mediated apoptosis. Oncogene *27*, 3211-3220.

Ghosh, S., May, M.J., and Kopp, E.B. (1998). NF-kappa B and Rel proteins: evolutionarily conserved mediators of immune responses. Annu Rev Immunol *16*, 225-260.

Gohda, J., Matsumura, T., and Inoue, J. (2004). Cutting edge: TNFR-associated factor (TRAF) 6 is essential for MyD88-dependent pathway but not toll/IL-1 receptor domain-containing adaptor-inducing IFN-beta (TRIF)-dependent pathway in TLR signaling. J Immunol *173*, 2913-2917.

Golstein, P., and Kroemer, G. (2007). Cell death by necrosis: towards a molecular definition. Trends Biochem Sci *32*, 37-43.

Graham, F.L., Smiley, J., Russell, W.C., and Nairn, R. (1977). Characteristics of a human cell line transformed by DNA from human adenovirus type 5. J Gen Virol *36*, 59-74.

Grell, M., Douni, E., Wajant, H., Lohden, M., Clauss, M., Maxeiner, B., Georgopoulos, S., Lesslauer, W., Kollias, G., Pfizenmaier, K., *et al.* (1995). The transmembrane form of tumor necrosis factor is the prime activating ligand of the 80 kDa tumor necrosis factor receptor. Cell *83*, 793-802.

Griffin, B.D., Mellett, M., Campos-Torres, A., Kinsella, G.K., Wang, B., and Moynagh, P.N. (2011). A poxviral homolog of the Pellino protein inhibits Toll and Toll-like receptor signalling. Eur J Immunol *41*, 798-812.

Grosshans, J., Schnorrer, F., and Nusslein-Volhard, C. (1999). Oligomerisation of Tube and Pelle leads to nuclear localisation of dorsal. Mech Dev *81*, 127-138.

Hacker, H., Redecke, V., Blagoev, B., Kratchmarova, I., Hsu, L.C., Wang, G.G., Kamps, M.P., Raz, E., Wagner, H., Hacker, G., *et al.* (2006). Specificity in Toll-like receptor signalling through distinct effector functions of TRAF3 and TRAF6. Nature *439*, 204-207.

Haghayeghi, A., Sarac, A., Czerniecki, S., Grosshans, J., and Schock, F. (2010). Pellino enhances innate immunity in Drosophila. Mech Dev *127*, 301-307.

Haranaka, K., Satomi, N., Sakurai, A., and Haranaka, R. (1984). Role of first stimulating agents in the production of tumor necrosis factor. Cancer Immunol Immunother *18*, 87-90.

Harlin, H., Reffey, S.B., Duckett, C.S., Lindsten, T., and Thompson, C.B. (2001). Characterization of XIAP-deficient mice. Mol Cell Biol *21*, 3604-3608.

Hasan, U., Chaffois, C., Gaillard, C., Saulnier, V., Merck, E., Tancredi, S., Guiet, C., Briere, F., Vlach, J., Lebecque, S., *et al.* (2005). Human TLR10 is a functional receptor, expressed by B cells and plasmacytoid dendritic cells, which activates gene transcription through MyD88. Journal of Immunology *174*, 2942-2950.

Hawari, F.I., Rouhani, F.N., Cui, X., Yu, Z.X., Buckley, C., Kaler, M., and Levine, S.J. (2004). Release of full-length 55-kDa TNF receptor 1 in exosome-like vesicles: a mechanism for generation of soluble cytokine receptors. Proc Natl Acad Sci U S A *101*, 1297-1302.

Hayashi, F., Smith, K.D., Ozinsky, A., Hawn, T.R., Yi, E.C., Goodlett, D.R., Eng, J.K., Akira, S., Underhill, D.M., and Aderem, A. (2001). The innate immune response to bacterial flagellin is mediated by Toll-like receptor 5. Nature *410*, 1099-1103.

Hayden, M.S., and Ghosh, S. (2008). Shared principles in NF-kappaB signaling. Cell *132*, 344-362.

He, S., Wang, L., Miao, L., Wang, T., Du, F., Zhao, L., and Wang, X. (2009). Receptor interacting protein kinase-3 determines cellular necrotic response to TNF-alpha. Cell *137*, 1100-1111.

Heil, F., Hemmi, H., Hochrein, H., Ampenberger, F., Kirschning, C., Akira, S., Lipford, G., Wagner, H., and Bauer, S. (2004). Species-specific recognition of single-stranded RNA via toll-like receptor 7 and 8. Science *303*, 1526-1529.

Hemmi, H., Kaisho, T., Takeuchi, O., Sato, S., Sanjo, H., Hoshino, K., Horiuchi, T., Tomizawa, H., Takeda, K., and Akira, S. (2002). Small anti-viral compounds activate

immune cells via the TLR7 MyD88-dependent signaling pathway. Nat Immunol *3*, 196-200.

Hitomi, J., Christofferson, D.E., Ng, A., Yao, J., Degterev, A., Xavier, R.J., and Yuan, J. (2008). Identification of a molecular signaling network that regulates a cellular necrotic cell death pathway. Cell *135*, 1311-1323.

Hoffmann, E., Thiefes, A., Buhrow, D., Dittrich-Breiholz, O., Schneider, H., Resch, K., and Kracht, M. (2005). MEK1-dependent delayed expression of Fos-related antigen-1 counteracts c-Fos and p65 NF-kappaB-mediated interleukin-8 transcription in response to cytokines or growth factors. J Biol Chem *280*, 9706-9718.

Holler, N., Zaru, R., Micheau, O., Thome, M., Attinger, A., Valitutti, S., Bodmer, J.L., Schneider, P., Seed, B., and Tschopp, J. (2000). Fas triggers an alternative, caspase-8-independent cell death pathway using the kinase RIP as effector molecule. Nat Immunol *1*, 489-495.

Holzberg, D., Knight, C.G., Dittrich-Breiholz, O., Schneider, H., Dorrie, A., Hoffmann, E., Resch, K., and Kracht, M. (2003). Disruption of the c-JUN-JNK complex by a cell-permeable peptide containing the c-JUN delta domain induces apoptosis and affects a distinct set of interleukin-1-induced inflammatory genes. J Biol Chem *278*, 40213-40223.

Honda, K., Takaoka, A., and Taniguchi, T. (2006). Type I interferon [corrected] gene induction by the interferon regulatory factor family of transcription factors. Immunity *25*, 349-360.

Horstmann, S., Kahle, P.J., and Borasio, G.D. (1998). Inhibitors of p38 mitogen-activated protein kinase promote neuronal survival in vitro. J Neurosci Res *52*, 483-490.

Hoshino, K., Takeuchi, O., Kawai, T., Sanjo, H., Ogawa, T., Takeda, Y., Takeda, K., and Akira, S. (1999). Cutting edge: Toll-like receptor 4 (TLR4)-deficient mice are hyporesponsive to lipopolysaccharide: evidence for TLR4 as the Lps gene product. J Immunol *162*, 3749-3752.

Hsu, H., Shu, H.B., Pan, M.G., and Goeddel, D.V. (1996). TRADD-TRAF2 and TRADD-FADD interactions define two distinct TNF receptor 1 signal transduction pathways. Cell *84*, 299-308.

Huang, Y., Chen, L., Zhou, Y., Liu, H., Yang, J., Liu, Z., and Wang, C. (2011). UXT-V1 protects cells against TNF-induced apoptosis through modulating complex II formation. Mol Biol Cell *22*, 1389-1397.

Irmler, M., Thome, M., Hahne, M., Schneider, P., Hofmann, K., Steiner, V., Bodmer, J.L., Schroter, M., Burns, K., Mattmann, C., *et al.* (1997). Inhibition of death receptor signals by cellular FLIP. Nature *388*, 190-195.

Jacchieri, S.G., Torquato, R., and Brentani, R.R. (2003). Structural study of binding of flagellin by Toll-like receptor 5. J Bacteriol *185*, 4243-4247.

Jap, A., and Chee, S.P. (2008). Immunosuppressive therapy for ocular diseases. Curr Opin Ophthalmol *19*, 535-540.

Jensen, L.E., and Whitehead, A.S. (2003a). Pellino2 activates the mitogen activated protein kinase pathway. FEBS Lett *545*, 199-202.

Jensen, L.E., and Whitehead, A.S. (2003b). Pellino3, a novel member of the Pellino protein family, promotes activation of c-Jun and Elk-1 and may act as a scaffolding protein. J Immunol *171*, 1500-1506.

Jeong, E.J., Bang, S., Lee, T.H., Park, Y.I., Sim, W.S., and Kim, K.S. (1999). The solution structure of FADD death domain. Structural basis of death domain interactions of Fas and FADD. J Biol Chem *274*, 16337-16342.

Jiang, Q., Akashi, S., Miyake, K., and Petty, H.R. (2000). Lipopolysaccharide induces physical proximity between CD14 and toll-like receptor 4 (TLR4) prior to nuclear translocation of NF-kappa B. J Immunol *165*, 3541-3544.

Jiang, Y., Woronicz, J.D., Liu, W., and Goeddel, D.V. (1999). Prevention of constitutive TNF receptor 1 signaling by silencer of death domains. Science *283*, 543-546.

Jiang, Z., Johnson, H.J., Nie, H., Qin, J., Bird, T.A., and Li, X. (2003). Pellino 1 is required for interleukin-1 (IL-1)-mediated signaling through its interaction with the IL-1 receptor-associated kinase 4 (IRAK4)-IRAK-tumor necrosis factor receptor-associated factor 6 (TRAF6) complex. J Biol Chem *278*, 10952-10956.

Jin, Z., and El-Deiry, W.S. (2006). Distinct signaling pathways in TRAIL- versus tumor necrosis factor-induced apoptosis. Mol Cell Biol *26*, 8136-8148.

Johnson, G.B., Brunn, G.J., Kodaira, Y., and Platt, J.L. (2002). Receptor-mediated monitoring of tissue well-being via detection of soluble heparan sulfate by Toll-like receptor 4. J Immunol *168*, 5233-5239.

Johnson, G.L., and Lapadat, R. (2002). Mitogen-activated protein kinase pathways mediated by ERK, JNK, and p38 protein kinases. Science *298*, 1911-1912.

Jourdan, M., De Vos, J., Mechti, N., and Klein, B. (2000). Regulation of Bcl-2-family proteins in myeloma cells by three myeloma survival factors: interleukin-6, interferon-alpha and insulin-like growth factor 1. Cell Death Differ *7*, 1244-1252.

Junttila, M.R., Li, S.P., and Westermarck, J. (2008). Phosphatase-mediated crosstalk between MAPK signaling pathways in the regulation of cell survival. FASEB J *22*, 954-965.

Karin, M. (1999). The beginning of the end: IkappaB kinase (IKK) and NF-kappaB activation. J Biol Chem *274*, 27339-27342.

Karin, M., and Ben-Neriah, Y. (2000). Phosphorylation meets ubiquitination: the control of NF-[kappa]B activity. Annu Rev Immunol *18*, 621-663.

Kawai, T., and Akira, S. (2008). Toll-like receptor and RIG-I-like receptor signaling. Ann N Y Acad Sci *1143*, 1-20.

Kawai, T., and Akira, S. (2010). The role of pattern-recognition receptors in innate immunity: update on Toll-like receptors. Nat Immunol *11*, 373-384.

Kawasaki, K., Akashi, S., Shimazu, R., Yoshida, T., Miyake, K., and Nishijima, M. (2000). Mouse toll-like receptor 4.MD-2 complex mediates lipopolysaccharide-mimetic signal transduction by Taxol. J Biol Chem *275*, 2251-2254.

Kelliher, M.A., Grimm, S., Ishida, Y., Kuo, F., Stanger, B.Z., and Leder, P. (1998). The death domain kinase RIP mediates the TNF-induced NF-kappaB signal. Immunity *8*, 297-303.

Kim, J.H., Sung, K.S., Jung, S.M., Lee, Y.S., Kwon, J.Y., Choi, C.Y., and Park, S.H. (2011). Pellino-1, an adaptor protein of interleukin-1 receptor/toll-like receptor signaling, is sumoylated by Ubc9. Mol Cells *31*, 85-89.

Kim, Y.M., Brinkmann, M.M., Paquet, M.E., and Ploegh, H.L. (2008). UNC93B1 delivers nucleotide-sensing toll-like receptors to endolysosomes. Nature *452*, 234-238.

Kim, Y.S., Morgan, M.J., Choksi, S., and Liu, Z.G. (2007). TNF-induced activation of the Nox1 NADPH oxidase and its role in the induction of necrotic cell death. Mol Cell *26*, 675-687.

Kobe, B., and Deisenhofer, J. (1995). Proteins with leucine-rich repeats. Curr Opin Struct Biol *5*, 409-416.

Koopman, G., Reutelingsperger, C.P., Kuijten, G.A., Keehnen, R.M., Pals, S.T., and van Oers, M.H. (1994). Annexin V for flow cytometric detection of phosphatidylserine expression on B cells undergoing apoptosis. Blood *84*, 1415-1420.

Kriegler, M., Perez, C., DeFay, K., Albert, I., and Lu, S.D. (1988). A novel form of TNF/cachectin is a cell surface cytotoxic transmembrane protein: ramifications for the complex physiology of TNF. Cell *53*, 45-53.

Krueger, A., Schmitz, I., Baumann, S., Krammer, P.H., and Kirchhoff, S. (2001). Cellular FLICE-inhibitory protein splice variants inhibit different steps of caspase-8 activation at the CD95 death-inducing signaling complex. J Biol Chem *276*, 20633-20640.

Kumar, S. (1995). ICE-like proteases in apoptosis. Trends Biochem Sci *20*, 198-202.

Lan, T., Kandimalla, E.R., Yu, D., Bhagat, L., Li, Y., Wang, D., Zhu, F., Tang, J.X., Putta, M.R., Cong, Y., *et al.* (2007). Stabilized immune modulatory RNA compounds as agonists of Toll-like receptors 7 and 8. Proc Natl Acad Sci U S A *104*, 13750-13755.

Lawen, A. (2003). Apoptosis-an introduction. Bioessays *25*, 888-896.

Lee, T.H., Shank, J., Cusson, N., and Kelliher, M.A. (2004). The kinase activity of Rip1 is not required for tumor necrosis factor-alpha-induced IkappaB kinase or p38 MAP kinase activation or for the ubiquitination of Rip1 by Traf2. J Biol Chem *279*, 33185-33191.

Lemaitre, B., Nicolas, E., Michaut, L., Reichhart, J.M., and Hoffmann, J.A. (1996). The dorsoventral regulatory gene cassette spatzle/Toll/cactus controls the potent antifungal response in Drosophila adults. Cell *86*, 973-983.

Li, H., Zhu, H., Xu, C.J., and Yuan, J. (1998). Cleavage of BID by caspase-8 mediates the mitochondrial damage in the Fas pathway of apoptosis. Cell *94*, 491-501.

Liang, X., Moseman, E.A., Farrar, M.A., Bachanova, V., Weisdorf, D.J., Blazar, B.R., and Chen, W. (2010). Toll-like receptor 9 signaling by CpG-B oligodeoxynucleotides induces an apoptotic pathway in human chronic lymphocytic leukemia B cells. Blood *115*, 5041-5052.

Lieb, K., Kaltschmidt, C., Kaltschmidt, B., Baeuerle, P.A., Berger, M., Bauer, J., and Fiebich, B.L. (1996). Interleukin-1 beta uses common and distinct signaling pathways for induction of the interleukin-6 and tumor necrosis factor alpha genes in the human astrocytoma cell line U373. J Neurochem *66*, 1496-1503.

Lin, C.C., Huoh, Y.S., Schmitz, K.R., Jensen, L.E., and Ferguson, K.M. (2008). Pellino proteins contain a cryptic FHA domain that mediates interaction with phosphorylated IRAK1. Structure *16*, 1806-1816.

Lin, R., Mamane, Y., and Hiscott, J. (1999a). Structural and functional analysis of interferon regulatory factor 3: localization of the transactivation and autoinhibitory domains. Mol Cell Biol *19*, 2465-2474.

Lin, Y., Devin, A., Rodriguez, Y., and Liu, Z.G. (1999b). Cleavage of the death domain kinase RIP by caspase-8 prompts TNF-induced apoptosis. Genes Dev *13*, 2514-2526.

Liu, Y., Dong, W., Chen, L., Xiang, R., Xiao, H., De, G., Wang, Z., and Qi, Y. (2004). BCL10 mediates lipopolysaccharide/toll-like receptor-4 signaling through interaction with Pellino2. J Biol Chem *279*, 37436-37444.

Locksley, R.M., Killeen, N., and Lenardo, M.J. (2001). The TNF and TNF receptor superfamilies: integrating mammalian biology. Cell *104*, 487-501.

Machein, U., Lieb, K., Hull, M., and Fiebich, B.L. (1995). IL-1 beta and TNF alpha, but not IL-6, induce alpha 1-antichymotrypsin expression in the human astrocytoma cell line U373 MG. Neuroreport *6*, 2283-2286.

Mahoney, D.J., Cheung, H.H., Mrad, R.L., Plenchette, S., Simard, C., Enwere, E., Arora, V., Mak, T.W., Lacasse, E.C., Waring, J., *et al.* (2008). Both cIAP1 and cIAP2 regulate TNFalpha-mediated NF-kappaB activation. Proc Natl Acad Sci U S A *105*, 11778-11783.

Mamane, Y., Heylbroeck, C., Genin, P., Algarte, M., Servant, M.J., LePage, C., DeLuca, C., Kwon, H., Lin, R., and Hiscott, J. (1999). Interferon regulatory factors: the next generation. Gene *237*, 1-14.

Margolin, N., Raybuck, S.A., Wilson, K.P., Chen, W., Fox, T., Gu, Y., and Livingston, D.J. (1997). Substrate and inhibitor specificity of interleukin-1 beta-converting enzyme and related caspases. J Biol Chem *272*, 7223-7228.

Martin, M., Bol, G.F., Eriksson, A., Resch, K., and Brigelius-Flohe, R. (1994). Interleukin-1-induced activation of a protein kinase co-precipitating with the type I interleukin-1 receptor in T cells. Eur J Immunol *24*, 1566-1571.

Medzhitov, R., Preston-Hurlburt, P., and Janeway, C.A., Jr. (1997). A human homologue of the Drosophila Toll protein signals activation of adaptive immunity. Nature *388*, 394-397.

Meylan, E., Burns, K., Hofmann, K., Blancheteau, V., Martinon, F., Kelliher, M., and Tschopp, J. (2004). RIP1 is an essential mediator of Toll-like receptor 3-induced NF-kappa B activation. Nat Immunol *5*, 503-507.

Micheau, O., Lens, S., Gaide, O., Alevizopoulos, K., and Tschopp, J. (2001). NF-kappaB signals induce the expression of c-FLIP. Mol Cell Biol *21*, 5299-5305.

Micheau, O., and Tschopp, J. (2003). Induction of TNF receptor I-mediated apoptosis via two sequential signaling complexes. Cell *114*, 181-190.

Miyake, K. (2007). Innate immune sensing of pathogens and danger signals by cell surface Toll-like receptors. Semin Immunol *19*, 3-10.

Mizel, S.B., Honko, A.N., Moors, M.A., Smith, P.S., and West, A.P. (2003). Induction of macrophage nitric oxide production by Gram-negative flagellin involves signaling via heteromeric Toll-like receptor 5/Toll-like receptor 4 complexes. J Immunol *170*, 6217-6223.

Mosmann, T. (1983). Rapid colorimetric assay for cellular growth and survival: application to proliferation and cytotoxicity assays. J Immunol Methods *65*, 55-63.

Moynagh, P. (2009). The Pellino family: IRAK E3 ligases with emerging roles in innate immune signalling. Trends in Immunology *30*, 33-42.

Moynagh, P.N. (2011). Peli1 (rel)ieves autoimmunity. Nat Immunol *12*, 927-929.

Muzio, M., Chinnaiyan, A.M., Kischkel, F.C., O'Rourke, K., Shevchenko, A., Ni, J., Scaffidi, C., Bretz, J.D., Zhang, M., Gentz, R., *et al.* (1996). FLICE, a novel FADD-homologous ICE/CED-3-like protease, is recruited to the CD95 (Fas/APO-1) death--inducing signaling complex. Cell *85*, 817-827.

Nagaki, M., Sugiyama, A., Osawa, Y., Naiki, T., Nakashima, S., Nozawa, Y., and Moriwaki, H. (1999). Lethal hepatic apoptosis mediated by tumor necrosis factor receptor, unlike Fas-mediated apoptosis, requires hepatocyte sensitization in mice. J Hepatol *31*, 997-1005.

Newton, K., Sun, X., and Dixit, V.M. (2004). Kinase RIP3 is dispensable for normal NF-kappa Bs, signaling by the B-cell and T-cell receptors, tumor necrosis factor receptor 1, and Toll-like receptors 2 and 4. Mol Cell Biol *24*, 1464-1469.

Nogueira, E., Ponciano, V.C., Naka, E.L., Marques, G.D., Cenedeze, M.A., Camara, N.O., and Pacheco-Silva, A. (2009). Toll-like receptors-related genes in kidney transplant patients with chronic allograft nephropathy and acute rejection. Int Immunopharmacol *9*, 673-676.

O'Neill, L.A. (1995). Towards an understanding of the signal transduction pathways for interleukin 1. Biochim Biophys Acta *1266*, 31-44.

O'Neill, L.A. (2006). Targeting signal transduction as a strategy to treat inflammatory diseases. Nat Rev Drug Discov *5*, 549-563.

Okamura, Y., Watari, M., Jerud, E.S., Young, D.W., Ishizaka, S.T., Rose, J., Chow, J.C., and Strauss, J.F., 3rd (2001). The extra domain A of fibronectin activates Toll-like receptor 4. J Biol Chem *276*, 10229-10233.

Ordureau, A., Smith, H., Windheim, M., Peggie, M., Carrick, E., Morrice, N., and Cohen, P. (2008). The IRAK-catalysed activation of the E3 ligase function of Pellino isoforms induces the Lys63-linked polyubiquitination of IRAK1. Biochem J *409*, 43-52.

Oshima, S., Turer, E.E., Callahan, J.A., Chai, S., Advincula, R., Barrera, J., Shifrin, N., Lee, B., Benedict Yen, T.S., Woo, T., *et al.* (2009). ABIN-1 is a ubiquitin sensor that restricts cell death and sustains embryonic development. Nature *457*, 906-909.

Ozinsky, A., Underhill, D.M., Fontenot, J.D., Hajjar, A.M., Smith, K.D., Wilson, C.B., Schroeder, L., and Aderem, A. (2000). The repertoire for pattern recognition of pathogens by the innate immune system is defined by cooperation between Toll-like receptors. P Natl Acad Sci USA *97*, 13766-13771.

Pandey, S., and Agrawal, D.K. (2006). Immunobiology of Toll-like receptors: emerging trends. Immunol Cell Biol *84*, 333-341.

Pfeffer, K., Matsuyama, T., Kundig, T.M., Wakeham, A., Kishihara, K., Shahinian, A., Wiegmann, K., Ohashi, P.S., Kronke, M., and Mak, T.W. (1993). Mice deficient for the 55 kd tumor necrosis factor receptor are resistant to endotoxic shock, yet succumb to L. monocytogenes infection. Cell *73*, 457-467.

Poltorak, A., He, X., Smirnova, I., Liu, M.Y., Van Huffel, C., Du, X., Birdwell, D., Alejos, E., Silva, M., Galanos, C., *et al.* (1998). Defective LPS signaling in C3H/HeJ and C57BL/10ScCr mice: mutations in Tlr4 gene. Science *282*, 2085-2088.

Rassa, J.C., Meyers, J.L., Zhang, Y., Kudaravalli, R., and Ross, S.R. (2002). Murine retroviruses activate B cells via interaction with toll-like receptor 4. Proc Natl Acad Sci U S A *99*, 2281-2286.

Reddy, P., Slack, J.L., Davis, R., Cerretti, D.P., Kozlosky, C.J., Blanton, R.A., Shows, D., Peschon, J.J., and Black, R.A. (2000). Functional analysis of the domain structure of tumor necrosis factor-alpha converting enzyme. J Biol Chem *275*, 14608-14614.

Resch, K., Jockusch, H., and Schmitt-John, T. (2001). Assignment of homologous genes, Peli1/PELI1 and Peli2/PELI2, for the Pelle adaptor protein Pellino to mouse chromosomes 11 and 14 and human chromosomes 2p13.3 and 14q21, respectively, by physical and radiation hybrid mapping. Cytogenet Cell Genet *92*, 172-174.

Rich, T., Allen, R.L., Lucas, A.M., Stewart, A., and Trowsdale, J. (2000). Pellino-related sequences from Caenorhabditis elegans and Homo sapiens. Immunogenetics *52*, 145-149.

Roach, J.C., Glusman, G., Rowen, L., Kaur, A., Purcell, M.K., Smith, K.D., Hood, L.E., and Aderem, A. (2005). The evolution of vertebrate Toll-like receptors. P Natl Acad Sci USA *102*, 9577-9582.

Rothe, M., Pan, M.G., Henzel, W.J., Ayres, T.M., and Goeddel, D.V. (1995). The TNFR2-TRAF signaling complex contains two novel proteins related to baculoviral inhibitor of apoptosis proteins. Cell *83*, 1243-1252.

Saitoh, S., and Miyake, K. (2009). Regulatory molecules required for nucleotide-sensing Toll-like receptors. Immunol Rev *227*, 32-43.

Sakamaki, K., Inoue, T., Asano, M., Sudo, K., Kazama, H., Sakagami, J., Sakata, S., Ozaki, M., Nakamura, S., Toyokuni, S., *et al.* (2002). Ex vivo whole-embryo culture of caspase-8-deficient embryos normalize their aberrant phenotypes in the developing neural tube and heart. Cell Death Differ *9*, 1196-1206.

Salvesen, G.S., and Dixit, V.M. (1997). Caspases: intracellular signaling by proteolysis. Cell *91*, 443-446.

Saraste, A., and Pulkki, K. (2000). Morphologic and biochemical hallmarks of apoptosis. Cardiovasc Res *45*, 528-537.

Scaffidi, C., Fulda, S., Srinivasan, A., Friesen, C., Li, F., Tomaselli, K.J., Debatin, K.M., Krammer, P.H., and Peter, M.E. (1998). Two CD95 (APO-1/Fas) signaling pathways. EMBO J *17*, 1675-1687.

Scaffidi, C., Kirchhoff, S., Krammer, P.H., and Peter, M.E. (1999). Apoptosis signaling in lymphocytes. Curr Opin Immunol *11*, 277-285.

Schauvliege, R., Janssens, S., and Beyaert, R. (2006). Pellino proteins are more than scaffold proteins in TLR/IL-1R signalling: a role as novel RING E3-ubiquitin-ligases. FEBS Lett *580*, 4697-4702.

Schauvliege, R., Janssens, S., and Beyaert, R. (2007). Pellino proteins: novel players in TLR and IL-1R signalling. J Cell Mol Med *11*, 453-461.

Sen, R., and Baltimore, D. (1986). Multiple nuclear factors interact with the immunoglobulin enhancer sequences. Cell *46*, 705-716.

Shembade, N., Ma, A., and Harhaj, E.W. (2010). Inhibition of NF-kappaB signaling by A20 through disruption of ubiquitin enzyme complexes. Science *327*, 1135-1139.

Smiley, S.T., King, J.A., and Hancock, W.W. (2001). Fibrinogen stimulates macrophage chemokine secretion through toll-like receptor 4. J Immunol *167*, 2887-2894.

Smith, H., Liu, X.Y., Dai, L., Goh, E.T., Chan, A.T., Xi, J., Seh, C.C., Qureshi, I.A., Lescar, J., Ruedl, C., *et al.* (2011). The role of TBK1 and IKKepsilon in the expression and activation of Pellino 1. Biochem J *434*, 537-548.

Smith, H., Peggie, M., Campbell, D.G., Vandermoere, F., Carrick, E., and Cohen, P. (2009). Identification of the phosphorylation sites on the E3 ubiquitin ligase Pellino that are critical for activation by IRAK1 and IRAK4. Proc Natl Acad Sci U S A *106*, 4584-4590.

Stanger, B.Z., Leder, P., Lee, T.H., Kim, E., and Seed, B. (1995). RIP: a novel protein containing a death domain that interacts with Fas/APO-1 (CD95) in yeast and causes cell death. Cell *81*, 513-523.

Stennicke, H.R., Jurgensmeier, J.M., Shin, H., Deveraux, Q., Wolf, B.B., Yang, X., Zhou, Q., Ellerby, H.M., Ellerby, L.M., Bredesen, D., *et al.* (1998). Pro-caspase-3 is a major physiologic target of caspase-8. J Biol Chem *273*, 27084-27090.

Stock, J.B., Ninfa, A.J., and Stock, A.M. (1989). Protein phosphorylation and regulation of adaptive responses in bacteria. Microbiol Rev *53*, 450-490.

Strelow, A., Kollewe, C., and Wesche, H. (2003). Characterization of Pellino2, a substrate of IRAK1 and IRAK4. FEBS Lett *547*, 157-161.

Strieter, R.M., Standiford, T.J., Huffnagle, G.B., Colletti, L.M., Lukacs, N.W., and Kunkel, S.L. (1996). "The good, the bad, and the ugly." The role of chemokines in models of human disease. J Immunol *156*, 3583-3586.

Sun, X., Yin, J., Starovasnik, M.A., Fairbrother, W.J., and Dixit, V.M. (2002). Identification of a novel homotypic interaction motif required for the phosphorylation of receptor-interacting protein (RIP) by RIP3. J Biol Chem *277*, 9505-9511.

Sun, X.M., MacFarlane, M., Zhuang, J., Wolf, B.B., Green, D.R., and Cohen, G.M. (1999). Distinct caspase cascades are initiated in receptor-mediated and chemical-induced apoptosis. J Biol Chem *274*, 5053-5060.

Symons, A., Beinke, S., and Ley, S.C. (2006). MAP kinase kinase kinases and innate immunity. Trends Immunol *27*, 40-48.

Takeda, K., Kaisho, T., and Akira, S. (2003). Toll-like receptors. Annu Rev Immunol *21*, 335-376.

Takeuchi, O., Kawai, T., Sanjo, H., Copeland, N.G., Gilbert, D.J., Jenkins, N.A., Takeda, K., and Akira, S. (1999). TLR6: A novel member of an expanding Toll-like receptor family. Gene *231*, 59-65.

Tang, G., Minemoto, Y., Dibling, B., Purcell, N.H., Li, Z., Karin, M., and Lin, A. (2001). Inhibition of JNK activation through NF-kappaB target genes. Nature *414*, 313-317.

Tao, Y., Yan, D., Yang, Q., Zeng, R., and Wang, Y. (2006). Low K+ promotes NF-kappaB/DNA binding in neuronal apoptosis induced by K+ loss. Mol Cell Biol *26*, 1038-1050.

Taub, D.D., Turcovski-Corrales, S.M., Key, M.L., Longo, D.L., and Murphy, W.J. (1996). Chemokines and T lymphocyte activation: I. Beta chemokines costimulate human T lymphocyte activation in vitro. J Immunol *156*, 2095-2103.

Tenev, T., Bianchi, K., Darding, M., Broemer, M., Langlais, C., Wallberg, F., Zachariou, A., Lopez, J., MacFarlane, M., Cain, K., *et al.* (2011). The Ripoptosome, a signaling platform that assembles in response to genotoxic stress and loss of IAPs. Mol Cell *43*, 432-448.

Termeer, C., Benedix, F., Sleeman, J., Fieber, C., Voith, U., Ahrens, T., Miyake, K., Freudenberg, M., Galanos, C., and Simon, J.C. (2002). Oligosaccharides of Hyaluronan activate dendritic cells via toll-like receptor 4. J Exp Med *195*, 99-111.

Tewari, M., Quan, L.T., O'Rourke, K., Desnoyers, S., Zeng, Z., Beidler, D.R., Poirier, G.G., Salvesen, G.S., and Dixit, V.M. (1995). Yama/CPP32 beta, a mammalian homolog of CED-3, is a CrmA-inhibitable protease that cleaves the death substrate poly(ADP-ribose) polymerase. Cell *81*, 801-809.

Theiner, G., Rossner, S., Dalpke, A., Bode, K., Berger, T., Gessner, A., and Lutz, M.B. (2008). TLR9 cooperates with TLR4 to increase IL-12 release by murine dendritic cells. Mol Immunol *45*, 244-252.

Thomas, P., and Smart, T.G. (2005). HEK293 cell line: a vehicle for the expression of recombinant proteins. J Pharmacol Toxicol Methods *51*, 187-200.

Thompson, C.B. (1995). New Insights into V(D)J Recombination and Its Role in the Evolution of the Immune-System. Immunity *3*, 531-539.

Thornberry, N.A. (1997). The caspase family of cysteine proteases. Br Med Bull *53*, 478-490.

Ting, A.T., Pimentel-Muinos, F.X., and Seed, B. (1996). RIP mediates tumor necrosis factor receptor 1 activation of NF-kappaB but not Fas/APO-1-initiated apoptosis. EMBO J *15*, 6189-6196.

Vabulas, R.M., Ahmad-Nejad, P., Ghose, S., Kirschning, C.J., Issels, R.D., and Wagner, H. (2002). HSP70 as endogenous stimulus of the Toll/interleukin-1 receptor signal pathway. J Biol Chem *277*, 15107-15112.

Van Molle, W., Libert, C., Fiers, W., and Brouckaert, P. (1997). Alpha 1-acid glycoprotein and alpha 1-antitrypsin inhibit TNF-induced but not anti-Fas-induced apoptosis of hepatocytes in mice. J Immunol *159*, 3555-3564.

Varfolomeev, E.E., Boldin, M.P., Goncharov, T.M., and Wallach, D. (1996). A potential mechanism of "cross-talk" between the p55 tumor necrosis factor receptor and Fas/APO1: proteins binding to the death domains of the two receptors also bind to each other. J Exp Med *183*, 1271-1275.

Vassalli, P. (1992). The pathophysiology of tumor necrosis factors. Annu Rev Immunol *10*, 411-452.

Wajant, H., Pfizenmaier, K., and Scheurich, P. (2003). Tumor necrosis factor signaling. Cell Death Differ *10*, 45-65.

Wallach, D., Varfolomeev, E.E., Malinin, N.L., Goltsev, Y.V., Kovalenko, A.V., and Boldin, M.P. (1999). Tumor necrosis factor receptor and Fas signaling mechanisms. Annu Rev Immunol *17*, 331-367.

Wang, C.Y., Mayo, M.W., Korneluk, R.G., Goeddel, D.V., and Baldwin, A.S., Jr. (1998). NF-kappaB antiapoptosis: induction of TRAF1 and TRAF2 and c-IAP1 and c-IAP2 to suppress caspase-8 activation. Science *281*, 1680-1683.

Wang, L., Du, F., and Wang, X. (2008). TNF-alpha induces two distinct caspase-8 activation pathways. Cell *133*, 693-703.

Weber, A., Wasiliew, P., and Kracht, M. (2010). Interleukin-1 (IL-1) pathway. Sci Signal *3*, cm1.

Weih, F., and Caamano, J. (2003). Regulation of secondary lymphoid organ development by the nuclear factor-kappaB signal transduction pathway. Immunol Rev *195*, 91-105.

Wertz, I.E., and Dixit, V.M. (2010). Regulation of death receptor signaling by the ubiquitin system. Cell Death Differ *17*, 14-24.

Wertz, I.E., O'Rourke, K.M., Zhou, H., Eby, M., Aravind, L., Seshagiri, S., Wu, P., Wiesmann, C., Baker, R., Boone, D.L., *et al.* (2004). De-ubiquitination and ubiquitin ligase domains of A20 downregulate NF-kappaB signalling. Nature *430*, 694-699.

Widmann, C., Gibson, S., Jarpe, M.B., and Johnson, G.L. (1999). Mitogen-activated protein kinase: conservation of a three-kinase module from yeast to human. Physiol Rev *79*, 143-180.

Wilson, N.S., Dixit, V., and Ashkenazi, A. (2009). Death receptor signal transducers: nodes of coordination in immune signaling networks. Nat Immunol *10*, 348-355.

Windheim, M., Stafford, M., Peggie, M., and Cohen, P. (2008). Interleukin-1 (IL-1) induces the Lys63-linked polyubiquitination of IL-1 receptor-associated kinase 1 to facilitate NEMO binding and the activation of IkappaBalpha kinase. Mol Cell Biol *28*, 1783-1791.

Wu, C.J., Conze, D.B., Li, T., Srinivasula, S.M., and Ashwell, J.D. (2006). Sensing of Lys 63-linked polyubiquitination by NEMO is a key event in NF-kappaB activation [corrected]. Nat Cell Biol *8*, 398-406.

Xiao, H., Qian, W., Staschke, K., Qian, Y., Cui, G., Deng, L., Ehsani, M., Wang, X., Qian, Y.W., Chen, Z.J., *et al.* (2008). Pellino 3b negatively regulates interleukin-1-induced TAK1-dependent NF kappaB activation. J Biol Chem *283*, 14654-14664.

Xu, G., Tan, X., Wang, H., Sun, W., Shi, Y., Burlingame, S., Gu, X., Cao, G., Zhang, T., Qin, J., *et al.* (2010). Ubiquitin-specific peptidase 21 inhibits tumor necrosis factor alpha-induced nuclear factor kappaB activation via binding to and deubiquitinating receptor-interacting protein 1. J Biol Chem *285*, 969-978.

Yamamoto, M., and Takeda, K. (2008). Role of nuclear IkappaB proteins in the regulation of host immune responses. J Infect Chemother *14*, 265-269.

Yarovinsky, F., Zhang, D., Andersen, J.F., Bannenberg, G.L., Serhan, C.N., Hayden, M.S., Hieny, S., Sutterwala, F.S., Flavell, R.A., Ghosh, S., *et al.* (2005). TLR11 activation of dendritic cells by a protozoan profilin-like protein. Science *308*, 1626-1629.

Yeh, W.C., Pompa, J.L., McCurrach, M.E., Shu, H.B., Elia, A.J., Shahinian, A., Ng, M., Wakeham, A., Khoo, W., Mitchell, K., *et al.* (1998). FADD: essential for embryo development and signaling from some, but not all, inducers of apoptosis. Science *279*, 1954-1958.

Yi, X., Yin, X.M., and Dong, Z. (2003). Inhibition of Bid-induced apoptosis by Bcl-2. tBid insertion, Bax translocation, and Bax/Bak oligomerization suppressed. J Biol Chem *278*, 16992-16999.

Yu, K.Y., Kwon, H.J., Norman, D.A., Vig, E., Goebl, M.G., and Harrington, M.A. (2002). Cutting edge: mouse pellino-2 modulates IL-1 and lipopolysaccharide signaling. J Immunol *169*, 4075-4078.

Yuan, J., Shaham, S., Ledoux, S., Ellis, H.M., and Horvitz, H.R. (1993). The C. elegans cell death gene ced-3 encodes a protein similar to mammalian interleukin-1 beta-converting enzyme. Cell *75*, 641-652.

Zandi, E., Rothwarf, D.M., Delhase, M., Hayakawa, M., and Karin, M. (1997). The IkappaB kinase complex (IKK) contains two kinase subunits, IKKalpha and IKKbeta, necessary for IkappaB phosphorylation and NF-kappaB activation. Cell *91*, 243-252.

Zhang, J., Cado, D., Chen, A., Kabra, N.H., and Winoto, A. (1998). Fas-mediated apoptosis and activation-induced T-cell proliferation are defective in mice lacking FADD/Mort1. Nature *392*, 296-300.

APPENDIX

Appendix I:

PrimerName	Primersequence(5'-3')	Application
HA-c8as	ATTGCGGCCGCTCAATCAGAAGGGAAGACAAGTTTTTTTC	HA-caspase-8
HA-c8s	CTGGTCGACCATGGACTTCAGCAGAAATCTTTATG	
P4-c8DEDs	CTGGATATCACCATGGACTTCAGCAGAAATCTTTATG	Myc- caspase-8 DED
P4-c8DEDas	ATTCTCGAGATCAGGACTTCCTTCAAGGCTGCTG	
PET-c8DEDs	CTGGATATCATGGACTTCAGCAGAAATCTTTATG	6 x his- caspase-8DED
PET-c8DEDas	ATTCTCGAGTATCAGGACTTCCTTCAAGGCTGCTG	

P4-c8DDEDs	CTGGATATCACCATGGAATTTTCAAATGGGGAGGAGTTG	Myc- caspase-8DDED
p4-C8DDEDas	ATTGCGGCCGCCAATCAGAAGGGAAGACAAGTTTTTTTC	
PRSET-C8bFLs	CTGGGATCCATGGACTTCAGCAGAAATCTTTATG	6 x his- caspase-8 full length
PRSET-C8bFLas	ATTAAGCTTCGATCAGAAGGGAAGACAAGTTTTTTTC	
PET-c8DDEDs	CTGGATATCGAATTTTCAAATGGGGAGGAGTTG	6 x his caspase-8DDED
PET-c8DDEDas	ATTGCGGCCGCAATCAGAAGGGAAGACAAGTTTTTTTC	
Retro-mP3s	CTGCTCGAGGCGATGGTGCTGGAAGGAAAC C	Retro-murine Pellino3
Retro-mP3as	ATTGTCGACCTACAGATCTTCTTCAGAAATAAGTTTTTGTTC	

Table I Primers for PCR amplification, cloning

PrimerName	Primersequence(5’-3’)	Application
mHPRTs	GTCCCAGCGTCGTGATTAGC	murine HPRT
mHPRTas	TGGCCTCCCATCTCCTTCA	
mA20s	TGCCAGTTTTGCCCACAGT	murine A20
mA20as	TTCAGAGCCACGAGCTTCCT	
cFLIPs	GCTCCAGAATGGGCGAAGT	murine cFLIP (both isoforms)
cFLIPas	CACGGATGTGCGGAGGTAA	
mP3t2s	ACATGCCAACGGAGTGAAGC	murine Pelino3 (both isoforms)
mP3t2as	AGCGGCCAATCTGGAACAT	

Table II Primers for mRNA relative quatification

Appenix II: Vectors and plasmids

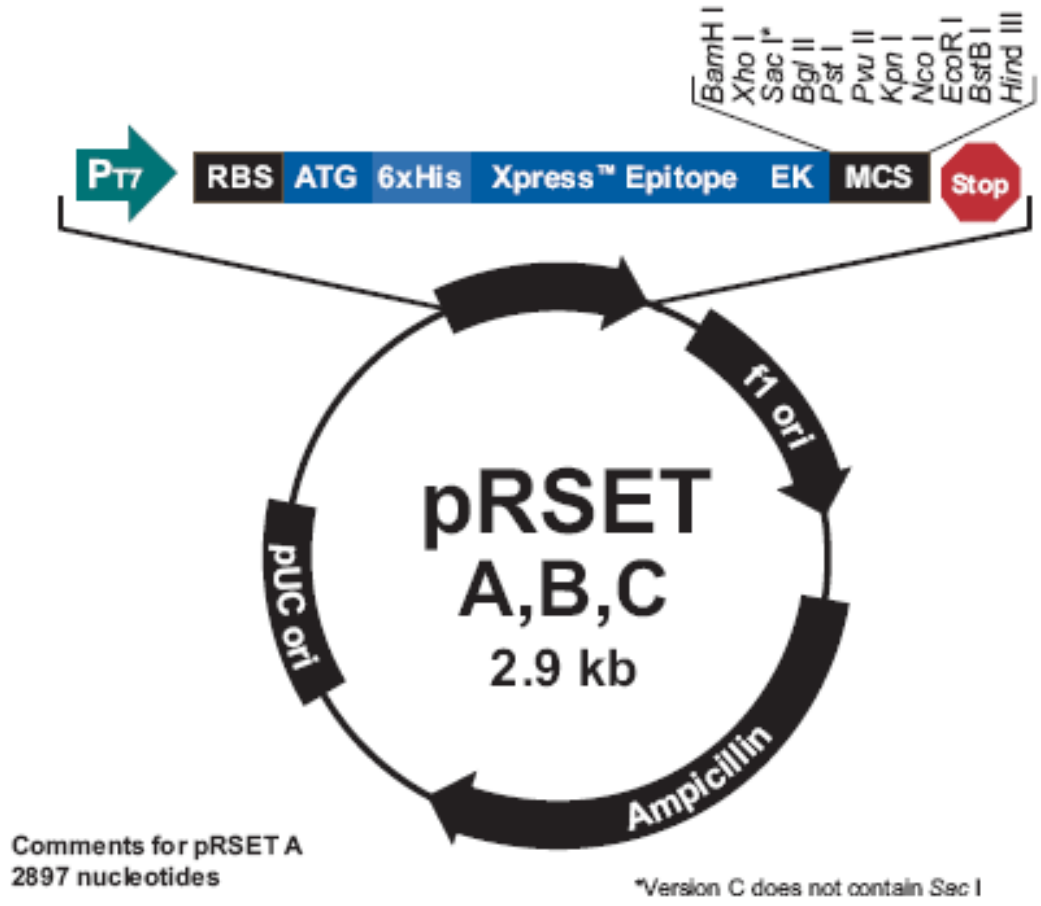

Figure I Maps of pRSET A

Adapted from http://products.invitrogen.com/ivgn/product/V35120

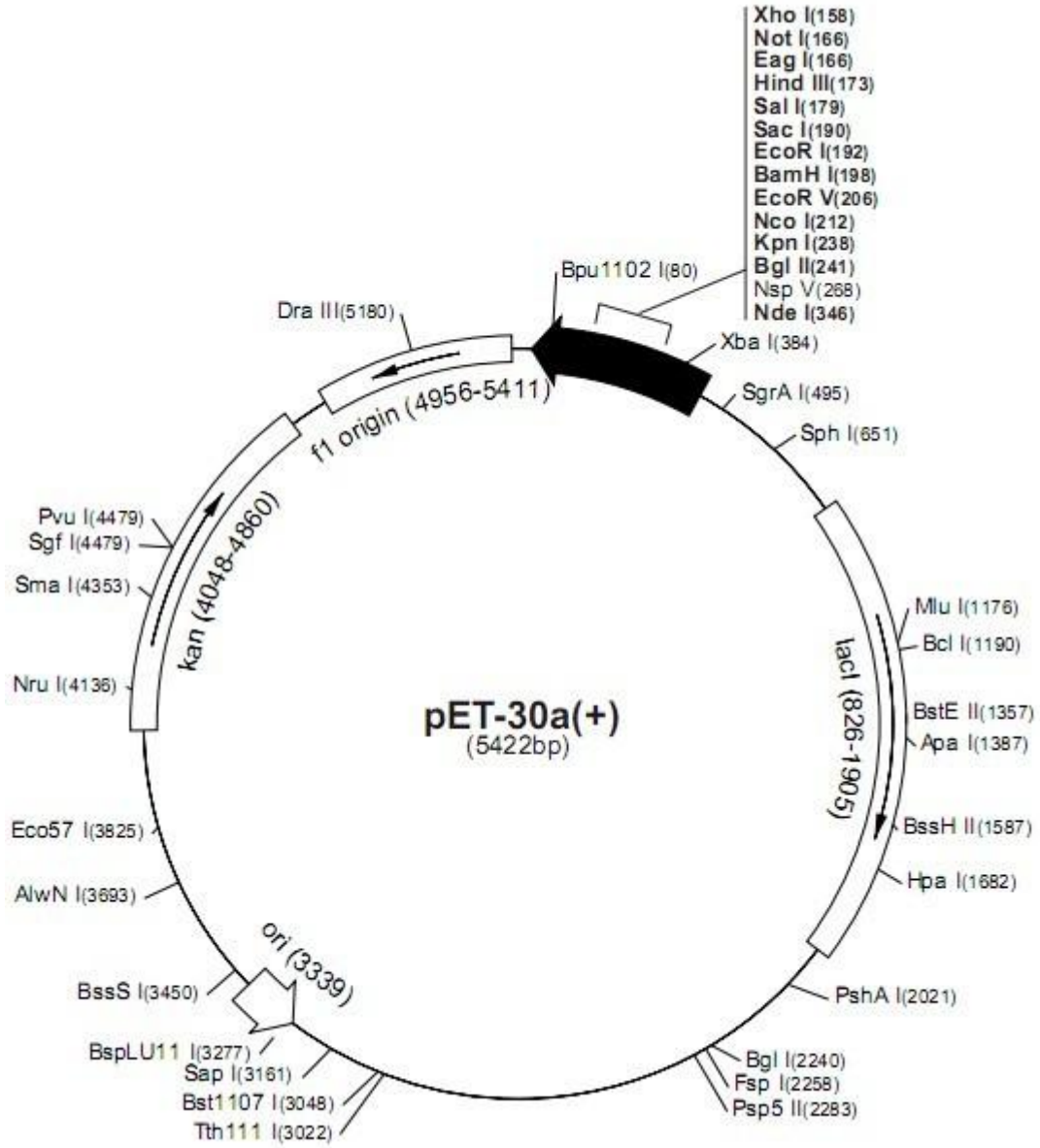

Figure II Maps of pET-30a

Adapted from

http://aether.sgc.ox.ac.uk:2784/structures/MM/Vectors/pET30a/pET30a_vector_sheet.pdf

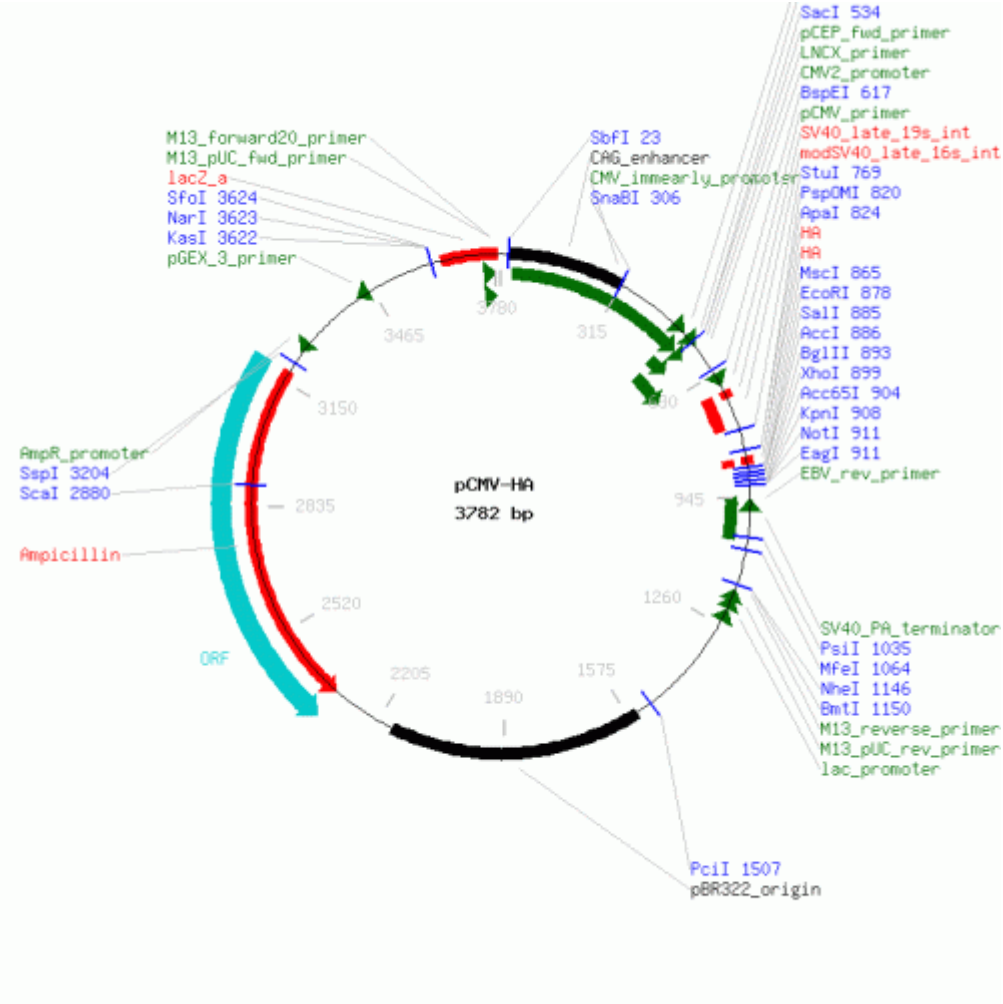

Figure III Maps of pCMV-HA Vector

Adapted from

http://www.clontech.com/IE/Products/Protein_Interactions_and_Profiling/Co-immunoprecipitation/Myc-Tagged_and_HA-Tagged_Vectors?sitex=10023:22372:US

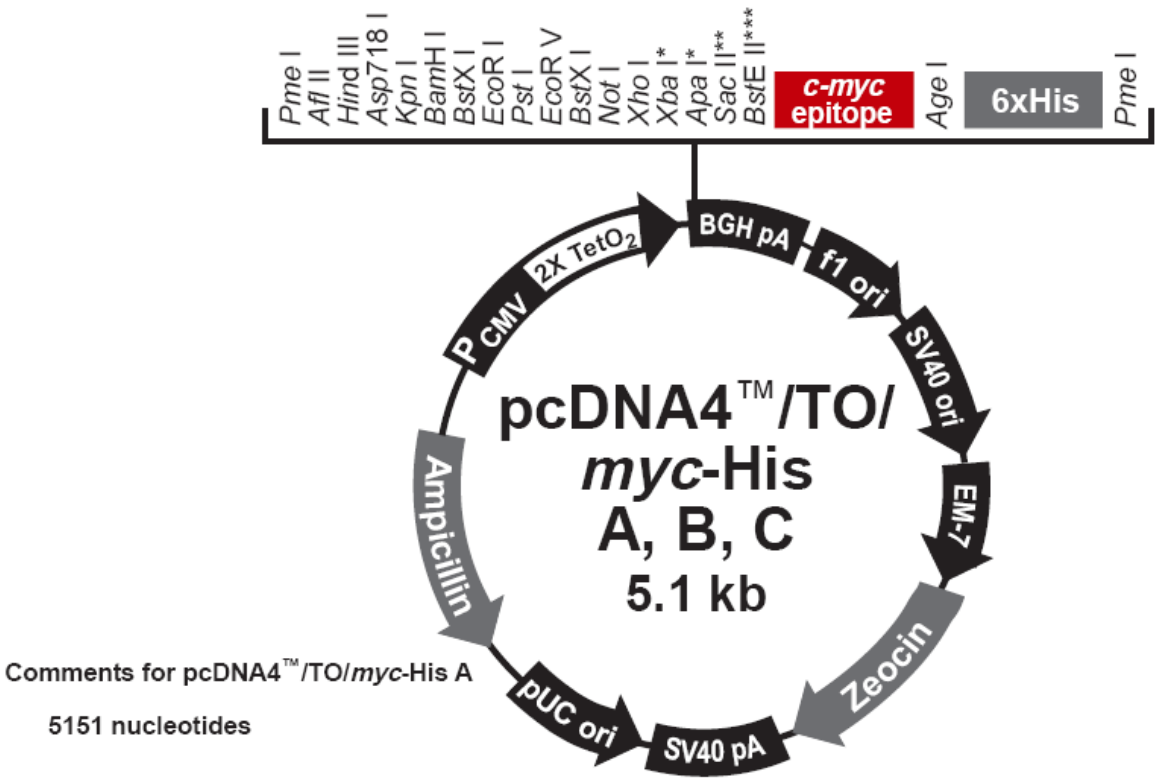

Figure IV Maps of pMSCV vectors.

Adapted from http://tools.invitrogen.com/content/sfs/vectors/pcdna4tomychis.pdf

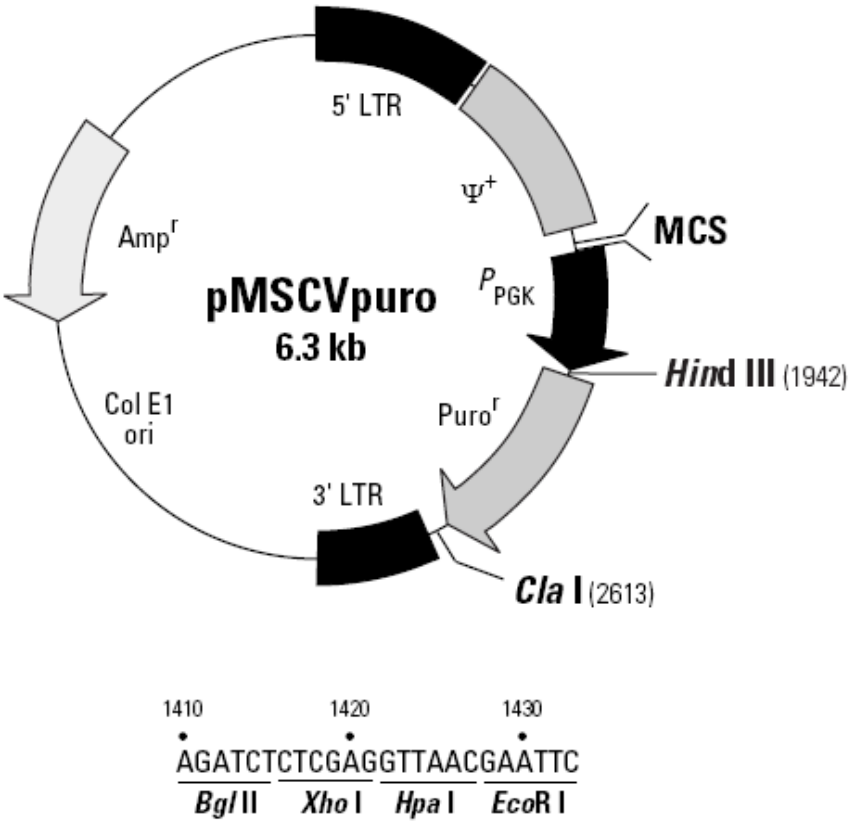

Figure V Maps of pMSCV vectors.

Adapted from

http://www.clontech.com/IE/Products/Viral_Transduction/Retroviral_Vector_Systems/MSCV?sitex=10023:22372:US